EXPLORATION AND PRODUCTION PROGRAM FOR LOCATING AND PRODUCING PROSPECTIVE AQUIFERS CONTAINING SOLUTION GAS AND FREE GAS--TEXAS GULF COAST

FINAL REPORT

(February 1, 1981 - January 31, 1983)

Prepared by

A. R. Gregory, Z. S. Lin, R. S. Reed,
R. A. Morton, and T. E. Ewing

Bureau of Economic Geology
W. L. Fisher, Director

The University of Texas at Austin
University Station, Box X
Austin, Texas 78712-7508

For

July 1983

GRI DISCLAIMER

RESEARCH SUMMARY

Title   Exploration and Production Program for Locating and Producing Prospective

Aquifers Containing Solution Gas and Free Gas--Texas Gulf Coast

Contractor   Bureau of Economic Geology

The University of Texas at Austin

GRI Contract No. 5080-321-0398

Accession Code: GRI-80/0141

Principal   A. R. Gregory
Investigator

Time Span   February 1, 1981 - January 31, 1983

Objective   This project was designed to locate and evaluate a prospective watered-out

gas reservoir in the Texas Gulf Coast inland area. The prospective reservoir

was to be suitable for application of enhanced gas recovery methods for

producing the unconventional gas that remained in the reservoir after primary

gas production ceased. A test well site would be located within a favorable

prospect area.

Technical   Previous work conducted by the Bureau of Economic Geology for the U.S.
Perspective   Department of Energy focused on the selection of test well sites in the Frio

Formation and Wilcox Group of the Texas Gulf Coast. These studies were

intended to make use of thermal energy, mechanical energy, and gas dissolved

in formation waters by producing large volumes of hot water from deep, highly

pressured formations. In this project, funded by the Gas Research Institute,

interest shifted to locating prospective reservoirs containing significant

quantities of free gas in addition to the gas dissolved in the water. Abandoned watered-out reservoirs and wet zones where large amounts of water must be produced to obtain the gas by co-production were identified.

The present project, funded by the Gas Research Institute, shows their continuing interest in unconventional gas and in developing prospects that are favorable for co-production of gas and water from watered-out gas reservoirs.

Results   Guidelines used to screen gas fields along the Texas Gulf Coast resulted in the selection of the Port Arthur field, Jefferson County, Texas, as a suitable prospect for application of enhanced gas recovery methods. Several watered-out gas sandstones in this field have excellent reservoir characteristics. All 18 wells in the field have been plugged and abandoned by previous operators; hence, leasing problems should be simplified. Abundant shallow Miocene sands in the area are available for salt-water disposal.

The "C" reservoir interval, located at an average depth of 11,130 ft, received the most extensive evaluation. Predicted gas recovery by natural flow is 5.1 billion standard cubic feet as reservoir pressure declines from 6,632 to 4,309 psig. A sample economic analysis showed a net present worth of $968,000, and a payout time of 3 yr. This prospect has the potential to be economically profitable in addition to being a good research and development test for evaluating co-production techniques.

It is recommended that a co-production well be drilled and tested on a site near the Meredith No. 2 Doornbos (Well 14).

Technical Approach The first task was to locate a prospective watered-out gas field where gas and water containing solution gas could be co-produced in economic quantities. Guidelines and test criteria were established for screening gas fields in the Texas Gulf Coast. These criteria included depth, pressure, salinity, temperature, and previous production history. More than 150 fields or reservoirs were considered, and 3 of these met most of the criteria. Eventually the Port Arthur field was selected as the most favorable prospect for further study and evaluation.

With the prime prospect located, the second task was to collect different types of data for the field and to analyze the data using various methods that are broadly classified as geological, reservoir engineering, geophysical, well log analysis, and economic analysis.

The amount of gas dissolved in formation waters was estimated from known values of pressure and temperature and calculated values of salinity. Bottom-hole pressures were obtained from drill-stem tests or calculated from wellhead shut-in measurements. Borehole temperatures were obtained from well logs and corrected to equilibrium values. Salinities were determined from spontaneous potential well logs.

More than 31 mi of seismic data were reprocessed in an effort to supplement geological interpretations, define reservoir boundaries, and identify the presence of free gas dispersed in the water-invaded zones of watered-out gas reservoirs.

Computer reservoir simulation studies were made to match past production and predict future production. A preliminary economic analysis was also made based on the future production predicted by the computer model.

ix

Project
Implications

This project is part of the GRI program to locate actual reservoirs or wells where co-production of natural gas and water can be evaluated. The search done by the BEG in Texas under this contract, along with similar work by others, has shown that there is a significant natural gas resource that may be producible by co-production techniques. The specific location identified and evaluated in detail by the BEG, the Port Arthur field, appears to be a good location for a GRI-supported research and development field test.

TABLE OF CONTENTS

Figures

xii

xiii

xiv

Tables

xv

Appendices

INTRODUCTION

Description of Project

This project was a comprehensive exploration and reservoir engineering program designed to locate and evaluate a prospective inland test area on the Texas Gulf Coast that will produce unconventional gas using enhanced gas recovery (EGR) methods. The search for suitable test areas was focused on watered-out gas fields. Unconventional gas in a watered-out gas field consists of mobile and producible free gas remaining in reservoir gas caps, immobile dispersed free gas trapped in water-invaded zones (fig. 1), solution gas, and mobile and producible free gas located in thin stringer sandstones (fig. 2).

Gas reservoirs that water out under moderate to strong water drives are usually abandoned when the expenses associated with salt-water disposal make continued operations uneconomical. Under favorable conditions, however, watered-out reservoirs can continue to produce substantial quantities of gas at competitive prices. Enhanced gas recovery (EGR) techniques can be used to extend the production from many reservoirs that are now watering out and that will soon be abandoned if conventional practices are followed. Now may be the time for the gas-producing industry to take another look at when to abandon reservoirs because of water production. Further gas production from these reservoirs would be a welcome addition to our nation's reserves.

The EGR method, which could prolong operations, involves the co-production of gas and water. Large volumes of water are deliberately produced to reduce reservoir pressure; the lower pressure causes expansion of free gas that was trapped in the water-invaded zone during the primary production period. Part of this free gas is mobilized and becomes producible. Pressure reduction at the surface releases additional but minor amounts of gas dissolved in the formation water.

A computer model that describes the performance of a geopressured watered-out reservoir (Geer and Cook, 1978) predicted that over 20 percent of the otherwise unrecovered gas could be produced by the co-production method. Field experience with EGR techniques has been favorable for hydropressured Wilcox and Frio reservoirs in the Texas Gulf Coast. Results from the Katy V-C reservoir (Lutes and others, 1977) and from the Lovells Lake Frio 1 reservoir (Brinkman, 1981) show that recovery factors exceed 20 percent of the original gas in place (OGIP) for additional gas produced during the blowdown period. A field test currently being conducted in the Double Bayou Frio 13 reservoir indicates that secondary gas recovery will be about 10 percent of the OGIP (Boyd and others, 1982). In another EGR project in the North
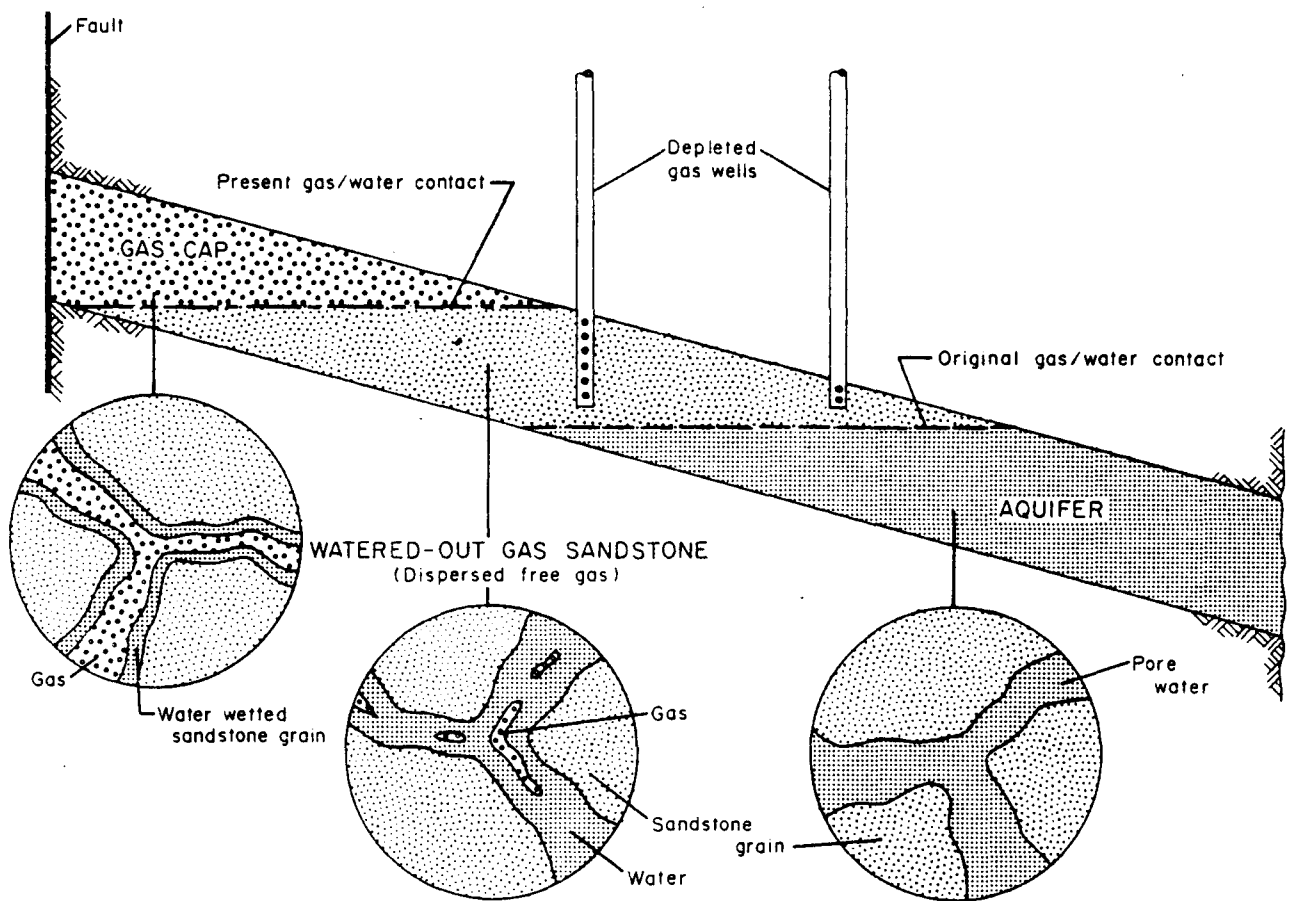
Figure 1. Fluid saturation zones within a hypothetical watered-out gas reservoir.

GAS CAP

GAS STRINGER

HYPOTHETICAL WELL

SP RES SP RES

GAS

WATER

100 ft

GAS

WATER

KILROY & MPS #1 DOORNBOS - PORT ARTHUR FIELD

GAS

11,300

WATER

11,350

GAS

WATER

11,150

11,200

KILROY & MPS #1 CITY OF PORT ARTHUR - PORT ARTHUR FIELD

GAS

WATER

11,300

GAS

11,400

WATER

11,450
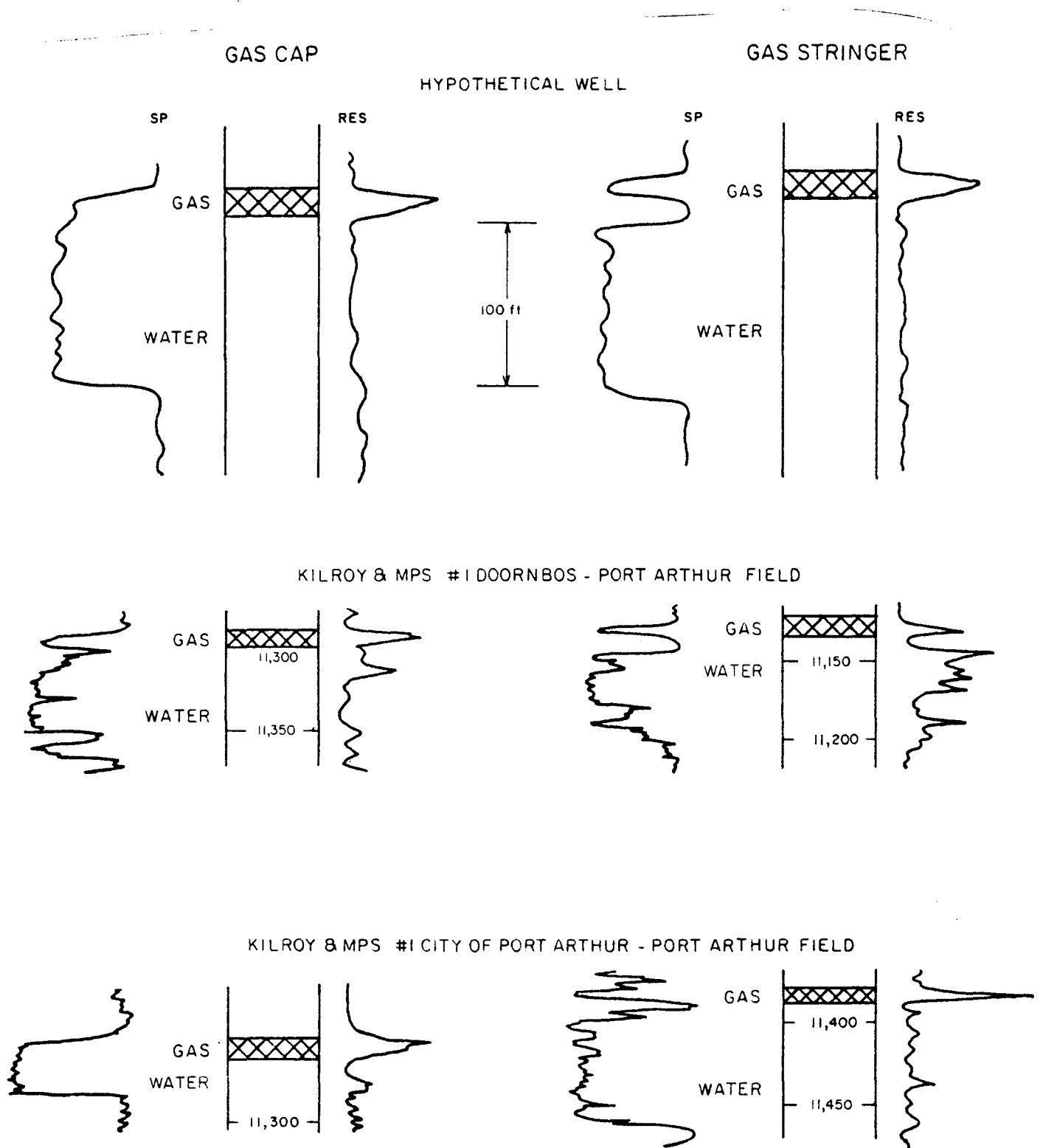
Figure 2. Typical well-log response for thick aquifers with a gas cap and thin gas stringers.

3

Alazan H-21 reservoir, Chesney and others (1982) concluded that the recovery process is dominated by gravity forces and is sensitive to vertical permeability and formation dip.

These four field cases involve pumping large volumes of water from water-drive hydropressured reservoirs located at depths between 7,200 and 8,750 ft. Although significant amounts of additional gas and some oil are recovered by EGR methods, discussion of the economic factors involved is not included in the published results. Generally, the economic outlook for EGR methods improves if (1) gas prices are high, (2) artificial lift methods are not required, and (3) waste brine can be injected into shallow aquifers or discharged at the surface.

In this project an integrated geological and engineering approach was used to select a prospective geopressured watered-out gas reservoir with characteristics favoring co-production of gas and water. During the screening phase of the project, several fields with potential were identified; one, the Port Arthur field in Jefferson County, Texas, was selected for more detailed evaluation (Gregory and others, 1981). All available data for the field were collected and analyzed using various methods that are broadly classified as reservoir engineering, geophysical interpretation, well log analysis, and economic analysis. More than 31 mi of seismic data obtained for lines in or near the Port Arthur field were reprocessed. Comparison of three independent reservoir simulation studies is made herein for the geopressured "C" sandstone; the top of this sandstone is located at an average depth of 11,130 ft. History matches are described, and predictions of reservoir performance and additional gas recovery by the EGR co-production method are made. Results of economic analyses are encouraging. The results of well log analyses are reported for seven reservoirs in the Port Arthur field. Gas-water contacts are established, and hydrocarbon pore volume maps are presented.

Formation fluid properties of pressure, temperature, and salinity have a significant influence on the amount of methane gas that can be held in solution. Solution gas, however, is less important in this project because it represents a relatively small part of the total gas resource. As a result, the influence of high salinity on the resource is minor, but high-salinity waters may cause scaling and corrosion of production equipment.

Finally, a drilling site for the recommended test well is delineated near the structural crest of the field.

Previous Related Work

Previous geological studies by the Bureau of Economic Geology, funded by the U.S. Department of Energy (DOE), concentrated on developing prospects in geothermal geopressured reservoirs in the Texas Gulf Coast area. These prospects were intended to produce large volumes of water from deep geopressured zones where fluid temperatures were at least

300°F* (Bebout and others, 1978a and b, 1979). Later studies, funded by the Gas Research Institute (GRI), were directed toward locating prospective areas that were favorable for producing solution gas from deep hydropressured and shallow geopressured zones where formation fluid temperatures were less than 300°F (Weise and others, 1981a). The GRI studies included the A, B, and C Zones that were defined on the basis of pressure gradients and temperatures (fig. 3). The A Zone is the deep hydropressured zone below a depth of 4,500 ft, in which the pressure gradient is hydrostatic (0.465 psi/ft). The B Zone is a relatively thin zone of transition from hydrostatic pressure gradients (0.465 psi/ft) to abnormally high pressure gradients of about 0.7 psi/ft. The C Zone has fluid pressure gradients greater than 0.7 psi/ft and fluid temperatures less than 300°F. In the D Zone, fluid pressure gradients are greater than 0.7 psi/ft and fluid temperatures are greater than 300°F. Broad sandstone corridors following trends of the Wilcox Group and Frio Formation were outlined. Areas with maximum net sandstone within these corridors were identified as the Matagorda, Corpus Christi, Kenedy, Cameron, and Montgomery fairways. Several areas within these fairways were considered to be favorable for testing the solution gas resource and were identified as prospects.

A continuation of the above work was later redirected to supplement the DOE conventional geopressured geothermal program and the GRI dispersed gas project (Weise and others, 1981b). Reconnaissance for conventional geopressured prospects of the interfairway Frio/Vicksburg and Wilcox sandstone trends showed that only five fault blocks had enough potential for further study. These fault blocks were identified as Point Comfort, Blue Lake, Devillier, and Port Arthur in the Frio/Vicksburg trend and Holzmark South in the Wilcox trend (fig. 4). A large number of watered-out gas fields located in most of the Wilcox and Frio/Vicksburg trends and in fairways were screened as possible test areas for the project described in this report.

PROSPECT SELECTION AND EVALUATION

Guidelines for Selecting Test Area

Guidelines for selecting favorable test reservoirs in watered-out gas fields are:

1. The area of the watered-out gas field, fault block, or aquifer should be equal to or greater than 5 mi^2.

2. There should be at least five watered-out gas wells.

3. There should be few or no active, producing gas or oil wells.

---

*Metric conversion factors are given in appendix E; nomenclature and abbreviations used in this report are given in appendix F.
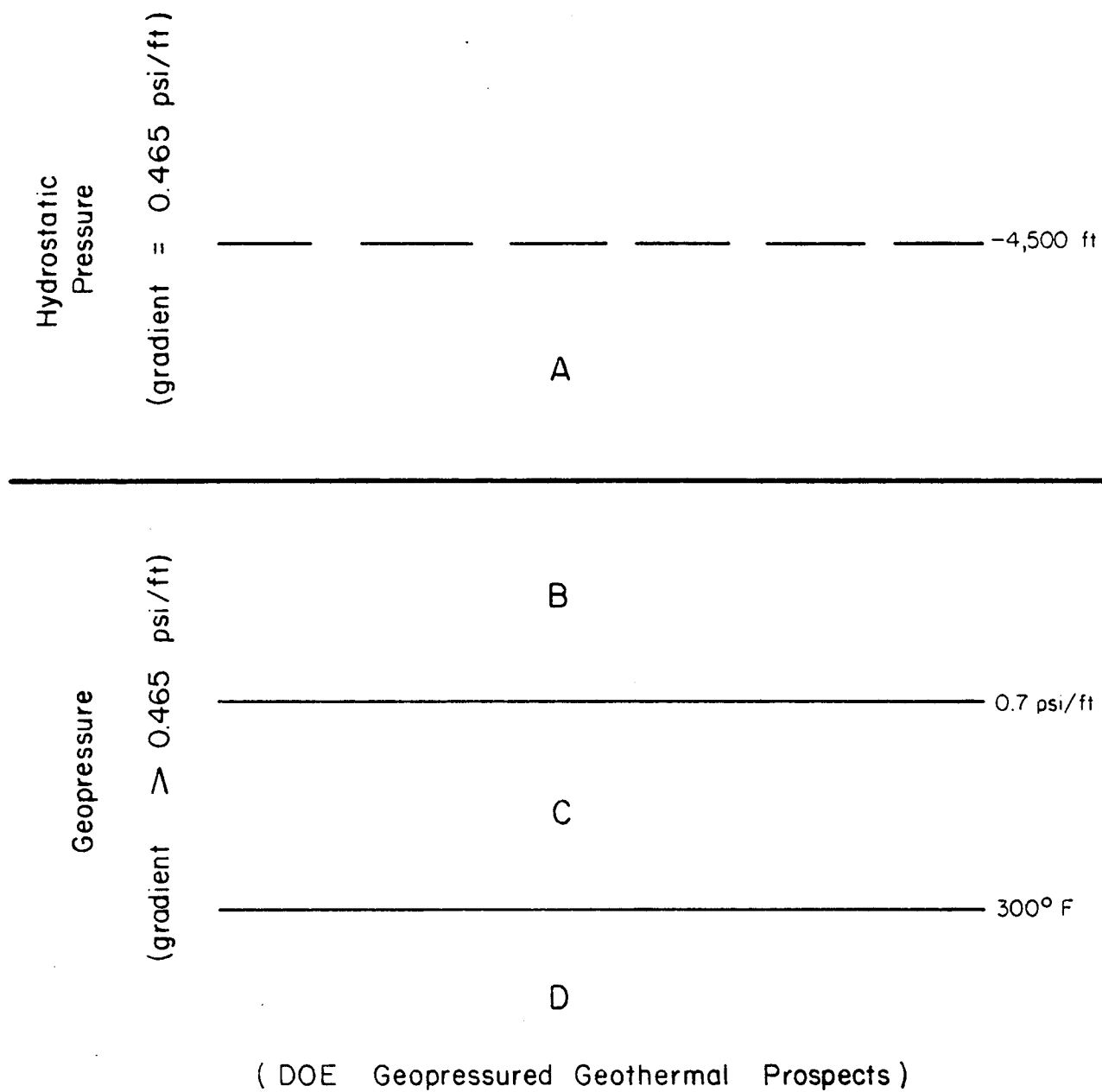
Figure 3. Definition of geopressured and deep hydropressured zones. Modified from Weise and others, 1981a.
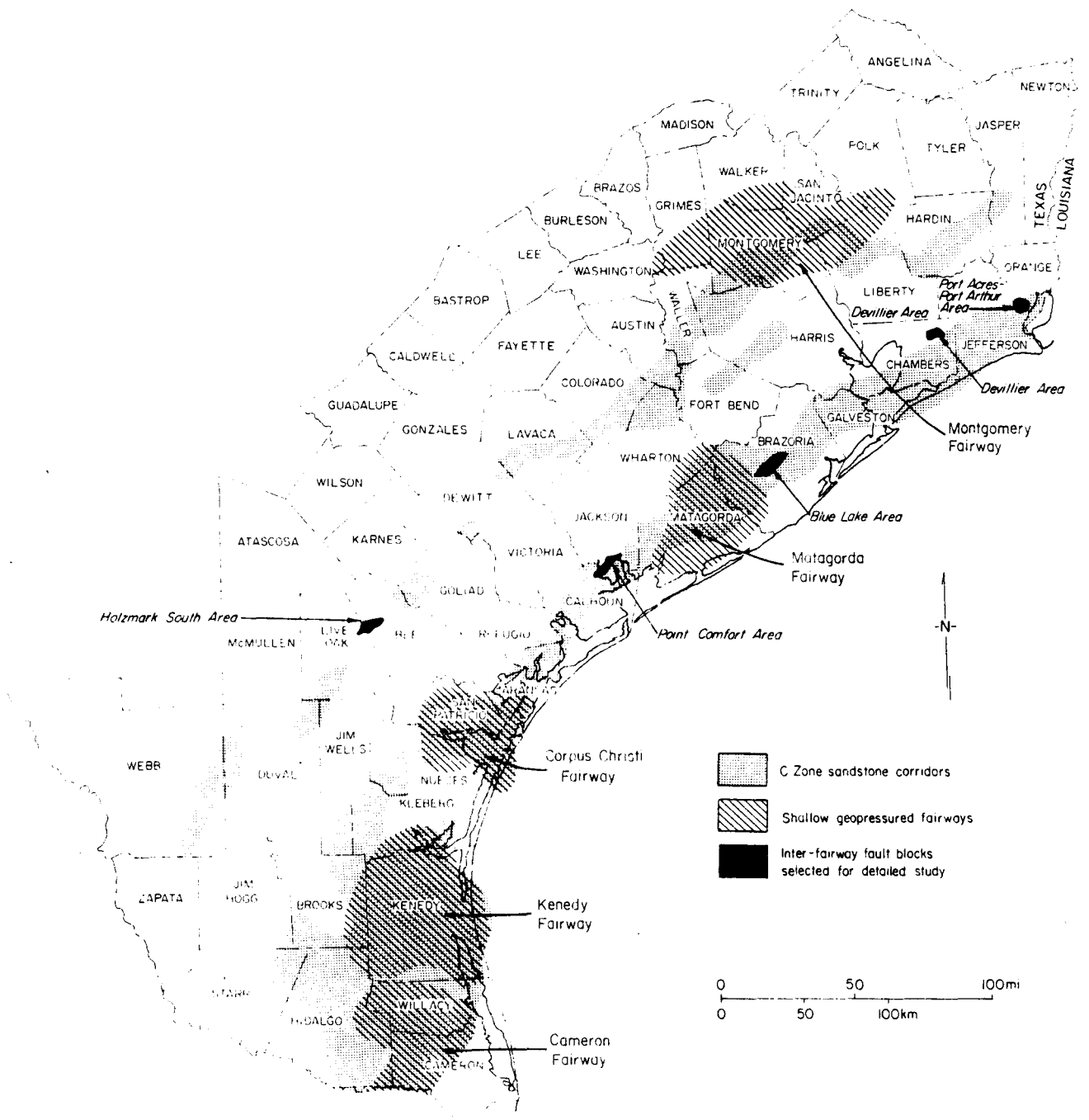
Figure 4. Fault blocks selected for detailed study along C Zone sandstone corridors between fairways (from Weise and others, 1981b).

7

4. Multiple prospective sands are preferred, but one thick sand with a gas cap or a thin gas sand associated with a thick aquifer having good lateral continuity should be adequate.

5. Approximate minimum thickness of the sand should be 5 ft of gas sand associated with a 40-ft-thick aquifer.

6. Formation pressures of abandoned gas reservoirs may vary from less than 0.3 psi/ft to more than 0.7 psi/ft. Normally, gas reservoirs with high pressure gradients are not abandoned without good reason; therefore, mechanical problems, sand or shale production, casing partings, and other production problems should be noted. These problems do not necessarily detract from the value of the prospect. High abandonment pressure means that more gas remains in the reservoir and increases the value of the prospect.

7. High temperature increases the methane solubility in formation water and adds to the value of the prospect. A temperature of 200°F $\pm$ 15°F may be considered a practical lower limit for producing unconventional gas from hydropressured reservoirs in Texas.

8. Permeability, which is particularly important for the aquifer because large volumes of water must be produced at high rates, should be at least 20 md. High porosity (20 percent) may or may not indicate good permeability.

9. Low salinity increases methane solubility in formation water and adds to the value of the prospect. Salinities below 100,000 ppm NaCl are preferred. Water samples recovered from the formation by an approved technique and analyzed for total dissolved solids give the most credible values of salinity. The SP well log is less credible but often is the only alternative for estimating salinity.

10. Existing seismic lines located in or near the field are very desirable. It is also desirable that some wells in the field have sonic and/or density logs as well as induction logs. A very good prospect should have strike and dip seismic lines and sonic and density logs for at least four wells in the field.

It is emphasized that these guidelines are not strict criteria. Most likely no field would meet all requirements, and compromises must be made.

Screening of Gas Fields

Numerous gas fields in the Frio/Vicksburg and Wilcox sandstone trends were screened initially. Attention was given to reservoirs in wells that were listed by Doherty (1981) as (1) watered-out geopressured gas cap wells (pressure gradient greater than 0.65 psi/ft), (2) wells

that lacked shut-in pressure data but had high water-production rates, and (3) rejected wells that had pressure gradients between 0.60 and 0.65 psi/ft. Many fields were rejected in the initial screening if factors such as too small an area or large numbers of wells actively producing could be readily determined. Fields that showed some potential in the initial evaluation or that needed more specific work to determine field area or production status were referred to a special study group for additional evaluation and determination of less readily available information. This information consisted of data on permeability, porosity, salinity, methane solubility, pressure and production history, and sandstone continuity, and seismic data and sonic and density logs.

Reservoir evaluation checklists (example in table 1) were prepared for individual wells in selected fields. After final evaluation of a field, favorable and unfavorable factors and a recommendation were given on a short form (table 2). The potential prospects were then classified in three categories: (1) a class A field is most favorable for a dispersed gas test area; (2) class B fields have marginal potential or lack certain data needed for full evaluation; and (3) class C fields were rejected.

Selection of Potential Test Areas

Class A Field

Screening of gas fields along the Frio/Vicksburg and Wilcox sandstone trends resulted in the selection of the Port Arthur field, Jefferson County, Texas, as the most favorable test area. The short form evaluation sheet (table 2) lists both its favorable and its unfavorable characteristics. The favorable features clearly predominate, making the Port Arthur field the only prime prospect (class A).

Class B Fields

Two fields with some attractive characteristics were classified as class B but are thought to have less potential than class A fields because of negative features such as small area, active production, shaly sands, and low permeability. The class B fields are Port Acres field, Jefferson County, Texas, and Algoa field, Brazoria and Galveston Counties, Texas. Evaluation sheets (appendix A, tables A1 and A2) summarize the favorable and unfavorable features of these fields.

The Port Acres field previously produced gas condensate primarily from a single interval (10,350 to 10,600 ft) in the lower Hackberry (Frio) sandstone units. Sandstone thickness in the producing interval varies from 30 to 120 ft. Porosity is high (28 to 35 percent), and permeability ranges from 5 to 1,000 md. Most wells have been plugged and abandoned.

Table 1. Example of Reservoir Evaluation Checklist.

(1) Name of operator

Meredith and Co.

(2) Well no. and name

#2 W. Doornbos (well #14)

(3) County

Jefferson

(4) Tobin Grid

1S-49E-4

(5) Located in gas field

Field name
Active gas well
Inactive (P & A), date
Inactive (shut-in), date

Yes X   No

Port Arthur
No
10/72

(6) Total depth
12,200   ft

(7) SS thickness

63   ft

(8) SS interval (ft)

Upper 11,117   Lower 11,160

(9) Perforation depths
"C" sandstone

11,136-11,144   ft

(10) Porosity
Whole core
SWC
Computed
(Identify method used)

_____ %

34.8 (average)
23
$F=0.62/\phi^{2.15}$ (HUMBLE)

(11) Permeability_____ md
Whole core _____
SWC   218 (avg)
BU/DD tests_____
Other   _____

(12) List types of logs available: induction   X   sonic _____
                                      SP   .   X   density _____
                                      gamma ray _____   other _____
                                                                        (identify)

(13) Temperature at reservoir depth:

Well bore temp.   210   °F   Annual mean
Equilibrium temp.   243   °F   surface temp. 70   °F
Temp. gradient   1.55   °F/100 ft

Table 1. continued

(14) Fluid pressure in reservoir

   a. Well head shut-in pressure (WHSIP)

      Initial _7593_ psig

      Last _3215_ psig

   b. Bottom-hole shut-in pressure (BHSIP)

      DST _9284_ psig

      Avg. perf. depth _11,140_ ft

      Gradient _0.833_ psi/ft

   c. Bottom-hole static pressure

      Computed from WHSIP _9,166 (initial) psig; 4,211 psig (last)_

(15) Salinity of formation water

      From SP _32,000_ ppm, NaCl

      R_{mf} method _80,000_ Mud type _Lime-base oil emulsion_

      Total solids from water analysis _not available_ ppm NaCl

(16) Methane solubility _26.7_ SCF/bbl

(17) a. Formation resistivity factor _14.66_ ($F = R_0/R_w = \dfrac{0.48}{0.033}$)

    b. Water resistivity (from SP) _0.033_ ohm-m; Res. Index (I) _6.94_ .

$$(I = R_t/R_0 = \frac{3.33}{0.48})$$

(18) Cumulative gas produced _12,362_ MMscf

    Years of production _July 1961 through July 1972_

(19) Last production date _July 1972_

(20) Gas gravity _0.67 (separator)_

(21) Gas compressibility factor (Z) _0.855 (last)_

Table 1. continued

(22) Free gas & water saturations S_w _32%_ S_g _68%_

Any oil in reservoir? _Condensate_ GOR _--_ SCF/bbl

Irreducible water saturation (S_{wirr}) _--_

(23) Water production - last rate reported _--_ bbl/day

- cumulative _--_ ·bbl

(24) Area of reservoir _5.1**_ mi^2

(25) Original free gas in-place ("C" reservoir) _56.2_ Bscf

(26) Primary gas produced _10.535_ Bscf

(27) Predicted gas recovery _5.1*_ Bscf

(28) BHP/Z at abandonment _4,925_ psia

(29) Seismic data in area Yes _X_ No _____

(30) Sonic logs in area Yes _X_ No _____

How many? _one_

*Value predicted for "C" reservoir by reservoir simulator for natural flow conditions.

**Drainage area for "C" reservoir calculated from pressure buildup test data.

Table 2. Example of Evaluation of Gas Fields.

(Short form)

Field name: <u>Port Arthur, 59 Hackberry sands, Frio (10,850-11,700 ft)</u>

Location: <u>Jefferson County, Texas 1S-49E</u>

Favorable Criteria:

1. <u>15 watered-out gas-distillate wells, no active wells in field</u>

2. <u>Multiple watered-out gas sands</u>

3. <u>Multiple thick aquifers: 30-150 ft</u>

4. <u>Abandonment pressure gradients: 0.4-0.74 psi/ft</u>

5. <u>Temp: 200°F, Porosity: 25-35%, Perm: 60-300 md</u>

6. <u>Recent (1973-1979) seismic lines in or near field</u>

7. <u>Pertinent geological and engineering data have been published</u>

Unfavorable Criteria:

1. <u>Productive area: 3 mi^2 (1,900 acres)</u>

2. <u>Possible sand and shale production problems</u>

3. <u>Only two sonic logs run in field (one available)</u>

4. <u>Salinity averages 90,400 ppm NaCl</u>

5. _____

6. _____

Recommendation:

<u>Favorable, because of multiple thick aquifers and watered-out gas sands</u>

<u>with excellent reservoir properties. All wells in field have been plugged</u>

<u>and abandoned, and all or most leases have expired. Some gas reservoirs</u>

<u>remain geopressured, and some aquifers appear to be geopressured. This is</u>

<u>considered to be a prime prospect and is rated as class A.</u>

13

Pressures recorded before abandonment were low. The field might be considered a viable hydropressured prospect, but the economics are questionable.

The Algoa field produces gas from the Frio 37 sandstone in the depth interval from 10,350 to 10,750 ft. The target sandstone is 150 to 300 ft thick, including gas cap and aquifer. There are five active wells in the field; three are recent completions. Core data are unavailable. Pressure gradients are low, but the reservoir might become a viable hydropressured prospect at some later date when the active wells are abandoned.

Both Algoa and Port Acres fields are definitely less favorable prospects than Port Arthur field. Considerable additional work would be required to evaluate their producibility and economic potential.

Class C Fields

Short form evaluation sheets have been prepared for eight gas fields that were previously considered candidates for the more favorable class B rating (appendix B, tables B1-B8). Further investigation showed that these fields were not good prospects. The most common unfavorable criteria are (1) active wells in target reservoir interval, (2) shaly sandstones, (3) poor aquifers, (4) presence of oil, (5) small area, (6) no core data, and (7) low porosity and permeability. Only the Lake Creek field, Montgomery County, Texas, might be upgraded to class B in the future when active production diminishes or ceases. Available core data for one well (Prairie Producing Company no. 1 E. G. Frost) in the Lake Creek area show high permeabilities (up to 1,050 md) in the perforated interval from 11,558 to 11,575 ft. A second interval from 11,269 to 11,297 ft has a maximum permeability of 10.2 md. Bottom-hole pressures are very low in this well. Although the sandstone bodies are 80 to 100 ft thick, the permeable zones are thin and their lateral extent is unknown. In general, permeabilities in the Lake Creek area are very low. Appendix B also lists 134 class C gas fields that were rejected as prospects because of unfavorable criteria (table B9). This list does not include the large number of fields rejected during the initial screening.

Many gas fields were rejected as prospects because they contained active gas-producing wells. Gas production in these fields will eventually decline as wells water out and are abandoned by the operators. When all wells that produce from a target reservoir are abandoned, the field may need to be reevaluated as a candidate for secondary gas recovery. If operators of active wells cooperate, some of these gas fields could become good prospects for secondary gas recovery before they water out.

14

STUDIES OF THE PORT ARTHUR AREA

Regional Geological Setting

The Frio Formation is one of the major clastic, progradational units of the Texas Gulf Coast (Galloway and others, 1982). Two large delta systems, the Norias in South Texas and the Houston in East Texas, prograded more than 60 mi basinward of the previous continental margin, causing the development of large regional growth fault systems and stimulating salt diapirism. Barrier-bar and strandplain systems extended both between the main deltas (the Greta-Carancahua system) and east of the Houston delta into Louisiana (the Buna system).

Shale and sandstone of the Hackberry member of the Frio Formation form a seaward-thickening wedge within the normal Frio marine succession in southeast Texas and southwestern Louisiana (fig. 5). The wedge pinches out to the north along a line which Bornhauser (1960) termed the "Hartburg flexure." The term "Hackberry" was first used for the bathyal (deep-water) foraminiferal assemblage at Hackberry salt dome in Louisiana by Garrett (1938) but was later generalized to refer to a member and/or facies of the Frio by Bornhauser (1960) and Paine (1968).

In most areas the lower Hackberry is a sand-rich unit that fills channels eroded up to 800 ft into the pre-Hackberry sediments. Previous studies have indicated that these sands were deposited in a submarine canyon-fan environment (Paine, 1968; Berg and Powers, 1980). A more uniformly distributed seaward-thickening wedge of shale overlies the lower Hackberry sands; it grades upward into upper Frio sediments of shallow-water origin. The lower Hackberry sands are significant oil and gas reservoirs in the area; exploration for deeper geopressured gas fields is currently active.

No adequate regional structural and stratigraphic study of the Hackberry in southeast Texas has been published. Thus, the location of the major submarine channels, the geometries of the sandstone bodies, and the evolution of the Hackberry depositional system are incompletely known. Reedy (1949) studied the Frio Formation in the area. Berg and Powers (1980) examined cores from two wells in Jefferson County.

The Port Arthur field and surrounding area was studied to achieve a better understanding of the regional geology. This area extends from the updip limit of the Hackberry wedge to the downdip limit of well control in Jefferson County, Orange County, and the adjacent parts of Louisiana. More than 220 logs of deep wells were obtained and correlated. Paleontological data were extensively used and assisted in picking the basal Hackberry unconformity and defining the lower Frio and Vicksburg units. Six seismic sections were interpreted to assist in determining structure and channel distribution downdip of the Port Arthur field. The
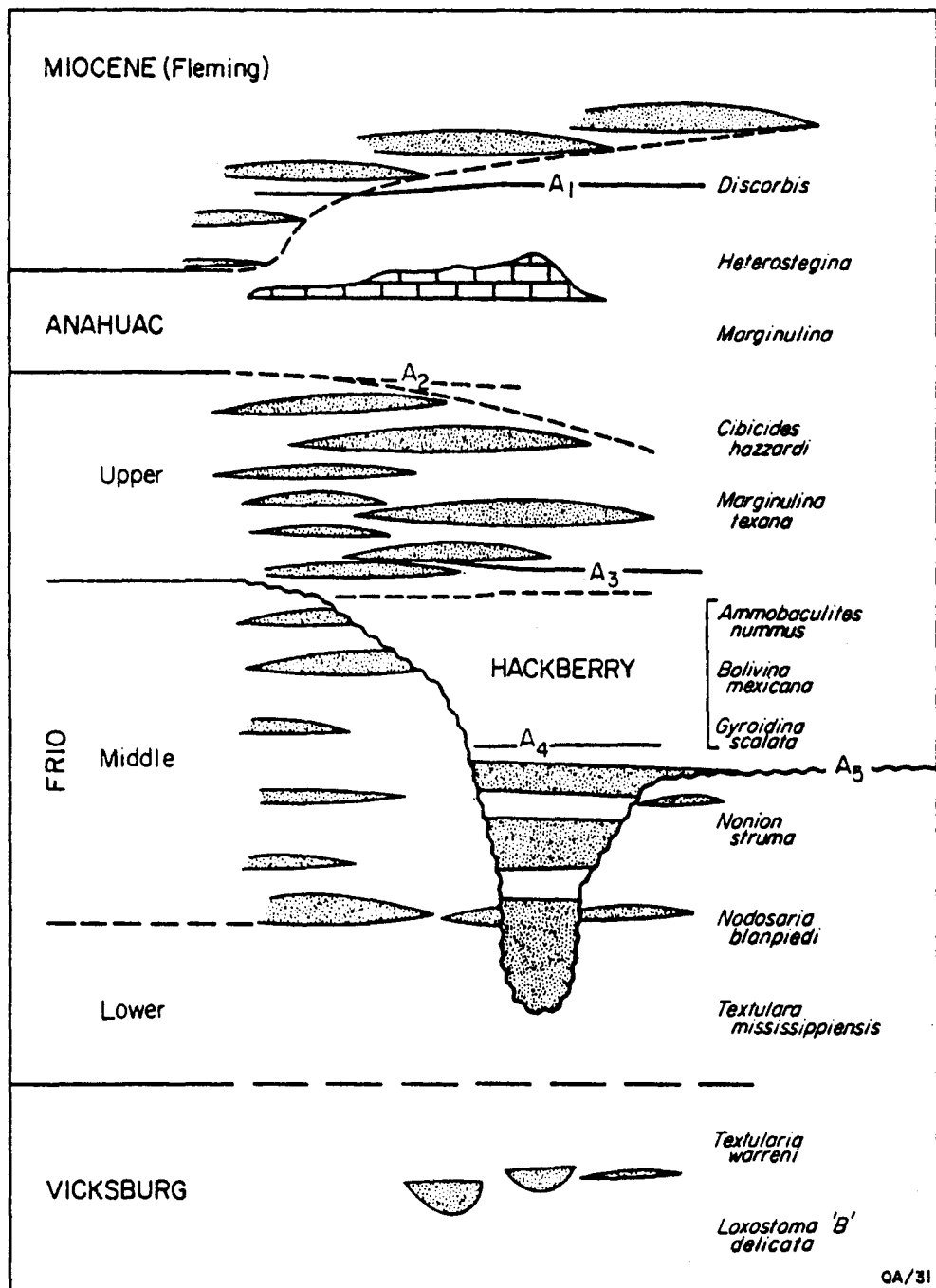
Figure 5. Stratigraphic diagram of Tertiary strata, paleontologic markers, diagrammatic sand-body distribution (stippled), and marker horizons, Jefferson County area.

16

information from seismic sections and well logs was merged to produce structural and net-sandstone maps of the study area. In addition, the well logs in Port Arthur field were studied to evaluate sand-body geometry, depositional setting, and continuity.

Frio Stratigraphy

The Frio Formation in the Port Arthur area ranges from approximately 2,000 ft to 6,000 ft thick; thickness increases basinward. In the updip portion of the area the Frio consists of stacked barrier-bar and strandplain sandstones of the Buna barrier system. Downdip the sands become less dominant, except within the deep-water sand-shale wedge of the Hackberry.

The Frio can be divided into three units (fig. 5). The lower unit (between the top of the Vicksburg at Textularia warreni and Nodosaria blanpiedi) is very thin and sand-poor and is distinguished only with difficulty from the underlying Vicksburg. The middle unit (from Nodosaria blanpiedi to about Marginulina texana) contains abundant sand updip but only a few discontinuous sands of undetermined origin downdip; this unit is extensively eroded at the pre-Hackberry unconformity, so that original thickness and geometry are difficult to determine. The Hackberry wedge lies between Nonion struma and Marginulina texana, that is, upper-middle Frio. The upper Frio consists of nearly continuous sand updip and alternating sand and shale downdip. These sands contain upward-coarsening cycles, are continuous along strike, but shale out fairly rapidly downdip and are inferred to represent barrier-bar and/or strandplain sand bodies. The upper Frio barrier system prograded with time, capping the deep-water Hackberry shale.

Within the downdip parts of the study area no units below the pre-Hackberry unconformity can be correlated in enough wells to reliably determine their structural configuration. Furthermore, the seismic data are not of good enough quality to determine the deep structures. Therefore, correlation markers A1 through A5 range from the top of the Anahuac to the pre-Hackberry unconformity (fig. 5). Progradation of the upper Frio and lower Miocene sand bodies is indicated as their respective correlation markers pass basinward from sand to shale sequences. Markers A1 through A3 subdivide shallow-water deposits, whereas A4 to A5 subdivide deep-water strata of the Hackberry member.

THE PORT ARTHUR FIELD

Geology

The Port Arthur field is located in east-central Jefferson County immediately northwest of the town of Port Arthur (fig. 6). The field is adjacent to the Port Acres field on the west;

17
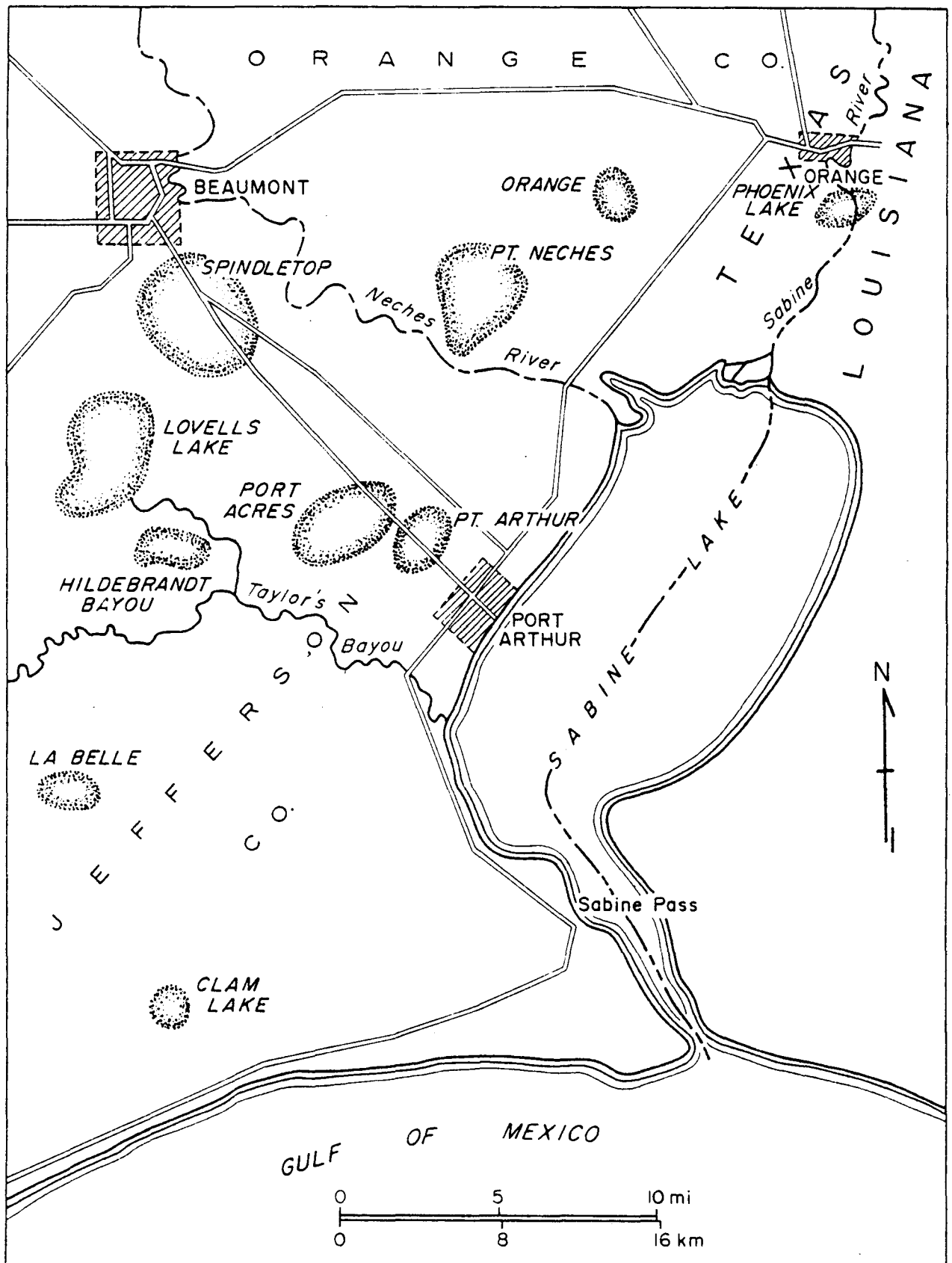
Figure 6. Map showing location of Port Arthur field and nearby fields (after Halbouty and Barber, 1961).

18

the two fields are separated by a major fault (fig. 7). The major sandstone deposits and productive area of the Port Arthur field cover about 1,900 acres (3 mi^2). Prior to abandonment, the field produced gas and condensate from lower Hackberry (Frio) sandstones that are interpreted as submarine fan deposits (Bornhauser, 1960; Paine, 1968; Berg and Powers, 1980). The Nodosaria sandstone and the Vicksburg Formation also produced gas in this field. The structure of the field is dominated by a northeast-trending anticline caused by the rollover into the major fault separating the Port Arthur and Port Acres fields (Weise and others, 1981b) (figs. 8 and 9). Closure on the structure is about 100 ft in all directions, but structure to the east is uncertain because of sparse well control.

The lower Hackberry sands are lenticular and range in thickness from a few feet to more than 150 ft. Some individual sandstones were correlated within the field, but cannot be correlated beyond the field area. The sandstones are thickest in relatively narrow, dip-aligned bands or channels (figs. 10 and 11); these geometries are consistent with a submarine-fan system. The channels contain massive sandstones with blocky SP patterns.

The field operators divided the lower Hackberry interval into 14 individual reservoirs (fig. 12). Log patterns for the six major reservoirs were studied to help determine the component depositional facies in the units. These patterns can be interpreted using the submarine-fan facies model by Walker (1979) (fig. 13).

The "H" sandstone is present in only six wells and does not produce hydrocarbons. It rests directly on the pre-Hackberry unconformity, filling a channel up to 6,000 ft wide. The "H" sandstone displays an SP pattern characteristic of confined channel-fill deposits. These deposits are massive, blocky sandstones with few shale partings. The axis of the channel has the thickest sand with no shale partings and an abrupt change in SP response from the overlying and underlying shale sections.

The "G" sandstone produced gas and condensate in the depth interval from 11,458 to 11,463 ft in Well 31. Log patterns for this sandstone indicate broad channel-fill deposits with some fan-plain overbank deposits (fig. 14). The SP curves for Wells 6, 30, and 31 show a blocky pattern with no shale partings. Progradation at the base of the sand suggests that the wells are located near the edge of the channel. Well 14, by contrast, has a blocky SP pattern with an abrupt change in SP response from the overlying and underlying shale sections, which suggests that the well is closer to the center or axis of the channel. Wells 12, 36, and 28 have generally blocky SP patterns but with more frequent shale partings than the confined-channel "H" sand, indicating broad channel-fill deposits. SP curves for Wells 11, 23, and 29 are inferred to be fan-plain overbank deposits, containing 2- to 10-ft-thick turbidite sandstones with interbedded shales.

19
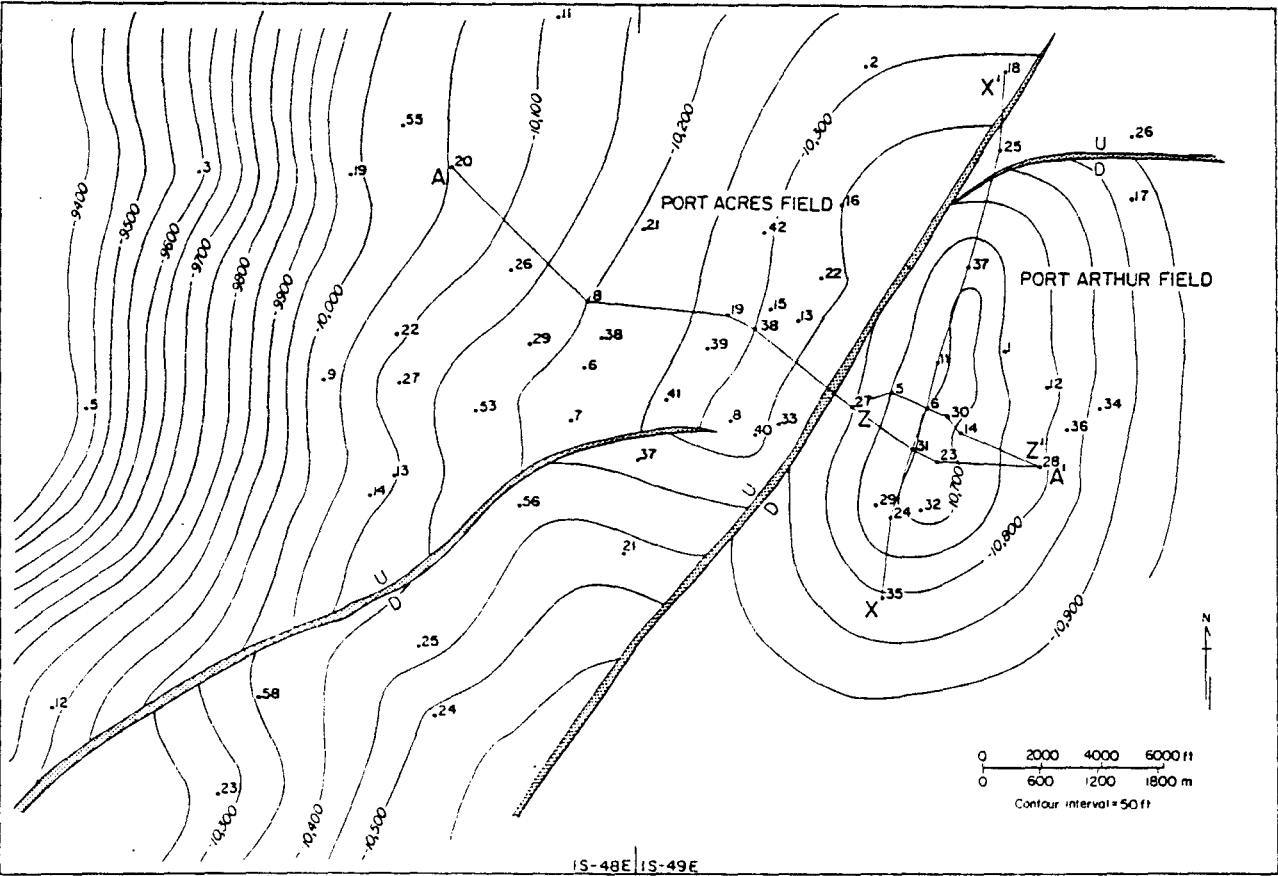
Figure 7. Well locations, lines of cross section, and structure on top of the lower Hackberry, Port Arthur - Port Acres area.

20
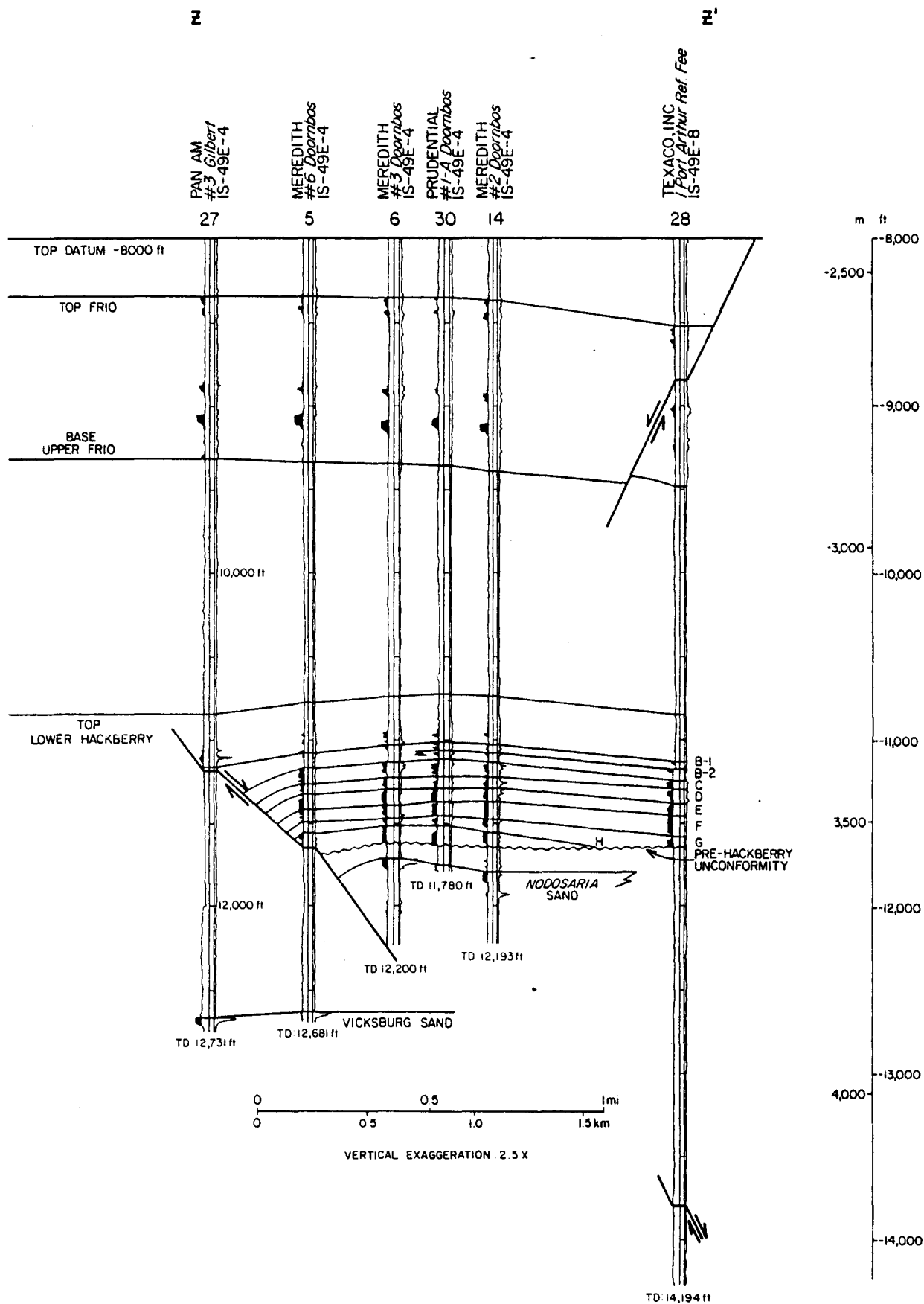
Figure 8. Structural dip section Z-Z', Port Arthur field. The field lies within a rollover anticline basinward of a regional fault. Sandstones are shaded.
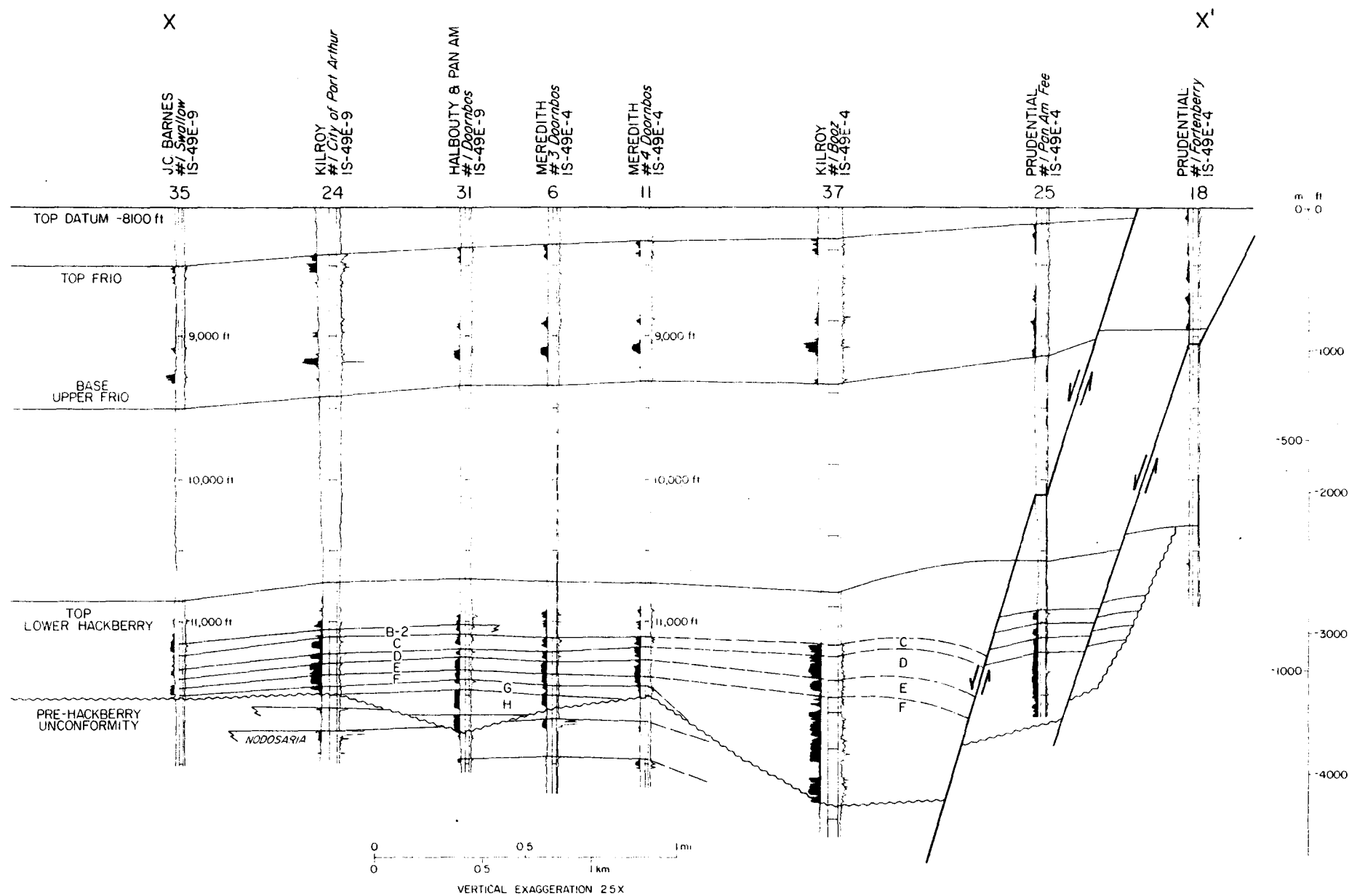
Figure 9. Structural strike section X-X', Port Arthur field. Note the channelling of the "F," "G," and "H" sands into the basal unconformity and rollover into the regional fault. Sandstones are shaded.

22

Figure 10. Structural dip section A-A', Port Arthur – Port Acres area (from Weise and others, 1981b).

23
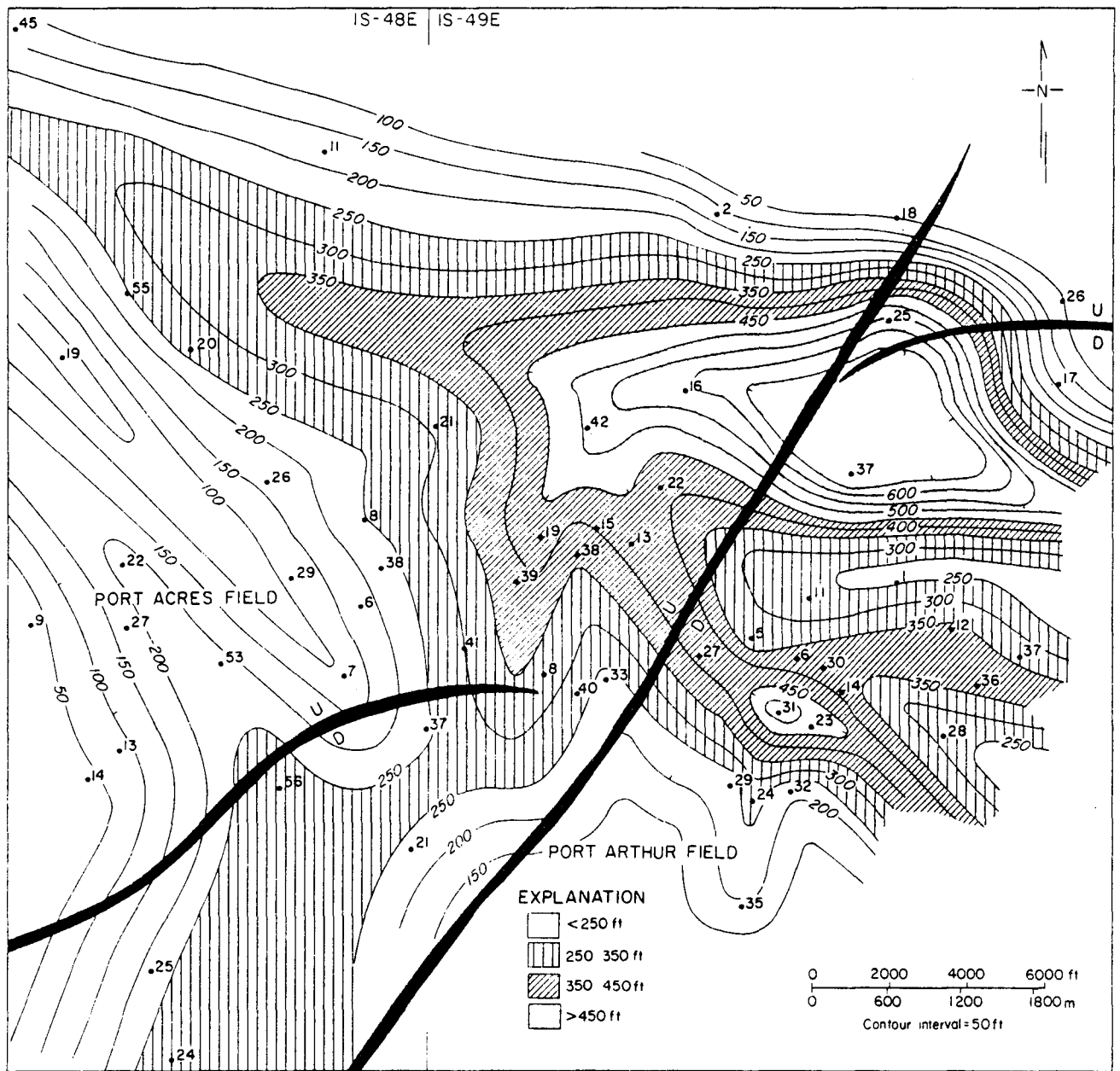
Figure 11. Net sandstone map of the lower Hackberry, Port Arthur - Port Acres area.
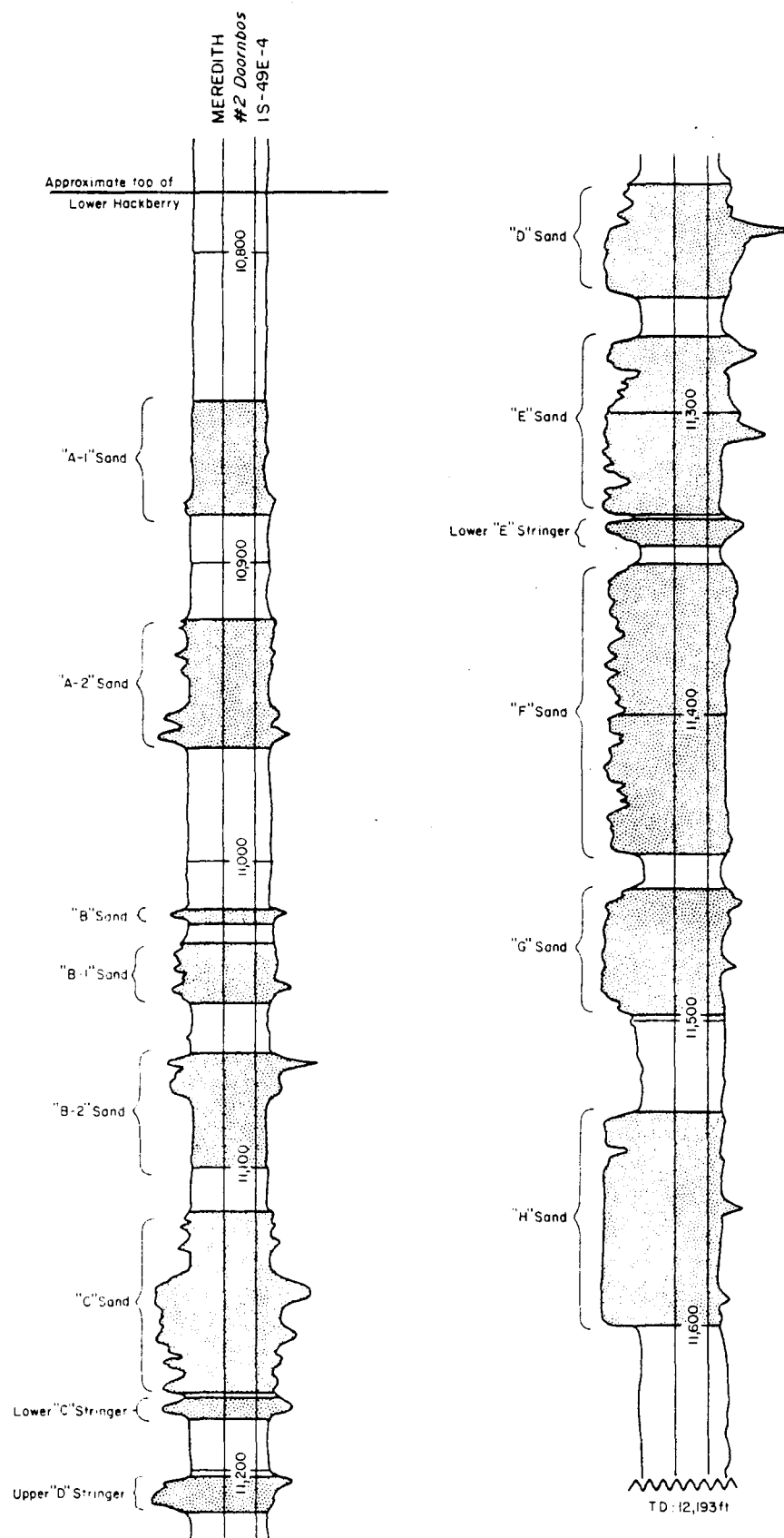
Figure 12. Type log showing reservoir intervals, Port Arthur field. The well is No. 14 on cross section Z-Z', figures 7 and 11 (from Weise and others, 1981b).

(confined)
FEEDER CHANNEL

Upward fining

Upward coarsening

Slope into basin

(35C)

Fan plain

Broad fan channel

(IC)

(34F)

(confined)
Incised channel

Suprafan lobes

Proximal
suprafan

(34C)

Intermediate
suprafan

New suprafan lobe

Modified from Walker (1979)

QA-221
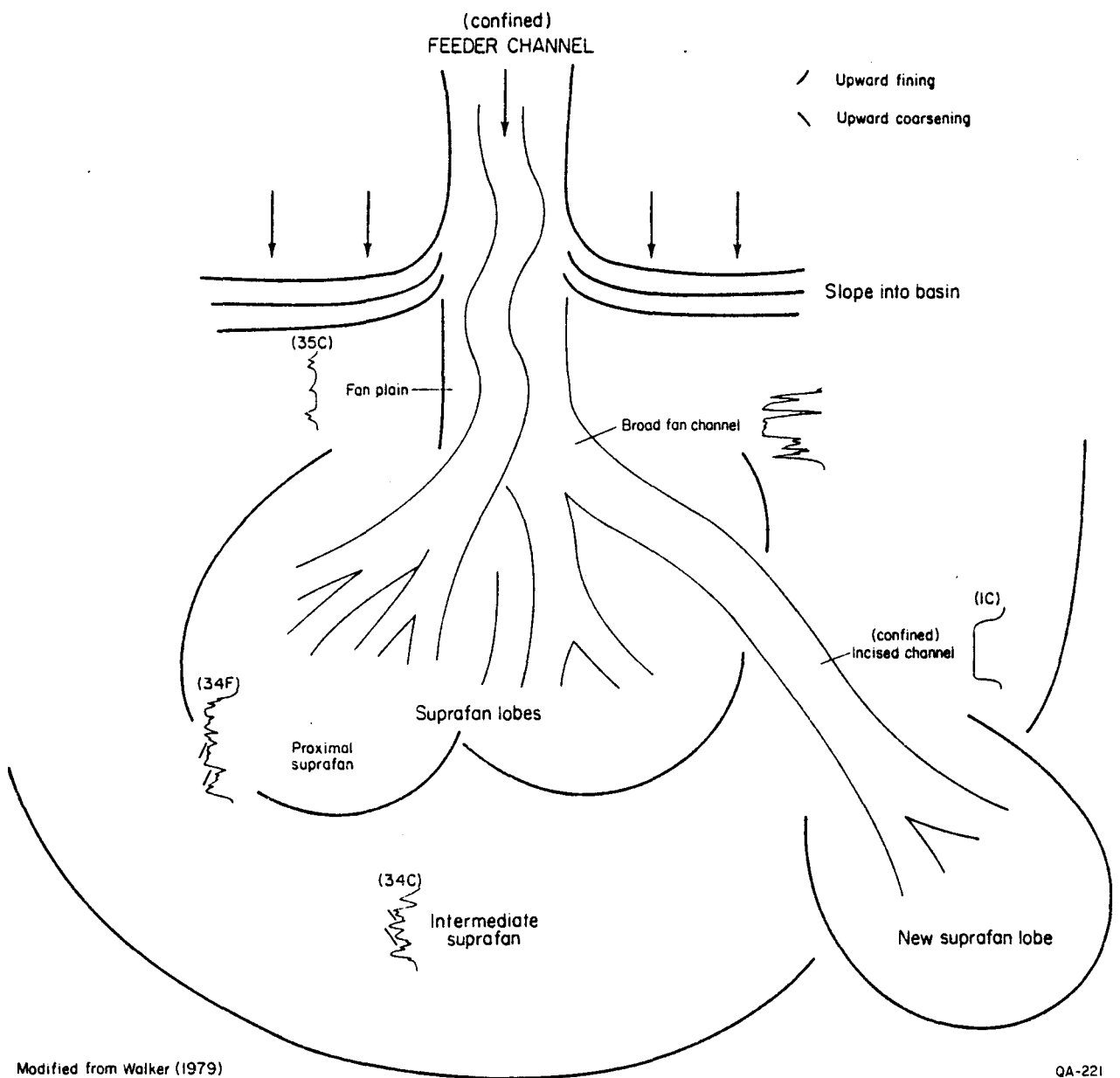
Figure 13. Submarine fan facies model with SP curves, Port Arthur field.

26
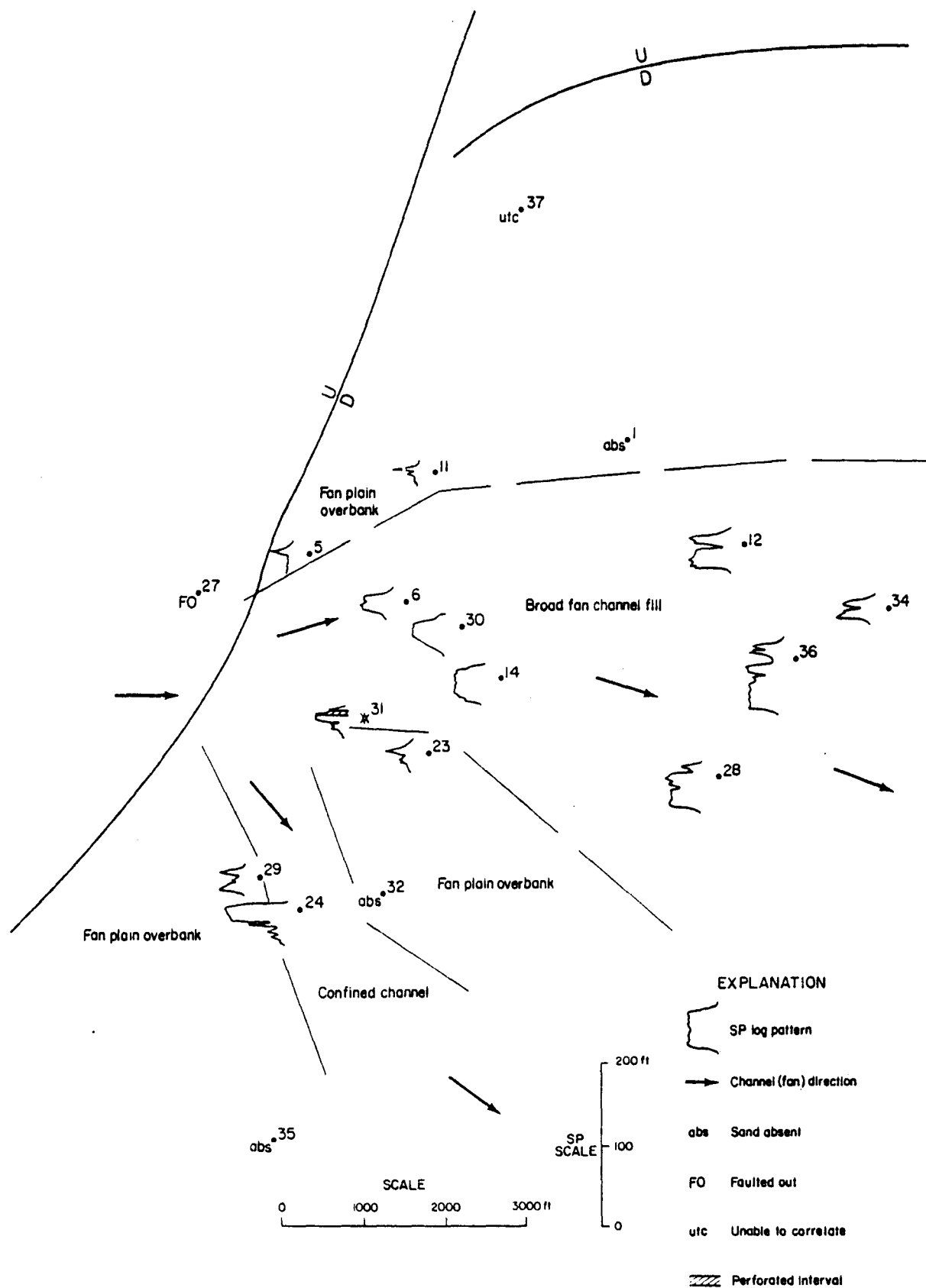
Figure 14. Distribution and log character of the "G" sandstone, Port Arthur field.

Well 14 produced gas and condensate from the "F" sandstone in the depth interval from 11,350 to 11,359 ft. The SP curve for the "F" sandstone in most of the wells is a serrated blocky pattern with an upward-fining pattern in some wells, indicating slight aggradation (fig. 15). This pattern is common to the proximal suprafan and is best seen in Wells 1, 12, 34, and 36. Wells 24, 29, and 32 have a blocky SP pattern indicative of broad fan channel-fill deposits. The SP curve for Well 35 is very blocky and shows a new confined channel developed at the southern end of the field.

Wells 6, 14, and 23 produced gas and condensate from the "E" sandstone in the depth interval from 11,276 to 11,301 ft. The "E" sandstone also shows serrate blocky patterns characteristic of broad fan channel-fill deposits. On the northeast side of the field, however, SP curves for Wells 1, 12, and 36 show that a younger confined fan channel cut through the field.

The "C" and "D" sandstones have SP curves characteristic of all the facies of the submarine-fan model as shown for the "C" sandstone on figure 16. The blocky shape of the SP curve with sharp upper and lower contacts for Well 1 is characteristic of a confined fan channel-fill deposit. Wells 12, 24, 29, and 32 are good examples of broad fan channel-fill deposits characterized by blocky SP patterns and thin shale partings. Wells 5, 6, 23, 30, and 31 are also broad fan channel-fill deposits showing irregular SP patterns. At the top of the section in Well 14, the SP pattern indicates a possible thin channel-fill deposit. At the base of the section the alternating thin sand-shale deposits suggest an overbank sequence. The SP curve for Well 11 has an overall blocky pattern with thin shale partings and characteristics indicating deposition in a proximal suprafan environment. Intermediate suprafan deposits are seen in Well 34. The SP curve is highly serrated, with SP deflections suggesting progradation (W. E. Galloway, personal communication, 1982). Finally, Well 35 has an SP curve characteristic of fan-plain overbank deposits: thin sandstones with thick interbedded shales. The "C" and "D" sandstones produce gas and condensate from numerous wells in the depth range from 11,128 to 11,257 ft.

The overlying "A-1," "A-2," "B," "B-1," and "B-2" reservoirs all appear to be thin turbidite sandstones with a few thin, scattered channel deposits. The lower "C," upper "D," and lower "E" sandstone stringers are similar to "A" and "B" sandstones.

The SP log patterns of the lower Hackberry sandstones clearly indicate deposition within a submarine-fan environment. An upward decrease in average channel-sand thickness suggests that the depth of scour decreased with time. In addition, the lateral continuity across the channel complex is greatest at the "C" sandstone level, decreasing downward. The "C" sandstone is the only sand that is easily correlatable with Well 37 north of the field.

28
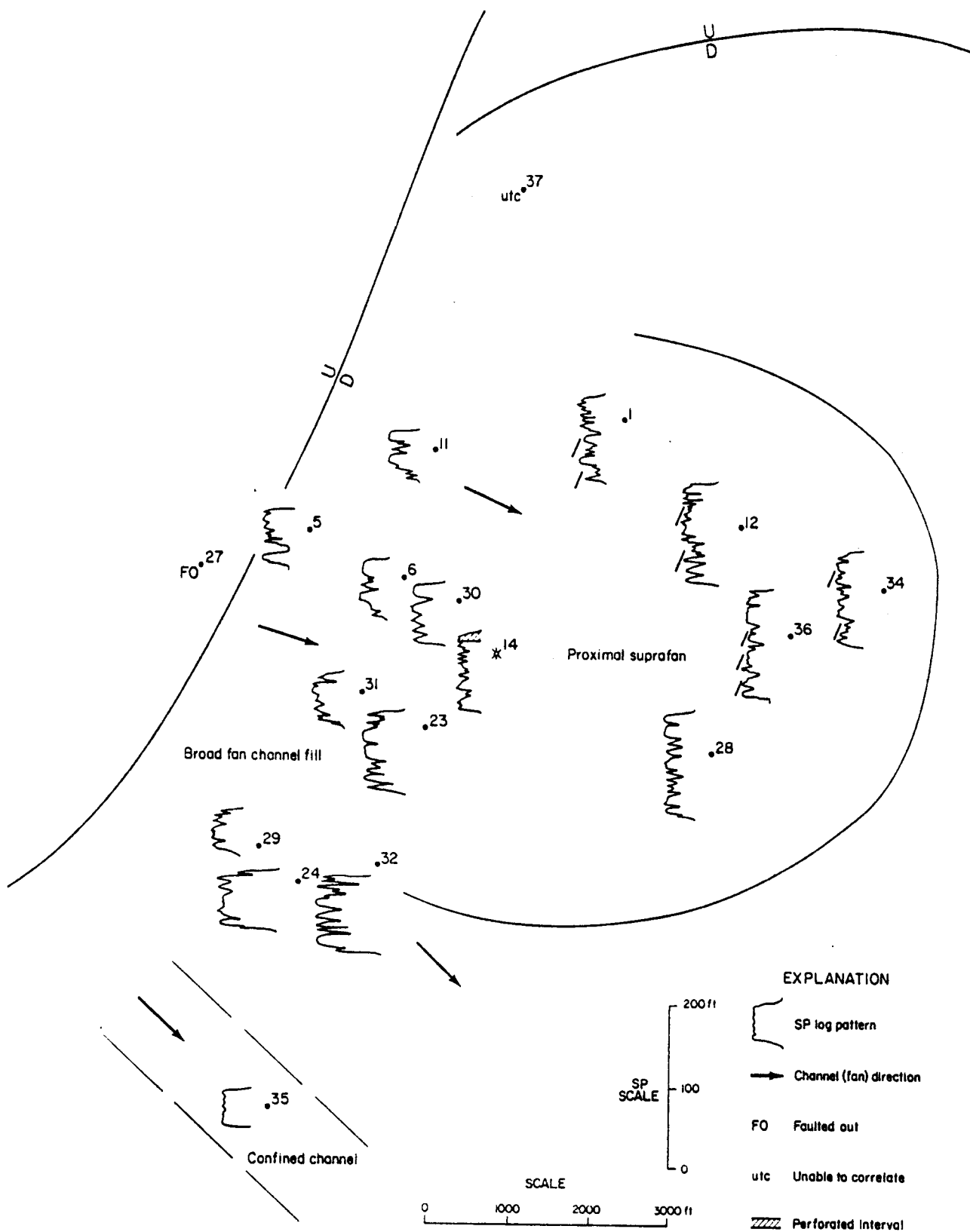
Figure 15. Distribution and log character of the "F" sandstone, Port Arthur field.
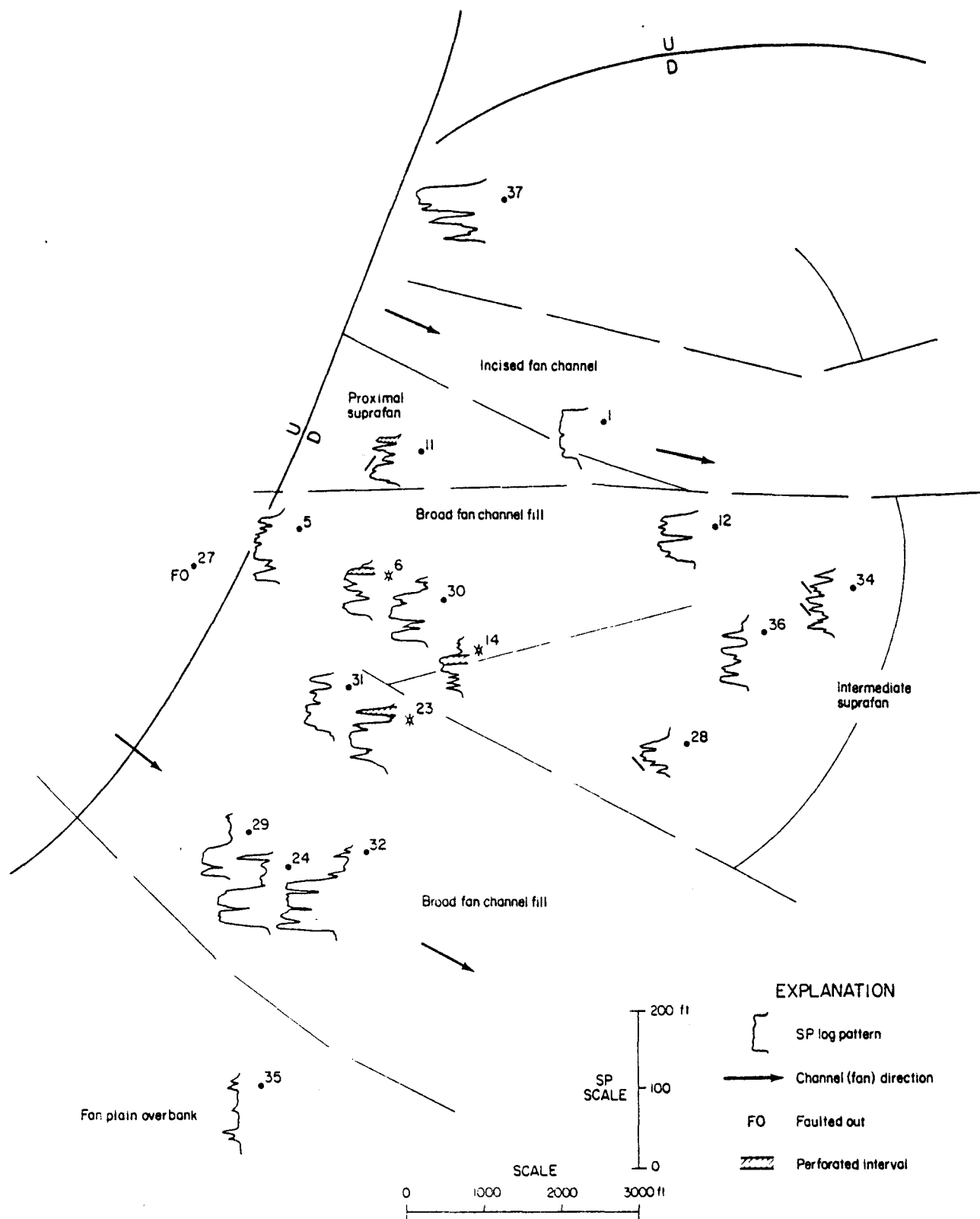
Figure 16. Distribution and log character of the "C" sandstone, Port Arthur field.

The geometry of the submarine channels and the succession of facies in the Port Arthur field suggest that the lower Hackberry unit formed as an aggrading submarine fan/channel sequence (fig. 17). The initial canyons were cut during headward erosion of the channels into the flank of the Buna strandplain/barrier-bar sand system and underlying muds. The channel at Port Arthur was first filled by a thick, coarse confined channel sand ("H" sandstone) representing the head of the fan complex; deposition of the sandstone may have been by grain flows and laminar flows as well as by proximal turbidity currents. As the fan aggraded, these deposits were overlain by proximal channel-fan deposits ("D," "E," and "F" sandstones). These sands occupied a broader valley in which broad-channel, proximal-fan, and overbank deposits were preserved. At about this stage, the secondary or crossover channels formed and were filled by confined fan-channel sands. Further aggradation of the fan led to the deposition of thinner, complex sand bodies ("B" and "C" sandstones), which include thin channels and suprafan deposits. Final deposition was either from turbidity currents of the distal fan or from suspension; these sediments form the upper Hackberry shale sequence.

Structure and Gas Production, Lower Hackberry Interval

The structure of the Port Arthur field is an anticline caused by rollover into a major fault (Weise and others, 1981b). Structure maps and net-sand isopach maps were constructed for the various Hackberry sands in the Port Arthur field, as was a structure map of the top of the pre-Hackberry unconformity. The pre-Hackberry unconformity and the various sands are discussed below in chronological order.

The structure map of the pre-Hackberry unconformity shows the effect of the canyon-cutting episode that preceded Hackberry deposition (fig. 18). Wells 23 and 31 are located near the axis of a canyon on the west side of the field. A major canyon occurs at and north of Well 37 along the northern fault (fig. 11). Wells 5, 6, 14, 29, and 30 are on the flanks of this canyon. There is a minor channel on the east side of the field, with an axis near Wells 34 and 36. Another small channel is at the south end of the field.

Comparison of the isopach map of the "H" sandstone (fig. 19) with the structure map of the pre-Hackberry unconformity shows that the "H" sandstone was deposited as a confined channel-fill deposit in the submarine canyon located on the west side of the field. Wells 23 and 31 penetrated the thickest sand interval due to their position near the axis of the canyon. The structure of the "H" sandstone is controlled by a north-south-trending anticline on strike with the major growth faults on the west (fig. 20).

The thickness and structure of the "G" sandstone are similar to those of the "H" sandstone. Deposition of the "G" sandstone, a broad fan channel-fill deposit, was concentrated

31
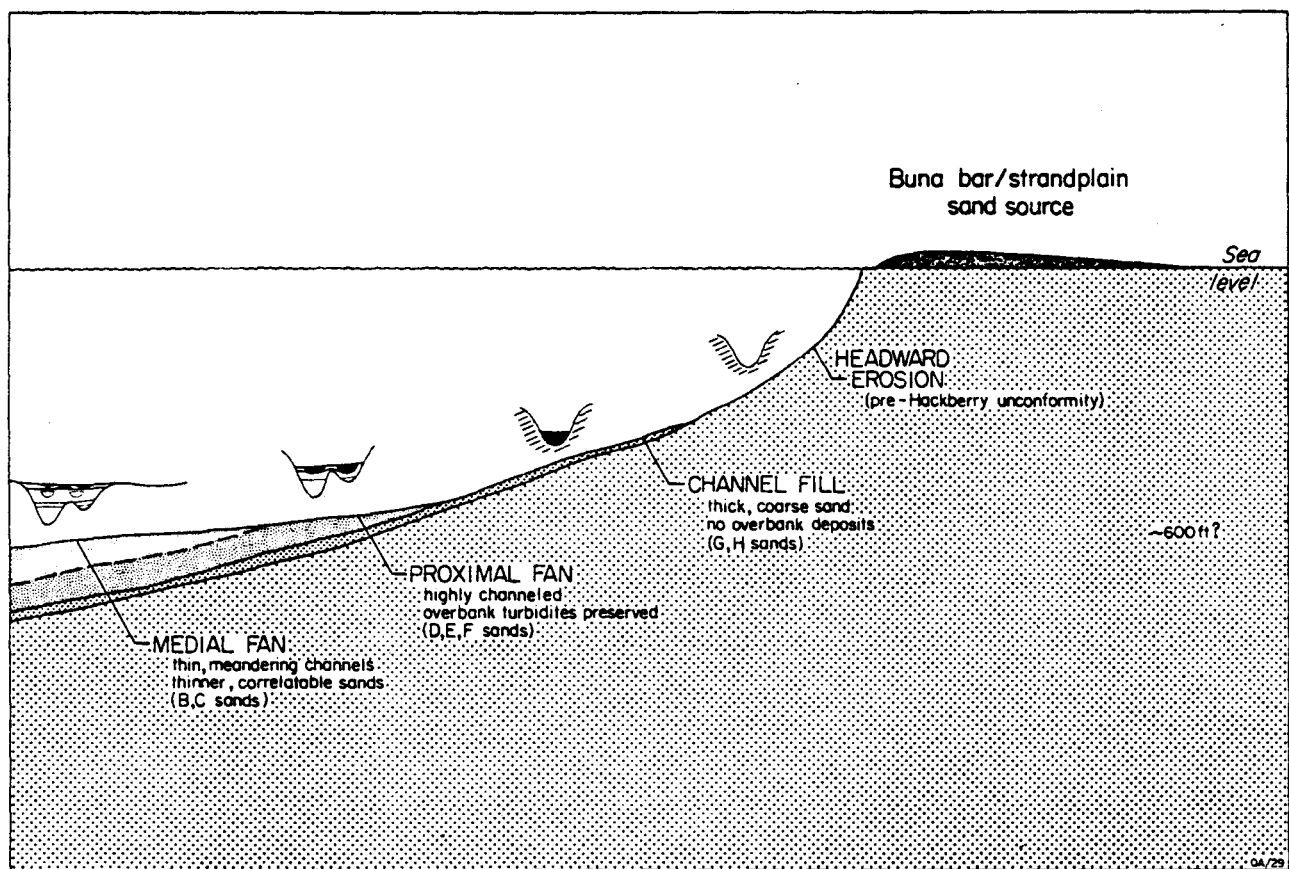
Figure 17. Onlapping submarine fan depositional model for lower Hackberry sandstones, Port Arthur field.

STRUCTURE MAP
TOP
Pre-Hackberry Unconformity
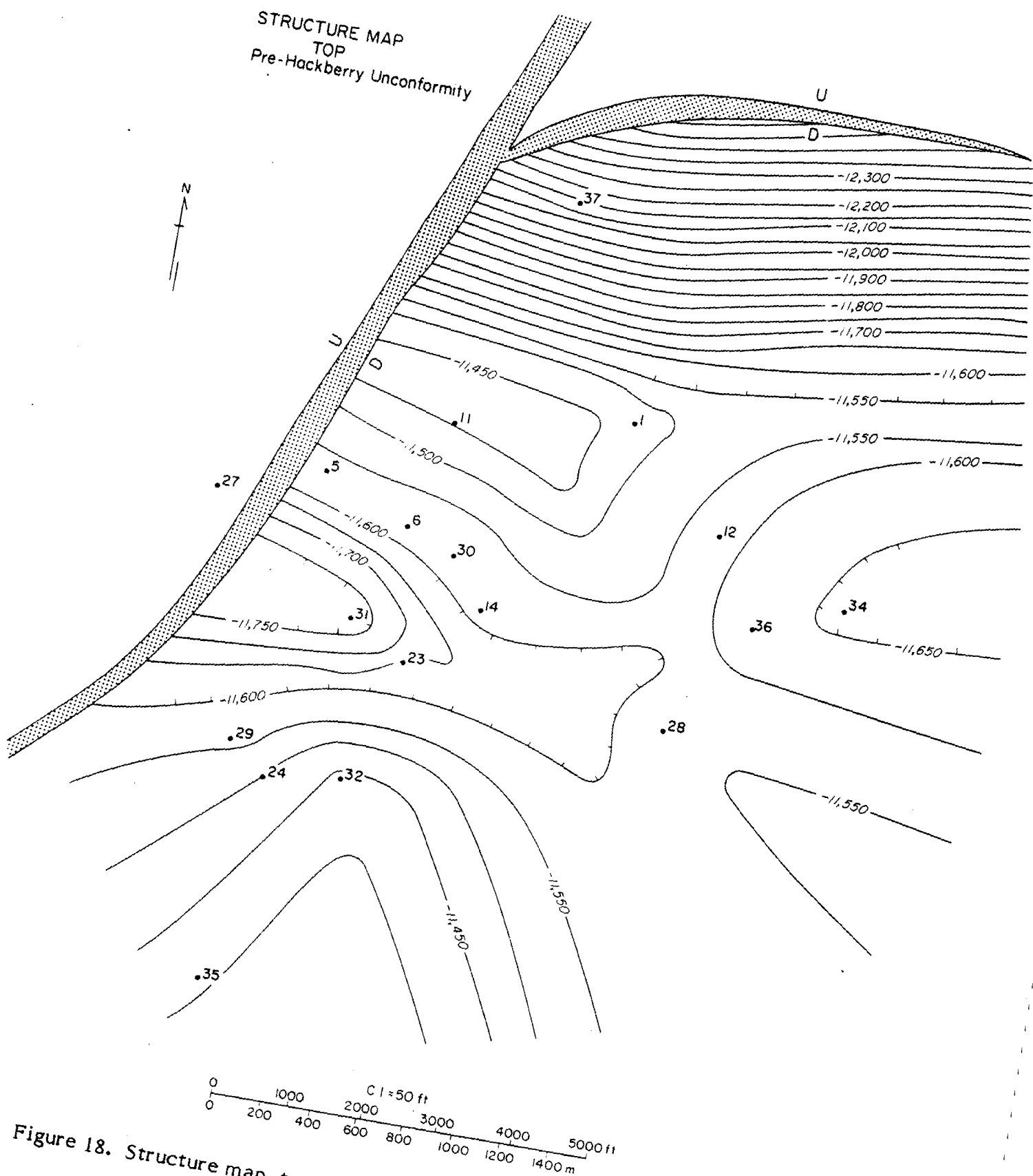
Figure 18. Structure map, top of pre-Hackberry unconformity, Port Arthur field.
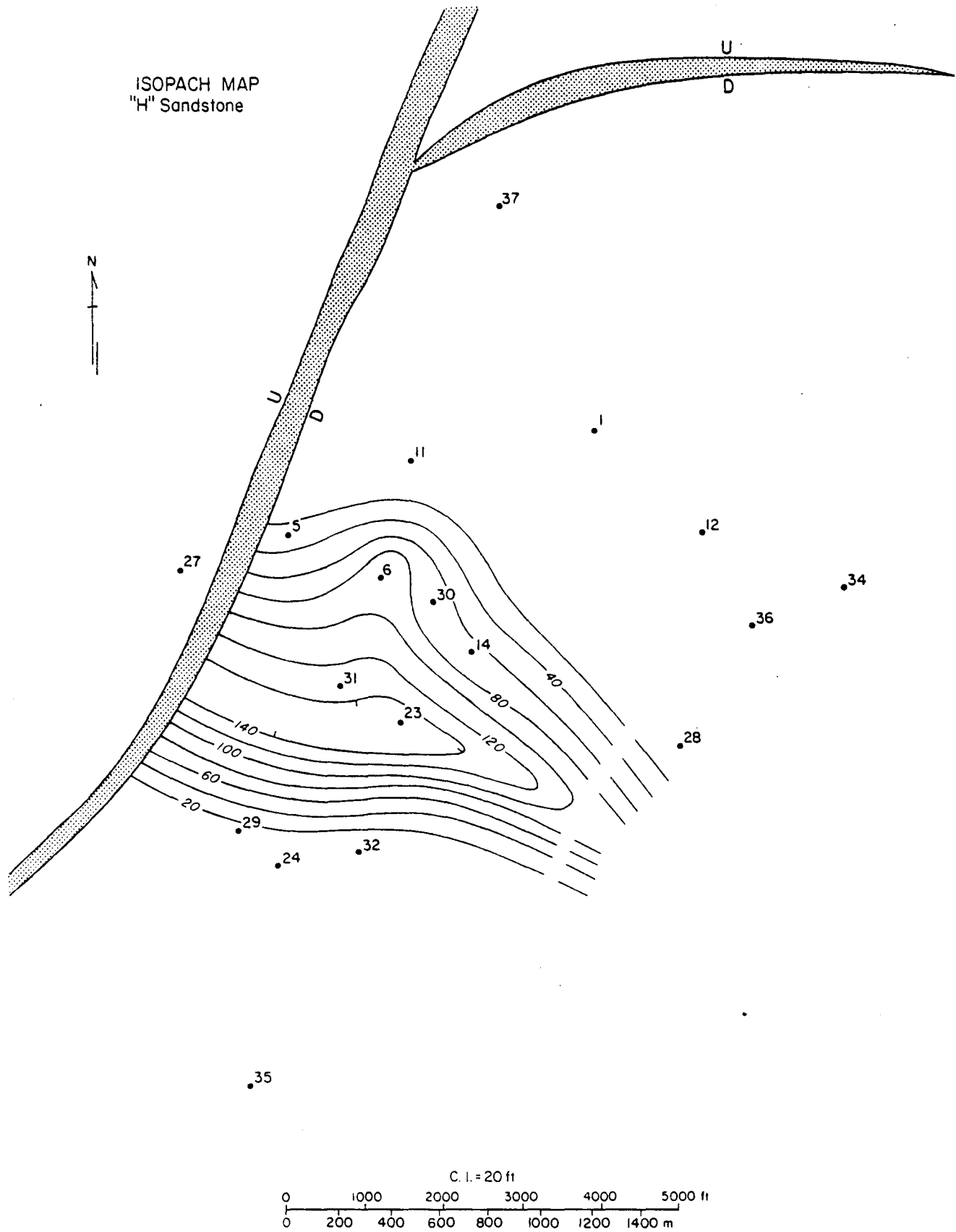
Figure 19. Isopach map, "H" sandstone, Port Arthur field.

STRUCTURE MAP
Top "H" Sandstone

N

C I = 20 ft

	0		1000		2000		3000		4000		5000 ft

0   200   400   600   800   1000   1200   1400 m
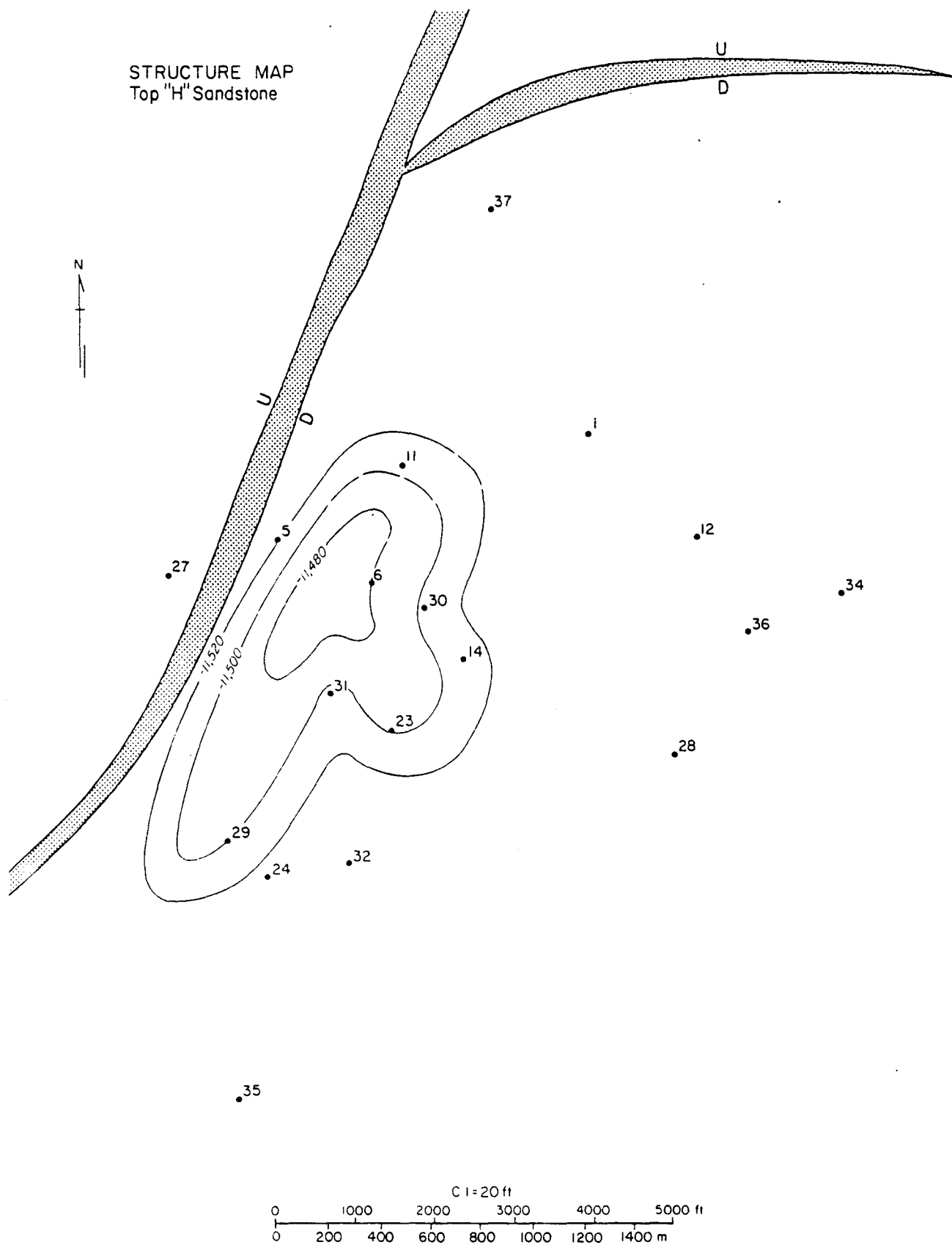
Figure 20. Structure map, "H" sandstone, Port Arthur field.

35

in the canyon area on the east side of the field (fig. 21). Well 31, which produces from this sandstone, is located on the flanks of the canyon and on the crest of the anticlinal structure (fig. 22).

By contrast, the "F" sandstone was primarily deposited within the major canyon at the north end of the field (fig. 23). Over the rest of the field area, "F" is interpreted to be a proximal suprafan deposit. It is productive only in Well 14, which is also located on the crest of the structure (fig. 24). The "E" sandstone, a broad fan channel-fill deposit similar to the "F" sandstone, was deposited by channels on the north and southwest of the field (fig. 25). Wells 6, 14, and 23 produce from this sand, being located on top of the anticline (fig. 26).

The composite "D" and "C" sandstones show a similar distribution. The "D" sandstone isopach map shows a confined fan channel at the south end of the field (fig. 27). Wells 6 and 11 produce from a broad, east-west-trending fan channel; there is also a larger channel to the north. The structure for the "D" sandstone is like that of the above-mentioned sandstones in this field (fig. 28); however, the structural high is shifted to the north. Wells 6, 14, 23, and 24 produce from this sand; they are located high on the structure but are not at its crest. The "C" sandstone is deposited in two main channels (fig. 29), one at each end of the field. Gas has been produced from Wells 6, 11, 14, and 23, which lie on top of the "C" sandstone structure (fig. 30).

The "B-2" sandstone was also deposited in a channel on the south end of the field (fig. 31), overlying the southern "C" sandstone channel. Well 31 was the only producer in this sand (fig. 32).

Potential Salt-Water Disposal Sands

The predicted production of 8.94 million bbl of salt water from natural flow over an 8-yr period, discussed later, requires that suitable disposal sands be located near the test well site. Over 2,000 ft of net sandstone are available for potential injection at depths between 2,000 and 7,500 ft in the Port Arthur field. Cross section T-T' (fig. 33) shows the sandstones available for salt-water injection at depths between 3,850 and 6,200 ft. These thick Miocene aquifers are found below the base of fresh water (-500 ft) and above the shallowest hydrocarbon production; they offer numerous zones for brine disposal. During primary production, brine was injected in two wells at depths of 1,400 to 3,500 ft. Since the proposed test site is near several plugged wells, it may be possible to use one of the abandoned wells for disposal rather than drilling a new injection well. Log calculations for Well 14 indicate that the Miocene sands contain waters with salinities of about 180,000 ppm NaCl compared with 90,000 ppm NaCl for the lower Hackberry sandstones. The effect on the stability of clays of mixing moderately saline and highly saline waters will need to be evaluated.

36

ISOPACH MAP
"G"Sandstone

N

37

U
D

U
D

1

11

5

10

30

12

27

6

50

30

14

60

34

36

31

23

28

40

29

20

24

32

20

20

35

10

C. I. = 10 ft

| 0 | 1000 | 2000 | 3000 | 4000 | 5000 ft |

| 0 | 200 | 400 | 600 | 800 | 1000 | 1200 | 1400 m |
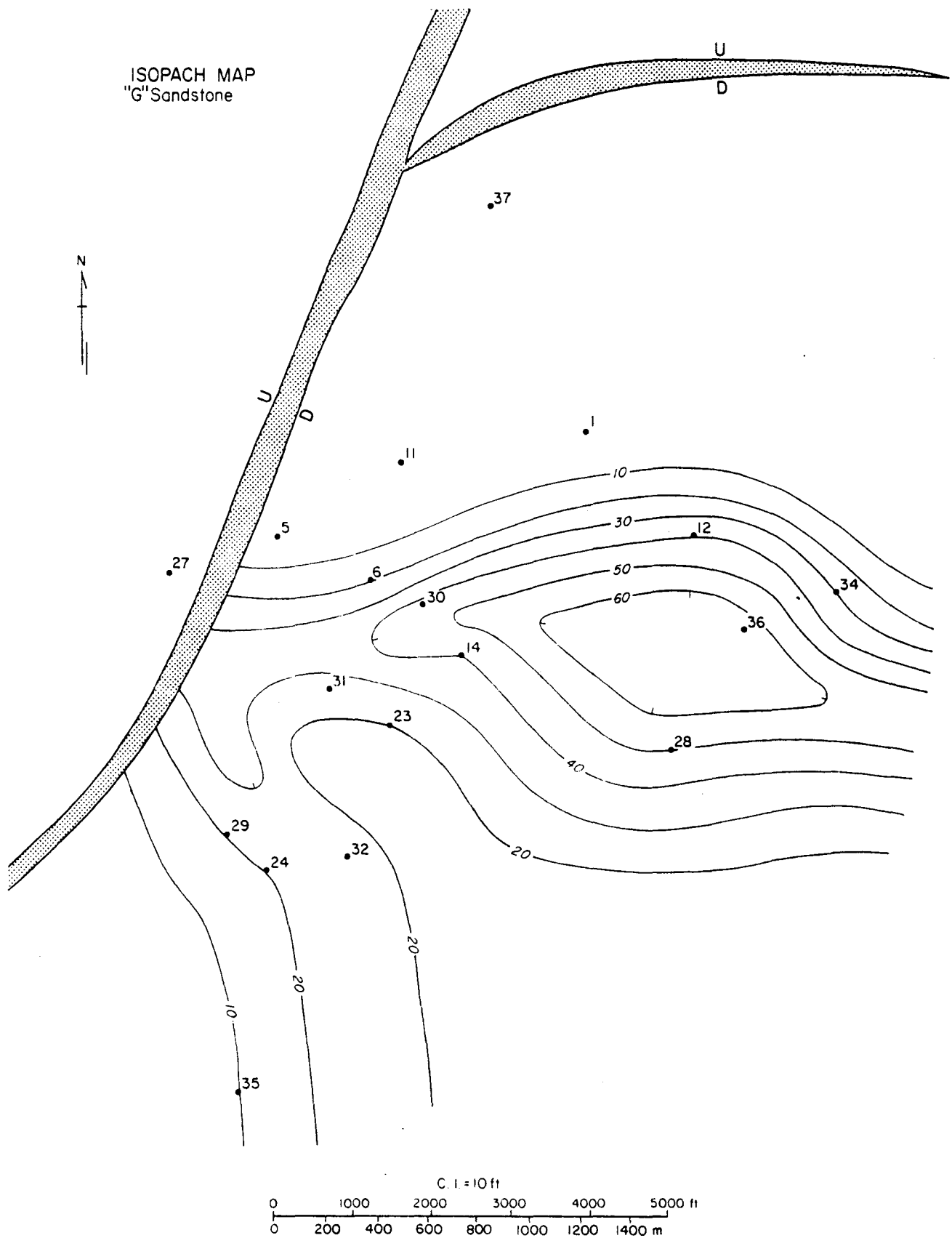
Figure 21. Isopach map, "G" sandstone, Port Arthur field.

37

STRUCTURE MAP
Top "G" Sandstone

C. I. = 20 ft

0	1000	2000	3000	4000	5000 ft
0	200 400 600 800 1000 1200 1400 m
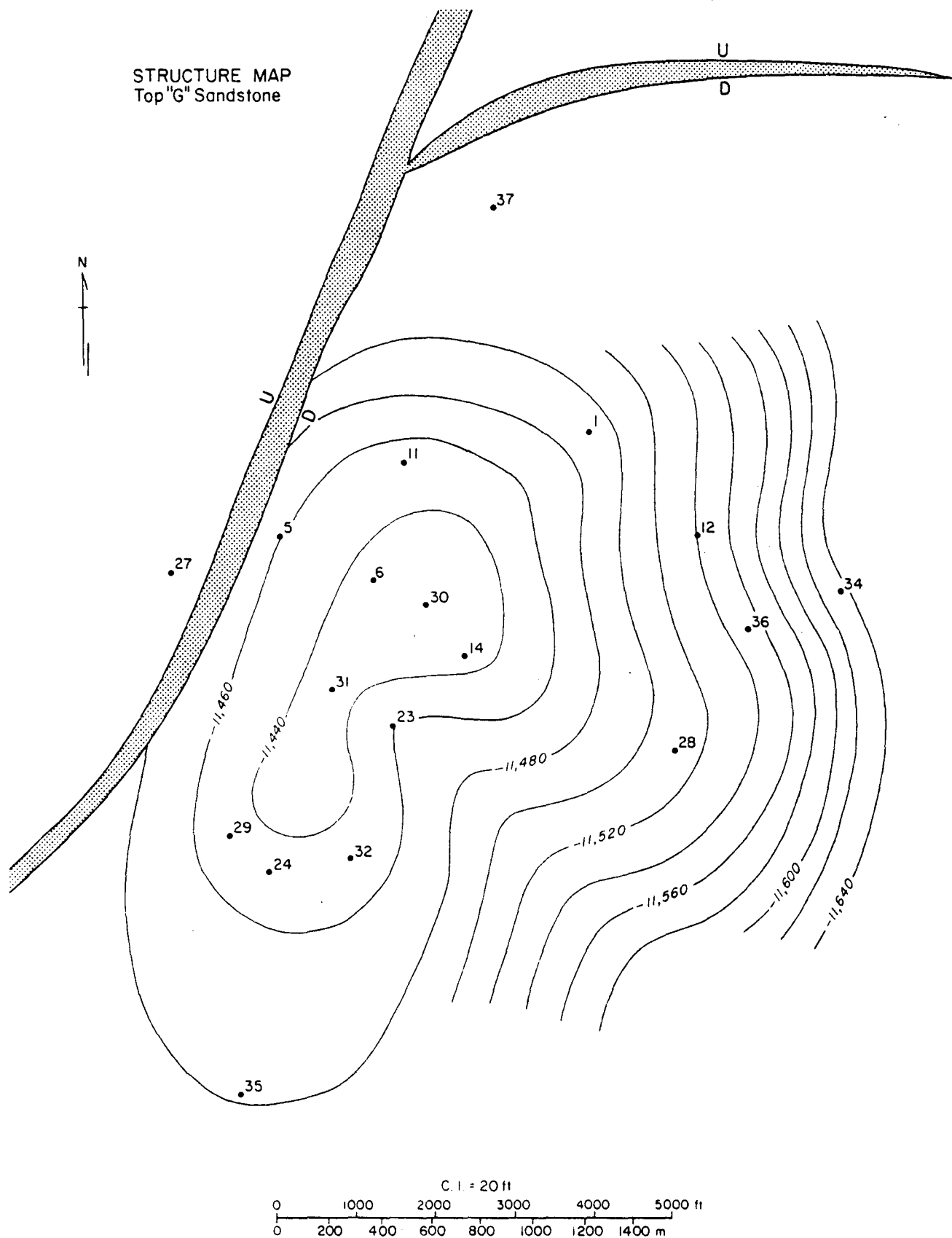
Figure 22. Structure map, "G" sandstone, Port Arthur field.

38
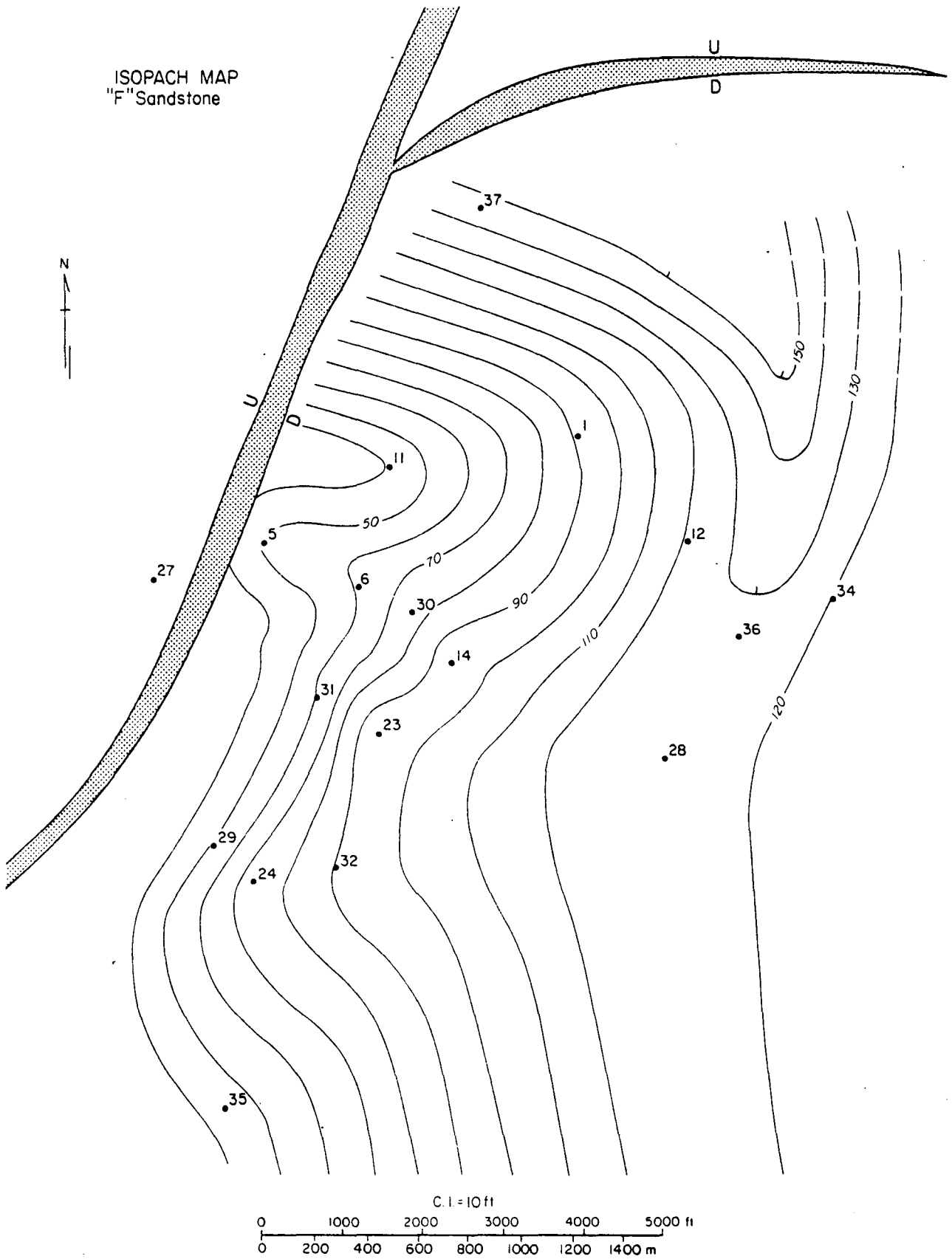
Figure 23. Isopach map, "F" sandstone, Port Arthur field.

39

STRUCTURE MAP
Top "F" Sandstone

C.I = 20 ft
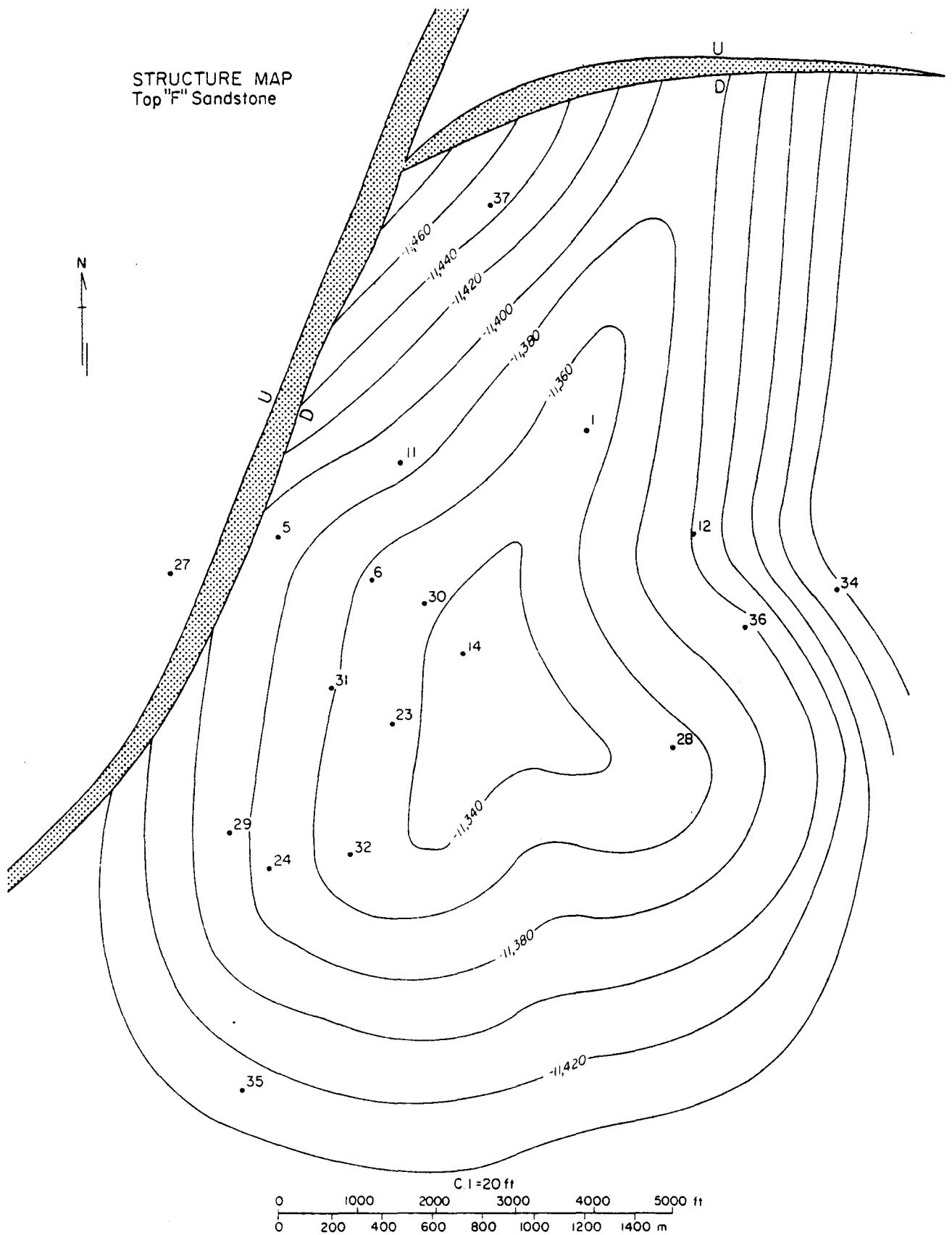
Figure 24. Structure map, "F" sandstone, Port Arthur field.

40

ISOPACH MAP
"E" Sandstone

N

CI = 10 ft

| 0 | 1000 | 2000 | 3000 | 4000 | 5000 ft |

| 0 | 200 | 400 | 600 | 800 | 1000 | 1200 | 1400 m |

Figure 25. Isopach map, "E" sandstone, Port Arthur field.

41

STRUCTURE MAP
Top "E" Sandstone

CI = 20 ft
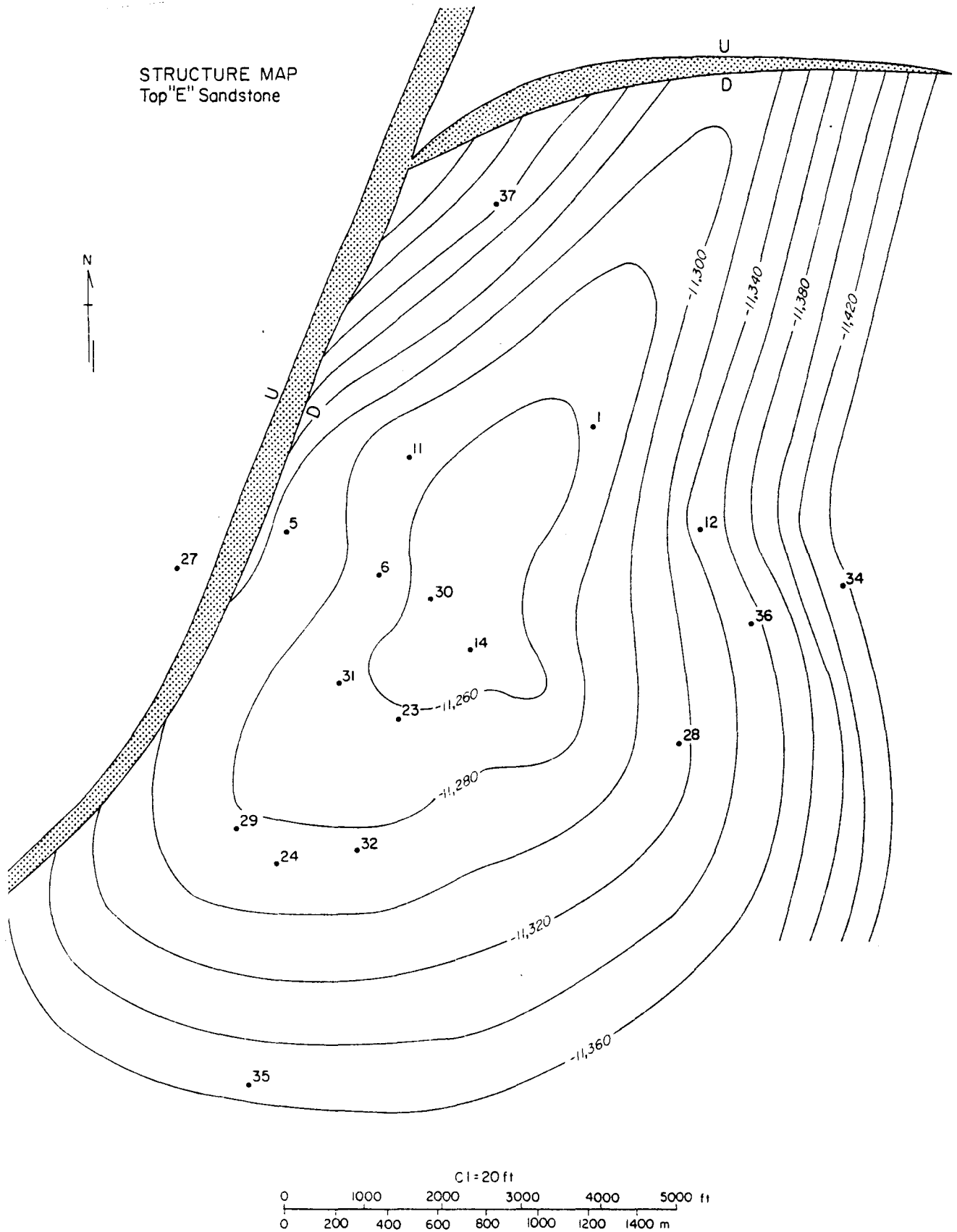
Figure 26. Structure map, "E" sandstone, Port Arthur field.

ISOPACH MAP
"D" Sandstone

C.I.=10 ft
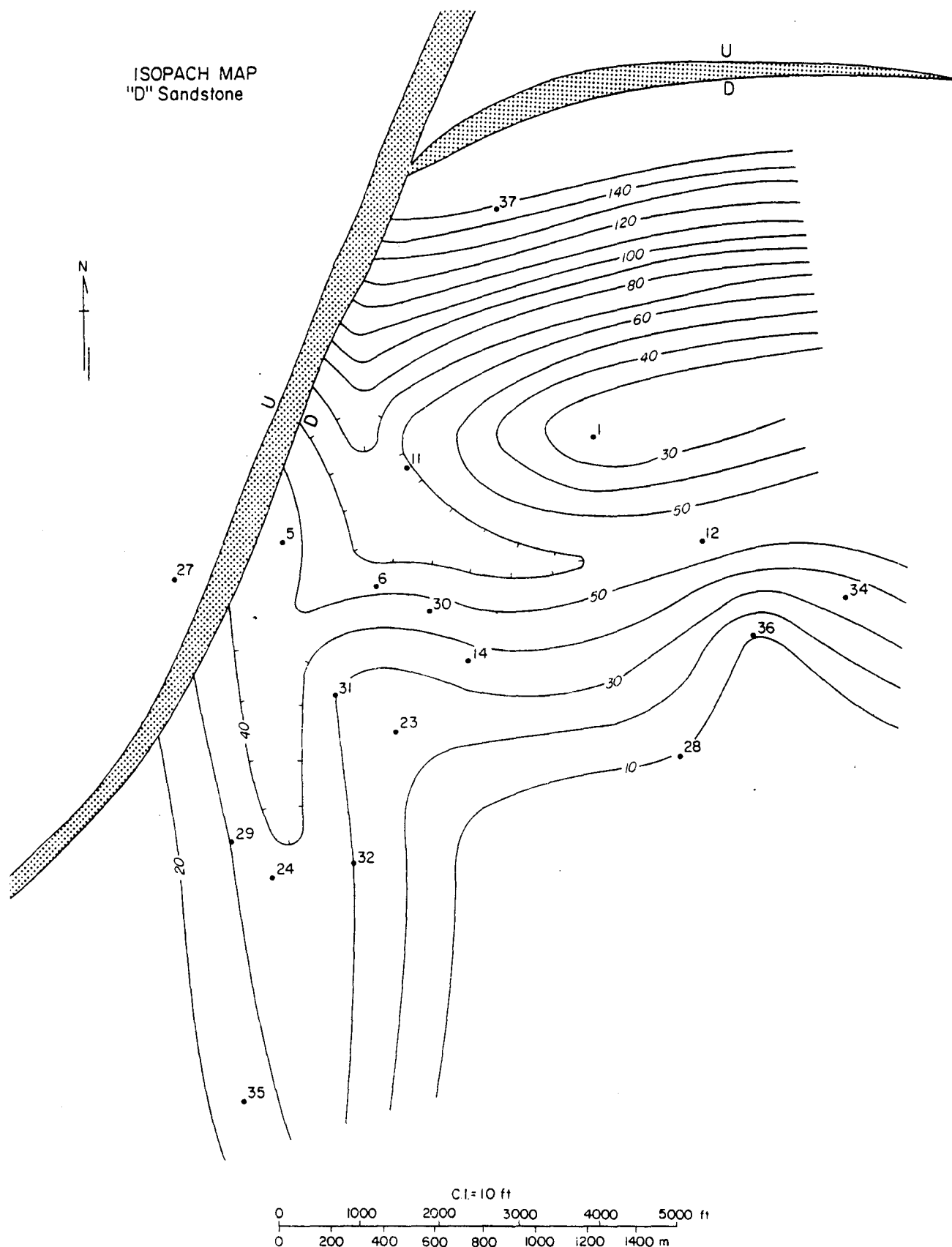
Figure 27. Isopach map, "D" sandstone, Port Arthur field.

STRUCTURE MAP
"D" Sandstone

C.I.=20 ft
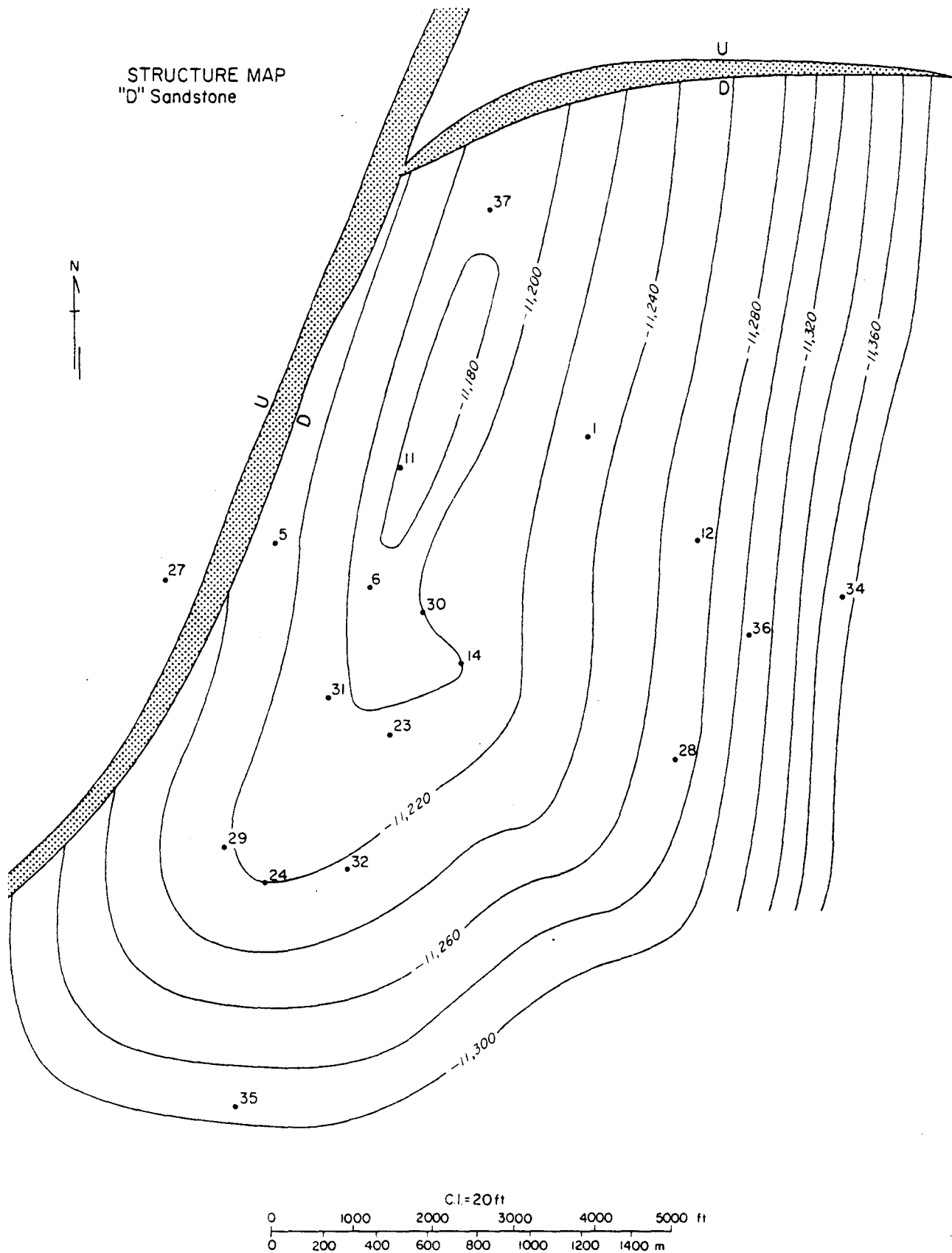
Figure 28. Structure map, "D" sandstone, Port Arthur field.
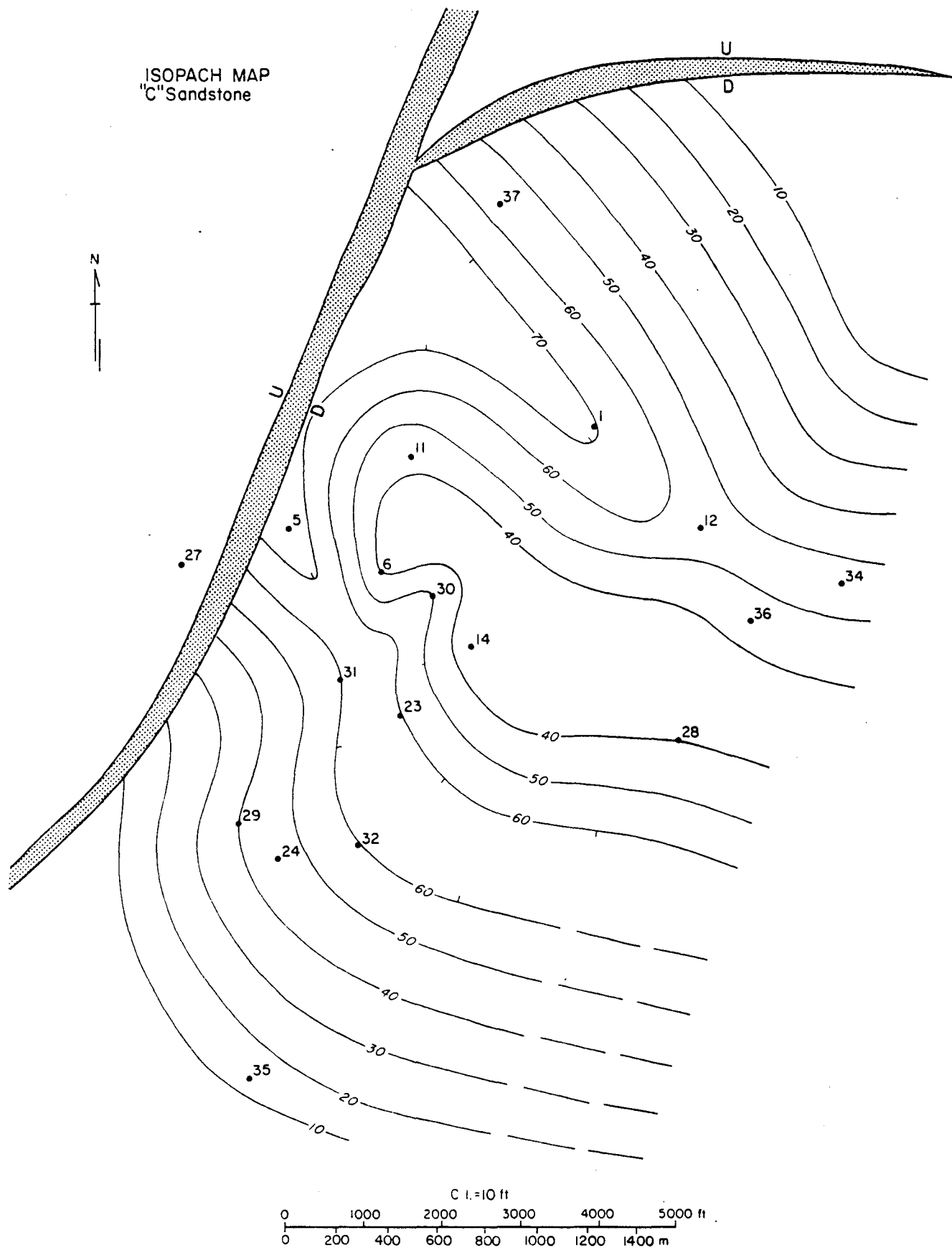
Figure 29. Isopach map, "C" sandstone, Port Arthur field.
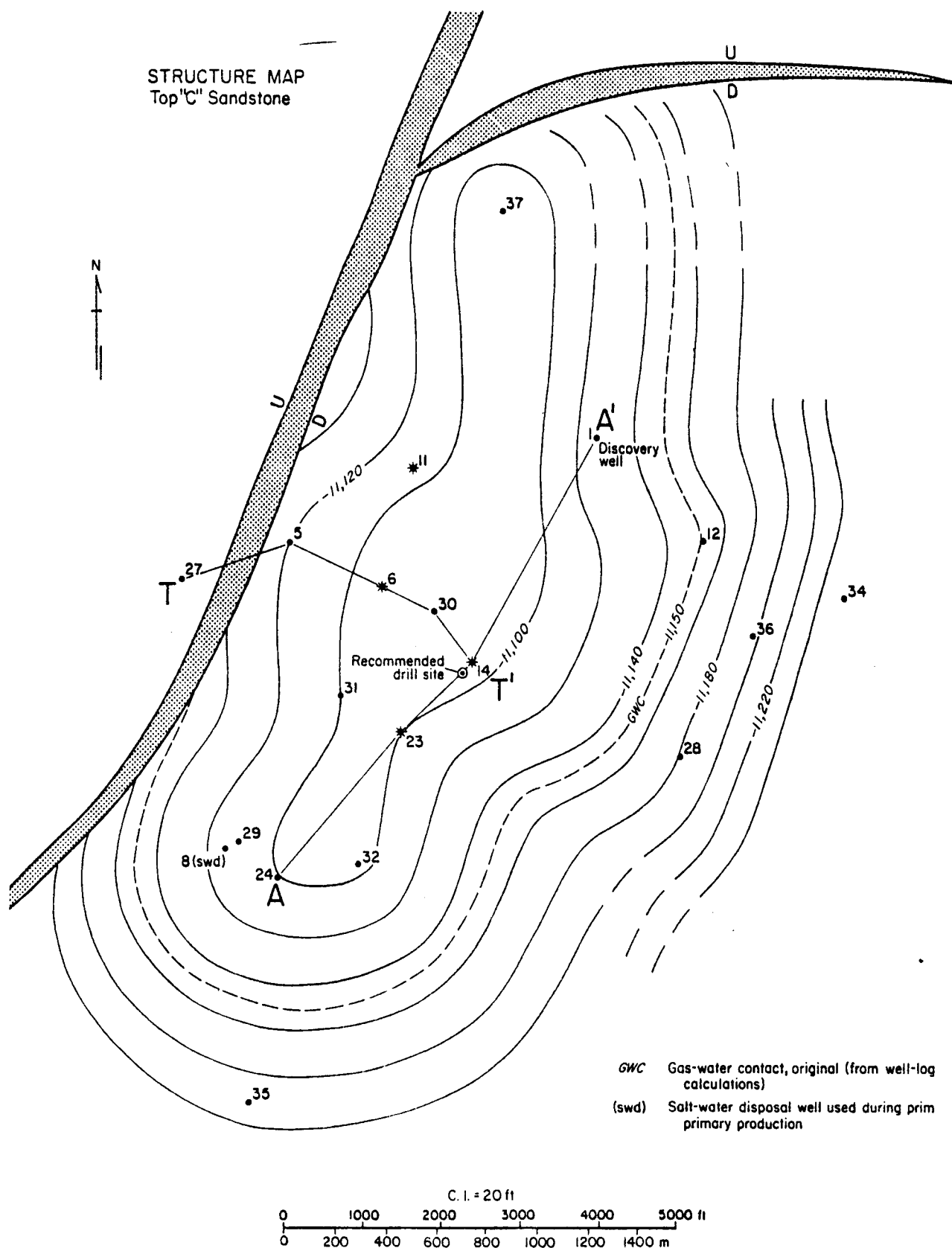
Figure 30. Structure map, "C" sandstone, Port Arthur field.

ISOPACH MAP
"B-2" Sandstone
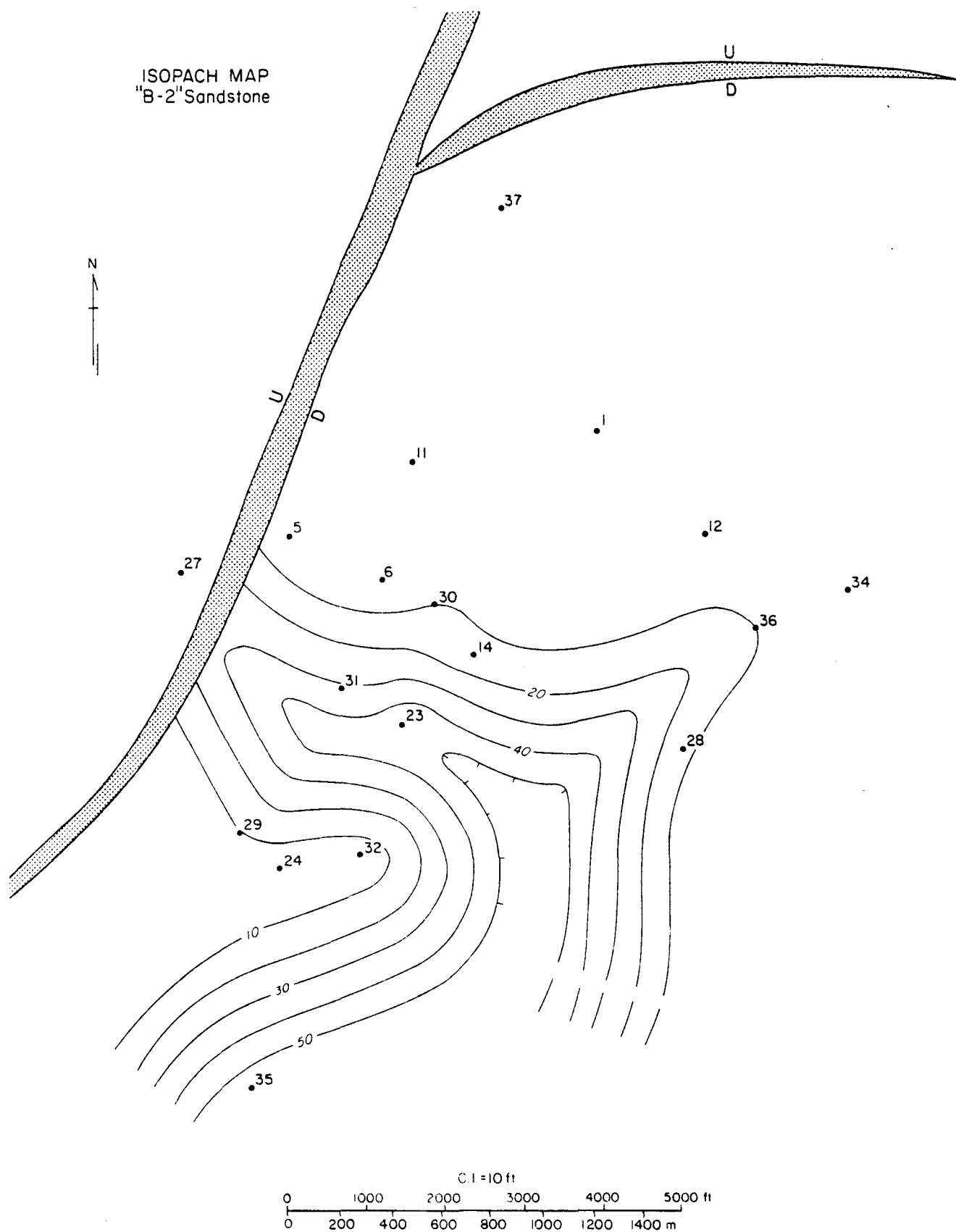
Figure 31. Isopach map, "B-2" sandstone, Port Arthur field.

47

STRUCTURE MAP
Top "B-2" Sandstone

No sand- contours on
B-2 shale marker

C. I. = 20 ft
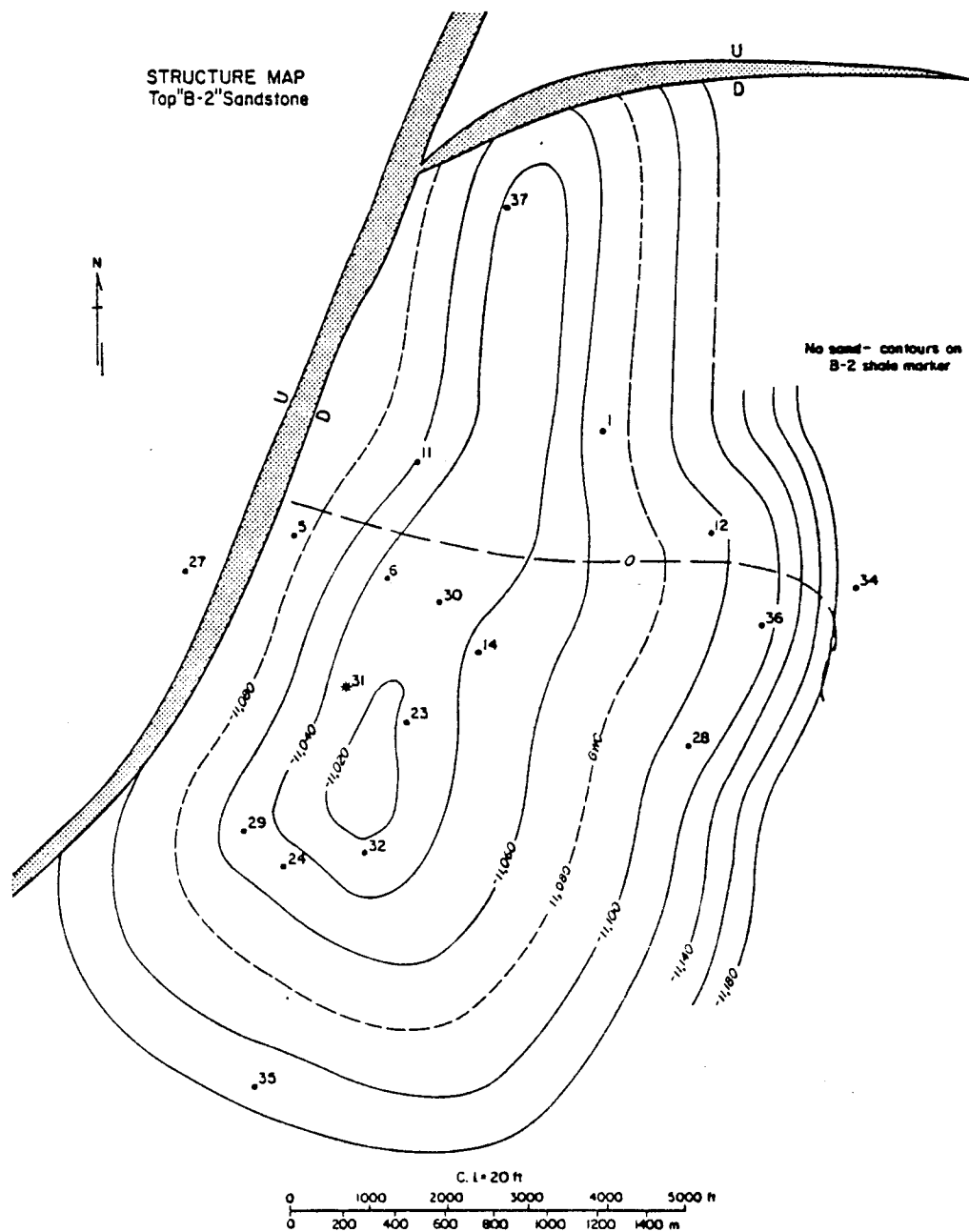
Figure 32. Structure map, "B-2" sandstone, Port Arthur field.
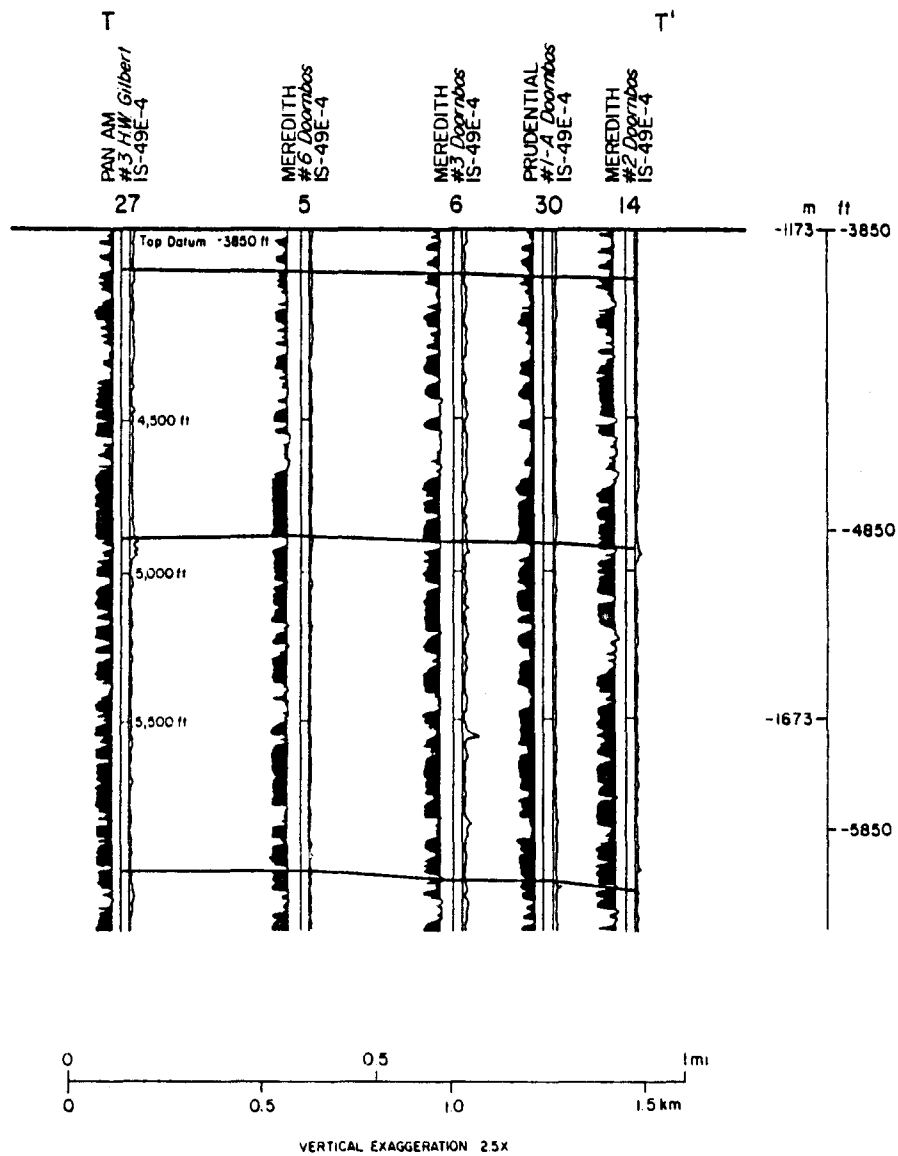
Figure 33. Cross section T-T' showing thickness of Miocene sands in the shallow subsurface suitable for disposal of waste salt water. See figure 30 for location of cross section.

Well Locations, Status, and Reservoir Properties

There are 18 wells in the Port Arthur field (table 3 and fig. 7). Eleven of these wells produced gas and condensate from one or more lower Hackberry reservoirs (table 4); four wells (1, 6, 24, and 32) produced from the Nodosaria sandstone; three wells (5, 27, and 36) produced from the Vicksburg interval; two wells (28 and 34) were dry holes; and production at Well 37 was reported as having been suspended (table 3).

Gas was produced from the lower Hackberry (Frio) sandstones in the depth interval from 10,850 to 11,700 ft. Reservoirs designated as "C," "D," and "E" are laterally continuous and have the best characteristics for producing gas and water. The last producing well watered out and was plugged and abandoned in March 1981.

The listing of average reservoir properties (table 5) shows that the lower Hackberry sandstones have high porosity, fairly high permeability, moderate temperature, and high-salinity fluids. Sidewall cores from seven wells in the field show that permeabilities range from 0.0 to 314 md and porosities vary from 12.9 to 36.5 percent in the "C" reservoir (appendix C). Two cores from the perforated interval of Well 14 had an average permeability of 156.5 md and an average porosity of 33.4 percent. Average water saturation and oil saturation in the perforated interval were 65.2 percent and 1.55 percent, respectively.

Reservoir Fluid Properties

Methane Solubility

The solubility of methane in water and NaCl solutions has been determined from laboratory measurements for salinities of 0 to 300 g/L, a temperature range of 160° to 464°F, and a pressure range of 3,500 to 22,500 psi (Price and others, 1981). Equations (1) and (2) below give the "best fit" to the average experimental data. Either equation can be used.

$$\log_e CH_4* = -1.4053 - 0.002332t + \tag{1}$$
$$6.30 \times 10^{-6}t^2 - 0.004038S - 7.579 \times 10^{-6}p$$
$$+ 0.5013 \log_e p + 3.235 \times 10^{-4} t \log_e p$$

Standard deviation of residuals = 0.0706
Multiple R = 0.9944

---

*CH_4 is in standard cubic feet (scf) per petroleum barrel (42 gallons) at 25°C (77°F) and one atmosphere pressure.

$$\log_e CH_4{}^* = -3.3544 - 0.002277t +$$
$$6.278 \times 10^{-6}t^2 - 0.004042S + 0.9904 \log_e p$$
$$-0.0311 (\log_e p)^2 + 3.204 \times 10^{-4}t \log_e p$$

(2)

Standard deviation of residuals $= 0.0709$

Multiple $R = 0.9943$

where

$t =$ temperature in degrees Fahrenheit

$S =$ salinity in grams per liter

$p =$ pressure in pounds per square inch

The equations show that methane solubility in water and NaCl solutions is a function of pressure, temperature, and salinity. An increase in pressure or temperature causes an increase in methane solubility. An increase in salinity reduces methane solubility. Pressure and temperature are more predictable than salinity, which varies greatly throughout the Gulf Coast area. Because of this variability and the difficulty of determining salinities accurately by indirect methods such as the well log analyses discussed below, salinity values generally are the least reliable of the three parameters that control methane solubility.

Several potential sources of error exist for salinities determined from the SP log. Dunlap and Dorfman (1981) pointed out that a major source of error lies in the use of incorrect values of mud filtrate resistivity R_{mf} that are listed on well log headers when high-density lignosulfonate muds and certain other types of mud are used (R_{mf} is too large). Lignosulfonate muds have been in use for over 15 yr; thus, the scope of the problem is large. Also, the method of determining R_{mf} from mud resistivity using the Schlumberger Limited (1978) chart, Gen 7, should not be applied to lignosulfonate muds, as clearly stated on the chart. The chart was based on the work of Overton (1958), which took place before the widespread use of lignosulfonate muds began. The present method of correcting R_{mf} from surface to downhole temperature, using resistivity versus temperature variations for NaCl solutions, may not be applicable to modern muds and mud filtrates, thus introducing further errors into salinity determinations.

Salinities in this report were determined from the SP log by the improved method of Dunlap and Dorfman (1981) and are commonly higher than those obtained from previous well log methods; these higher salinities result in lower estimates of methane solubility.

As stated earlier, formation fluid temperature influences methane solubility. In this report, well-bore temperatures taken from well logs are corrected to equilibrium values that represent formation fluid temperatures by the following equation of Kehle (1971):

51

Table 3. Identification, location, and status of wells, Port Arthur field, Jefferson County, Texas.

Well no.	Original operator and well name	Current operator and well name	Tobin grid	Well status*	Total depth (ft)
1	Meredith no. 1 Doornbos	Prudential no. 1 Doornbos Loidold	1S-49E-4	P & A	12,290
5	Meredith no. 6 Doornbos	Prudential no. 6 Doornbos	1S-49E-4	P & A	12,681
6	Meredith no. 3 Doornbos	Prudential no. 3 Port Arthur Hack. Unit	1S-49E-4	P & A	12,200
11	Meredith no. 4 Doornbos	Prudential no. 4 Port Arthur Hack. Unit	1S-49E-4	P & A	12,175
12	Meredith no. 5 Doornbos	Prudential no. 5 Port Arthur Hack. Unit	1S-49E-5	P & A	12,352
14	Meredith no. 2 Doornbos	Prudential no. 2 Port Arthur Hack. Unit	1S-49E-4	P & A	12,200
23	Kilroy & MPS no. 1 Doornbos	Prudential no. 1 Port Arthur Hack. Unit	1S-49E-9	P & A	12,160
24	Kilroy & MPS no. 1 City of Port Arthur	Prudential no. 9 Port Arthur Hack. Unit	1S-49E-9	P & A	12,001
27	Pan Am. no. 3, H.W. Gilbert	Amoco no. 3 H.W. Gilbert	1S-49E-4	P & A	12,751
28	Texaco, Inc. no. 1 Port Arthur Refinery Fee	no change	1S-49E-8	Dry	14,200
29	Halbouty & Pan Am. no. 2 Doornbos	Prudential no. 7 Port Arthur Hack. Unit	1S-49E-9	P & A	12,202
30	Prudential no. 1-A Doornbos	no change	1S-49E-4	P & A	11,809
31	Halbouty & Pan Am. no. 1 Doornbos	Prudential no. 6 Port Arthur Hack. Unit	1S-49E-9	P & A	12,103
32	Kilroy & MPS no. 2 Doornbos	Kilroy & M.P.S. no. 1 Doornbos Nodosaria Gas Unit 1	1S-49E-9	P & A	12,208
34	Meredith no. 1 Doornbos-Port Arthur Vicksburg Gas Unit 1	no change	1S-49E-5	Dry	14,125
35	J. C. Barnes no. 1 Swallow	Tex-Star Oil & Gas no. 1 Swallow	1S-49E-9	P & A	12,000
36	Texaco, Inc. no. 1 Park Place Gas Unit	no change (slanted hole)	1S-49E-8	P & A	14,050
37	Kilroy no. 1 Booz	no change (slanted hole)	1S-49E-4	Sus.	12,641

*P & A = plugged and abandoned; Sus. = production suspended.

52

Table 4. Pressure gradients and production history by reservoir
and well, Port Arthur field, Jefferson County, Texas.

Lower Hackberry reservoirs	Well no.*	Perforated interval (ft)	BHSIP gradient (psi/ft) Initial	BHSIP gradient (psi/ft) Last	Production period	Cumulative production Gas (Bscf)	Cumulative production Condensate (bbl)
A-1	12	10,946-10,956	0.84	0.57	12/59-7/68	0.989	93,934
	35	10,966-10,978	0.80	0.74	8/60-5/61	0.138	-
A-2	29	10,925-10,955	0.82	0.59	9/59-2/62	0.054	228
	6	10,936-10,946	0.83	0.54	3/66-8/71	0.784	31,492
	11	10,934-10,950	0.69	-	12/59-9/61	0.121	-
Upper B Stringer	31	10,986-10,994	0.83	0.64	3/66-1/72	0.200	8,115
B	6	10,995-11,000	0.81	0.77	5/67-5/79	0.088	4,952
	30	10,994-11,002	0.73	-	8/78-2/80	0.002	387
B-1	24	11,052-11,058	0.58	0.44	9/68-3/70	0.003	148
	23	11,021-11,029	0.82	0.78	6/62-9/65	3.323	172,158
B-2	31	11,077-11,101	0.84	0.69	9/59-1/66	13.343	720,286
C	23	11,128-11,131	0.75	0.64	7/65-8/71	1.249	38,404
	14	11,136-11,144	0.83	0.70	7/61-7/72	10.535	455,783
	6	11,130-11,135	0.70	0.45	8/71-12/72	0.099	2,301
	11	11,130-11,138	0.75	0.60	9/61-10/69	7.754	366,494
Upper D Stringer	30	11,204-11,208	0.73	0.68	5/75-5/79	0.616	27,963
D	14	11,225-11,243	0.53	0.50	6/68-10/72	0.517	19,719
	6	11,218-11,228	0.82	0.63	3/60-4/66	4.310	174,229
	23	11,251-11,256	0.67	0.63	7/65-8/71	1.881	66,583
	24	11,250-11,257	0.65	0.62	1/68-8/68	0.126	6,430
E	14	11,276-11,286	0.83	0.66	5/59-12/60	1.620	87,638
	23	11,290-11,299	0.81	0.73	11/59-6/62	2.072	109,115
	6	11,296-11,301	0.80	0.73	3/66-8/71	0.552	24,357
Lower E Stringer	24	11,387-11,391	0.70	-	11/67-12/67	0.034	1,225
F	14	11,350-11,359	0.81	0.80	7/61-6/68	6.212	224,288
G	31	11,458-11,463	0.79	0.76	3/66-1/67	0.449	17,606
					Total	57.071	2,653,835

*Well locations shown in figure 7; Tobin grids are shown in table 3.

Table 5. Average reservoir properties, lower Hackberry (Frio) sandstones,
Port Arthur field, Jefferson County, Texas.

Depth to top	10,850 ft
Net sandstone	350 ft
Bed thickness	30 to 150 ft
Porosity[1]	30%
Permeability[1]	60 md
Equilibrium temperature	231°F
Pressure gradient (initial)	0.76 psi/ft
Salinity[2]	90,400 ppm NaC1
Methane solubility[3]	23.5 scf/bbl
Productive area[1]	3 mi[2]

[1]Modified from Halbouty and Barber (1961).

[2]Calculated from SP well logs using method of Dunlap and Dorfman (1981).

[3]Calculated at initial pressure, temperature, and salinity, using equation of Price and others (1981).

$$T_E = T_L - 8.819 \times 10^{-12}D^3 - 2.143 \times 10^{-8}D^2 + 4.375 \times 10^{-3}D - 1.018 \tag{3}$$

where T_E = equilibrium temperature (°F)

T_L = temperature recorded on well log header (°F)

D = depth (ft).

Formation fluid pressures can be derived from shale resistivity or acoustic travel time data using the method of Hottmann and Johnson (1965). Shale resistivity values (R_{sh}) from amplified short-normal resistivity curves of induction logs are plotted as a function of depth for both hydropressured and geopressured zones. The normal compaction curve is drawn by a least-squares regression method. All R_{sh} data fall near this curve when shales are normally pressured or slightly geopressured; R_{sh} data to the left of this curve are lower than normal, indicating that pressure gradients are significantly greater than normal and may approach 1 psi/ft in highly geopressured zones. Deviations of R_{sh} data points from the normal compaction curve are calibrated in terms of pressure or pressure gradient by bottom-hole shut-in pressures measured by drill-stem tests in wells located in the area of interest. Details of the method are explained in previous reports (Gregory and others, 1980; Weise and others, 1981a).

Aquifers in the lower Hackberry sandstones in the Port Arthur field initially contained waters characterized by high geopressures, high salinities, moderate temperatures, and moderate methane solubilities (table 6). Distribution maps (figs. 34 to 38) show the interrelationships among these parameters in the "C" sandstone. There are two high-pressure areas in the field (fig. 34): one is a large area aligned along strike that includes Well 12; the other is a smaller area updip that includes Wells 5 and 6. The highest temperatures occur near the center of the structural high (fig. 35) and exceed 240°F only in Wells 14 and 24. Salinities increase rapidly from 80,000 ppm NaCl in Well 14 to more than 160,000 ppm NaCl in Well 30, located less than 1,000 ft to the northwest (fig. 36). Methane solubility in formation water increases from about 18 scf/bbl at the outer fringe of the field to about 26 scf/bbl at the center of the structure and also at the proposed test well site located near Well 14 (fig. 37).

Values of pressure, pressure gradient, salinity, temperature, and methane solubility of the best thick aquifers are plotted and tabulated versus depth at original reservoir conditions for Well 14 (fig. 38 and table 7). Solubility values in the Port Arthur field increase with depth; typical data vary from 4 to 5 scf/bbl at a depth of 2,000 ft and from 24 to 30 scf/bbl at approximately 12,000 ft. In the lower Hackberry sandstone units the average methane solubility is 23.5 scf/bbl, based on a pressure gradient of 0.76 psi/ft, a salinity of 90,400 ppm, a temperature of 231°F, and an average depth of 11,150 ft (table 5). This means that on the average, only 470 Mscf/d of solution gas will be obtained from a well producing methane-saturated formation water at a rate of 20,000 bbl/d. It is essential, therefore, to produce a

Table 6. Salinity, temperature, pressure, and methane solubility at initial reservoir conditions, lower Hackberry reservoirs, Port Arthur field, Jefferson County, Texas.

Lower Hackberry reservoirs	Well no.[1]	Perforated interval (ft)	Salinity (ppm NaCl)[2]	Equilibrium temperature (°F)	Initial BHSIP (psi)[3]	Methane solubility (scf/bbl)[4]
A-1	12	10,946-10,956	28,300	214	9,192	30.10
	35	10,966-10,978	45,900	224	8,778	28.20
A-2	29	10,925-10,955	37,000	208	8,917	27.99
	6	10,936-10,946	77,300	212	9,059	23.96
	11	10,934-10,950	55,900	217	7,542	24.44
Upper B Stringer	31	10,944-10,986	95,000	219	9,171	22.76
B	6	10,995-11,000	60,500	214	8,955	25.84
	30	10,994-11,002	98,600	232	8,029	21.91
B-1	24	11,052-11,058	110,000	237	6,412	18.84
	23	11,021-11,029	89,900	230	9,041	24.04
B-2	31	11,077-11,101	112,000	223	9,302	21.47
C	23	11,128-11,131	95,100	232	8,398	22.78
	14	11,136-11,144	80,000	243	9,284	26.70
	6	11,130-11,135	88,100	218	7,775	21.57
	11	11,130-11,138	69,000	224	8,350	24.86
Upper D Stringer	30	11,204-11,208	144,000	238	8,180	18.20
D	14	11,225-11,243	88,600	247	5,954	20.74
	6	11,218-11,228	74,700	222	9,203	25.26
	23	11,251-11,256	112,000	234	7,540	20.08
	24	11,250-11,257	134,000	246	7,315	18.58
E	14	11,276-11,286	87,500	249	9,400	26.56
	23	11,290-11,299	108,000	235	9,148	22.63
	6	11,296-11,301	87,600	224	9,023	23.76
Lower E Stringer	24	11,387-11,391	129,000	250	8,012	20.24
F	14	11,350-11,359	83,500	252	9,197	27.06
G	31	11,458-11,463	121,000	237	8,820	21.05

[1]Well locations shown in figure 7; Tobin grid given in table 3.

[2]From SP log using method of Dunlap and Dorfman (1981).

[3]From completion cards or calculated from WHSIP.

[4]Calculated from equation of Price and others (1981) at initial conditions of pressure, temperature, and salinity.

INITIAL PRESSURE GRADIENT
"C" Sandstone

C I = 0.05 psi/ft
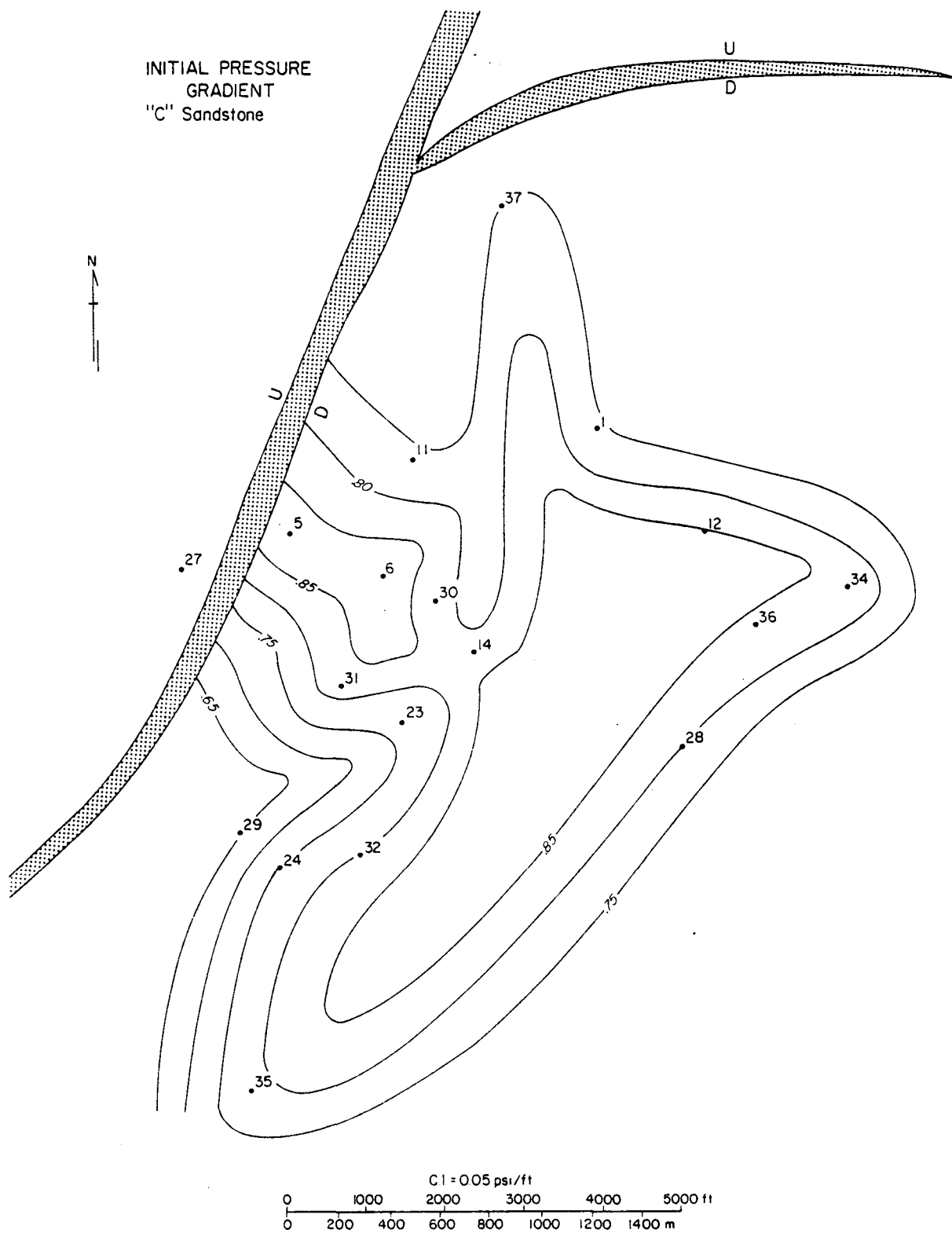
Figure 34. Distribution of initial pressure gradients (psi/ft), "C" sandstone, Port Arthur field.
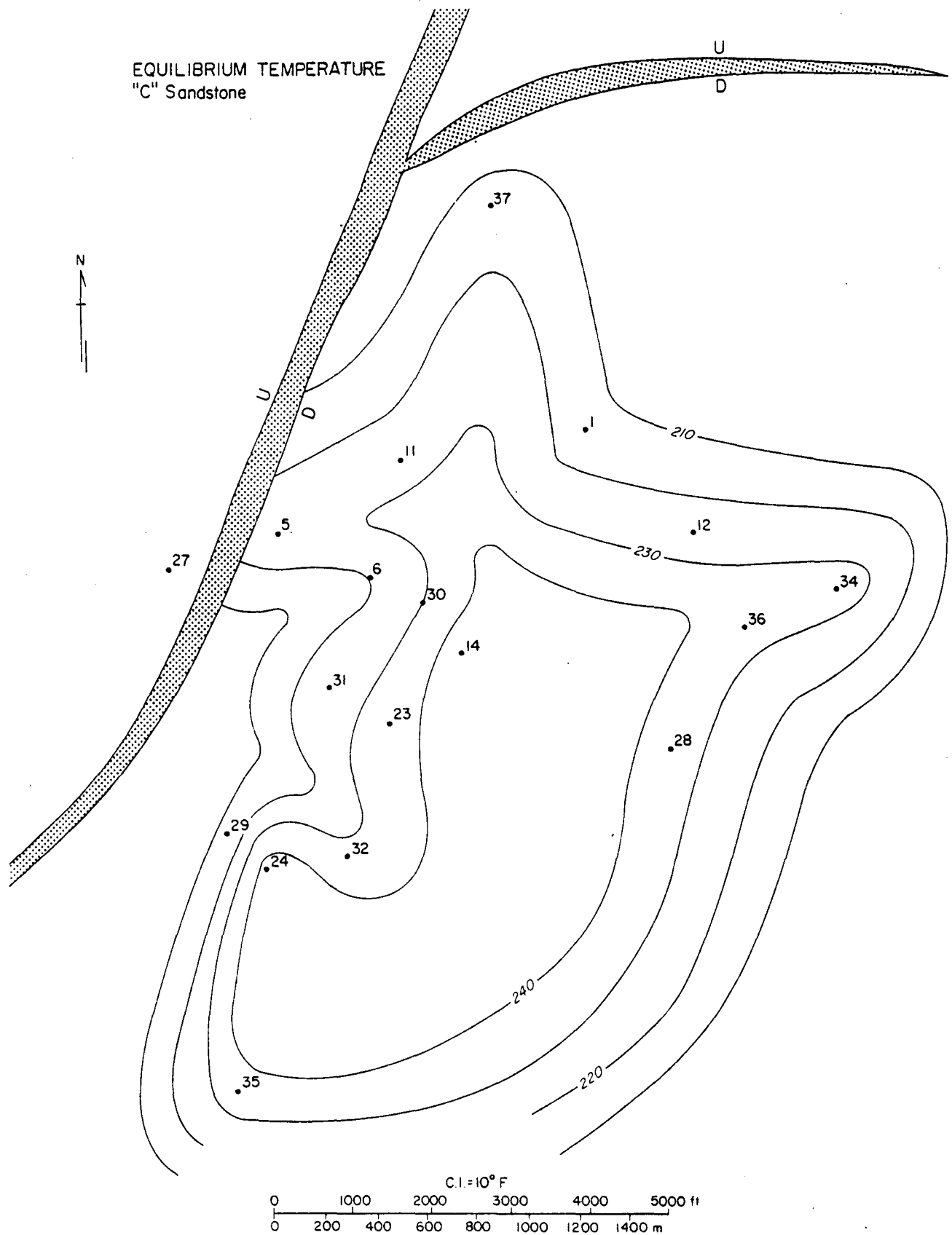
Figure 35. Distribution of temperature (°F), "C" sandstone, Port Arthur field.

58

Figure 36. Distribution of salinity (ppm NaCl), "C" sandstone, Port Arthur field.

INITIAL METHANE
SOLUBILITY
"C" Sandstone

C I. = 2 scf/bbl
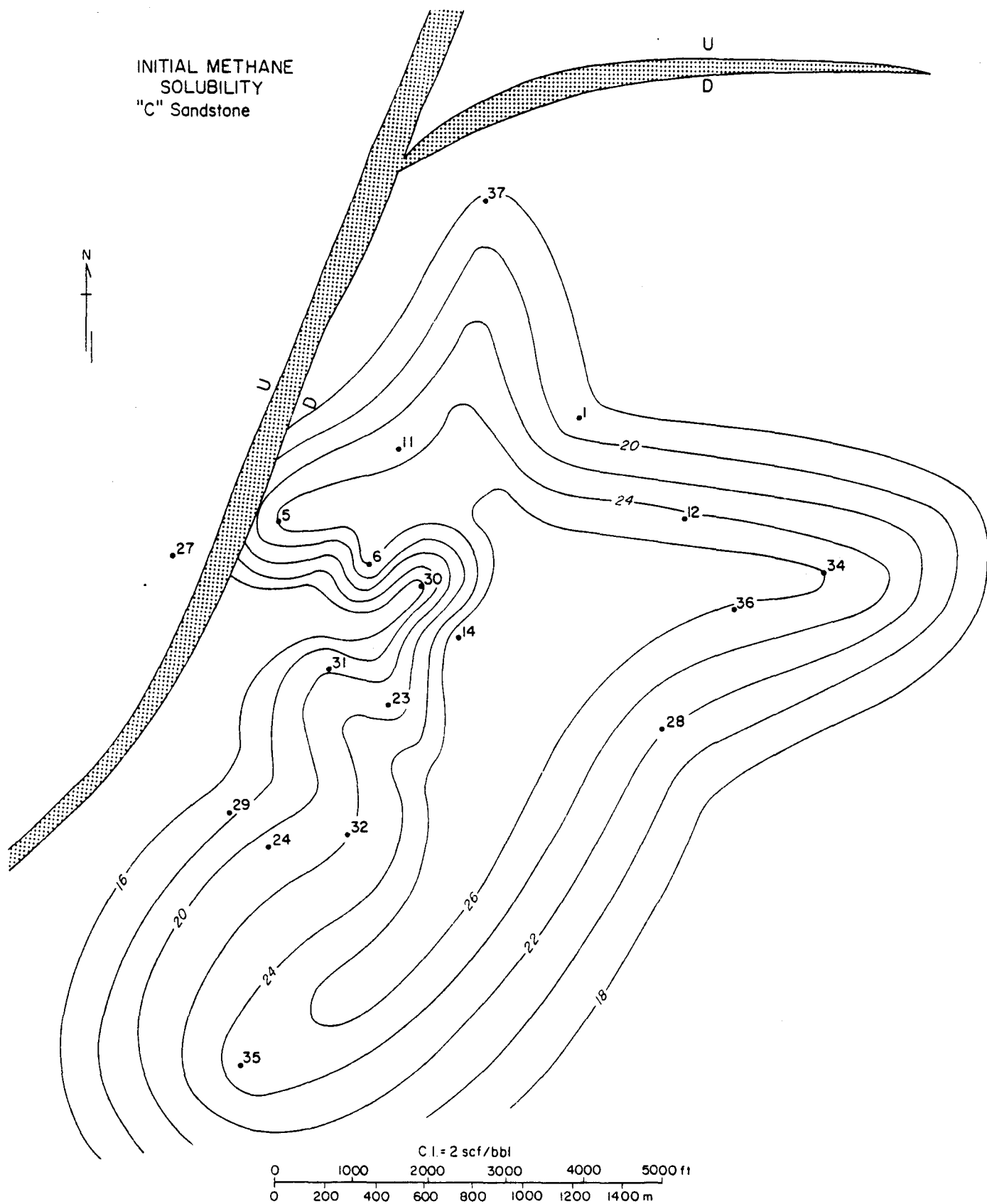
Figure 37. Distribution of initial methane solubility (scf/bbl), "C" sandstone, Port Arthur field.

60
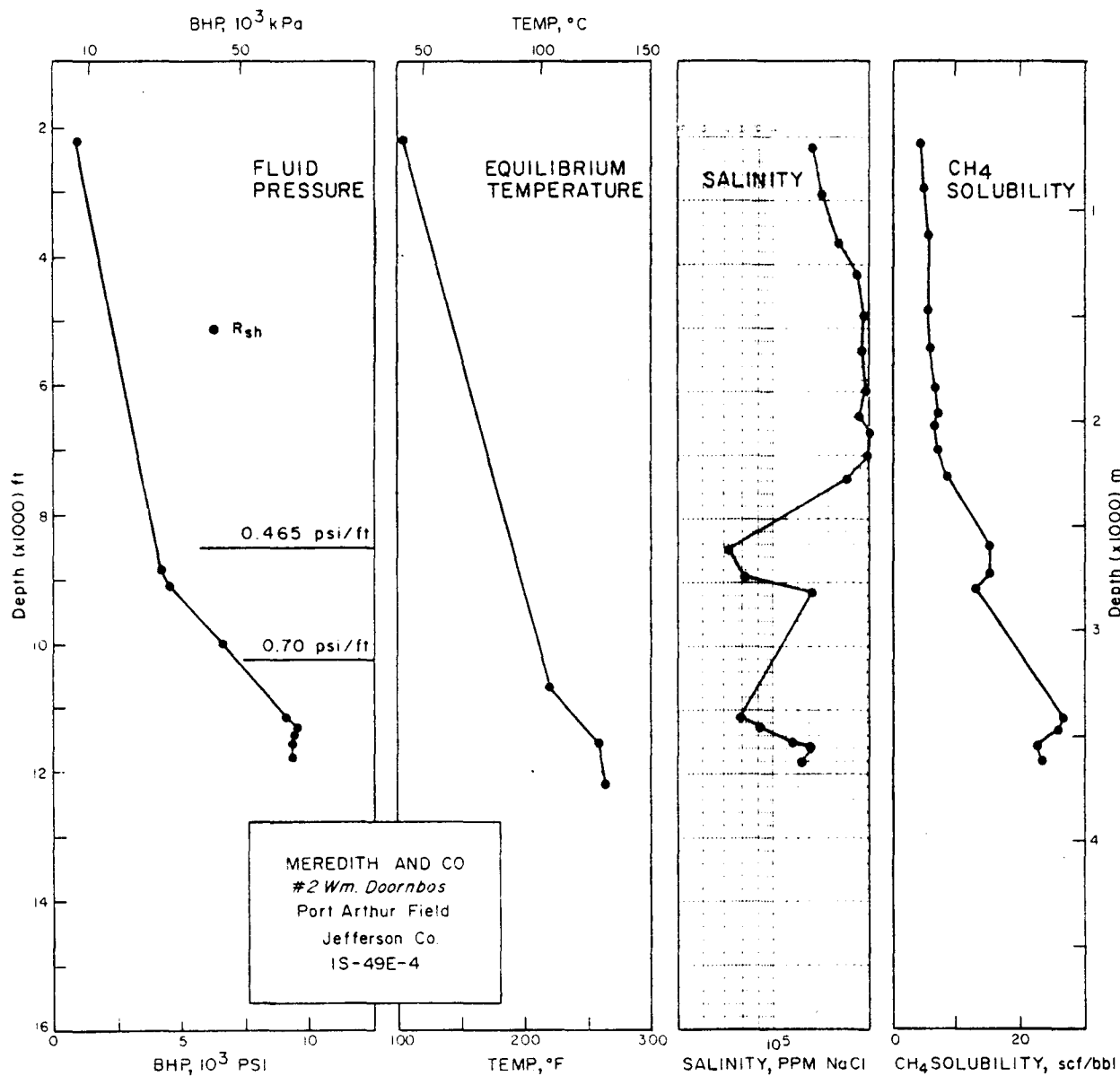
Figure 38. Pressure, temperature, salinity, and methane solubility versus depth, Well 14.

Table 7. Well 14 data: fluid pressure, equilibrium temperature, salinity, and methane solubility versus depth at original reservoir conditions, Meredith No. 2 Doornbos, Port Arthur field, Jefferson County, Texas.

Depth (ft)	Pressure (psi)	Pressure gradient (psi/ft)	Salinity (ppm NaCl)	Temperature (°F)	Methane solubility (scf/bbl)
2,200	1,023	0.465	134,000	104	4.4
2,920	1,358	0.465	144,000	113	5.0
3,650	1,697	0.465	162,000	125	5.3
4,160	1,934	0.465	187,000	135	5.1
4,800	2,232	0.465	195,000	142	5.4
5,350	2,488	0.465	193,000	150	5.9
6,000	2,790	0.465	196,000	161	6.3
6,400	2,976	0.465	189,000	166	6.9
6,600	3,069	0.465	204,000	169	6.5
7,000	3,255	0.465	200,000	175	6.9
7,350	3,418	0.465	174,000	179	8.2
8,480	3,943	0.465	72,300	195	15.2
9,120	4,560	0.500	135,000	203	12.5
11,150	9,255	0.830	80,000	244	26.8
11,250	9,338	0.830	90,100	247	26.0
11,360	9,656	0.850	91,900	252	26.7
11,470	9,520	0.830	116,000	256	24.0
11,550	9,471	0.820	130,000	259	22.7
11,800	9,440	0.800	124,000	261	23.5

substantial amount of free gas in addition to solution gas to make the drilling of a test well economically viable. The presence of multiple thick aquifers in the Hackberry sandstone units should simplify the task of finding reservoirs with suitable combinations of gas and water that will produce with a gas/brine ratio that greatly exceeds the solution gas/brine ratio.

During the production period, the amount of methane dissolved in formation waters decreases as reservoir pressures decline. An example is the "C" reservoir (11,136 to 11,144 ft) in the Meredith No. 2 Doornbos, where the bottom-hole flowing pressure decreased 24 percent over a period of about 10 yr. The corresponding decrease in methane solubility was 13 percent, changing from 26.5 scf/bbl in 1961 to 23.0 scf/bbl in 1971. It was assumed that reservoir temperature and formation water salinity remained constant at 243°F and 80,000 ppm NaCl, respectively.

Temperature and Pressure Gradients

Temperatures from well log headers were corrected to equilibrium values and plotted versus depth (fig. 39). A geothermal gradient of 2.58°F/100 ft was determined by least-squares fit to the temperature data on sand below a depth of 10,500 ft in the geopressured zone. The top of the lower Hackberry sandstones near the structural high occurs at an average depth of about 10,850 ft.

Temperature data from well logs in the Port Arthur field were very limited for sands at depths less than 10,500 ft. Additional temperature data from other wells in Jefferson County were used to extrapolate the temperature trend in the depth interval above 10,500 ft to a mean surface temperature of 72°F. A geothermal gradient of 1.3°F/100 ft was established for the shallow section.

The original formation fluid pressures in the Port Arthur field were obtained from bottom-hole shut-in pressures (BHSIP) measured by drill-stem tests (DST) and from shale resistivity (R_{sh}) data using the method of Hottmann and Johnson (1965). The top of geopressure in the lower Hackberry sandstones was estimated to be 8,900 ft by plotting BHSIP from DST versus depth and using average pressure gradients from shale resistivity data to extrapolate the trend line until it crosses the pressure gradient line of 0.465 psi/ft (fig. 40). Top of geopressure (8,900 ft) appears to be deeper in the Port Arthur field, compared with 8,000 ft estimated for Jefferson County (fig. 41).

Well Log Analyses

The main purpose of log analyses of Frio sandstones in the Port Arthur field was to provide a basis for determining porosity and the original gas-water contact (GWC) from

63
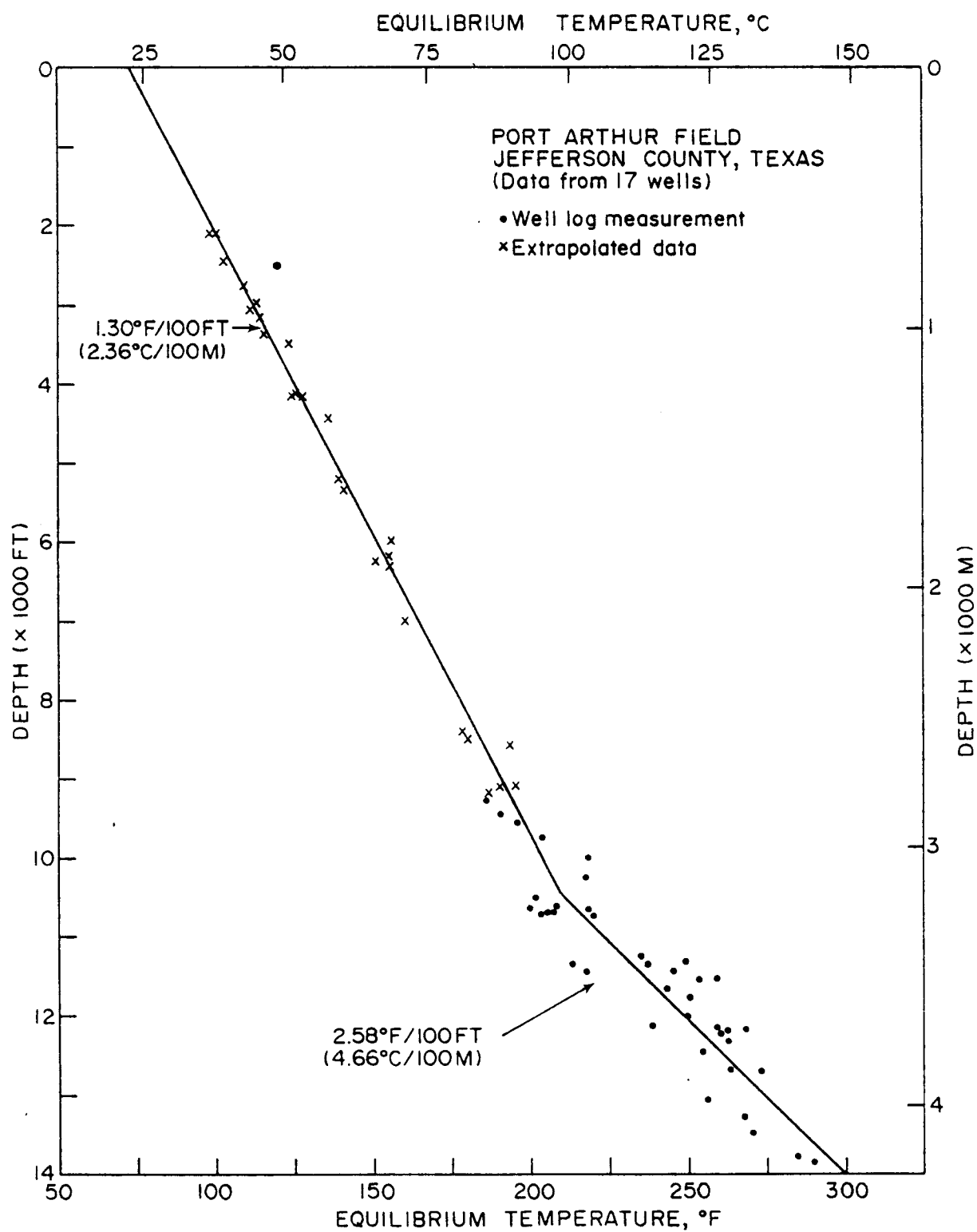
Figure 39. Geothermal gradients, Port Arthur field.
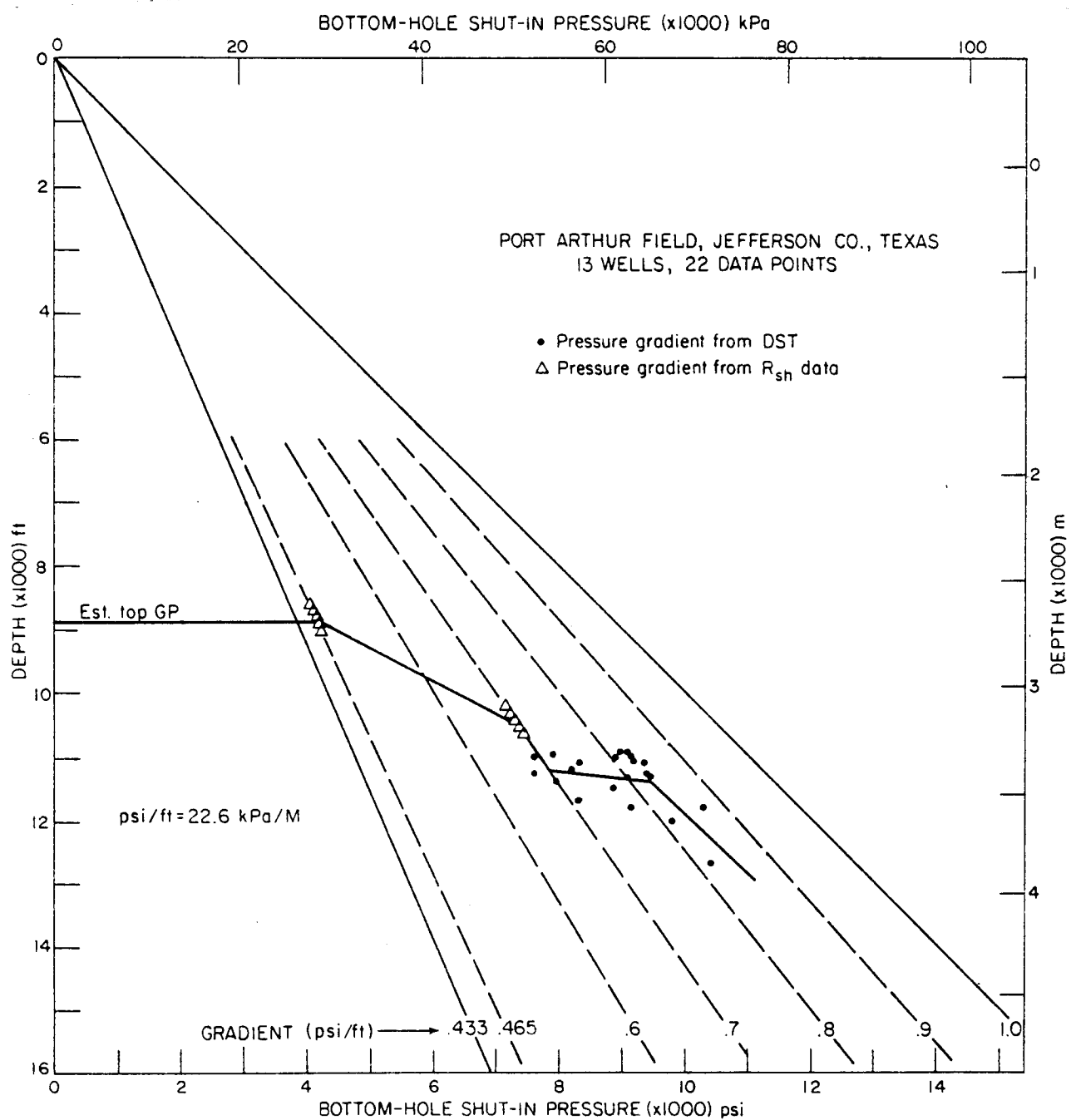
Figure 40. Bottom-hole shut-in pressure versus depth for 13 wells, Port Arthur field.
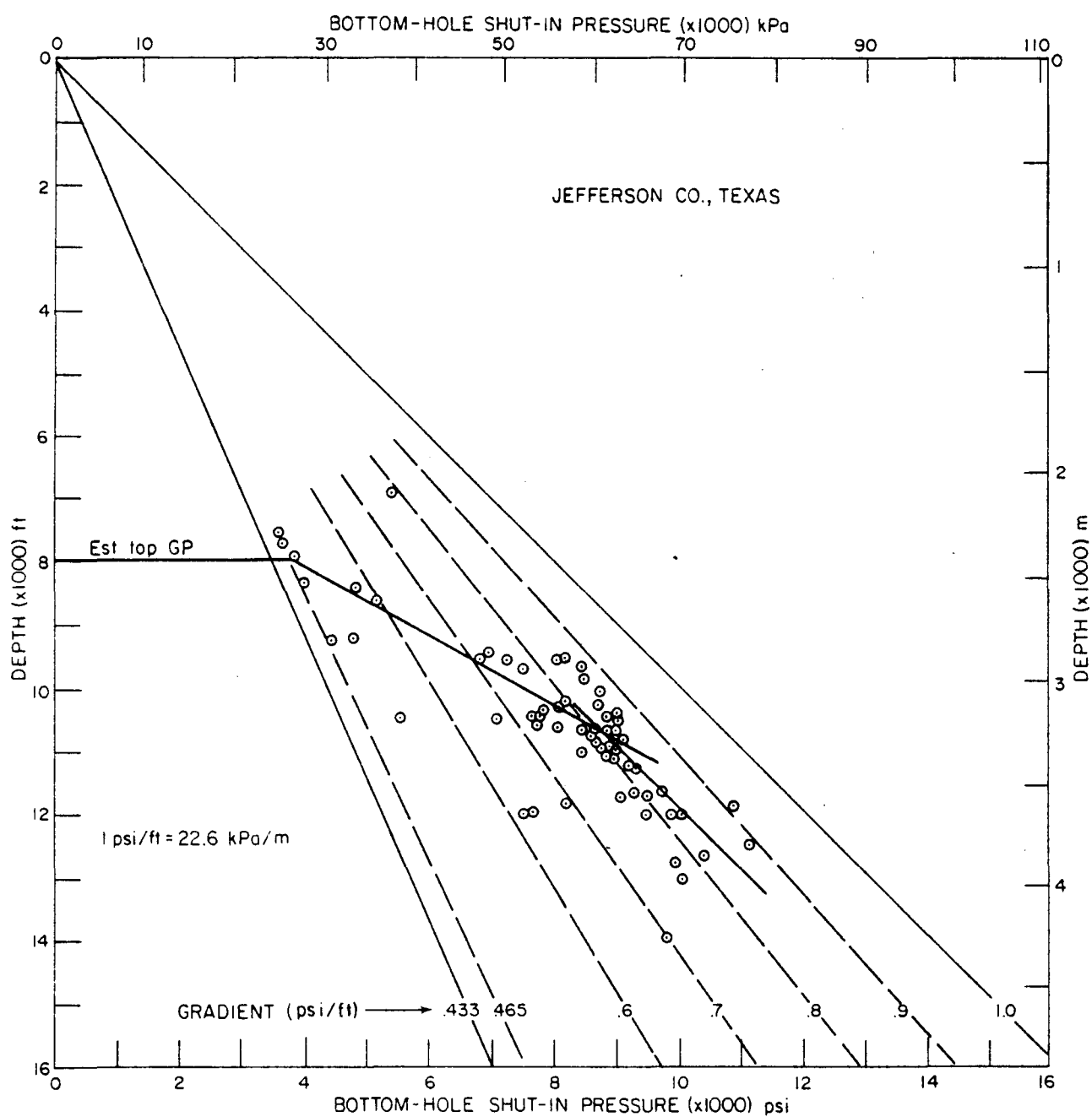
Figure 41. Bottom-hole shut-in pressure versus depth for wells in Jefferson County, Texas.

volumetric calculations. To do this, it was necessary to establish net gas sandstone thickness, porosity, and water saturation at each penetration of the "B-2," "C," "D," "E," "F," "G," and "H" sandstones. The major findings of this study (Ausburn and others, 1982) are summarized below; details of the computation methods and results are given in appendix D.

Only one porosity log was available for the field (sonic log for Well 37). The interval transit times and the correlative induction log resistivities provided a basis for estimating formation factor relationships. The apparent relationship between formation factor (F) and porosity ($\emptyset$) was found to be

$$F = 1.75 \times \emptyset^{-1.81} \tag{4}$$

and water saturation (S_w) was related to the resistivity ratio (R_o/R_t) by the equation

$$S_w = (R_o/R_t)^{-1/n} \tag{5}$$

where R_t = true resistivity of rock obtained from the induction log in the zone of interest, ohm-meters

   R_o = resistivity of rock obtained from the induction log in a zone that is interpreted to be 100-percent saturated with water, ohm-meters

   n = saturation exponent, assumed to be 1.8.

Using the established formation factor relation (equation 4) and resistivity values in zones interpreted to be wet (S_w = 100), it was possible to estimate porosity from resistivity values for zones near the intervals of interest in each well bore. For example, the porosity $\emptyset_w$ of the wet zone was computed from the relation

$$\emptyset_w = (aR_w/R_o)^{1/m} \tag{6}$$

where   a = 1.75

   m = 1.81

   R_w = resistivity of water computed from salinity data, ohm-meters.

These wet-zone porosities were usually assigned to nearby zones of interest, but sidewall core data, when available, were used as a guide in the assignments. A comparison of porosity distribution plots (fig. 42) shows that porosity from sidewall core data peaks at higher values than porosities from sonic log data or resistivity data.

The original gas-water contact (GWC) was determined by inspection of the computed values of S_w. When values of S_w were consistently above 65 percent, a possible GWC was noted. These individual well values were compared and the best estimate of GWC was determined by finding the subsea depth compatible with the individual well determinations and

67
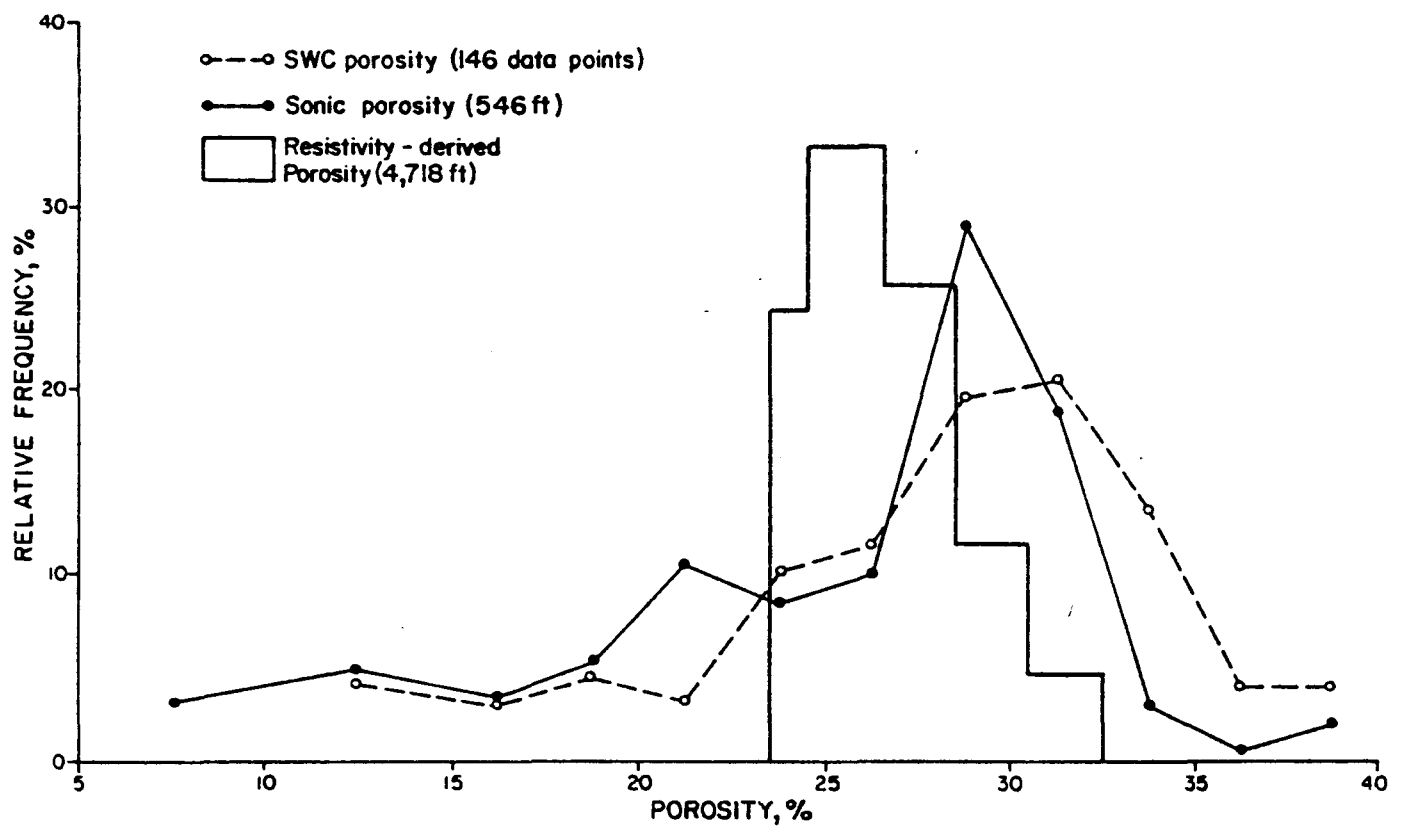
Figure 42. Porosity distribution, lower Hackberry sandstones, Port Arthur field.

existing structure and stratigraphic interpretations. The apparent original GWC was determined to be -11,150 ft for the "C" sandstone, as indicated on the structure map (fig. 30). The GWC in other sandstones ranges from 11,075 ft to 11,470 ft (table 8).

Values of net feet of gas in place obtained from the relation ($\emptyset$ h (1-S_w) = $\emptyset$ h S_g) are computed for each penetration and are listed in appendix D, part 3. These values were plotted on maps for each sandstone and then contoured and planimetered to obtain in-place gas volumes (appendix D, part 4). The in-place gas value for the "C" sandstone is 1,789 acre-ft. Dividing by the gas volume factor yields an estimated 26.24 Bscf in-place gas compared with 19.64 Bscf that was produced from this reservoir by conventional primary production methods. The apparent recovery efficiency of 74.8 percent is considerably higher than reservoir simulation studies (discussed later) indicate.

Seismic Data Acquisition and Processing

Seismic data were obtained for this project to (1) provide structural information to supplement geological interpretations in areas with poor well control, (2) determine location and geometry of faults, (3) locate boundaries of gas reservoirs and aquifers, and (4) evaluate seismic reflection response to low saturations of free gas dispersed in the water-invaded zones of watered-out gas reservoirs. The detection of low free-gas saturations of 5 percent or less seems to be possible from general theoretical considerations (Geertsma, 1961) and from laboratory velocity measurements (Domenico, 1976). Item 4 above was intended to address the crucial, basic question of whether dispersed gas can be detected in Tertiary sediments by real seismic data.

Seismic data for this project were purchased from data brokers and oil companies. This method is quick and relatively inexpensive but allows no control over acquisition parameters or quality. The data selected were the best that were available for purchase. The orientation of the seismic lines relative to the Port Arthur field is shown in figure 43. Several types of data were obtained, as listed below.

1. Line A was recorded in 1980, using a thumper as a source. The data were recorded with a 220-ft group interval and a 24-fold stack from a 48-trace cable.

2. Lines 1, 2, and 3 were recorded in 1973, using Vibroseis as a source (sweep 48-12 Hz). A 330-ft group interval, 24-trace cable developed a 12-fold stack.

3. Line B was recorded in 1979, using dynamite as a source (10 lb at 77 ft). A 330-ft group interval, 48-trace cable, and 12-fold stack were recorded.

4. Line 4 was recorded in 1969, using dynamite as a source (15 lb at 73 ft). A 300-ft group interval, 24-trace cable, and 6-fold stack were used.

Table 8. Summary of volumetric calculations.

Sand ID	Volumetric calculations							Remarks
	G. Fact.[1] 10^{-3}	P. Area[2] (acres)	AF[3] (acre-ft)	OGIP (Bcf)	OOIP (bbl)	R.E.[4] (%)	GWC subsea	
B_2	2.80	800.7	896.1	13.941	752,800	95.7	11075	R.E. too high
C	2.97	855.9	1,886.7	27.672	1,205,375	49.7	11150	
D	2.86	449.4	962.3	14.657	580,400	50.8	11240	
E	2.88	422.4	674.6	10.203	538,736	40.5	11296	88 Mbbls condensate for Well 14, back calculation results in 1.66 Bcf additional gas
E_L	2.94							
		400.2	640.4	9.488	342,530	65.8	11368	Combination of lower "E" and "F" sands
F	2.94							
G	2.95	294.2	302.7	4.470	175,212	10.0	11470	
H								No hydrocarbons detected
TOTAL			5,362.8	80.431	3,595,053			

[1]G. Fact. = gas volume factor

[2]P. Area = area circumscribed by zero gas contour

[3]Acre-ft of gas at reservoir conditions. One acre-ft = 43,560 ft^3

[4]Apparent recovery efficiency
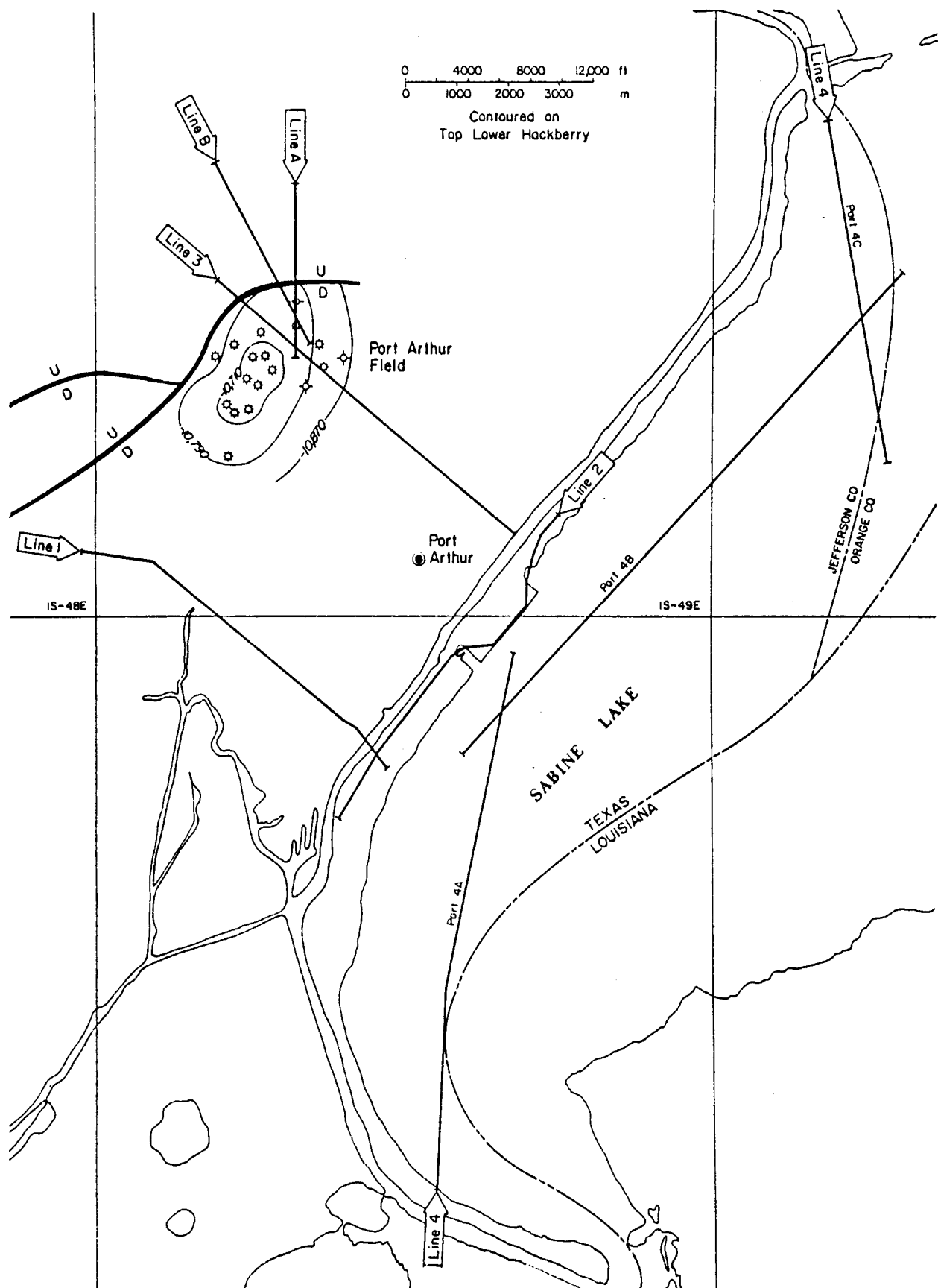
Figure 43. Location of seismic lines in the Port Arthur area and structure contour map of top of lower Hackberry in the Port Arthur field.

This wide variation in source, geometry, and stack fold results in appreciable differences in data quality, particularly when a broad-band spectral content is needed for detailed stratigraphic interpretation. Wavelet processing was used to compensate for source differences and the resulting character differences.

Data processing* was done to improve the interpretation of seismic sections. The first approach was to shape the wavelet to a narrow, symmetrical form and the second was to migrate the data to enhance lateral resolution. The processing sequence (listed below) was intended to produce seismic sections with a near-zero-phase wavelet having the broadest spectral content that can be supported with the signal-to-noise ratio of the data.

1. Demultiplexing
2. Correlating, if needed
3. Applying a gain-leveling function
4. Trace-to-trace normalization
5. Field statics and geometry corrections
6. Sorting to CDP gathers
7. Velocity determination (one per km)
8. Residual static corrections
9. Stacking
10. Deconvolution (predictive)
11. Time variant statistical wavelet enhancement
12. Migration
13. Conversion to relative acoustic impedance sections

The objective of enhancing resolution by broadening the spectral bandwidth and by migration was severely hampered by the very poor signal-to-noise ratio in the data. Data quality was adequate for structural interpretation but was not suitable for detailed reservoir delineation or detection of gas zones.

Seismic Modeling

Seismic modeling was used to show what kind of seismic response should be expected from known subsurface geology. Only limited well data were available for predicting acoustic properties. Thus the modeling effort focused on demonstrating the detectability of

---

*The data processing and seismic modeling were done by GeoQuest International, Inc. This discussion is a summary of the more detailed report by Meanley (1982).

reservoir details in synthetic seismic data and relating these data to the real seismic data, where possible. The modeling was done for varying conditions of bandwidth, noise, and rock velocities.

The subsurface geologic model (fig. 44) was developed from well data. The thick beds of lower Hackberry sandstones were correlated from well to well and projected onto the line of section that coincides with seismic line 3. The projection was guided by structure maps prepared on sand tops. Locations of the five wells (top of fig. 44) closest to seismic line 3 are shown in figure 30. The velocities assigned to the beds were derived in part from the sonic log of the Kilroy No. 1 Booz (Well 37). Different gas sandstone velocities were assumed in the five models (fig. 44) because of the uncertainty of the values of this important parameter. Density was computed from the relation developed by Gardner and others (1974). The uncertainty of density was included in the velocity uncertainty where determining acoustic impedance values for gas zones.

The modeled synthetic sections discussed below can be compared directly with the corresponding portion of seismic line 3 (fig. 45). The real seismic data are very noisy and have poor reflection coherence. The interpreted top of the "C" sandstone does not roll over into the major fault as much as the geologic model suggests.

The effects of bandwidth are examined in the synthetic seismic sections of figures 46, 47, and 48. Each bed boundary of the geologic model (fig. 44) is represented by a spike that is two samples (2 ms) wide (fig. 46). The spikes are very broad-band (0-500 Hz) and represent the ultimate resolution for the sample rate used. The amplitudes and polarities of the reflection coefficients at each bed boundary and each fluid contact are indicated by the size and sign of the spikes. The location of gas sandstones is shown by the shaded zones (fig. 46). The Butterworth bandpass wavelets used in each synthetic section are shown at CDP 205 near the time of 2.97 seconds.

Synthetic sections, based on bed velocities in model 1, were made in part to show the effect of increasing the bandwidth (with no noise) from 15-45 Hz (fig. 47) to 15-65 Hz (fig. 48). It is clear that the broader bandwidth data with higher resolution and no noise (fig. 48) bring out details that are essential to reservoir delineation. However, it is still not possible to map the reservoirs or to determine the lateral extent of hydrocarbon zones. The only clear indication of gas is the dimming of the reflection from the top of the "C" sandstone over the crest of the structure. This is caused by the reduction of velocity contrast with respect to the overlying shales. The gas sandstone velocity (9,500 ft/sec) is intermediate between the water sandstone velocity (11,000 ft/sec) and the shale velocity (9,000 ft/sec), as specified in model 1 (fig. 44). In the real seismic data (fig. 45) there is no clear indication of amplitude reduction (dimming);
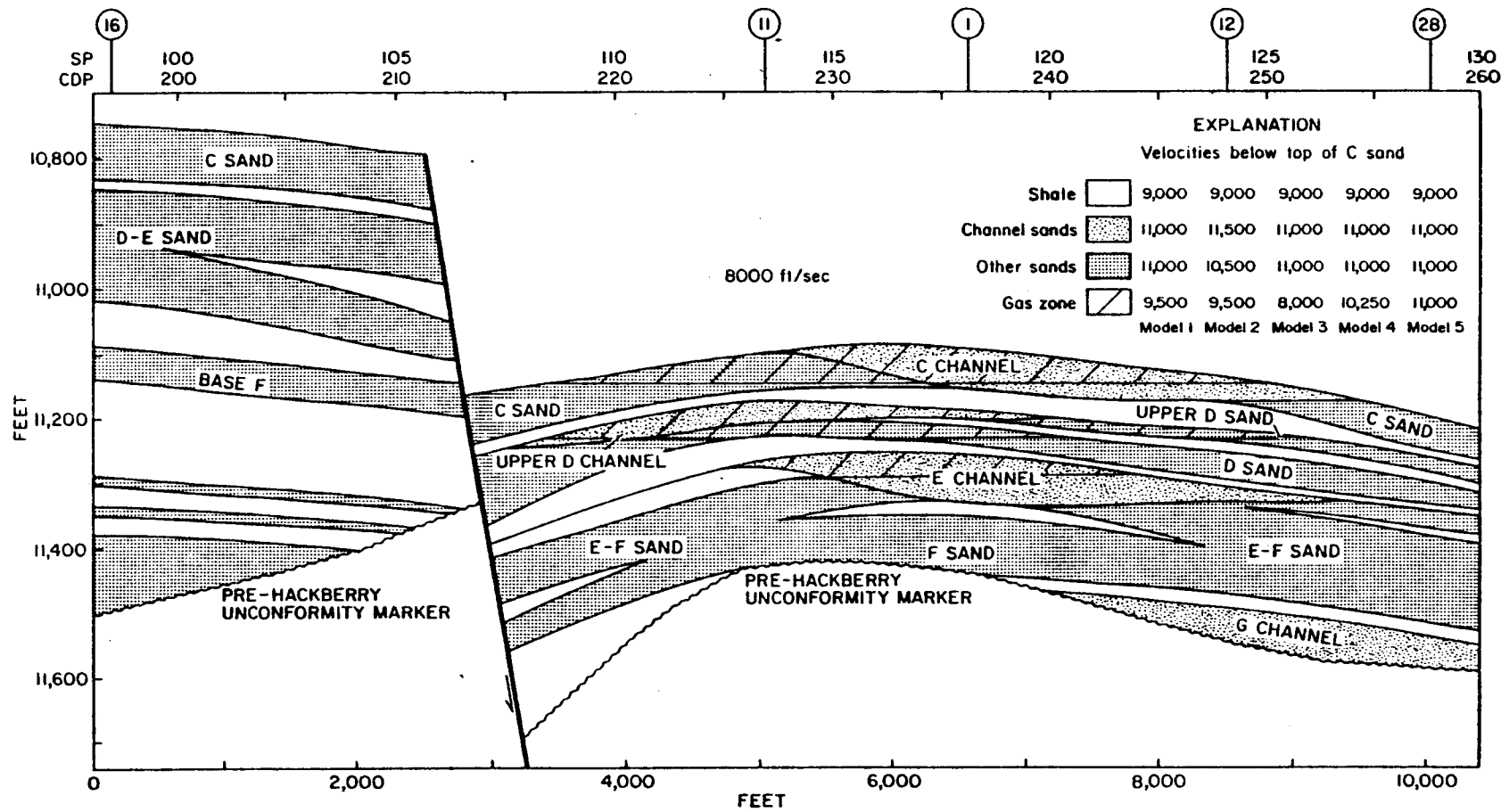
Figure 44. Model of the Hackberry sands along a cross section following seismic line 3.
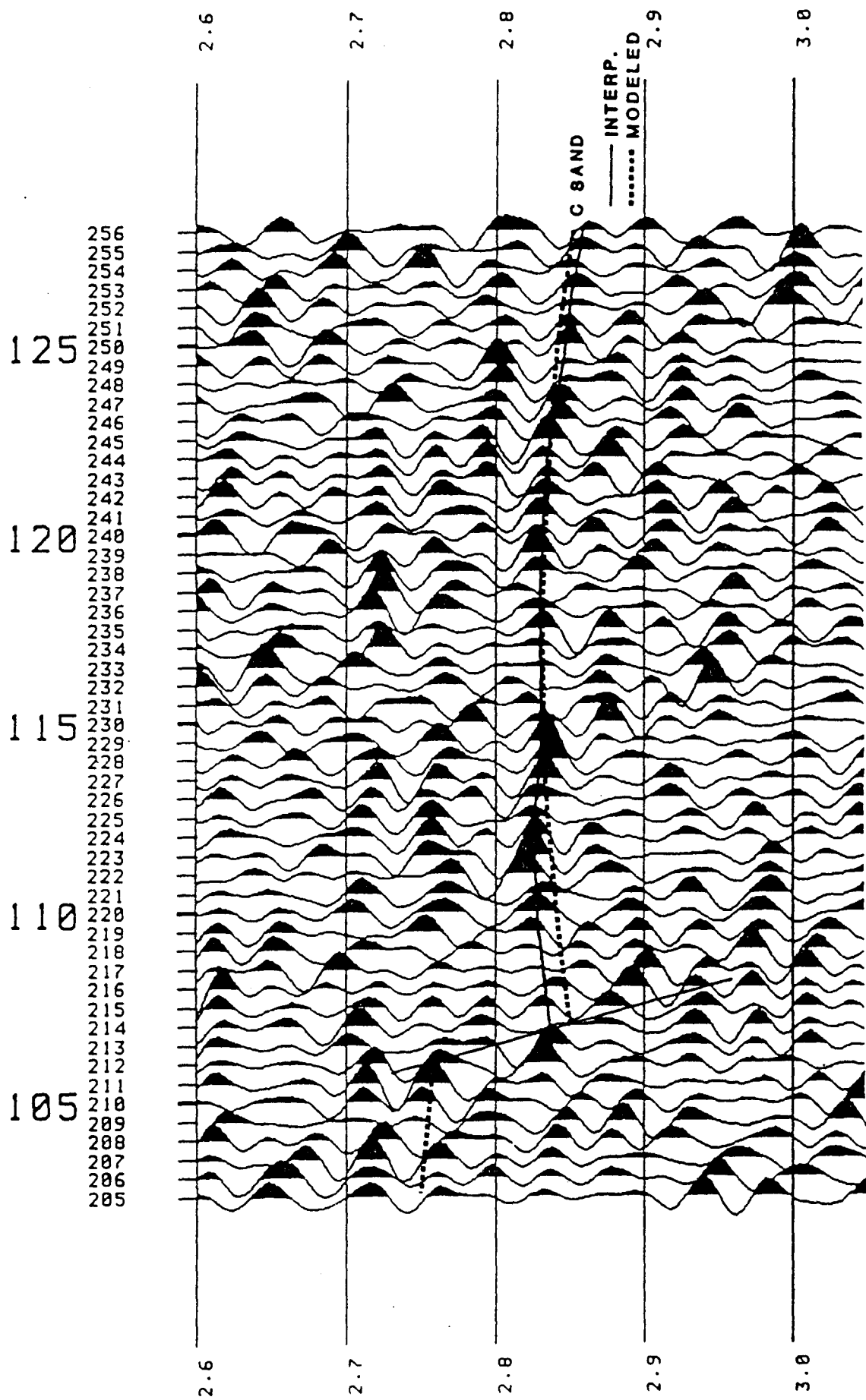
Figure 45. Line 3 showing interpreted and modeled top of "C" sandstone.
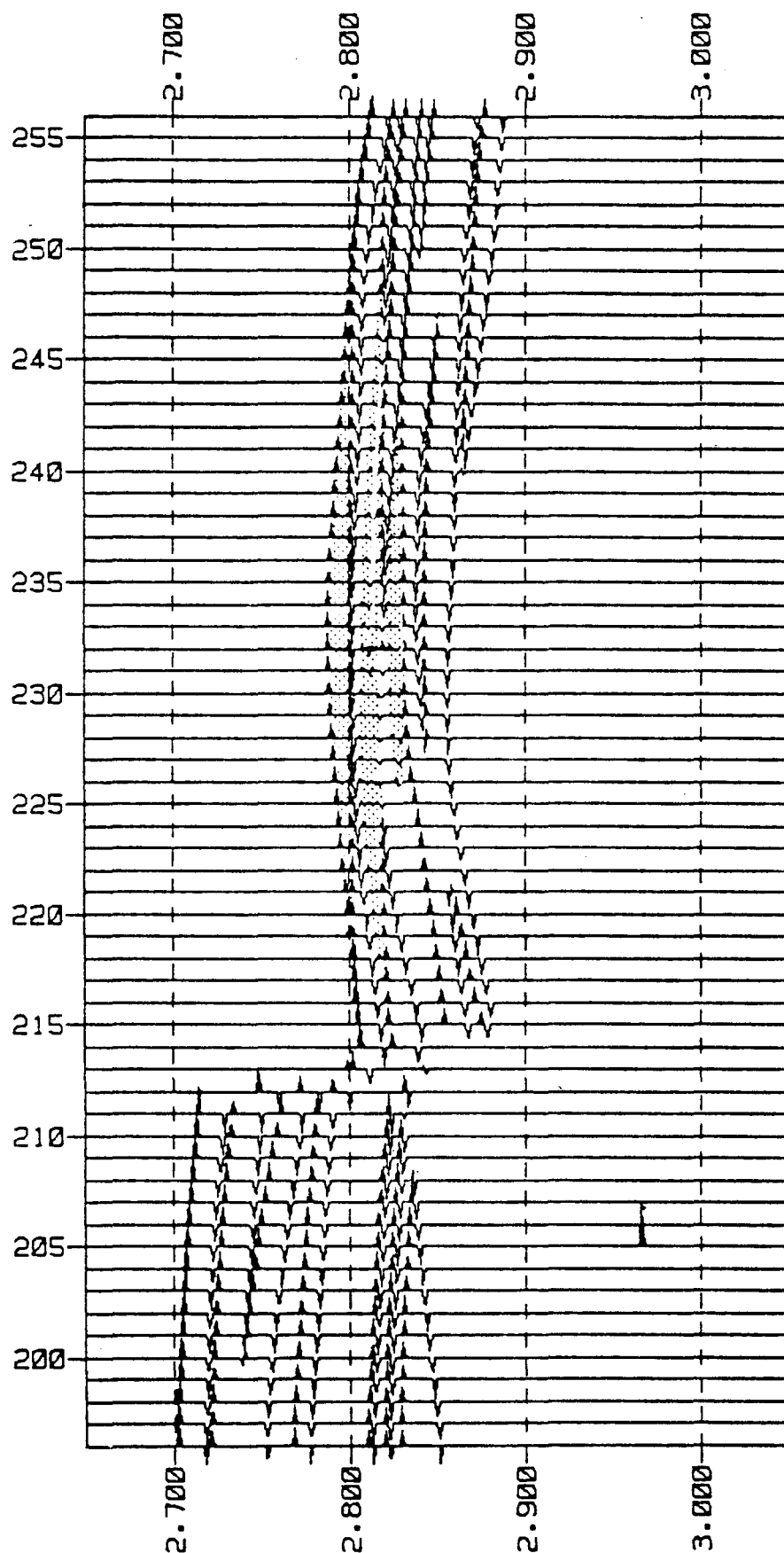
Figure 46. Spike synthetic seismic section with gas sands shaded (model 1).
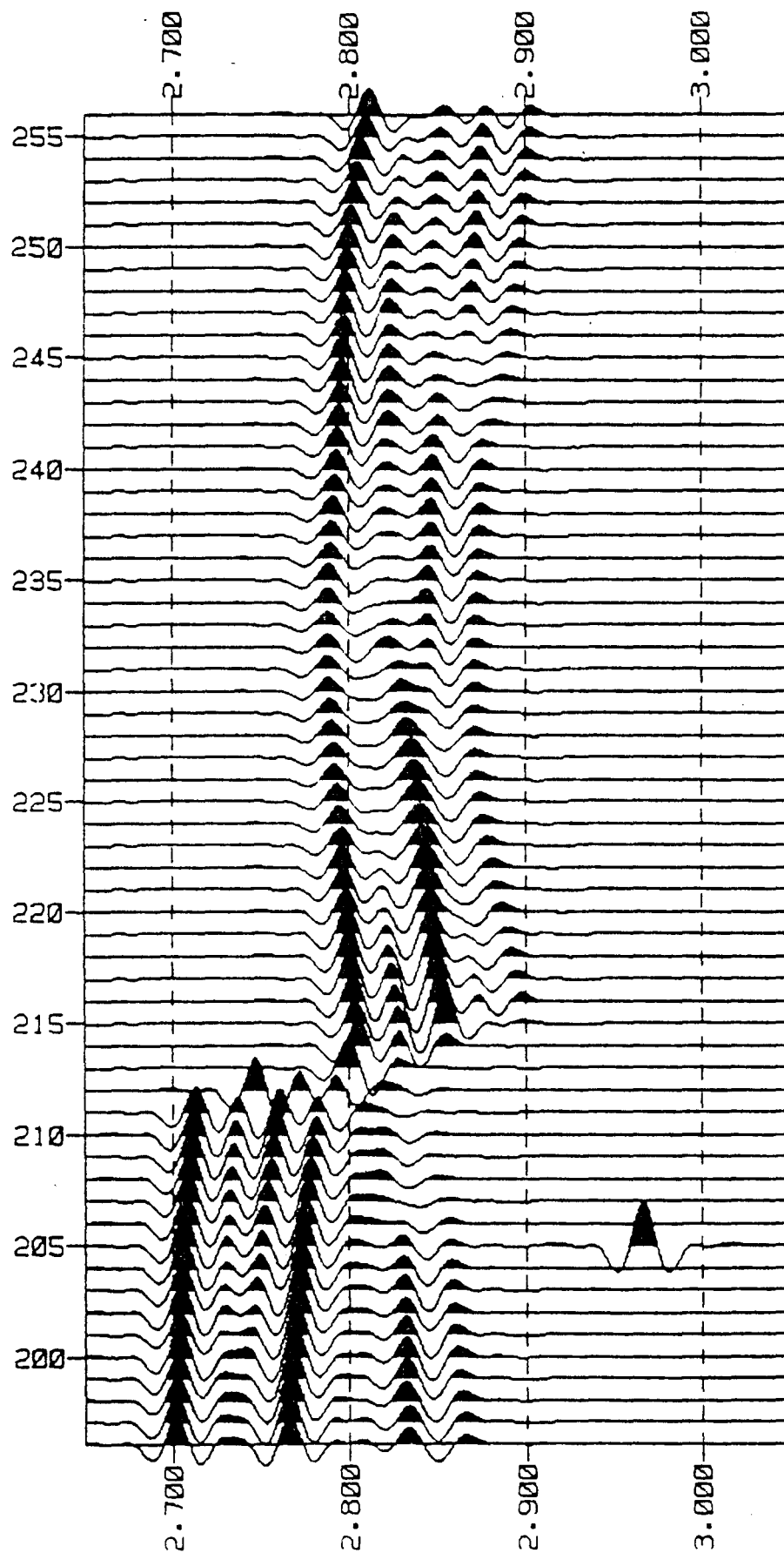
Figure 47. Synthetic seismic section with wavelet bandpass = 15-45 Hz (model 1).
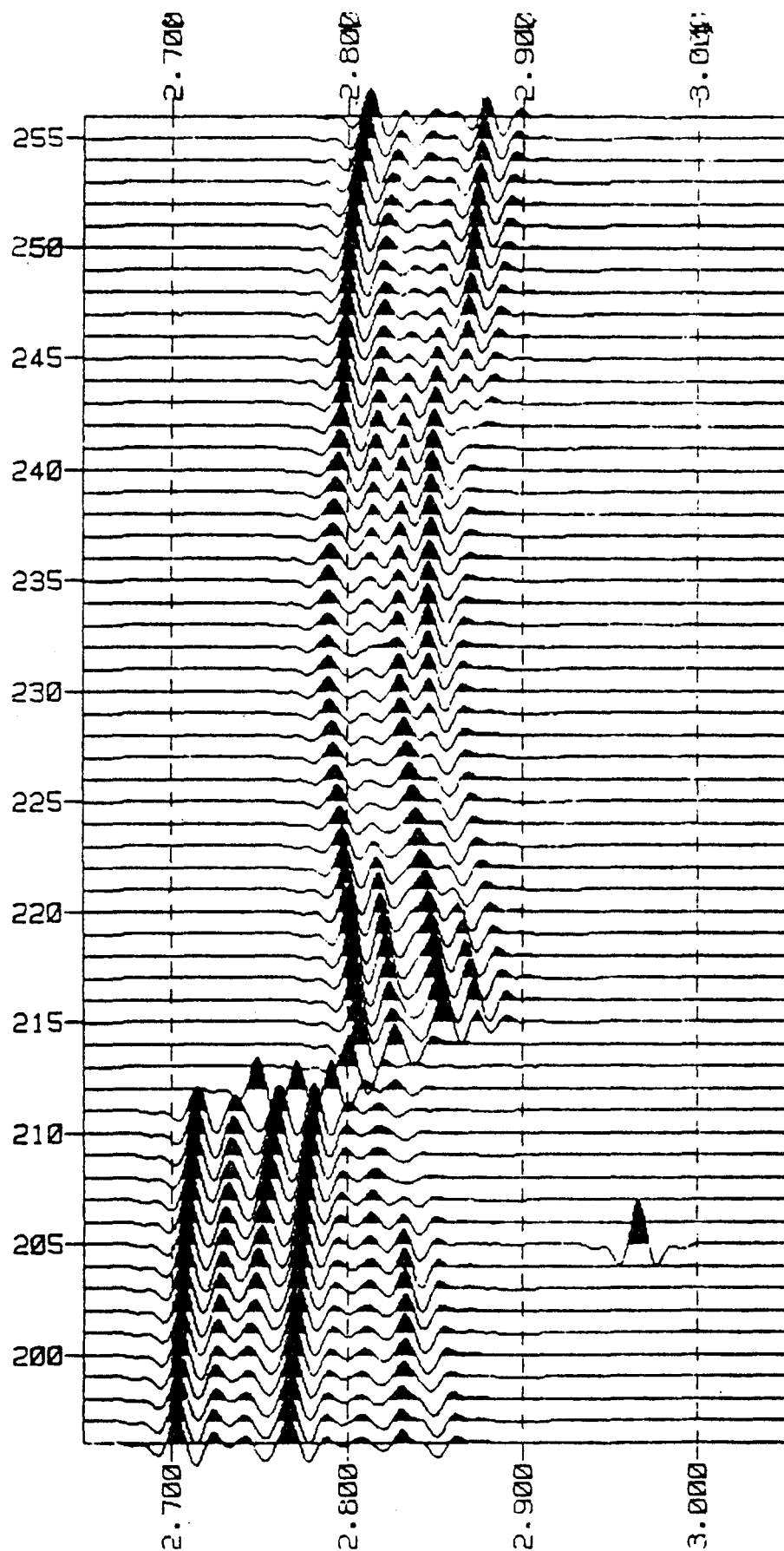
Figure 48. Synthetic seismic section with wavelet bandpass = 15-65 Hz (model 1).

only noise fluctuations occur. A second dim zone in the synthetic sections occurs at the structural crest of the central portion of the reservoir complex at a time of 2.82 seconds. This dimming feature simply shows that the acoustic contrasts approach zero here. A reduction of amplitude (dimming) can also be caused by thinning of the reservoir bed or by contamination by non-reservoir rock. These other causes of dimming introduce ambiguity and complicate the interpretation. The only classic hydrocarbon indicator present in these synthetic sections is the flat spot at the base of the "E" sandstone at 2.83 seconds (fig. 48). The flat spot just below the "E" sandstone is a shale stringer, not a fluid contact.

The addition of noise to the synthetic seismic sections reduces the detectability of reservoir details. The noise is measured here as the ratio of the largest signal amplitude (the amplitude of the wavelet) to the RMS value of the noise. For the signal-to-noise ratio of 25.1 (28 db), a bandpass of 15-45 Hz and velocity data of model 1 (fig. 49) illustrate that essential reservoir elements found in the noise-free section (fig. 47) are still discernible. As more noise is added (fig. 50), the usefulness of the section for modeling purposes deteriorates drastically. The section now begins to look like the real seismic section in figure 45. This suggests that the noise level in the real data is four times the maximum tolerable level for modeling.

Detectability in synthetic sections with broader bandwidth (15-85 Hz) seems to be affected less by noise because of higher resolution and the decline of destructive interference from adjacent beds. However, the improvement in detectability is not dramatic and no classic indicators of gas sands, fluid contacts, or phase changes are obvious. The presence of gas has more subtle features, which can only be verified in this case by comparing different velocity models with the seismic data.

Five velocity models (fig. 44) are considered by Meanley (1982). Different assumptions about bed velocities are made and their effect on the synthetic sections is observed. This approach is useful for understanding how important the knowledge of acoustic impedances is to the detection of reservoir elements. It was found that changing the velocities of channel sandstones and other sandstones (model 2) had little effect on the synthetic sections. Changing the gas sandstone velocity had a much greater effect.

In model 4 the gas sandstone velocity was increased from 9,500 ft/sec to 10,250 ft/sec. The difference between the gas sandstone and the water sandstone (11,000 ft/sec) decreases while the difference between gas sandstone and shale (9,000 ft/sec) increases. The resulting synthetic section (fig. 51) exhibits relatively small and subtle changes when compared with figure 48. The presence of gas causes less loss of amplitude at the tops of the "C" and "D" sandstones and reduces the amplitude of the flat spot (fluid contact) on the third black cycle.

79
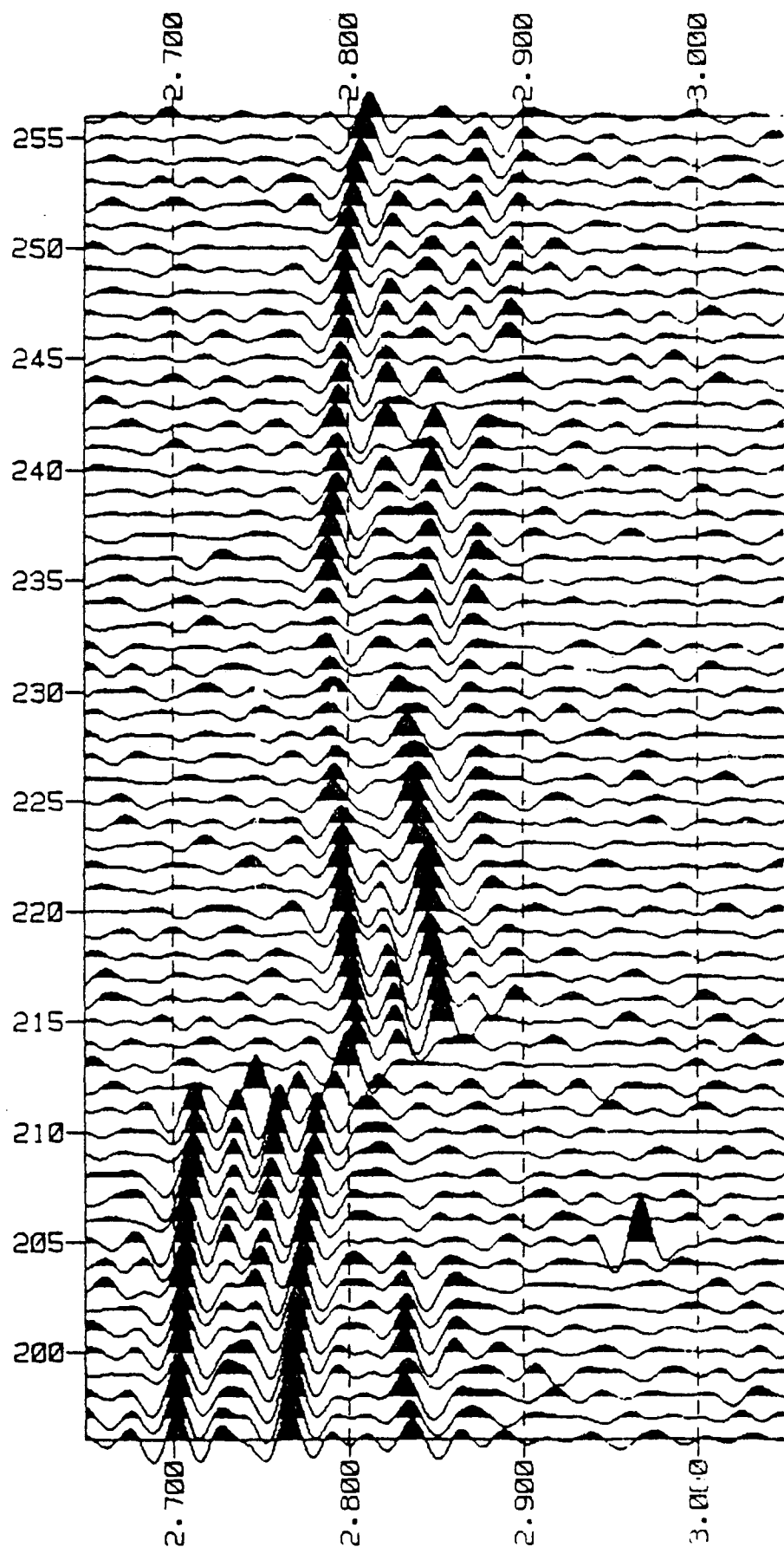
Figure 49. Synthetic seismic section with signal-to-noise = 25.1 (bandpass = 15-45 Hz, model 1).
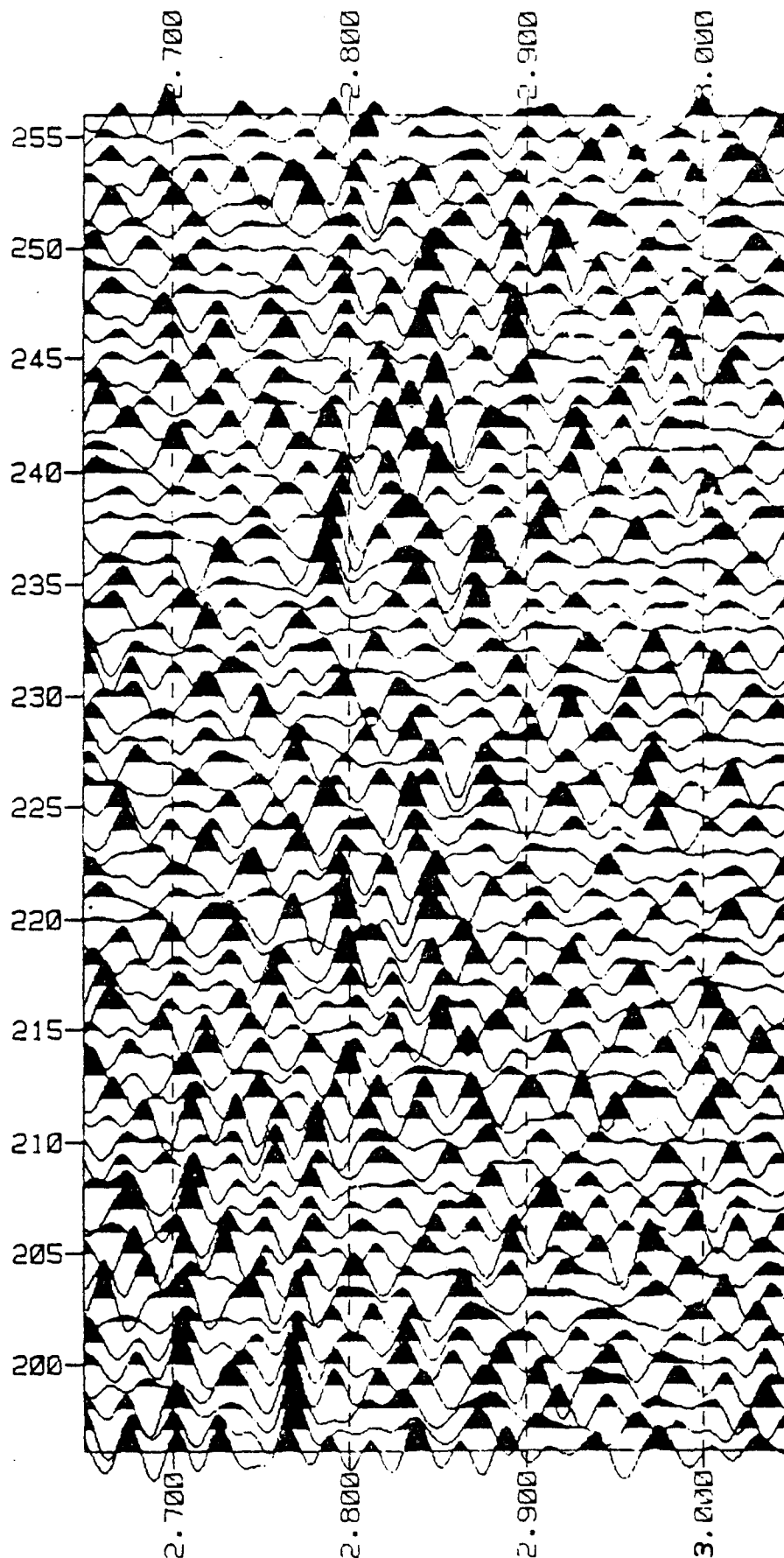
Figure 50. Synthetic seismic section with signal-to-noise = 6.3 (bandpass = 15-45 Hz, model 1).

81
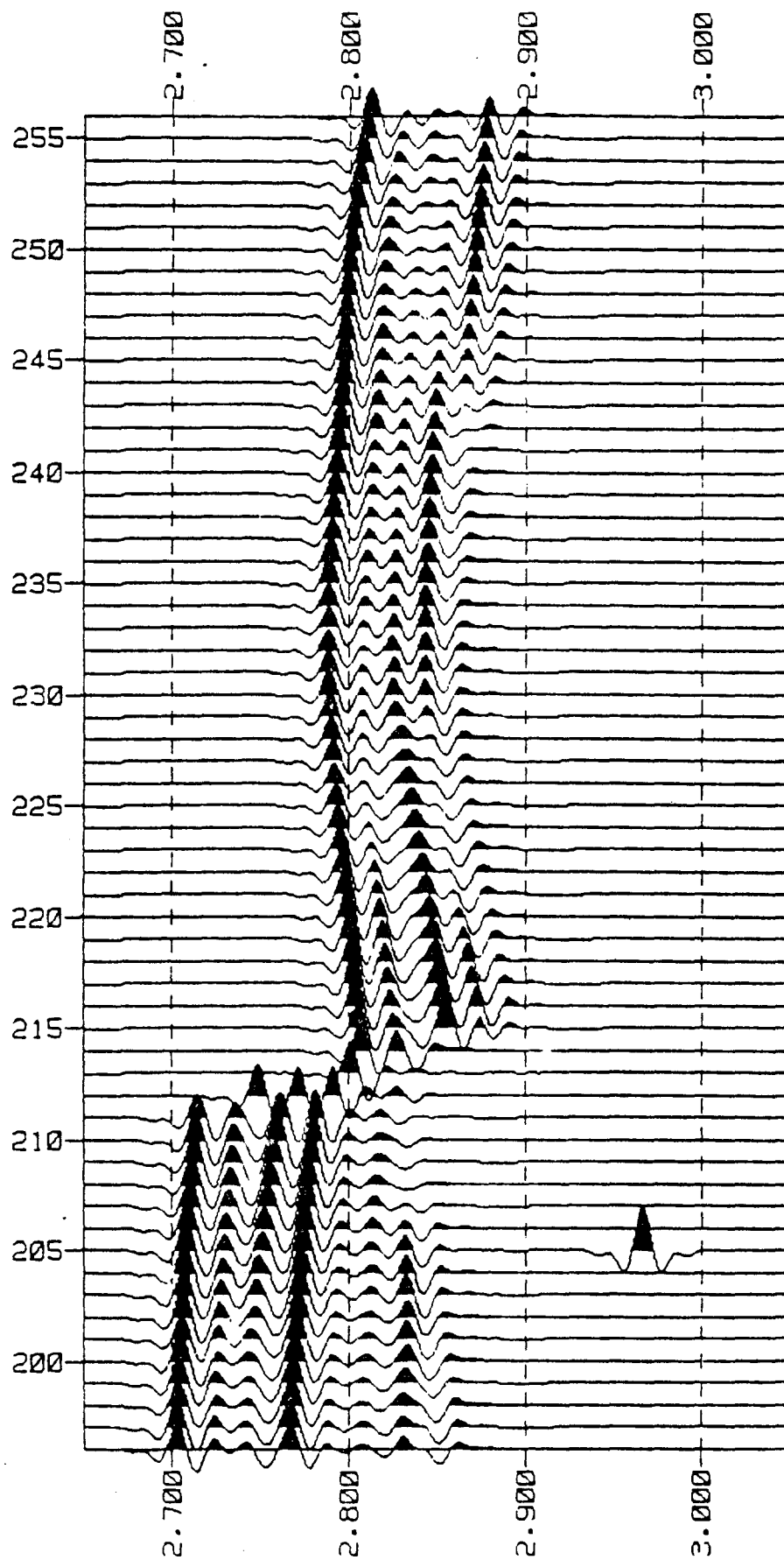
Figure 51. Synthetic seismic section with gas sand velocity = 10,250 ft/sec, model 4 (bandpass = 15-65 Hz).

Other factors, such as sidelobes from different reflectors and the gas-water contact in the "E" sandstone, also contribute to the observed changes in reflection amplitudes.

It is interesting to compare two extreme cases represented by model 3, which has a gas sand velocity of 8,000 ft/sec (fig. 52), and model 5, which has no gas present in the reservoir (fig. 53). In model 3 the top of the "C" sandstone is lost because there is no contrast in acoustic impedance with the upper shale. The "D" and "E" sandstones are more visible because the largest amplitudes are associated with the gas (fig. 52). In model 5 (fig. 53) the reflectors look strong and continuous. Amplitude changes can be related to the coming and going of shale stringers. Comparing this section to model 1 with a gas sandstone velocity of 9,500 ft/sec (fig. 48), the clues to the presence of hydrocarbons become more evident. These clues consist of the dimming of the top cycle, the central dim spot, and the fluid contact.

The modeling has been instructive in showing the possibilities of better reservoir delineation with increased bandwidth, improved signal-to-noise ratio, and better knowledge of reservoir acoustic impedances. In general, the noise level in the real seismic data precludes the detection of gas and reservoir details in the synthetic seismic data. The models also show that the thin reservoir beds and rapid lateral variations cause problems which challenge the seismic state-of-the-art for detailed reservoir delineation in the Port Arthur field. Thus, the question posed at the beginning of this study as to whether dispersed gas in a watered-out gas reservoir can be detected in seismic data remains unanswered.

The final question concerning the type of seismic data that would be needed to see reservoir details desired in studies of this nature is answered as follows: (1) a signal-to-noise level of four times that observed in seismic line 3 must be achieved; (2) a bandwidth of 10 to 85 Hz would be satisfactory but may not be possible; (3) dynamite would be the best source for both signal strength and static corrections but may not be practical due to cultural features of the environment; and (4) recording of the shot signature with a special uphole geophone would improve the wavelet processing. In planning a new seismic survey, many different field parameters and geometries must be considered to provide maximum data quality and resolution in the zone of interest. For a discussion of these parameters, the reader is referred to Denham (1981).

Production History

The discovery well drilled by Meredith et al. (the No. 1 Doornbos, fig. 30) encountered gas condensate in several lower Hackberry sandstones and in a deeper Nodosaria sandstone. Later development of the field identified 24 separate reservoirs; 14 of these were productive in different wells during the life of the field. The productive reservoirs include thick sandstones
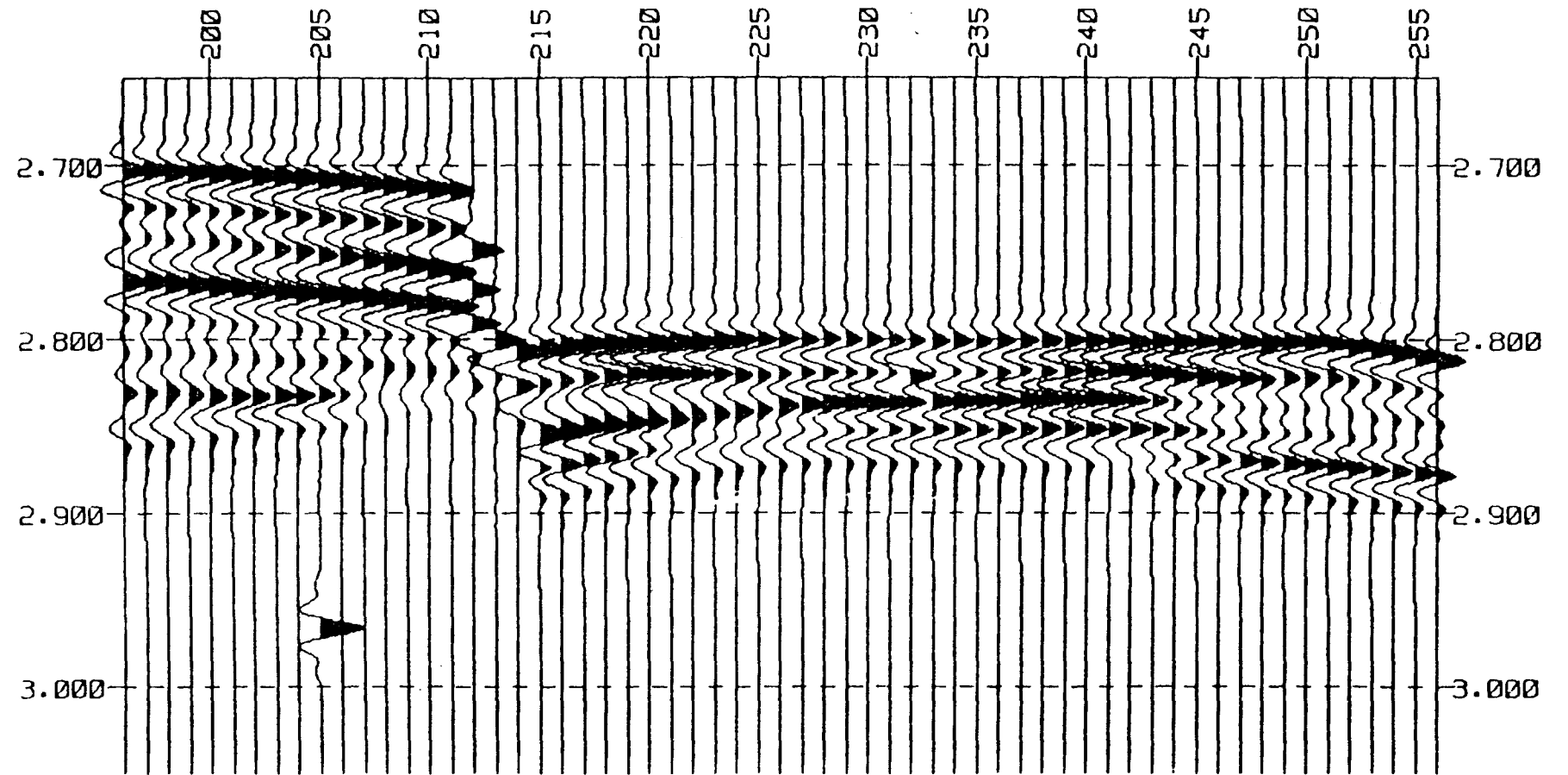
Figure 52. Synthetic seismic section with low velocity gas sand = 8,000 ft/sec, model 3 (bandpass = 15-65 Hz). Compare this figure to figure 48.
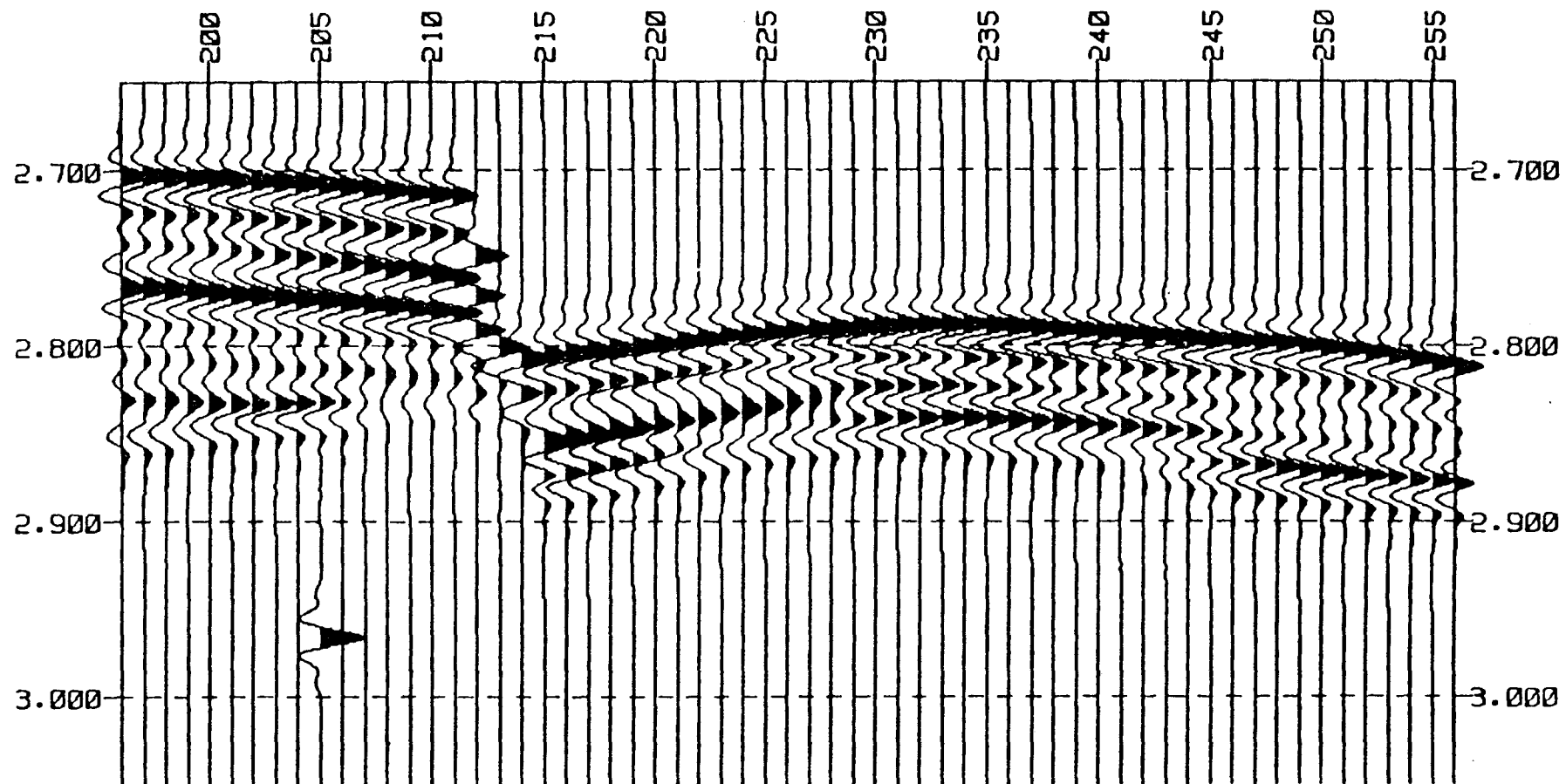
Figure 53. Synthetic seismic section with no gas, model 5 (bandpass = 15–65 Hz).

with gas caps and thin stringer sandstones saturated with gas (fig. 54). Of the 18 wells drilled in the Port Arthur field, 10 wells produced a total of 57.1 Bcf of gas and 2.65 MMbbl of condensate from lower Hackberry sandstones during the primary production period (1959 to 1981).

The "C" Reservoir

The "C" reservoir was chosen for detailed study because of high abandonment pressure, excellent reservoir quality, high productivity, and good lateral continuity. Cumulative production from the "C" reservoir was 19.6 Bcf (table 9). Well 14 produced 54 percent of the gas and 53 percent of the condensate from the depth interval from 11,136 to 11,144 ft over a period of about 11 years (July 1961 to July 1972). The well was plugged and abandoned in October 1972.

Table 9. Cumulative production from "C" reservoir, Port Arthur field.

Well no.*	Original operator and well name	Gas (Bcf)	Condensate oil (Mbbl)
14	Meredith No. 2 Doornbos	10.535	456
23	Kilroy & MPS, No. 1 Doornbos	1.250	38
11	Meredith No. 4 Doornbos	7.754	366
6	Meredith No. 3 Doornbos	0.099	2
	Total	19.638	862

*Location of wells shown in figure 30.

Peak production of hydrocarbons from Well 14 occurred between 1961 and 1965 when water production increased rapidly and peaked at 1,400 bbl/d (fig. 55). The bottom-hole flowing pressure decreased from 9,115 psi in 1961 to about 6,632 psi in 1971. A plot of P/Z versus cumulative gas production does not give a straight line and cannot be used to estimate the original gas in place because of substantial water production and encroachment of water into the gas reservoir. Using reservoir simulation studies that are discussed later in this report, the OGIP was estimated to be 56.2 Bcf.

86
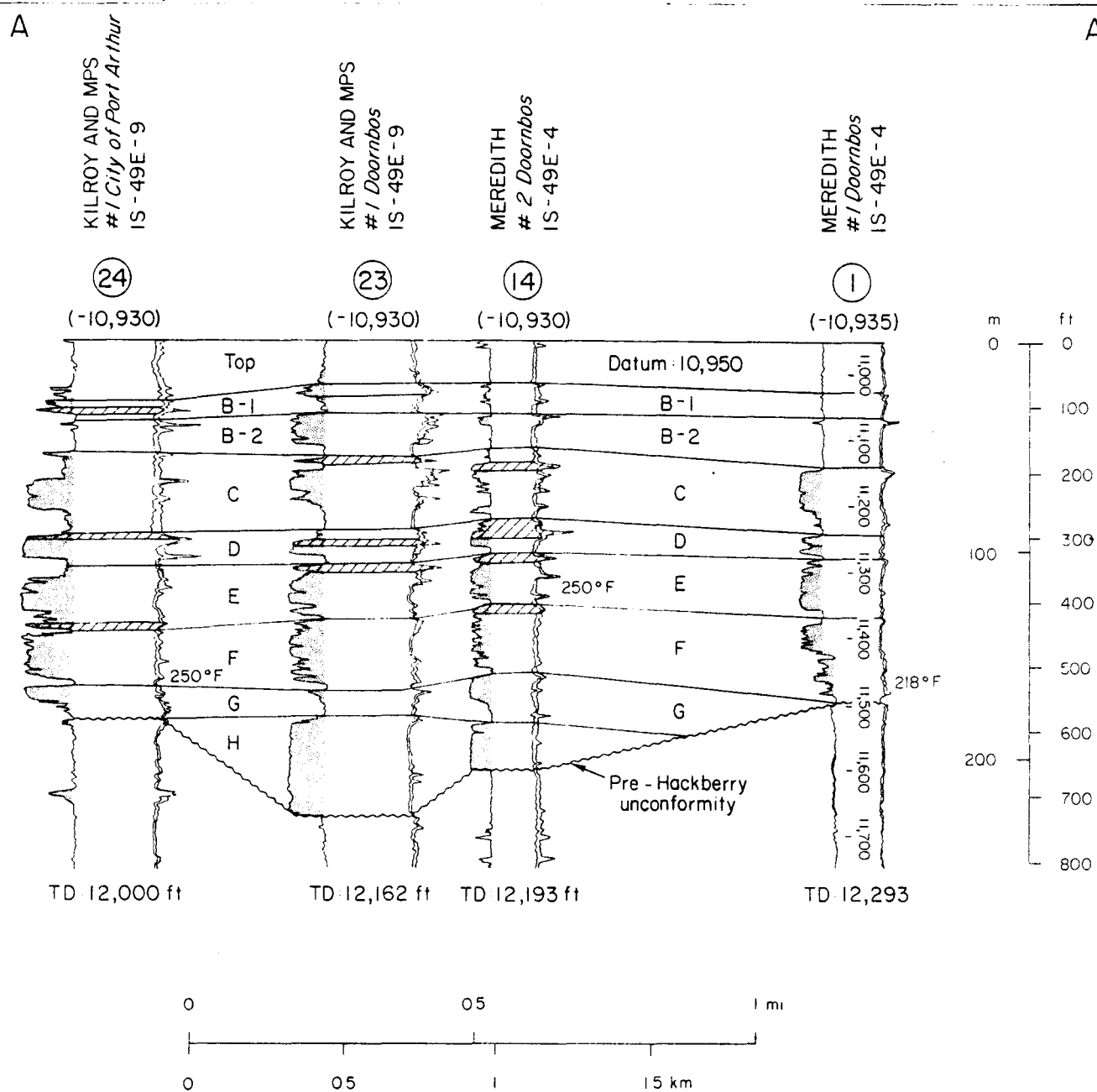
Figure 54. Structural strike section A-A' showing lower Hackberry sandstone intervals and perforated gas production zones (hachured intervals), Port Arthur field. Line of section shown in figure 30.
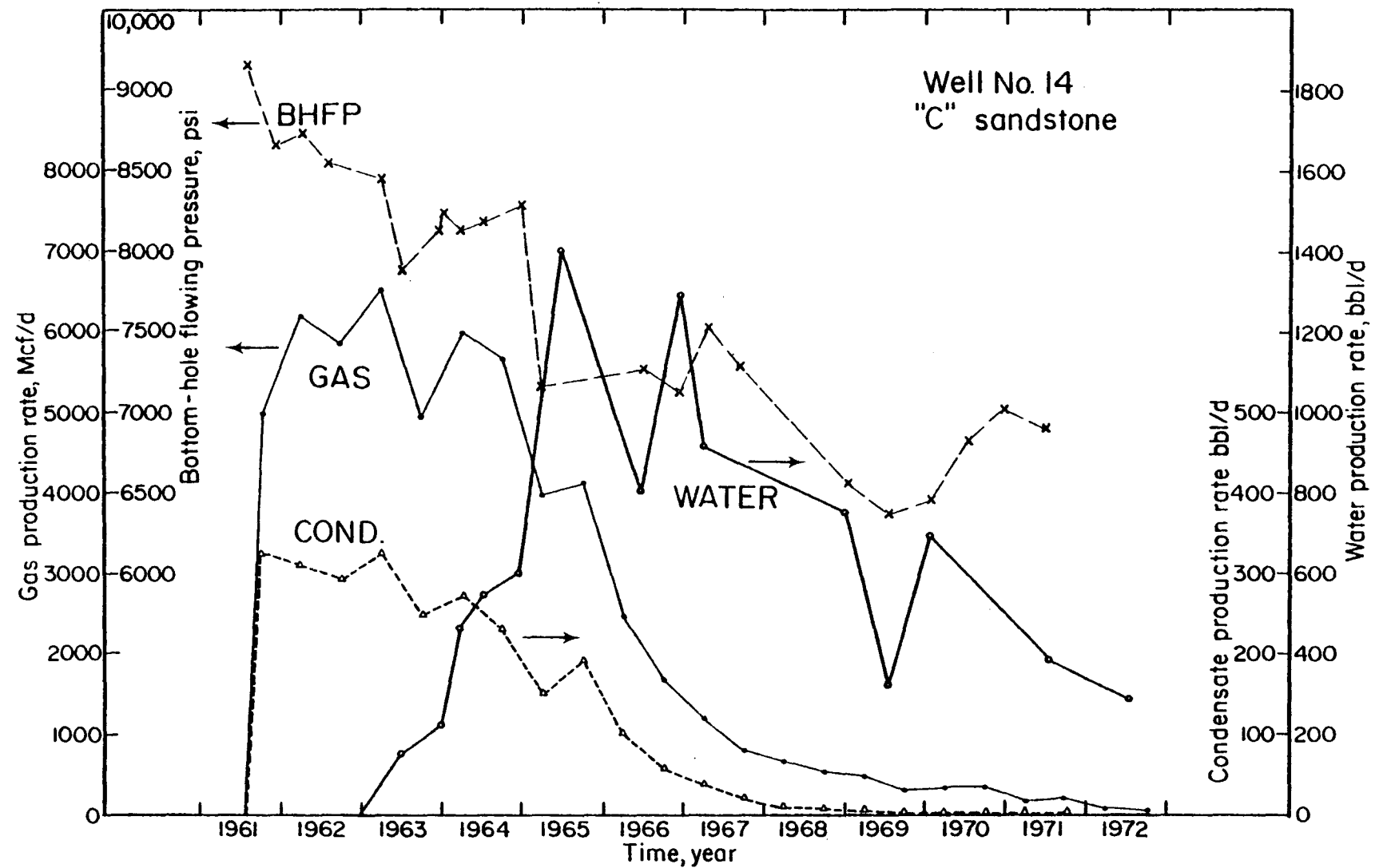
Figure 55. Reservoir production rates and bottom-hole flowing pressure versus time, "C" sandstone, Well 14, Port Arthur field.

Other Reservoirs

Several other lower Hackberry reservoirs ("A-1" through "F") produced enough hydrocarbons to merit some attention in evaluating the Port Arthur field as an EGR prospect. Collectively these other reservoirs contributed 66 percent of the gas and 68 percent of the condensate that was produced from the field during primary production. Some of these reservoirs are lenticular and have limited lateral continuity; however, they may have sufficient production potential to influence the economic feasibility of an EGR test. For example, the "B-2" reservoir produced more than 13 Bcf of gas (table 4) from 1959 to 1966 in Well 31. The last recorded bottom-hole shut-in pressure gradients (table 4) indicate that some of these reservoirs were geopressured when abandoned. Salinity, pressure, temperature, and methane solubility data are listed in table 6. Structure and isopach maps for other reservoirs appear elsewhere in this report (figs. 18 to 28, 31, 32), and sidewall core data are in appendix C. Results of well log analysis of most of these reservoirs ("B-2" through "H" sandstones) are included in appendix D.

A new well drilled near the top of the structure at the specified test site location near Well 14 (fig. 30) in the Port Arthur field would offer numerous potentially productive lower Hackberry sandstones for testing and completion programs. An alternate drill site located about 200 ft from Well 31 along a line connecting Wells 31 and 14 would give a better exposure of the "B-2" sandstone. If a new well is drilled deeper, a Nodosaria sandstone and the Vicksburg interval would become potential producers.

Predicted Reservoir Performance and Economic Analysis

Reservoir Simulation Studies

The objective of this work was to predict the amount of gas that can be produced from the "C" reservoir by drilling a new well and co-producing the gas and gas-saturated reservoir brine. A numerical reservoir simulator model was used to approximate the physical characteristics of the reservoir by matching the production history. Future reservoir behavior can then be predicted by the model.

Three independent studies were made to increase the credibility of results. These studies were carried out by (1) Wattenbarger and Associates (W&A), (2) Lewis Technical Services, Inc. (LTS), and (3) the Bureau of Economic Geology (BEG).

A two-dimensional gas-water simulator was used by W&A and three dimensional gas-water simulators were used by LTS and BEG. The Cartesian coordinate system was used in all three simulators. The W&A simulator made use of pseudo relative permeability curves, which allow a two-dimensional simulator to model three-dimensional fluid flow (Coats and others, 1967;

89

Hearn, 1971). The simulators used by LTS and BEG are the same; only the input parameters differ.

Simulator Grids

The model grid used by W&A (fig. 56) and the grid used by LTS and BEG (fig. 57) represent the "C" sandstone and include both the gas reservoir and its contiguous aquifer. A small block size was used to represent reservoir variations in the area of initial gas saturation, whereas a coarser grid was used to represent aquifers away from the gas cap. An overall grid dimension of 10 x 13 blocks is shown; however, certain blocks were deleted from the active system (fig. 57, hachured area) because some areas are not in communication with the primary area of interest. Elevation and thickness values were assigned to individual blocks by overlaying the grid on the isopach map (fig. 29) and structure map (fig. 30) for the "C" sandstone.

In all three studies, only Wells 14 and 23 were modeled, although four wells actually produced from the "C" sandstone. Well 6 was not modeled because it produced a negligible amount of gas, whereas Well 11 was deleted because it has a limited drainage area and had poor interconnection to the area of interest. There appears to be some geological support for believing that the "C" sandstone in Well 11 is not in communication with the "C" sandstone in Wells 14 and 23. The SP characterization study of the "C" sandstone, discussed earlier, shows that Well 11 intersects a proximal suprafan facies whereas Wells 14 and 23 intersect a broad fan channel-fill facies. The "C" sandstone is a composite of smaller sand bodies, each deposited in sedimentary environments of limited extent; the individual sand bodies may or may not be in communication.

Model Data and History Matches

The same basic field data were used for these reservoir simulation studies; however, different interpretations were made when converting field data to input data for the simulator. For example, the LTS simulation study used extrapolated formation pressures (bottom-hole static pressures), whereas calculated bottom-hole flowing pressures were used by W&A and BEG.

The model data used in the three simulation studies are shown in table 10. The large differences between the values of original water in place are caused by the different areas that are assumed for the "C" sandstone and the different values of porosity and water saturation assigned to the gas cap and aquifer. There are also substantial differences in the distributions assumed for permeability. W&A assumes that a constant permeability of 60 md exists throughout the "C" sandstone. LTS assumed that there are two sharp, narrow permeability barriers (fig. 58). Inserting the barriers is an attempt to account for the lack of good communication between Wells 14 and 23 and the restriction in aquifer support to Well 23 which

90
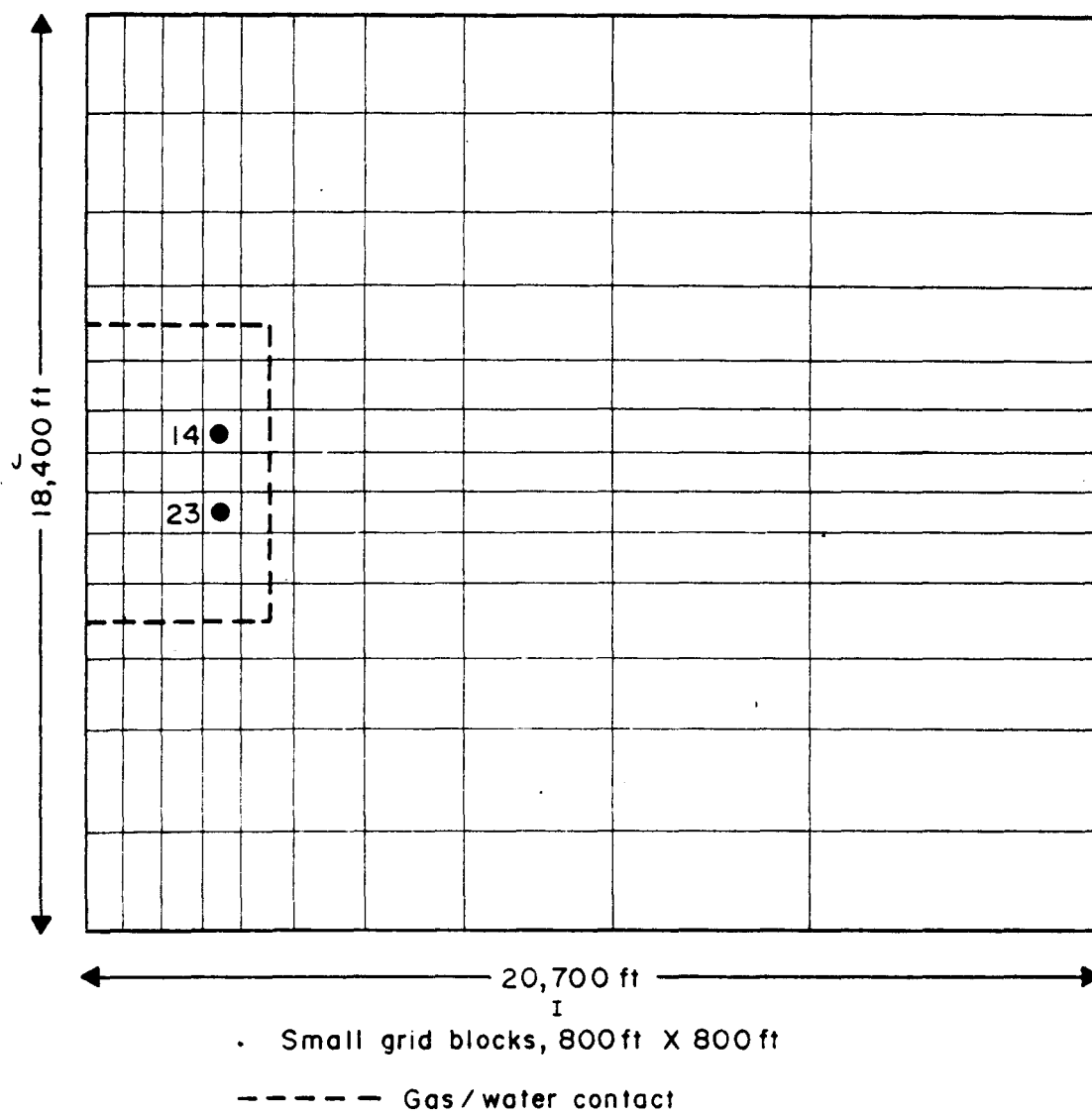
Figure 56. Simulator grid used by W&A.

91
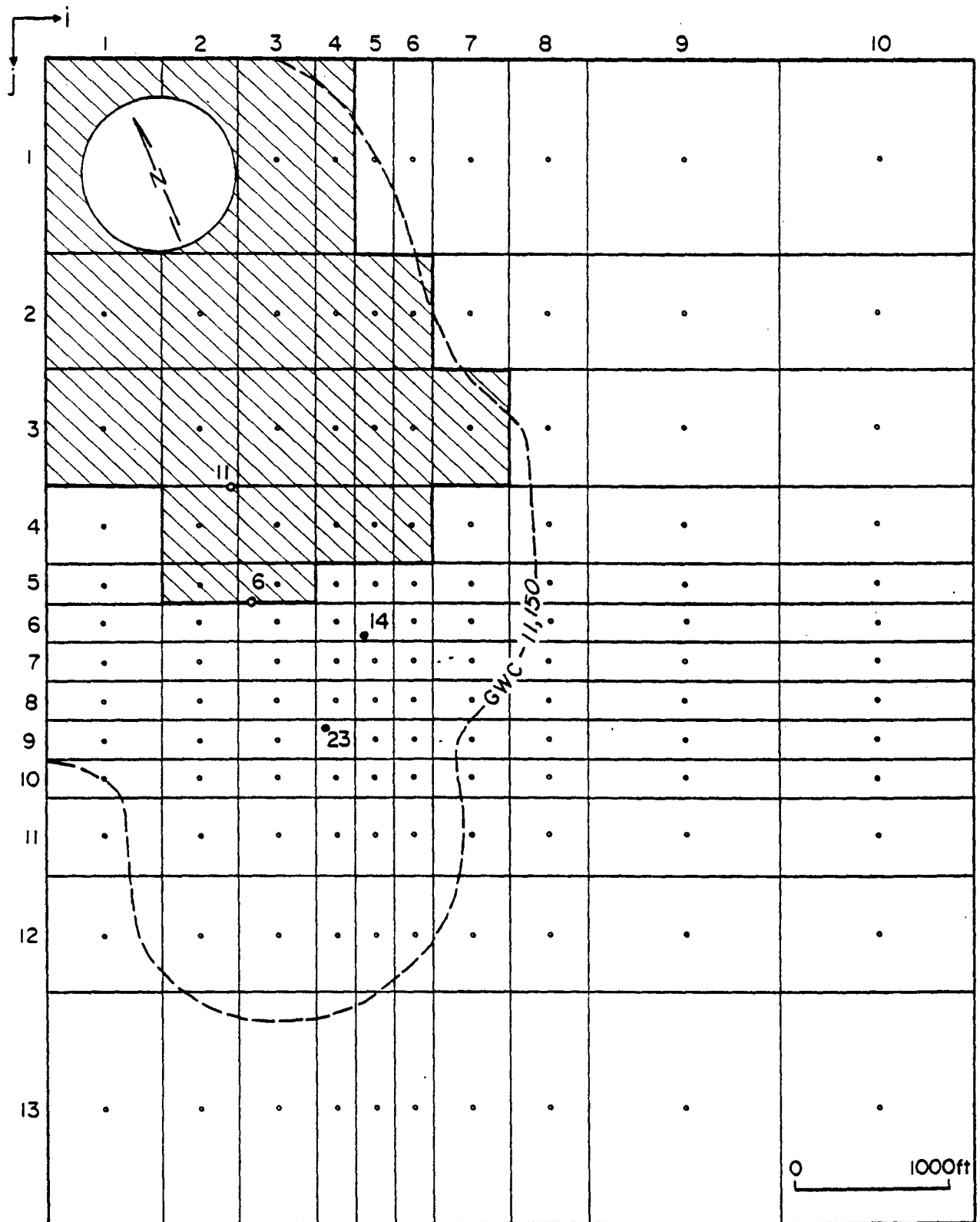
Figure 57. Simulator grid used by LTS and BEG. Hachured blocks are outside the area of interest.

Table 10. Comparison of model data used in the simulation studies.

	W&A	LTS	BEG
Original water in place, MMbbl	656.312	862.0	314.9
Original free gas in place, Bcf	29.479	52.3	56.2
Reservoir temperature, °F	235	230	230
Initial pressure, psi	9425	9115	9115
Reservoir gas gravity	0.8	0.7	0.7
Initial gas formation-volume factor, reservoir cf/scf	0.00297	0.00289	0.00289
Initial gas viscosity, cp	0.0365	0.0365	0.0365
Water viscosity, cp	0.40	0.3	0.3
Permeability, md	figure 60	figure 58	figure 59
Relative permeability curve	figure 60	figure 60	figure 60
Porosity, %	30	variable	30
Net-sandstone thickness, ft	33	figure 61	figure 61
Net gas sand thickness, ft	16	--	--
Water compressibility, psi^{-1}	2.5×10^{-6}	5×10^{-6}	7×10^{-6}
Rock compressibility, psi^{-1}	3.0×10^{-6}	--	--

is confirmed by the higher rate of pressure decline during the time that Well 23 was producing. BEG assumes that there are two zones with permeabilities of 200 and 300 md (fig. 59).

Differences also exist in the way relative permeabilities to gas and water were handled in the three simulation studies. W&A used pseudo relative permeability curves to model the three-dimensional fluid flow, as stated previously. LTS and BEG varied the exponent values in the equation developed by Corey (1954) to obtain a good history match. Wide differences are observed in the resulting relative permeability curves for the "C" sandstone (fig. 60).

W&A used a constant gross sandstone thickness of 30 ft and a net gas sand thickness of 16 ft. LTS and BEG used the isopach map for the "C" sandstone to obtain a distribution of sandstone thickness (fig. 61).

Comparisons of history matches for pressures and water production rates measured in the field and those calculated by the model for Wells 14 and 23 are shown in figures 62 to 67, inclusive. W&A did not provide calculated pressure data for Well 23. As stated earlier, W&A and BEG used bottom-hole flowing pressures and LTS used formation pressures. Based on the input data in table 10, W&A, LTS, and BEG believe that reasonably good history matches were obtained for pressure and for water production rates.

Predictions

Reservoir simulation predictions were made for a single test well located near Well 14. A 10-yr shut-in period (1973 to 1982) was modeled, followed by a 10-yr production period predicted by W&A and LTS, and an 8-yr production period predicted by BEG. Comparisons are shown for gas flow rates (fig. 68) and water flow rates (fig. 69) predicted for natural flow conditions by the three independent studies. Cumulative recoveries of gas, condensate, and water (table 11) predicted by the three studies are not greatly different and average 4.64 Bcf of gas, 53.21 Mbbl of condensate, and 7.97 MMbbl of water.

In summary, the results of the three independent reservoir simulation studies are considered to be substantially the same for the purpose of evaluating the Port Arthur field as a prospect. Additional details of these studies are given by Wattenbarger (1981a and b, 1982), Ridings (1982), and Gregory and others (1982, 1983).

Economic Analysis

Estimated total drilling costs for a test well to -11,650 ft and a salt-water disposal well to -4,500 ft are $3,837,280 (table 12) with operating costs during the testing and production period averaging an additional $33,000/mo. The economic indicators (table 13) are obtained from cash flow calculations based on the cost data (table 12) and the predicted flow rates (figs. 68 and 69). The break-even gas price from the BEG analysis is $2.40/Mcf for a 15-percent rate of return after federal income tax is paid (fig. 70). The break-even gas price is the price

	(1)	(2)	(3)	(4)	(5)	(6)	(7)	(8)	(9)	(10)
(1)					300	300	300	300	300	300
(2)							300	300	300	300
(3)								300	300	300
(4)							300	300	300	300
(5)	300			300	300	300	300	300	300	300
(6)	300	300	300	300	300	300	300	300	300	300
(7)	300	300	300	300	300	300	300	300	300	300
(8)	300	300	300	300	300	300	300	300	300	300
(9)	300	300	300	0.03y 0.3x	0.03y 300x	0.03y 300x	0.03y 300x	0.03y 300x	0.015y 150x	0.015y 15x
(10)	300	300	300	300y 0.3x	300	300	300	300	150	15
(11)	300	300	300	300y 0.3x	300	300	300	300	150	15
(12)	300	300	300	300y 0.3x	300	300	300	300	150	15
(13)	300	300	300	300y 0.3x	300	300	300	300	150	15

0   1000 ft

Figure 58. Permeability distribution for reservoir simulation by LTS.

95

j \ i	(1)	(2)	(3)	(4)	(5)	(6)	(7)	(8)	(9)	(10)
(1)					300	300	300	300	300	300
(2)							300	300	300	300
(3)								300	300	300
(4)							300	300	300	300
(5)	300			300	300	300	300	300	300	300
(6)	300	300	300	300	300	300	300	300	300	300
(7)	300	300	300	300	300	300	300	300	300	300
(8)	200	200	200	300	300	300	300	300	300	300
(9)	200	200	200	200	200	200	200	300	300	300
(10)	200	200	200	200	200	200	200	200	300	300
(11)	200	200	200	200	200	200	200	200	200	200
(12)	200	200	200	200	200	200	200	200	200	200
(13)	200	200	200	200	200	200	200	200	200	200

0   1000 ft

Figure 59. Permeability distribution for reservoir simulation by BEG.

96
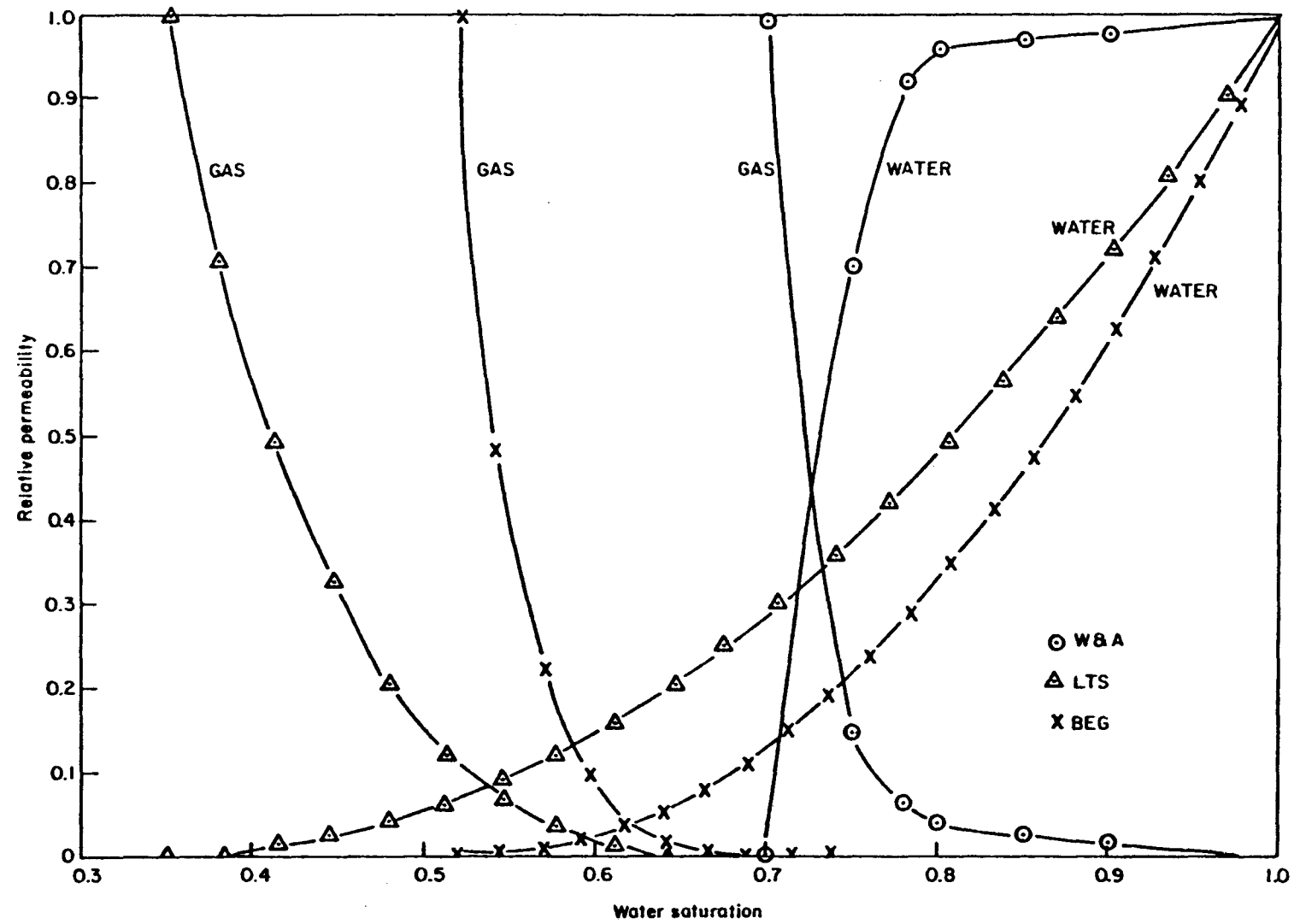
Figure 60. Comparison of relative permeability curves used in reservoir simulation.

	(1)	(2)	(3)	(4)	(5)	(6)	(7)	(8)	(9)	(10)
(1)	░	░	░	░	42	38	35	25	15	10
(2)	░	░	░	░	░	░	53	43	39	36
(3)	░	░	░	░	░	░	░	50	50	50
(4)	░	░	░	░	░	░	40	40	43	46
(5)	70	░	░	46	40	40	40	40	40	40
(6)	70	55	40	40	40	40	40	40	40	40
(7)	70	60	45	40	40	40	42	44	41	40
(8)	60	60	55	51	47	45	46	50	48	40
(9)	55	60	60	60	55	43	54	55	54	57
(10)	45	50	60	60	60	60	60	60	60	55
(11)	32	42	58	60	60	60	60	60	60	60
(12)	18	34	47	56	58	60	60	60	60	60
(13)	5	17	25	28	30	31	35	28	38	38

0   1000 ft
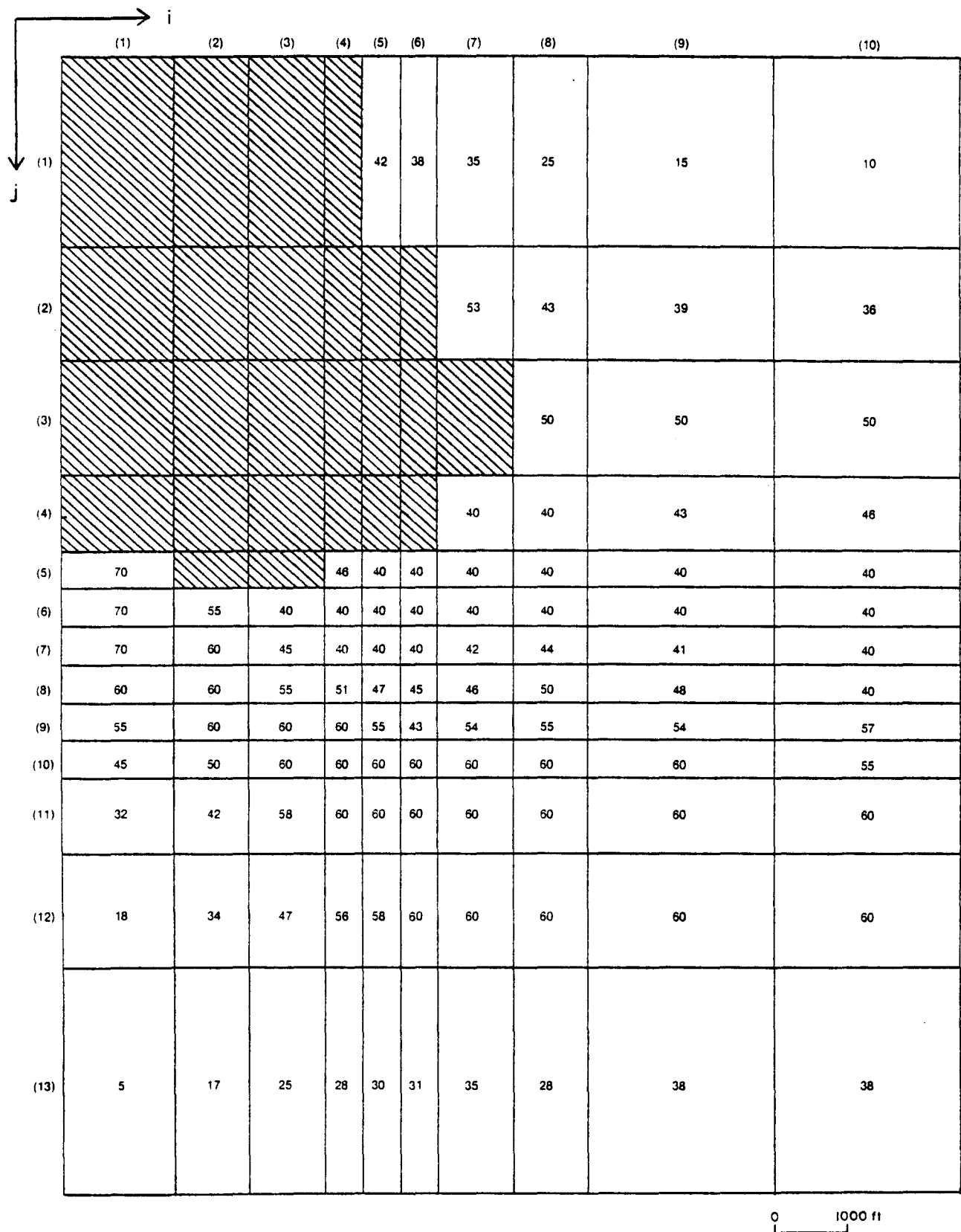
Figure 61. Distribution of sandstone thickness used in reservoir simulation by LTS and BEG.

98
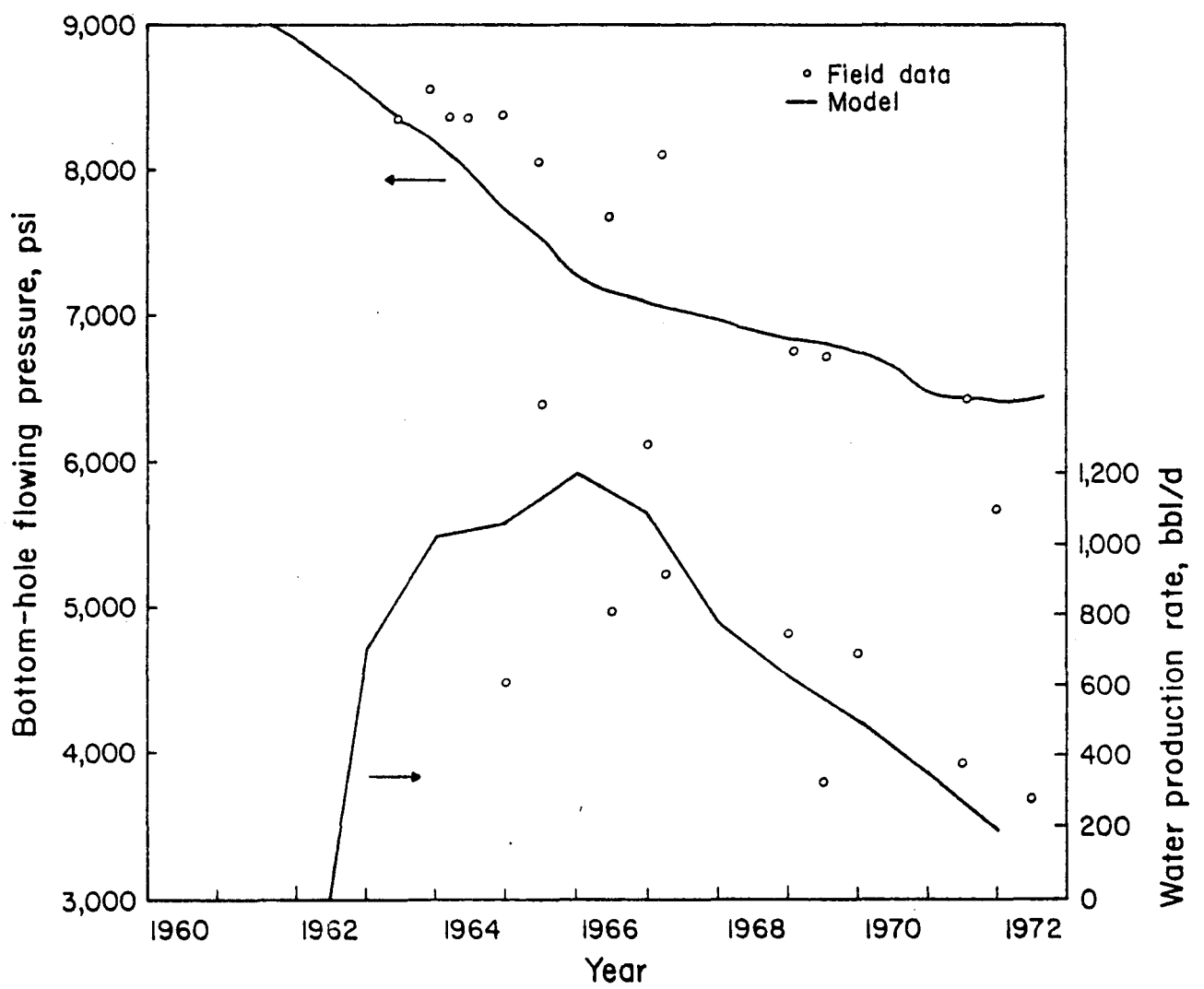
Figure 62. History matches for pressure and water production rates, "C" sandstone, Well 14 (W&A).
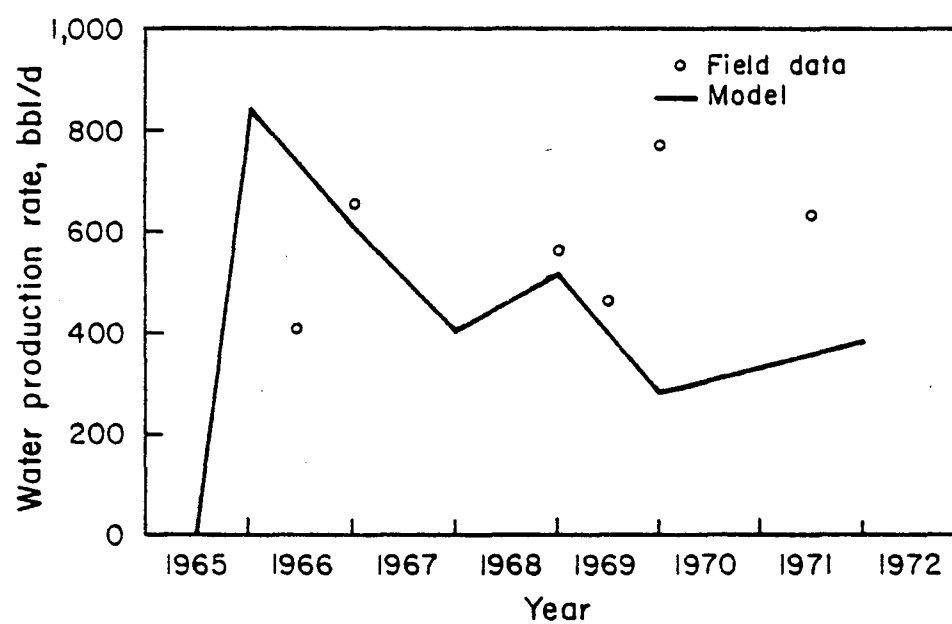
Figure 63. History match for water production rate, "C" sandstone, Well 23 (W&A).

100
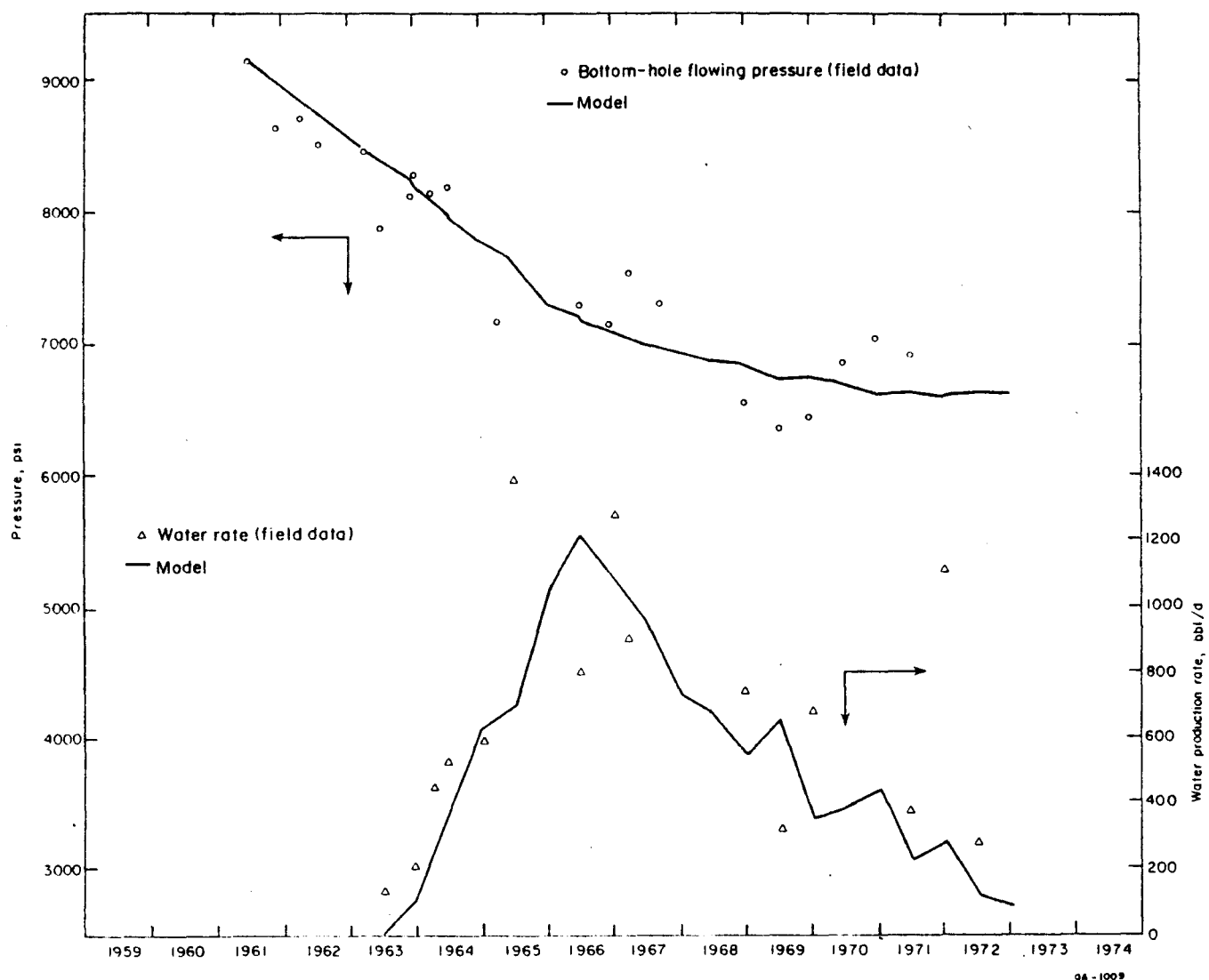
Figure 64. History matches for pressure and water production rates, "C" sandstone, Well 14 (BEG).
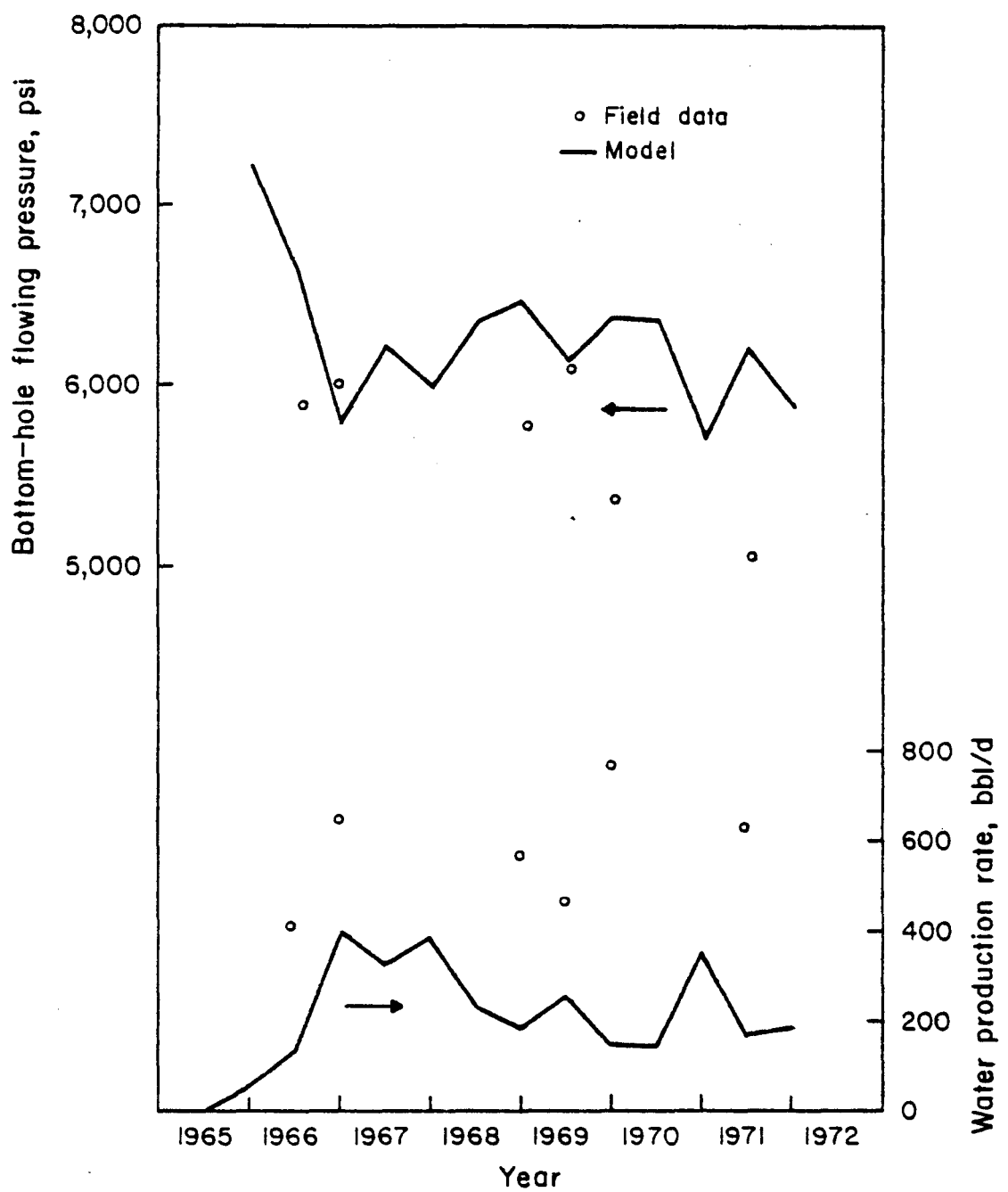
Figure 65. History matches for pressure and water production rates, "C" sandstone, Well 23 (BEG).
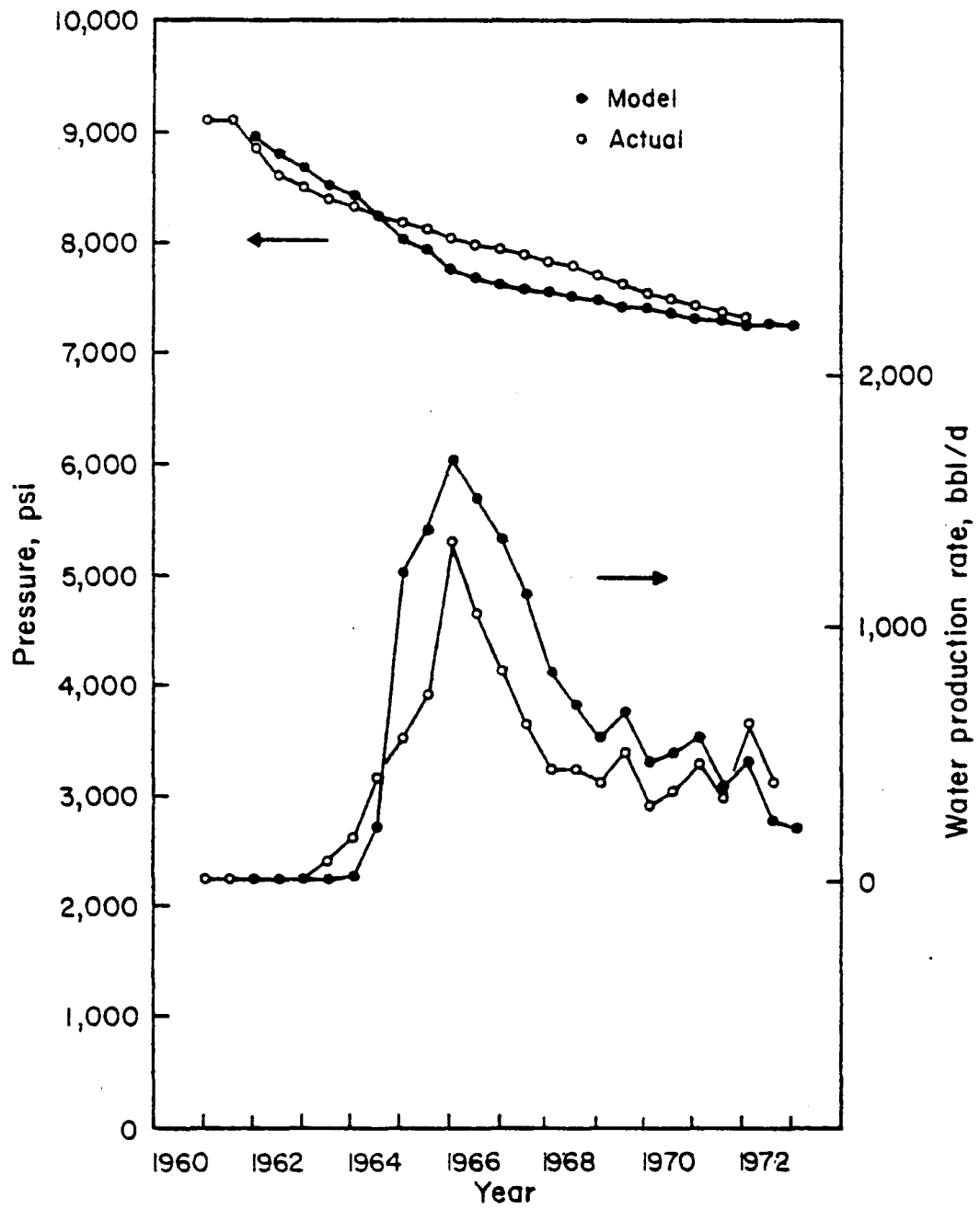
Figure 66. History matches for formation pressure and water production rate, "C" sandstone, Well 14 (LTS).
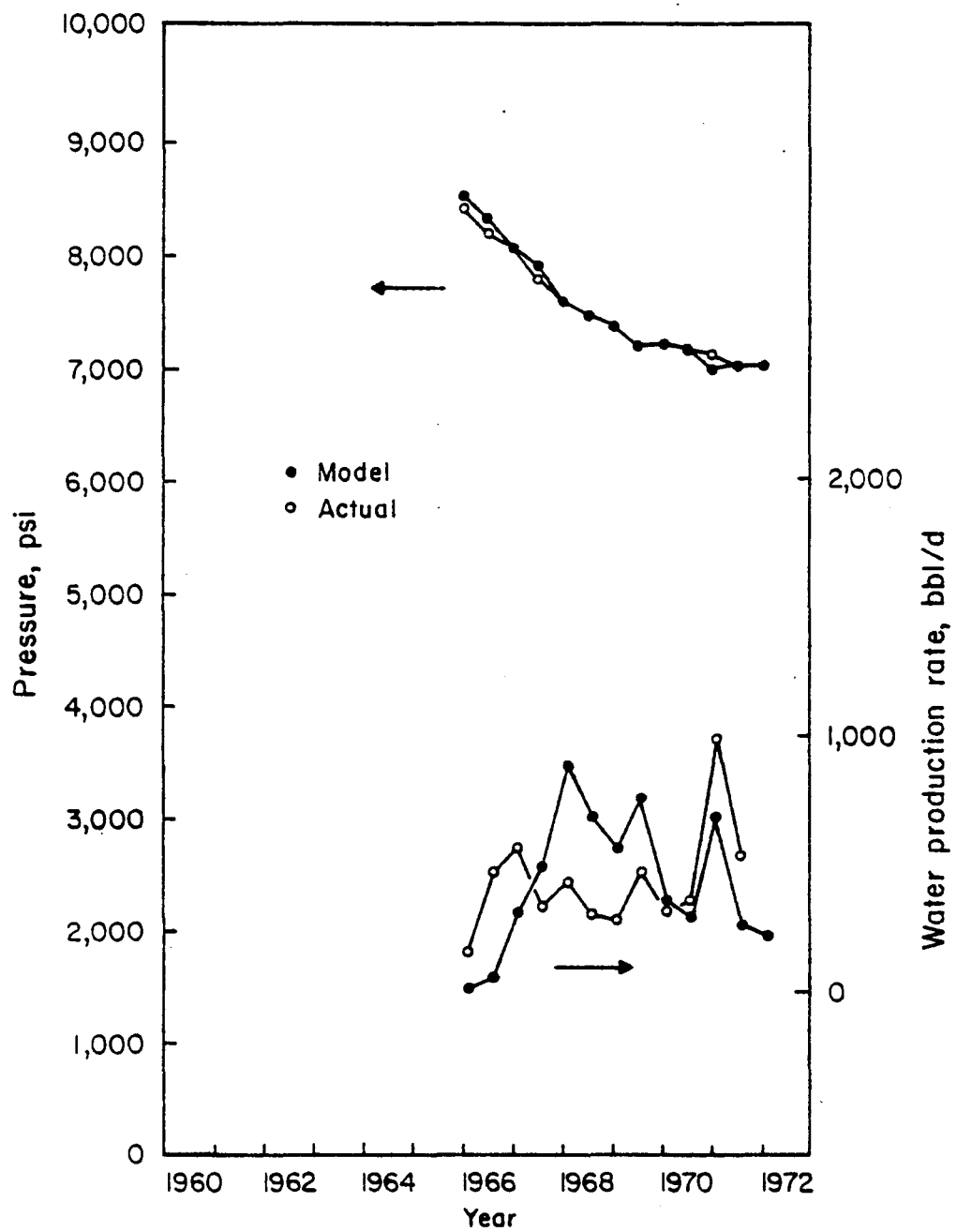
Figure 67. History matches for formation pressure and water production rate, "C" sandstone, Well 23 (LTS).
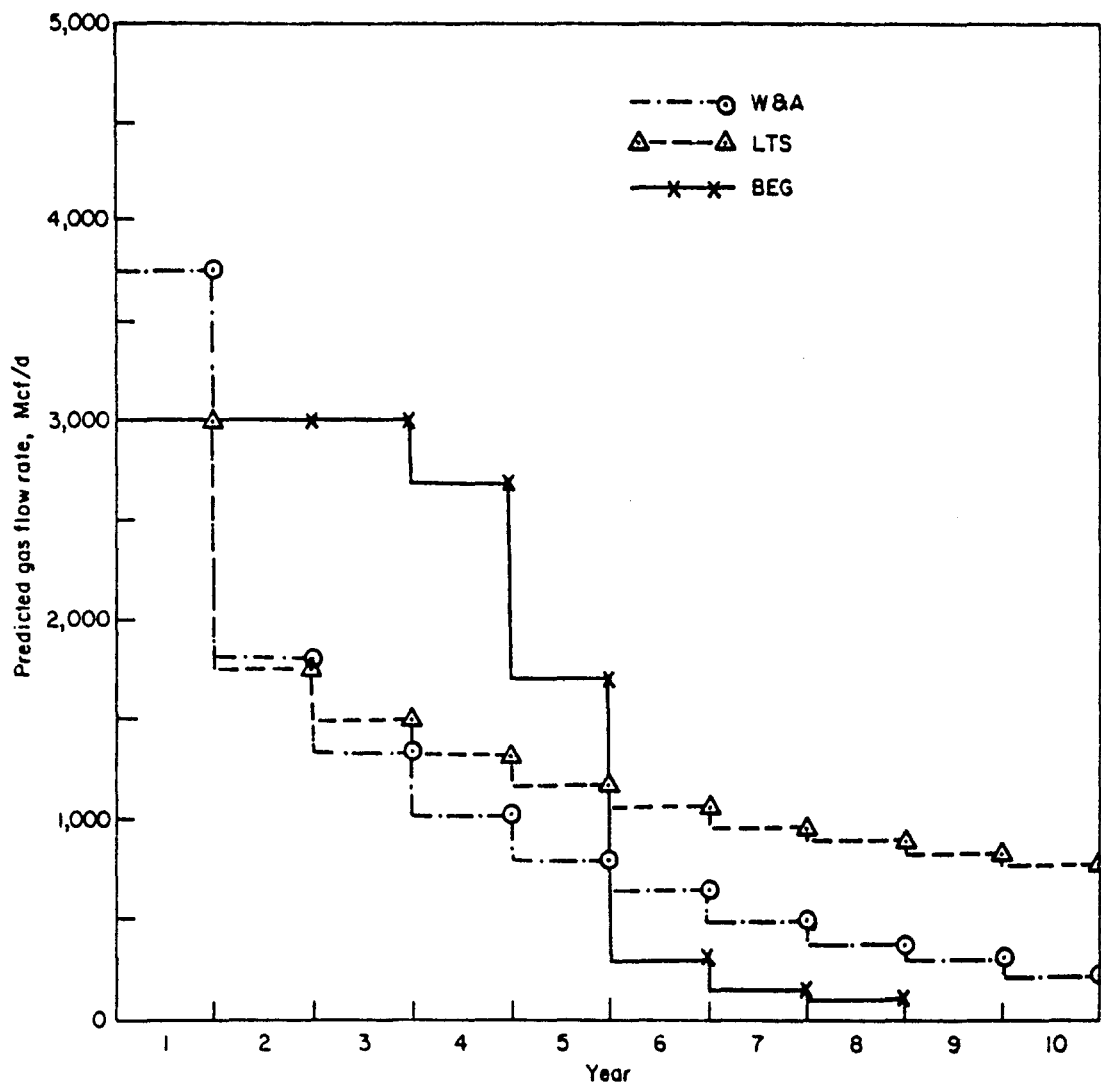
Figure 68. Comparison of predicted gas flow rates by three independent simulation studies—one by W&A, one by LTS, and one by BEG.
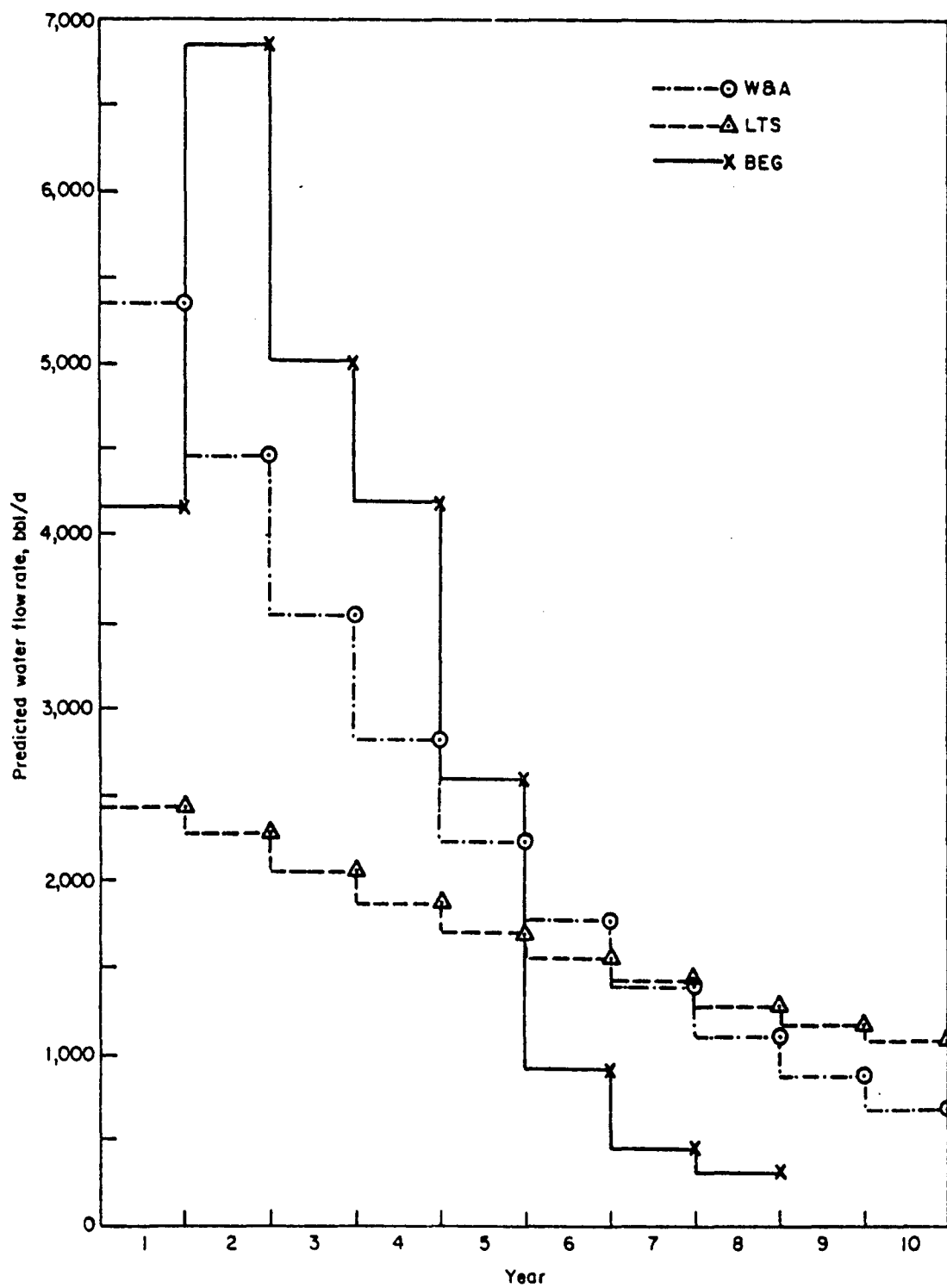
Figure 69. Comparison of predicted water flow rates by three independent simulation studies--one by W&A, one by LTS, and one by BEG.

Table 11. Comparison of cumulative recovery of gas, condensate, and water predicted by different reservoir simulation studies.

	W&A	LTS	BEG
Gas, Bcf	3.977	4.84	5.10
Condensate, Mbbl	58.62	50	51
Water, MMbbl	8.825	6.15	8.94
Estimated OGIP,* Bcf	29.479	52.3	56.2
Production period, yrs	10	10	8
Initial reservoir pressure at end of shut-in period, psi	6500	7248	6632
Average reservoir pressure at end of prediction period, psi	4018	5699	4320

* Original gas in place.

Table 12. Cost data used in economic analyses.

Production test well		
	Tangible	$1,783,040
	Intangible	1,322,720
Disposal well		
	Tangible	103,040
	Intangible	224,560
Other capital costs		
	Tangible	0
	Intangible	403,920
	Total	$3,837,280

Table 13. Comparison of economic indicators.

	W&A	LTS	BEG
*Break-even gas price, $/Mcf	3.05	3.00	2.40
†*Net present worth, $	-50,000	0	986,000
†Pay-out period, years	-	4.0	3.0

* Assume 15-percent rate of return after federal income tax.
† Assume gas price of $3.00/Mcf after federal income tax.
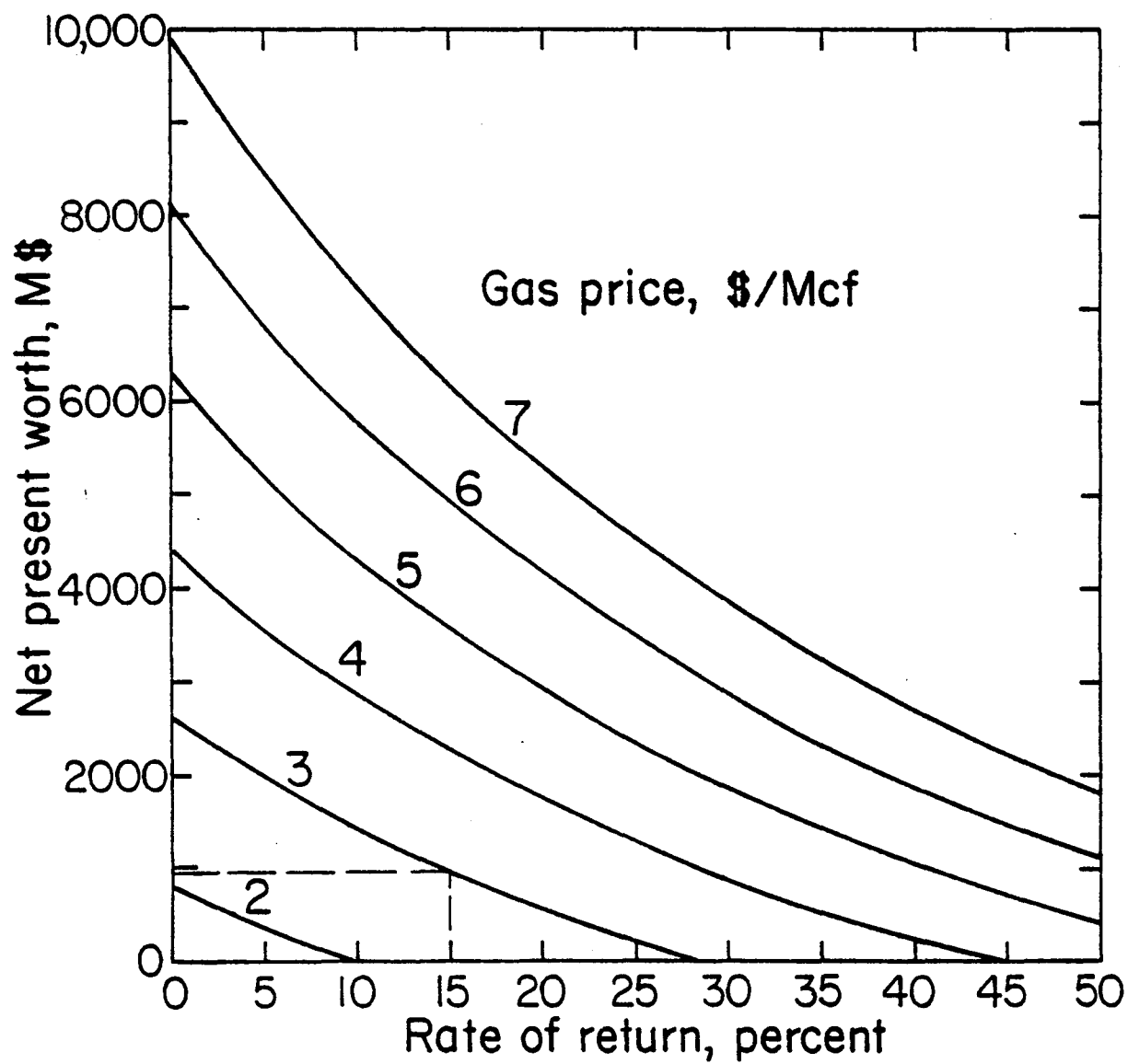
Figure 70. Net present worth versus rate of return for different gas prices.

109

at which the project breaks even on a zero net present worth basis. The BEG study shows that the net present worth of the investment is about $986,000 for a gas price of $3.00/Mcf and increases rapidly for higher gas prices (fig. 71). The original investment would pay off in 3 yr. The economic outlook for the prospect might be even better if production from the "C" sandstone and from other watered-out reservoirs in the field were commingled.

TECHNICAL PROBLEMS ENCOUNTERED

A problem that is common for this type of project is the unavailability of certain data or well logs that are necessary or desirable for evaluating the prospect. The reasons for unavailability of data may be that the key measurements were not made or the data were destroyed, misplaced, or considered proprietary. Reliable porosity and permeability data are commonly lacking. Whole-core porosity and permeability data were not available for the Port Arthur field. In situ permeability in some reservoirs could not be calculated because pressure buildup data were lacking. However, sidewall core porosity and permeability data were found for several zones of interest in the lower Hackberry sandstones. Sidewall core data are much better than no data at all, but usually overestimate both porosity and permeability.

Only one sonic log and no density logs were available for the field. Normally, several sonic and density logs are needed to develop acoustic impedance trends in the subsurface and to calibrate seismic response to lithology and fluid content by using synthetic seismograms and models.

The poor quality of the raw seismic data purchased for this project severely limited its usefulness for delineating reservoir details or detection of gas zones. The objective of improving resolution by reprocessing the data was not successful because of the poor signal-to-noise ratio.

Reservoir simulation computer programs for modeling the reservoir mechanics of a watered-out gas field were not readily available at the beginning of this project. The development of suitable programs has been slow and has caused delay in evaluating individual reservoirs in the Port Arthur field. We had hoped to model several other reservoirs in addition to the "C" reservoir, but this was not possible because of time constraints.

Gregory and others (1982) were unable to convert wellhead shut-in pressure (WHSIP) to bottom-hole shut-in pressure (BHSIP) unless it was assumed that the only fluid in the well bore was gas. To account for the presence of both liquid and gas in the borehole, this conversion technique has been modified in this report by the method of Orkiszewski (1967).

A reservoir simulation study by Wattenbarger in 1982 (documented in the BEG first quarterly report to GRI, 1982) predicted that gas recovery from the "C" sandstone could be

110
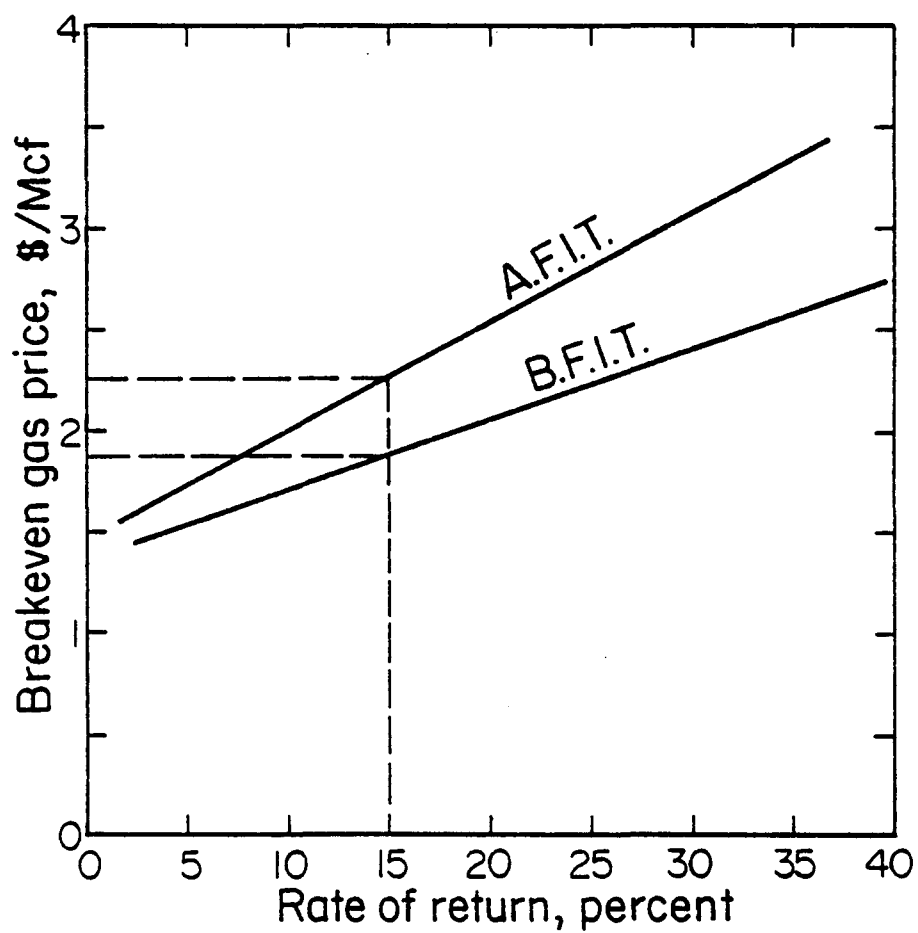
Figure 71. Break-even gas price versus rate of return before federal income tax (B.F.I.T.) and after federal income tax (A.F.I.T.).

increased more than 90 percent by using gas lift. The higher recovery for the gas-lift case is attributed mainly to the lower reservoir pressures achieved. This optional method of gas production was not considered further, however, when studies by Louisiana State University and Eaton Operating Company indicated that the "C" sandstone in the Port Arthur field is too deep for the gas-lift technique to be effective.

CONCLUSIONS AND RECOMMENDATION

1. Co-production of gas and water is an EGR method that has considerable potential for increasing the ultimate hydrocarbon recovery from abandoned reservoirs.

2. Reservoir simulation studies for the Port Arthur field predict that the gas remaining in the abandoned "C" reservoir exceeds 60 percent of the OGIP; an additional 9 percent can be recovered by the co-production method during the natural flowing life of a test well.

3. Results obtained from reservoir modeling suggest that a field test conducted for research and development would pay off the original investment in 3 yr. The break-even gas price is $2.40/Mcf for a 15-percent return on the investment after payment of federal income taxes.

4. Only the "C" reservoir has been considered in this analysis. The co-production of several additional abandoned reservoirs in the Port Arthur field could substantially improve the economic outlook.

5. This analysis of the Port Arthur field is a case example of how new technology and increased prices can make it worthwhile to reconsider these types of reservoirs.

It is recommended that a design test well be drilled on a site about 200 ft southwest of Well 14. The exact location may be determined by the location of good elevated roads and by the condition of the old surface site of Well 14, which is located in a marshy area. Projected depths of the well are 11,650 ft to penetrate all of the lower Hackberry sandstones, 11,850 ft to penetrate the Nodosaria sandstone, and about 13,500 ft to penetrate the Vicksburg interval. An alternate drill site located about 200 ft from Well 31 along a line connecting Wells 31 and 14 would give a better exposure of the "B-2" sandstone.

ACKNOWLEDGMENTS

113

REFERENCES

Ausburn, B. E., Skirvin, R. T., and Hyun, I. S., 1982, Volumetric analysis of Frio sands, Port Arthur field: J. R. Butler Company report to Bureau of Economic Geology, The University of Texas at Austin, 85 p.

Bateman, R. M., and Konen, C. E., 1977, The log analyst and the programmable pocket calculator: The Log Analyst, v. 18, no. 5, p. 3-11.

Bebout, D. G., Gavenda, V. J., and Gregory, A. R., 1978a, Geothermal resources, Wilcox Group, Texas Gulf Coast: The University of Texas at Austin, Bureau of Economic Geology, report to the U.S. Department of Energy, Division of Geothermal Energy, Contract No. AT-E(40-1)-4891 (EY-76-S-05-4891), 82 p.

Bebout, D. G., Loucks, R. G., and Gregory, A. R., 1978b, Frio sandstone reservoirs in the deep subsurface along the Texas Gulf Coast--their potential for the production of geopressured geothermal energy: The University of Texas at Austin, Bureau of Economic Geology Report of Investigations No. 91, 92 p.

Bebout, D. G., Weise, B. R., Gregory, A. R., and Edwards, M. B., 1979, Wilcox sandstone reservoirs in the deep subsurface along the Texas Gulf Coast, their potential for production of geopressured geothermal energy: The University of Texas at Austin, Bureau of Economic Geology, report to the U.S. Department of Energy, Division of Geothermal Energy, Contract No. DE-AS05-76ET28461, 219 p.

Berg, R. R., and Powers, B. K., 1980, Morphology of turbidite-channel reservoirs, lower Hackberry (Oligocene), southeast Texas: Gulf Coast Association of Geological Societies Transactions, v. 30, p. 41-48.

Bornhauser, Max, 1960, Depositional and structural history of Northeast Hartburg field, Newton County, Texas: American Association of Petroleum Geologists, v. 44, no. 4, p. 458-470.

Boyd, W. E., Jr., Christian, L. D., and Danielsen, C. L., 1982, Secondary gas recovery from a watered-out reservoir: Society of Petroleum Engineers of AIME, SPE paper no. 11158, 10 p.

Brinkman, F. P., 1981, Increased gas recovery from a moderate water drive reservoir: Journal of Petroleum Technology, v. 33, no. 12, p. 2375-2480.

Chesney, T. P., Lewis, R. C., and Trice, M. L., 1982, Secondary gas recovery from a moderately strong water drive reservoir, a case history: Journal of Petroleum Technology, v. 34, no. 9, p. 2149-2157.

Coats, G. R., and Dumanoir, J. L., 1974, A new approach to improved log-derived permeability: The Log Analyst, January-February issue.

Coats, K. H., Nielsen, R. L., Terhune, M. H., and Weber, A. G., 1967, Simulation of three-dimensional, two-phase flow in oil and gas reservoirs: Society of Petroleum Engineers Transactions, v. 240, p. 377-388.

Collins, H. N., and Piles, D., 1981, Benefits of linear bivariate log analysis models: Preprint, Society of Petroleum Engineers, paper no. 10105.

Corey, A. T., 1954, The interrelation between gas and oil relative permeabilities: Producers Monthly, November issue, p. 38-41.

Denham, L. R., 1981, Extending the resolution of seismic reflection exploration: Journal of Canadian Society of Exploration Geophysicists, v. 17, no. 1, p. 43-54.

Doherty, M. G., 1981, Analysis of geopressured aquifers: Institute of Gas Technology, 1980 Annual Report to the Gas Research Institute, Contract No. 5011-0109, 145 p.

Domenico, S. N., 1976, Effects of brine-gas mixture velocity in an unconsolidated sand reservoir: Geophysics, v. 41, p. 882-894.

Dunlap, H. F., and Dorfman, M. H., 1981, Problems and partial solutions in using the S.P. log to predict water salinity in deep hot wells: Proceedings, Fifth United States Geopressured-Geothermal Energy Conference, Louisiana State University, p. 189-192.

Galloway, W. E., Hobday, D. K., and Magara, K., 1982, Frio Formation of the Texas Gulf Coast Basin--depositional systems, structural framework, and hydrocarbon origin, migration, distribution, and exploration potential: The University of Texas at Austin, Bureau of Economic Geology Report of Investigations No. 122, 78 p.

Gardner, G. H. F., Gardner, L. W., and Gregory, A. R., 1974, Formation velocity and density--the diagnostic basics of stratigraphic traps: Geophysics, v. 39, p. 770-780.

Garrett, J. H., 1938, The Hackberry Assemblage--an interesting foraminiferal fauna of post-Vicksburg age from deep wells in the Gulf Coast: Journal of Paleontology, v. 12, p. 309-317.

Geer, E. C., and Cook, H. L., 1978, Enhanced gas recovery from geopressured aquifers: Society of Petroleum Engineers of AIME, SPE paper 7541, 8 p.

Geertsma, J., 1961, Velocity log interpretation: the effect of rock bulk compressibility: Society of Petroleum Engineers AIME Transactions, v. 222, p. 235-253.

Gregory, A. R., Dodge, M. M., Posey, J. S., and Morton, R. A., 1980, Volume and accessibility of entrained (solution) methane in deep geopressured reservoirs--Tertiary formations of the Texas Gulf Coast: The University of Texas at Austin, Bureau of Economic Geology, report to the U.S. Department of Energy, Division of Geothermal Energy, Contract No. DE-AC08-78ET01580, 390 p.

Gregory, A. R., Jirik, L. A., Reed, R. S., Weise, B. R., and Morton, R. A., 1981, Location and evaluation of reservoirs containing solution gas and free gas--Texas Gulf Coast: Proceedings, Fifth United States Geopressured-Geothermal Energy Conference, Louisiana State University, p. 255-257.

Gregory, A. R., Lin, Z. S., Reed, R. S., and Morton, R. A., 1982, Exploration and production program for locating and producing prospective aquifers containing solution gas and free gas--Texas Gulf Coast: The University of Texas at Austin, Bureau of Economic Geology, annual report to the Gas Research Institute, Contract No. 5080-321-0398, 170 p.

Gregory, A. R., Lin, Z. S., Reed, R. S., Morton, R. A., and Rogers, L. A., 1983, Watered-out gas reservoirs profitable via enhanced recovery: Oil and Gas Journal, v. 81, no. 11, p. 55-60.

Halbouty, M. T., and Barber, T. D., 1961, Port Acres and Port Arthur fields, Jefferson County, Texas: Gulf Coast Association of Geological Societies Transactions, v. 11, p. 225-234.

_____ 1962, Port Acres and Port Arthur fields, Jefferson County, Texas: Houston Geological Society, p. 169-173.

Hearn, C. L., 1971, Simulation of stratified waterflooding by pseudo relative permeability curves: Journal of Petroleum Technology, v. 23, p. 805-813.

Hottmann, C. E., and Johnson, R. K., 1965, Estimation of formation pressures from log-derived shale properties: Journal of Petroleum Technology, v. 17, p. 717-723.

Kehle, R. O., 1971, Geothermal survey of North America, 1971 annual progress report: American Association of Petroleum Geologists, Research Committee (unpublished), 31 p.

Lutes, J. L., Chiang, C. P., Rossen, R. H., and Brady, M. M., 1977, Accelerated blowdown of a strong water-drive gas reservoir: Journal of Petroleum Technology, v. 29, no. 12, p. 1533-1538.

Meanley, E. S., 1982 (reviewed by Kelm, D. L., and Patch, J. R.), Seismic processing and modeling, Port Arthur field: GeoQuest International, Inc., report to Bureau of Economic Geology, The University of Texas at Austin, 84 p.

Orkiszewski, J., 1967, Predicting two-phase pressure drops in vertical pipe: Society of Petroleum Engineers/AIME Transactions, v. 240, p. 829-838.

Overton, H. L., 1958, A correlation of electrical properties of drilling fluids with solids content: American Institute of Mining, Metallurgical, and Petroleum Engineers Transactions, v. 213, p. 333-336.

Paine, W. R., 1968, Stratigraphy and sedimentation of subsurface Hackberry wedge and associated beds of southwestern Louisiana: American Association of Petroleum Geologists Bulletin, v. 52, no. 2, p. 322-342.

116

Porter, C. R., and Carothers, J. E., 1970, Formation factor-porosity relation derived from well log data: Society of Professional Well Log Analysts Transactions, paper A1-A19.

Price, L. C., Blount, C. W., MacGowen, D., and Wenger, L., 1981, Methane solubility in brines with application to the geopressured resource: Proceedings, Fifth United States Geopressured-Geothermal Energy Conference, Louisiana State University, p. 205-214.

Ransom, R. C., 1974, The bulk volume water concept of resistivity well log interpretation: The Log Analyst, January-February issue.

Reedy, F., Jr., 1949, Stratigraphy of Frio Formation, Orange and Jefferson Counties, Texas: American Association of Petroleum Geologists Bulletin, v. 33, no. 11, p. 1830-1858.

Ridings, R. L., 1982, Evaluation of the lower Hackberry "C" sand, Port Arthur field: Lewis Technical Services, Inc., report prepared for the Gas Research Institute, 30 p.

Ritch, H. J., and Kozik, H. G., 1971, Petrophysical study of overpressured sandstone reservoirs, Vicksburg Formation, McAllen Ranch field: Society of Professional Well Log Analysts, Transactions, paper BB1-BB14.

Schlumberger Limited, 1978, Log interpretation charts, Gen 7: p. 3.

Walker, R. G., 1979, Facies models --2. Turbidites and associated coarse clastic deposits, in Walker, R. G., ed., Facies models: Geological Association of Canada, Geoscience Canada, reprint series 1, p. 91-103.

Wattenbarger, R. A., 1981a, Dispersed Gas Project, Port Arthur field, preliminary economic analysis: Wattenbarger and Associates report to Bureau of Economic Geology, The University of Texas at Austin, 15 p.

_____ 1981b, Port Arthur field, "C" sand reservoir simulation study for the Dispersed Gas Project: Wattenbarger and Associates report to Bureau of Economic Geology, The University of Texas at Austin, 20 p.

_____ 1982, Port Arthur "C" sandstone, reservoir mechanics natural flow versus artificial lift predictions: Wattenbarger and Associates report to Bureau of Economic Geology, The University of Texas at Austin, 22 p.

Weise, B. R., Edwards, M. B., Gregory, A. R., Hamlin, H. S., Jirik, L. A., and Morton, R. A., 1981a, Geologic studies of geopressured and hydropressured zones in Texas: test-well site selection: The University of Texas at Austin, Bureau of Economic Geology, final report to the Gas Research Institute, Contract No. 5011-321-0125, 308 p.

Weise, B. R., Jirik, L. A., Hamlin, H. S., Hallam, S. L., Edwards, M. B., Schatzinger, R. A., Tyler, N., and Morton, R. A., 1981b, Geologic studies of geopressured and hydropressured zones in Texas: supplementary tasks: The University of Texas at Austin, Bureau of Economic Geology, final report to the Gas Research Institute, Contract No. 5011-321-0125, 120 p.

APPENDIX A

CLASS B FIELDS

EVALUATION SHEETS

CONTENTS

TABLES A-1 AND A-2

Table A-1. EVALUATION OF GAS FIELDS

DISPERSED GAS PROJECT

(Short form)

Field name: Port Acres, 57 Hackberry sands, Frio (10,350-10,600 ft)

Location: Jefferson County, Texas, 1S-48E, 1S-49E

Favorable Criteria:

    1. Reservoir area: 5 mi^2, multiple Hackberry sands (Frio)

    2. Essentially one producing sand; 30-120 ft thick

    3. Porosity: 28-35%, Permeability: 5-1,000 md

    4. Seismic lines penetrate field

    5. 5 sonic logs in general area

    6. Geological and engineering data have been published

Unfavorable Criteria:

    1. Active wells in field: one in Hackberry @ 10,600 ft; two in
       Frio 5 sand

    2. Possible sand/shale production problems

    3. Limited seismic coverage

    4. Abandonment pressure gradients average 0.25 psi/ft

    5. _____

    6. _____

Recommendation:

    Favorable, because good sand, most wells P & A, good porosity and
    permeability (Rated: Class B)

    Unfavorable, because low pressure gradients

119

Table A-2. EVALUATION OF GAS FIELDS

DISPERSED GAS PROJECT

(Short form)

Field name: Algoa, 49 (Frio 37 sd, 10,350-10,750 ft interval)

Location: Brazoria-Galveston Counties, Texas, 5S-39E

Favorable Criteria:

1. Fault block: 6.6 mi^2, anticlinal structure

2. Average equilibrium temperature: 227°F @ 10,400 ft

3. One thick sand (gas stringer + aquifer) 150-300 ft

4. Three gas wells in target zone P & A

5. Range of salinities: 62,000 - 150,000 ppm NaCl

6. _____

Unfavorable Criteria:

1. Core data unavailable; possible core data in files of Superior Oil
   for their #1 Evans unit

2. Reservoir area <5 mi^2

3. Five active wells in field (3 comp. 1978-1979)

4. 2 sonic logs, 1 density log in area

5. Abandonment pressure gradients: 0.3 to 0.4 psi/ft

6. _____

Recommendation:

Favorable, because good sand (Rated: Class B)

_____

_____

Unfavorable, because field is still active, might become viable prospect
when active wells are abandoned.

_____

120

APPENDIX B

CLASS C FIELDS

EVALUATION SHEETS

CONTENTS

Table B-1. EVALUATION OF GAS FIELDS

DISPERSED GAS PROJECT

(Short form)

Field name: Blessing (F-19 sand at 8,500 ft)

 Location: Matagorda County, Texas, 10S-31E

Favorable Criteria:

1. Located in large fault block (35 mi^2) but producing area is small

2. Target sand 100 ft thick (35 ft gas sand, 65 ft aquifer)

3. No active wells in target sand

4. 8 wells P & A in target sandstone

5. Seismic lines through field

6. At least 4 sonic logs in immediate area

Unfavorable Criteria:

1. Oil production primarily from F-14 sand which is above the F-19 sand.

2. 8 active gas wells in field, shallower than target sand

3. Recent completions 1978, 1979

4. Average abandonment pressure gradient = 0.25 psi/ft

5. No core data for target sand

6. Target sand is shaly in much of area

Recommendation:

Favorable, because

Unfavorable, because active oil and gas production occurs near target sand. Sands are shaly (Rated: Class C).

122

Table B-2. EVALUATION OF GAS FIELDS

DISPERSED GAS PROJECT

(Short form)

Field name: Blue Lake, 45 (Frio 10,280 ft sand)

Location: Brazoria County, Texas, 7S-37E

Favorable Criteria:

1. Seven inactive wells (P & A)

2. Sand thickness = 30-70 ft with 10-30 ft of gas sand

3. Equilibrium temperature of reservoir is about 230°F

4. _____

5. _____

6. _____

Unfavorable Criteria:

1. Estimated reservoir size: <2 square miles

2. Only two sonic logs in area

3. There are two active wells which produce from intervals that
    bracket the target sand: one is in 8,900 ft sand, the other is
    in 10,500 ft sand

4. Average abandonment pressure gradient = 0.24 psi/ft

5. No core data available in target sand interval

Recommendation:

Favorable, because _____

_____

_____

Unfavorable, because area is small and sands are shaly (Rated: Class C).

_____

_____

123

Table B-3.   EVALUATION OF GAS FIELDS

DISPERSED GAS PROJECT

(Short form)

Field name: Devillier, 75 (Vicksburg, 10,750-10,920 ft interval)

Location: Chambers County, Texas, 2S-44E, 2S-45E

Favorable Criteria:

1. Gas productive area: 4 to 5 square miles

2. Four wells P & A

3. Conv. core data (Gulf no. 1 Hankamer) avg. perm. >300 md,

   range 25-980 md, avg. porosity 29% in interval 10,850-10,875 ft.

   Avg. perm. = 200 md, avg. porosity = 26% from 10,876-10,888 ft.

4. Five sonic logs run in area; BHT >200°F.

Unfavorable Criteria:

1. Gas sand thickness: 10-30 ft

2. 3 active wells producing from Vicksburg

3. Thin aquifer sands, very shaly

4. Oil produced from reservoir

5.

6.

Recommendation:

Favorable, because

Unfavorable, because thin shaly aquifer sands not laterally extensive,

considerable oil production from reservoir (Rated: Class C).

124

Table B-4. EVALUATION OF GAS FIELDS

DISPERSED GAS PROJECT

(Short form)

Field name: Harris, 47 (Wilcox, Luling and Massive sands in depth interval

7,600-8,600 ft

Location: Live Oak County, Texas, 14S-16E

Favorable Criteria:

1. Located in fault block, 25 mi^2 area

2. Structure--fault-bounded anticline with 200 ft closure

3. More than one sand

4.

5.

6.

Unfavorable Criteria:

1. At least 12 active wells (most in target sand zone)

2. Perforated intervals range from 2 to 30 ft

3. Recent completion - 1979

4. Core data not available

5. Only two sonic logs in area

6. Abandonment pressures average 0.3 psi/ft from 7,600-8,600 ft

Recommendation:

Favorable, because

Unfavorable, because field is still active (Rated: Class C).

Table B-5. EVALUATION OF GAS FIELDS

DISPERSED GAS PROJECT

(Short form)

Field name: Lake Creek, Wilcox 11,508-11,758 ft sand

Location: Montgomery County, Texas, 3N-36E, 2N-36E

Favorable Criteria:

1. Fault block size is 14.4 square miles

2. 6 inactive wells in target sand; all P & A

3. 75 ft gas cap associated with 150 ft aquifer (Delhi Taylor, #1 Sealy Smith

4. Permeability varies from 0 to 1,050 md and averages 234 md in interval from 11,537 to 11,564 ft in Prairie Prod. #1 Frost

5. Salinity averages 72,000 ppm NaCl in aquifers nearest target gas sands

Unfavorable Criteria:

1. 9 active wells producing from above and below target sand.

2. _____

3. _____

4. _____

5. _____

Recommendation:

Favorable, because _____

_____

Unfavorable, because field is too active (Rated: Class C). Reservoir might become viable prospect when production ceases.

Table B-6. EVALUATION OF GAS FIELDS

DISPERSED GAS PROJECT

(Short form)

Field name: NADA (67) & NADA, NE (62) Wilcox 9,700 ft sand

 Location: Colorado County, Texas, 5S-29E-8/9

Favorable Criteria:

1. Reservoir size: $\geq$4.5 mi^2

2. Fault block, anticlinal structure

3. 9 inactive wells (P & A)

4. Sand thickness: 45-260 ft

5. Average salinity = 45,000 ppm NaCl

6.

Unfavorable Criteria:

1. Two active wells near top of anticline with last pressure gradient = 0.06-0.07 psi/ft

2. Average porosity = 15.2%, and permeability = 10.7 md, based on conv. core data from Shell Oil, no. 1 Engstrom.

3. Only two sonic logs (for Shell, no. 1 Engstrom and Chambers and Kenedy, #1 Dalco Oil Co.)

4. Abandonment pressure grad. $\geq$ 0.3 psi/ft

Recommendation:

Favorable, because

Unfavorable, because the target reservoir has low porosity and permeability, shaly sand, low pressure gradients, and active wells near top of structure (Rated: Class C).

127

Table B-7. EVALUATION OF GAS FIELDS

DISPERSED GAS PROJECT

(Short form)

Field name: Petronilla (8,000-8,100 ft sand interval)

Location: Nueces County, Texas, 19S-20E-3

Favorable Criteria:

1. Area of field is about 5 mi^2

2. There are 19 gas wells P & A

3. Five sonic logs, one density log

4. Average equilibrium temperature at 8,050 ft = 192°F

5. Average sand thickness in depth interval 8,000-8,100 ft = 90 ft

6. _____

Unfavorable Criteria:

1. 4 gas wells active from sands near target sand

2. 12 oil wells active from sand near target sand

3. No core data

4. Abandonment pressure gradients: 0.3 to 0.4 psi/ft

5. _____

6. _____

Recommendation:

Favorable, because _____

_____

_____

Unfavorable, because the field is very active (Rated: Class C).

_____

_____

128

Table B-8. EVALUATION OF GAS FIELDS

DISPERSED GAS PROJECT

(Short form)

Field name: Sarah White, 58 (Frio 9,200 ft sand)

Location: Galveston County, Texas, 6S-40E

Favorable Criteria:

1. Field is essentially abandoned with the exception of one well

2. Target sand is abandoned (originally contained gas, oil, and H_2O)

3. Target area >12 mi^2

4. Equilibrium temperature: 216°F

Unfavorable Criteria:

1. No core data available, but core taken in Tex East Trans.

   #1 Sadie Henck

2. Only one sonic log in fault block

3. Fault cuts target sand and reduces thickness from 80 to 30 ft

4. Area of aquifer is reduced by fault

5. Salinity: Indeterminate from SP log

6. Reservoir originally produced oil in western part of field and gas

   distillate from eastern part.

7. Pressure gradient in abandoned sand = 0.05-0.16 psi/ft

Recommendation:

Favorable, because _____

_____

_____

Unfavorable, because thin isolated gas sand, oil production, poor aquifer ·

(Rated: Class C).

129

Table B-9. Gas fields rejected as non-prospective for dispersed gas test areas.

County	Field Name, Discovery Year	Area <5 mi^2	Active Field	<5 Watered-Out Gas Wells	Recent Gas Completions Since 1975
Aransas	[3]Nine Mile Pt., 65		x		
	Rattlesnake Pt., 68	x	x		
	Rockport W., 54				x
	Salt Lake, 48	x			
Bee	[2]Caesar S., 42		x		
	Holzmark S., 56		x		x
	Karon S., 49		x		x
	Mosca, 59			x	
	Norbee, 65		x		x
	Orangedale, 63		x		
	Ragsdale, 52		x		x
	[2]Tuleta N., 61	x			
	Tuleta W., 37		x		
Brazoria	[2]Angleton, 39		x		x
	Bailey's Prairie, 40				No Aquifer
	Bell Lake, 76		x	x	
	Bonney, 50	x			
	Bonney N., 54			x	
	Collins Lake, 49		x		x
	Drum Point, 53			x	
	Lake Alaska, 63			x	
	Manor Lake, 55		x		
	Oyster Creek, 75			x	
	Peach Point, 48			x	
	Rattlesnake Mound, 61		x		
	Rowan, 40				x
	Rowan N., 53	x			
Chambers	Anahuac E., 64			x	
	[1,3]Devillier, 75		x		x
	Fig Ridge N.W., 44	x			
	Fishers Reef, 40		x		
	Mayes S., 46		x		x
	Red Fish Reef, 46		x		
	Umbrella Point, 57		x		x
	Willow Slough N., 51	x	x		

[1]One or more wells in field were classified by Doherty (1981) as watered-out geopressured gas cap wells.

[2]One or more field wells reported by Doherty (1981) as having high water production rates but lacked shut-in pressure data.

[3]One or more wells classified by Doherty (1981) as bottom hole rejects (pressure gradient between 0.6 and 0.65 psi/ft).

County	Field Name, Discovery Year	Area <5 mi²	Active Field	<5 Watered-Out Gas Wells	Recent Gas Completions Since 1975
Colorado	Altair, 45		x		No Aquifer
	Buck Snag, 42		x		x
	Cecil Noble, 50		x		x
	2Chesterville, 43		x		x
	Columbus, 44		x		x
	Eagle Lake S., 69		x		x
	Frelsburg, 44				x
	Glasscock, 44		x		x
	Hamel, 45		x		x
	Lissie, 50		x		
	New Ulm, 45				x
	Orangehill, 42				x
	Ramsey, 43		x		x
	Rock Island, .45		x		
	2Sheridan, 40		x		
	Tait, 50			x	
De Witt	Anna Barre, 54				x
	Arneckeville, 51		x		x
	Arneckeville S., 53		x		x
	Helen Gohlke, 51		x		
	Hix Green, 65		x		x
	Jennie Bell, 52		x		x
	Nordheim, 42		x		
	Smith Creek, 61		x		
	Sucher, 78				x
	Thomaston, 40				x
	Tinsley, 64			x	
	2Yorktown, 54		x		x
Goliad	Cabeza Creek S., 44		x		x
	Dallas Husky E., 53		x		x
	Dial, 44		x		
	Karen Beauchamp, 57		x		x
	Marshall, 48			x	x
	2Soleberg, 62			x	x
Hardin	Hickory Creek, 69			x	
	Longs Station, 60			x	
Karnes	2Burnell, 44		x		

County	Field Name, Discovery Year	Area <5 mi²	Active Field	<5 Watered-Out Gas Wells	Recent Gas Completions Since 1975
Kleberg	Baffin Bay, 66	x		x	
	Bina, 76		x		
	Kings Inn, 77		x		x
	²Laguna Larga, 49		x		x
	May, 55		x		
	Yeary, 58		x		
Liberty	Blanding, 75		x		
	Hull, 18		x		
	McCoy, 46				No Aquifer
	Raywood, 53		x		
	Rich Ranch, 60			x	
Live Oak	²Braslau S., 58		x		
	Clayton, 44		x		x
	Dunn, 56	x		x	
	George West, 62		x		x
	Karon, 51		x		
	Katz-Slick, 59	x			x
	²Sierra Vista, 67	x			x
Matagorda	Bay City, 34		x		
	Duncan Slough, 60		x		
	El Maton, 59				No Aquifer
	Old Ocean, 34		x		
	Pheasant S., 61		x		
	Pheasant S.W., 59		x		
	Sugar Valley, 43		x		
	Sugar Valley N., 66		x		
	³Tidehaven, 46		x		
	Trull, 57		x		x
	Van Vleck N., 62			x	
	Wilson Creek, 52			x	
Montgomery	Conroe N., 53			x	
	Fostoria, 42		x		No Aquifer
	Grand Lake, 52			x	
Newton	Quicksand Creek, 59		x		x

County	Field Name, Discovery Year	Area <5 mi^2	Active Field	<5 Watered-Out Gas Wells	Recent Gas Completions Since 1975
Nueces	[2]Agua Dulce, 28		x		x
	Bobby Lynn King, 78		x		x
	Bohemian Colony, 64			x	
	Chapman Ranch, 37		x		x
	Corpus Channel, 53		x		
	Corpus Christi, 35		x		x
	[3]Encinal Channel, 65		x		x
	Flour Bluff S.S.E., 78		x		x
	Nor Am., 70			x	
	Ransom Island, 53			x	
	[3]Red Fish Bay, 50		x		x
	[3]Red Fish Bay N., 59		x		x
	Stedman Island, 51		x		
Refugio	Bayside, 57			x	
	Bonnie View, 76		x		x
	Roche N., 62		x		
	Rooke Ranch, 75		x		
	Woodsboro S., 75		x		x
San Jacinto	Cold Springs, 40		x		x
	Urbana, 59		x	x	x
San Patricio	Enos Cooper, 53		x		x
	Gregory E., 60			x	
	Mary Lou Patrick, 68			x	
	Patrick, 51			x	
Tyler	Hillister E., 48		x	x	x
	Hyatt S., 45			x	
Victoria	Mission Valley N., 51		x		x
	Mission Valley W., 49		x		x

APPENDIX C

SIDEWALL CORE DATA,

LOWER HACKBERRY RESERVOIRS,

PORT ARTHUR FIELD

APPENDIX C—Sidewall core data, lower Hackberry

reservoirs, Port Arthur field.

Well No.	Depth (ft)	K (md)	φ (%)	Sw (%)	So (%)	Gas (by vol.)
			"A-1" Reservoir			
14	10,882	52.8	27.9	64.9	tr	9.8
			"A-2" Reservoir			
6	10,938†	7.1	27.3	82.0	0.0	4.9
	10,947	12.6	27.9	71.6	0.0	7.9
	10,951	335.0	32.6	49.7	tr	16.4
11	10,937†	84.5	27.5	61.8	0.4	10.4
	10,948†	58.2	27.2	63.1	0.7	9.8
14	10,923	41.9	27.5	63.3	tr	10.1
	10,960	238.0	30.8	60.4	tr	12.2
24	10,930	*	24.2	62.3	0.4	9.0
	10,945	11.0	24.4	77.9	0.4	5.3
	10,948	14.0	25.2	64.3	0.4	8.9
	10,951	0.0	19.6	64.6	0.5	6.8
29	10,927	15.2	24.1	63.2	0.0	8.9
	10,933.5	0.0	12.1	76.9	0.0	2.8
	10,938.5	1.3	15.2	67.2	0.0	5.0
	10,944	2.9	16.3	62.6	0.0	6.1
	10,961	0.0	11.2	81.2	0.0	2.1
			"B" Reservoir			
11	11,022	104.0	29.0	57.2	8.6	9.9
24	11,032	0.0	24.0	89.5	0.0	2.6
29	11,051	2.9	19.1	87.4	0.0	2.2
31	11,025.5	*	31.8	74.7	0.1	6.9
	11,029	*	30.9	63.7	3.9	10.0
	11,032	*	31.2	68.3	0.4	9.8
	11,034	*	30.3	79.3	3.6	5.2
	11,044	*	33.7	63.3	8.9	9.4
	11,045	*	34.1	63.7	9.3	10.2
			"B-1" Reservoir			
6	11,022	21.2	28.4	51.0	tr	13.9
11	11,041	0.0	15.7	70.6	0.0	4.6
	11,042	7.6	17.3	71.1	0.0	5.0
14	11,043	141.0	28.1	64.1	tr	10.1
24	11,040	*	24.9	54.3	0.4	11.3
	11,045	5.4	26.1	58.2	0.0	6.9
	11,048	0.0	25.6	83.2	0.0	4.3

Well No.	Depth (ft)	K (md)	φ (%)	Sw (%)	So (%)	Gas (by vol.)
			"B-2" Reservoir			
31	11,078.5	*	29.4	75.4	1.4	6.8
	11,091	*	32.6	71.3	0.3	9.4
	11,097	*	27.2	76.5	1.5	6.0
14	11,067	182.0	30.7	61.6	1.1	11.8
29	11,071	0.0	14.3	77.6	0.0	3.2
	11,074	127.0	31.1	.68.6	0.8	9.6
	11,087	0.0	12.1	83.5	0.0	2.0
			"C" Reservoir			
1	11,147.5	60.0	28.9	76.4	0.0	6.8
	11,149	95.2	30.0	71.1	0.3	8.9
	11,152	74.3	31.2	69.2	0.2	9.6
	11,156	110.0	30.7	66.2	0.3	10.4
	11,162	88.0	29.6	60.3	0.1	11.8
	11,168	132.0	30.8	59.3	0.2	11.6
	11,173.5	120.0	31.4	76.6	0.0	7.4
6	11,131	*	32.4	44.5	15.4	13.3
11	11,157	41.2	22.0	64.0	3.2	7.2
	11,160	10.8	19.4	73.7	0.0	5.1
14	11,142†	207.0	33.3	60.1	1.5	12.7
	11,144†	106.0	33.5	70.2	1.6	9.5
	11,147	248.0	35.7	66.1	1.4	11.6
	11,148	310.0	36.5	63.3	2.7	12.4
	11,157	122.0	31.1	63.2	tr	11.4
	11,164	0.0	28.8	83.7	1.2	4.8
	11,174	35.2	27.1	57.1	3.2	10.6
	11,182	262.0	30.5	56.7	3.0	12.2
24	11,122	4.2	23.3	35.6	0.4	11.2
	11,161	0.0	25.0	83.1	0.0	2.8
	11,165	4.6	29.7	66.0	1.1	9.3
	11,170	113.0	31.6	67.6	0.3	10.1
	11,189	67.0	29.6	48.1	0.3	15.3
	11,200	226.0	31.9	56.2	0.3	13.9
29	11,129	0.0	12.9	69.0	0.0	4.0
31	11,132	*	28.6	75.0	1.1	6.8
	11,152	*	28.3	71.3	0.2	8.1
	11,155	13.1	26.4	78.0	0.0	5.8
	11,163	84.3	31.2	61.2	1.3	11.7
	11,165	314.0	33.3	58.9	1.5	13.2
			Upper "D" Reservoir			
14	11,206	15.2	20.7	56.1	4.5	8.1
	11,209.5	176.0	34.4	58.7	2.9	13.2

Well No.	Depth (ft)	K (md)	φ (%)	Sw (%)	So (%)	Gas (by vol.)
			"D" Reservoir			
6	11,231	67.0	28.8	70.1	tr	8.6
	11,240	49.2	29.7	70.8	5.4	7.1
	11,244	*	28.0	57.5	8.6	9.5
11	11,205	12.1	19.7	59.0	0.3	8.1
	11,211	18.5	22.0	70.5	0.0	6.5
	11,219	*	22.6	65.5	0.0	7.8
14	11,232†	285.0	32.5	66.2	3.0	10.1
	11,238†	101.0	28.2	57.1	2.8	11.0
	11,249	89.7	31.8	65.6	3.0	10.0
	11,255	241.0	38.4	64.7	2.6	12.6
	11,261	187.0	35.1	63.7	1.4	12.2
24	11,250†	*	34.2	58.7	0.3	14.0
	11,255†	110.0	31.0	60.3	0.3	12.2
	11,260	173.0	32.3	52.9	0.3	15.1
29	11,240	8.1	13.7	67.1	0.0	4.5
	11,253	98.1	26.0	53.2	0.4	12.2
	11,267	3.2	18.4	62.1	0.0	7.0
31	11,250	149.0	30.7	61.3	0.2	11.8
	11,252	*	29.9	45.8	3.7	15.1
	11,253	310.0	31.1	58.8	0.2	11.8
			"E" Reservoir			
11	11,303	*	27.7	59.5	0.0	11.2
14	11,281†	327.0	37.5	63.3	1.3	13.3
	11,283†	119.0	32.5	61.1	tr	12.6
	11,285†	137.0	31.5	66.0	1.5	10.9
	11,302	128.0	32.6	64.1	tr	10.6
	11,305.5	89.7	36.7	68.1	1.3	12.2
	11,315	122.0	32.7	68.2	tr	12.0
	11,339	27.5	26.5	70.1	1.9	7.4
	11,341	91.9	33.8	66.5	1.5	10.8
24	11,309	44.0	24.3	56.6	0.3	12.3
	11,310	11.0	26.6	67.0	0.4	8.7
	11,318	44.0	33.4	58.5	0.3	15.4
	11,322	35.0	31.4	68.9	0.3	9.7
	11,327	112.0	31.4	67.3	0.3	10.2
	11,333	29.0	31.4	59.9	0.3	12.5
	11,362	27.0	29.7	65.0	0.3	10.3
	11,369	12.0	29.8	78.2	0.3	6.4
	11,380	51.0	34.7	65.2	0.3	12.0
29	11,312	69.1	27.1	55.3	0.0	12.1

138

Well No.	Depth (ft)	K (md)	φ (%)	Sw (%)	So (%)	Gas (by vol.)
			"E" Reservoir (cont.)			
31	11,289	4.7	24.3	85.2	0.0	4.1
	11,296	80.9	29.2	44.5	0.7	16.2
	11,300.5	64.3	28.7	61.3	0.7	10.9
	11,306	71.1	28.2	69.6	0.3	7.8
			"F" Reservoir			
14	11,359†	182.0	35.0	62.3	tr	14.2
	11,364	137.0	38.7	65.5	2.6	12.5
	11,370	218.0	38.0	62.9	2.4	*
	11,385	87.2	33.2	62.0	tr	12.6
24	11,394	37.0	32.5	75.5	0.3	7.9
	11,400	69.0	31.0	72.3	0.3	8.5
29	11,413	7.6	17.1	46.9	0.0	9.1
31	11,386.5	7.4	24.4	88.0	0.0	3.1
	11,390	27.6	28.3	73.3	0.0	7.0
	11,440	*	26.1	81.8	0.0	4.7
			"G" Reservoir			
14	11,463	167.0	36.5	59.4	2.7	*
	11,467	151.0	38.8	59.2	2.1	15.0
	11,470	139.0	34.8	64.2	tr	2.4
	11,479	119.0	38.3	69.9	tr	11.5
24	11,478	74.0	31.2	73.6	0.3	8.1
	11,482	101.0	32.8	68.9	0.3	9.1
	11,489	16.0	29.2	50.6	0.4	14.3
	11,493	8.0	27.9	60.0	0.3	11.1
	11,499	*	29.8	74.0	0.3	8.4
	11,528	2.5	23.4	67.8	0.0	7.5
29	11,480	54.1	21.1	48.8	0.0	10.8
	11,481	29.7	25.1	53.7	0.0	10.7
	11,490	2.7	17.9	70.9	0.0	5.2
	11,496	16.8	18.1	46.4	0.0	9.7
	11,501	23.1	24.2	54.1	0.0	11.1
	11,502	73.9	23.4	40.6	0.4	13.9
	11,503	31.4	20.9	42.1	0.6	12.1
	11,525	47.3	21.8	46.8	0.9	11.2
	11,527	15.1	24.2	58.3	0.0	10.1
31	11,461†	*	31.3	63.0	3.8	10.4
	11,464	112.0	32.6	72.0	0.2	9.1
	11,468	184.0	32.9	66.0	0.2	11.2
	11,474	8.7	26.8	82.8	0.1	4.6

Well No.	Depth (ft)	K (md)	φ (%)	Sw (%)	So (%)	Gas (by vol.)
			Nodosaria Reservoir			
1	12,043	6.7	27.2	69.4	0.0	8.3
	12,045	16.8	28.6	68.7	tr	9.0
	12,048	14.3	27.4	76.3	0.0	6.5
	12,050	15.2	27.9	71.4	0.0	8.0
	12,053	5.3	26.3	81.3	0.0	4.9
	12,063	14.9	28.5	67.4	0.1	9.3
	12,067	8.8	27.2	72.4	0.0	7.5
6	11,708	*	28.9	45.8	2.1	14.3
	11,723	238.0	28.4	37.0	10.9	14.8
	11,733	*	29.6	44.6	11.5	13.0
	11,738	341.0	30.6	49.3	7.5	13.2
14	11,787	16.5	31.4	62.8	tr	11.6
	11,797	42.8	30.5	65.1	tr	10.6
	11,804	452.0	34.3	64.1	tr	12.3
24	11,802	132.0	34.8	64.6	0.3	12.2
	11,806	135.0	34.0	57.0	0.3	14.5
	11,810	171.0	34.6	63.7	0.6	12.3
	11,815	256.0	33.0	54.0	0.3	15.1
	11,820	15.0	28.9	56.2	0.4	12.2
	11,824	*	29.4	56.9	0.7	12.5
	11,852	97.0	33.3	34.8	0.3	14.5

* No test
† Depths fall within perforated intervals.
tr = trace

APPENDIX D

VOLUMETRIC ANALYSES OF FRIO
SANDS USING WELL LOG METHODS,
PORT ARTHUR FIELD

Contents

APPENDIX D

Part 1

Matrix Interval Transit Time (Δtm)

Ninety-five sets of data (R_t vs. Δt) were extracted from Well No. 37 and used to approximate matrix interval transit time for several thousand feet of water bearing section (4,000 - 12,000 feet).

$$\text{Log } R_t = m \cdot \text{Log } \emptyset_s + \text{Log } A$$

where

$$A = a \cdot R_w \cdot I$$

$$\emptyset = \frac{\Delta t - \Delta tm}{\Delta tf - \Delta tm} \left(\frac{1}{C_p}\right)$$

Sonic derived porosity ($\emptyset_s$) was calculated in the conventional manner. Compaction factor C_p was approximated by the magnitude of Δtsh and was considered a function of depth as demonstrated by the following relationship:

$$C_p = 1.54 - (6 \cdot 10^{-5} \cdot \text{Depth}) \qquad \text{if depth} < 9000 \text{ feet}$$

$$\text{ie.} \quad \begin{aligned} C_p &= 1.36 \quad @ \quad 3000' \\ C_p &= 1.00 \quad @ \quad 9000' \end{aligned}$$

and

$$C_p = 1.15 \qquad \text{if depth} > 9000 \text{ feet}$$

Using the approximate C_p value and an assumed Δtf (189 μsec/ft.), a series of regression analyses were made by varying Δtm from 40 to 60 μsec/ft. Regression coefficients, R_c, were calculated for the varying Δtm values in order to select the relationship with the best mathematical fit (Table D-1). The highest degree of correlation was found when $\Delta tm = 53$ μsec/ft. In this phase only the applicable Δtm value was determined without calculating cementation constant 'm'.

Formation Factor-Porosity Relationship

The sonic log for Well No. 37 was the only porosity log available in the field. The interval transit times and the correlative induction log resistivities provided a basis to estimate formation factor relationships. The results of the following analysis compare favorably with published data (Table D-2).

Using a value of 53 μsec/ft. for Δtm to compute porosity and 63 sets of data points below 11,000 feet (zones of interest in Well No. 37), two regression analyses were made to determine 'a' and 'm' for the equation $F = a\emptyset^{-m}$. Figure D-1 shows a linear bivariate relationship between R_t and $\emptyset_S$ represented by two lines. These two lines are the result of the two regression analyses. One considers porosity as the independent variable. The other considers porosity as the dependent variable. The spread between the lines is a measure of random error and heterogeneity effects operating on each variable. The equations for the two lines are:

Run 1 ($\emptyset$ independent): $R_t = A \cdot \emptyset^m$

Run 2 (R_t independent): $\emptyset_S = A* \cdot R_t^{m*}$, or $R_t = A*^{-1/m*} \cdot \emptyset^{1/m*}$

If $m = 1/m*$ and $A = A*^{(-m)}$

then $R_t = A \cdot \emptyset^m$

Assuming the saturation index $I = 1$ and $R_w = 0.0212$ (136,000 ppm @ 217°F), 'a' was obtained by:

$$a = \frac{A}{R_w \cdot I} = \frac{A}{R_w}$$

It is recognized that a saturation index of 1.00 produces a value of 'a' which may be too high. Therefore, instead of attempting a reduced regression (Collins and Piles, 1981), values obtained by regressing R_t as the independent variable were selected. Values of 'a' and 'm' obtained by pattern recognition technique are shown below.

Run	m*	A*	m	A	a	
#1			-1.532	.0549	2.59	$\emptyset$ independent
#2	-.5527	.1619	-1.809	.0371	1.75	R_t independent

143

Therefore, based on Well No. 37, the apparent formation factor-porosity relationship is $F = 1.75 \cdot \emptyset^{-1.81}$.

Since the quality of porosity data in Well No. 37 is unknown, determining the true functional relationship between $\emptyset$ and R_t is difficult. However, by noting the intersection of the two lines in Figure D-1, an approximation of average porosity and water-bearing formation resistivity can be made:

Porosity = 0.243 fraction of bulk volume

R_o = 0.479 ohm-meters

These values may be used as a reference when there are insufficient data to determine specific values for an interval.

Saturation Exponent

According to the October 1981 study on Well No. 1 by Ausburn and the study of the Vicksburg Formation by Ritch and Kozik, the value of 1.8 for 'n' was chosen.

At this point, working parameters for the Port Arthur Field were fixed as follows:

Δtm	=	53 μsec/ft	m	=	1.81
Δtf	=	189 μsec/ft	n	=	1.8
a	=	1.75	C_p	=	1.1 to 1.2

Laboratory measured 'm' and 'n' values for various Texas formations (Coats and Dumanoir, 1974, and Porter and Carothers, 1970) are shown for reference on Table D-2.

Resistivity Values

Temperature,

Instead of interpolating BHT, nearby equilibrium temperature was adopted as Tf.

Mud Resistivities

Mud and mud filtrate resistivities were converted to formation temperature.

Formation Water Resistivity

R_W was calculated from salinity data supplied by BEG according to the following conversion formulas (Bateman and Konen, 1977).

$$R_W \ @ \ 75^\circ F \ = \ 10^{(3.562 \ - \ .955 \ Log \ (ppm))} + .0123$$

$$R_W \ @ \ Tf \ = \ R_W \ @ \ 75 \ x \ \frac{82}{Tf + 7}$$

R_O

R_O was assumed from conductivity of a nearby apparent wet zone. The ranges in R_W and R_O were:

Item	Range	Average
R_W	.017 - .036	.025
R_O	.37 - .50	.44

145

TABLE D - 1

REGRESSION COEFFICIENTS

Δtm	Rc
41	.8516
43	.8521
45	.8526
47	.8530
49	.8534
51	.8536
*53	.8538; Best Fit
55	.8537
57	.8534
59	.8525

TABLE D - 2

LABORATORY MEASURED 'm' AND 'n'

	Litho.	Average m	Average n	a
Wilcox, Gulf Coast	SS	1.9	1.8	
Government Wells, South Texas	SS	1.7	1.9	
Frio, South Texas	SS	1.8	1.8	
Miocene, South Texas	SS	1.95	2.1	
Rodessa, East Texas	LS	2.0	1.6	
Woodbine, East Texas	SS	2.0	2.5	
Ellenburger, West Texas	LS,DOL	2.0	3.8	
Ordovician, West Texas	SS	1.6	1.6	
Pennsylvanian, West Texas	LS	1.9	1.8	
Permian, West Texas	SS	1.8	1.9	
Frio, Agua Dulce, South Texas	SS	1.71	1.66	
Frio, Edinburgh, South Texas	SS	1.82	1.5	
Frio, Hollow Tree, South Texas	SS	1.83	1.66	
Jackson, Cole, South Texas	SS	2.01	1.66	
Navarro, Olmos, South Texas	SS	1.89	1.49	
Viola, Bowie, North Texas	LS	1.77	1.15	
*Miocene, Gulf Coast	SS	1.35		1.8
*Miocene, Gulf Coast	SS	1.35		1.6
*Miocene, Gulf Coast	SS	1.3		2.0
*Miocene, Gulf Coast	SS	1.2		2.0
*Miocene, Gulf Coast	SS	1.29		1.97

*Data taken from Porter and Carothers (1970)

147
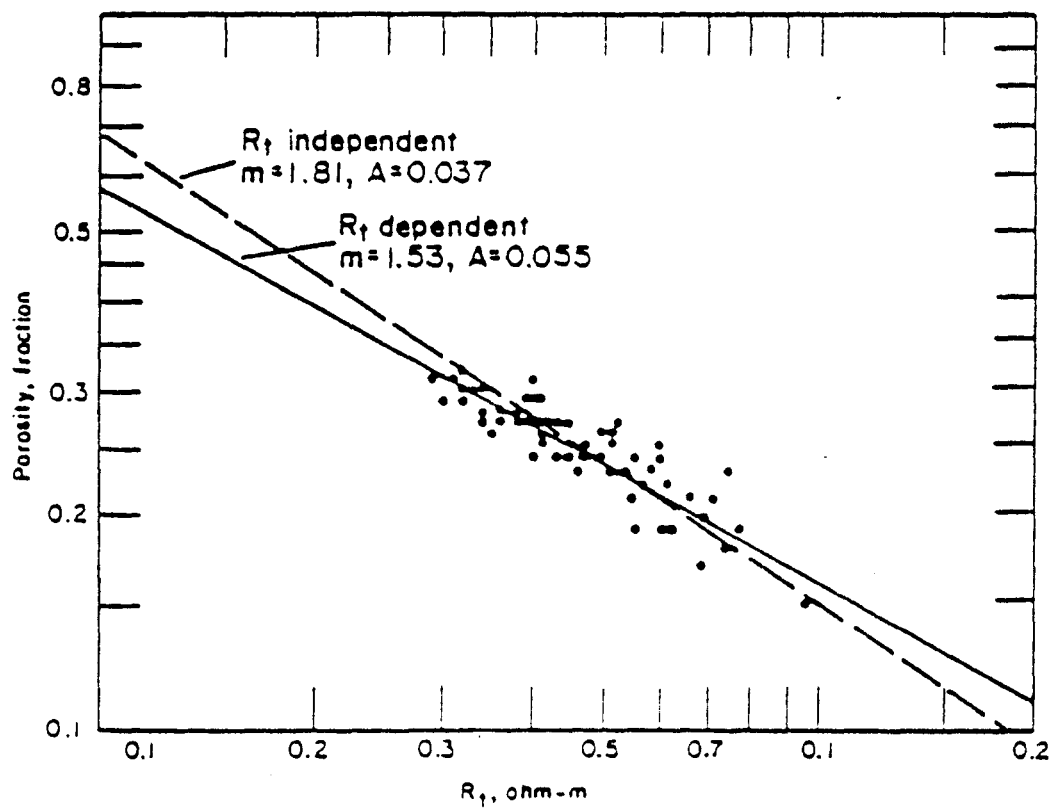
FIGURE D-1, R_t VS. SONIC POROSITY (WELL NO. 37)

$$\Delta t_m = 53, \quad \Delta t_f = 189$$

148

Part 2

Computer Plots

FIG. D-2   SW VS. SUBSEA DEPTH

B-2 SAND (FRIO)   60 DATA, $\bar{X}=$ 0.702 $\bar{Y}=11070.350$
L. HACKBERRY SD.   TYPE   LINER   EXPNT   POWER   LOGAR
PORT ARTHUR FIELD   EQ.   Y=A+BX   Y=A.E^{BX} Y=A.X^B Y=A+BLX
JEFFERSON CO., TEXAS   A =   11028.   11028.   11086.   11087.
APP. GWC = -11075   B =   60.036   0.005   0.004   43.048
                          R =   0.048   0.018   0.020   0.055
       EACH SYMBOL REPRESENTS APPROX. 5 FT. INTERVAL

SUBSEA DEPTH, FT

SW, (CUTOFF=.65)

Special Symbols
☐ Producer
☒ Perf. Interval
○ Well #30
   (recent in-fill well)

LKG

$S_w = 65\%$

150
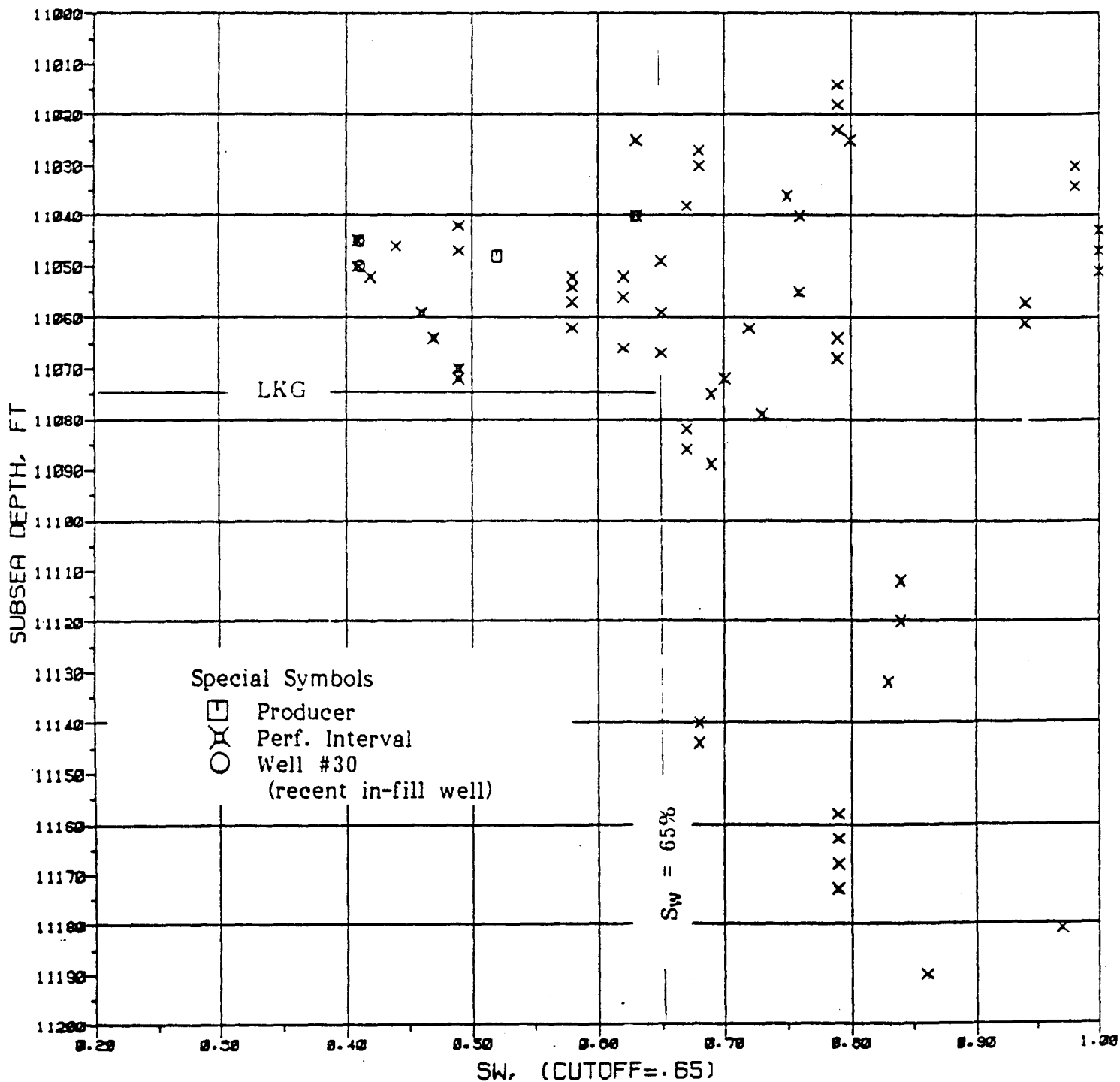
FIG. D-3 SW VS. SUBSEA DEPTH

C SAND (FRIO)
L. HACKBERRY SD.
PORT ARTHUR FIELD
JEFFERSON CO., TEXAS
APP. GWC = -11150 FT

157 DATA, $\bar{X}=$ 0.728 $\bar{Y}=11155.548$

TYPE	LINER	EXPNT	POWER	LOGAR
EQ.	$Y=A+BX$	$Y=A.E^{BX}$	$Y=A.X^B$	$Y=A+BLX$
A =	11087.	11088.	11178.	11177.
B =	94.672	0.008	0.005	60.913
R =	0.271	0.022	0.023	0.246

EACH SYMBOL REPRESENTS APPROX. 5 FT. INTERVAL

Special Symbols

⊡ Producer
⋈ Perf. Interval
○ Well #30
    (recent in-fill well)

LKG

$S_W = 65\%$

SUBSEA DEPTH, FT

SW, (CUTOFF=.65)

151
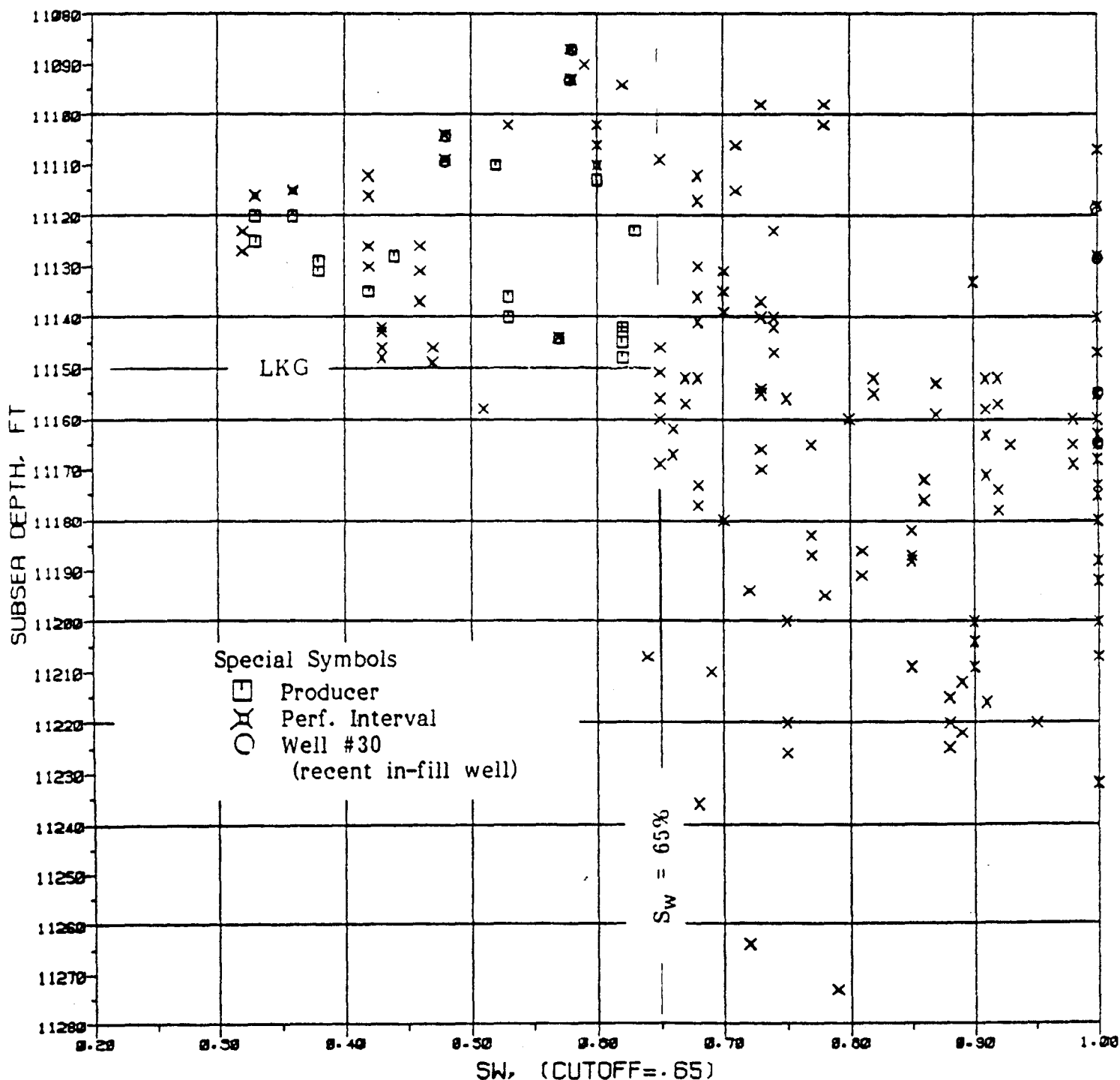
FIG. D-4   SW VS. SUBSEA DEPTH

D SAND (FRIO)   147 DATA,   X̄=   0.759   Ȳ=11241.619
L. HACKBERRY SD.   TYPE   LINER   EXPNT   POWER   LOGAR
PORT ARTHUR FIELD   EQ.   Y=A+BX   Y=A·E^{BX} Y=A·X^B Y=A+BLX
JEFFERSON CO., TEXAS   A =   11164.   11165.   11263.   11263.
APP. GWC = -11240 FT   B =   102.090   0.009   0.006   71.140
                                    R =   0.231   0.027   0.028   0.221
            EACH SYMBOL REPRESENTS APPROX. 5 FT. INTERVAL

Special Symbols
▯ Producer
✗ Perf. Interval
○ Well #30
   (recent in-fill well)

LKG

S$_W$ = 65%

SUBSEA DEPTH, FT

SW, (CUTOFF=.65)

152
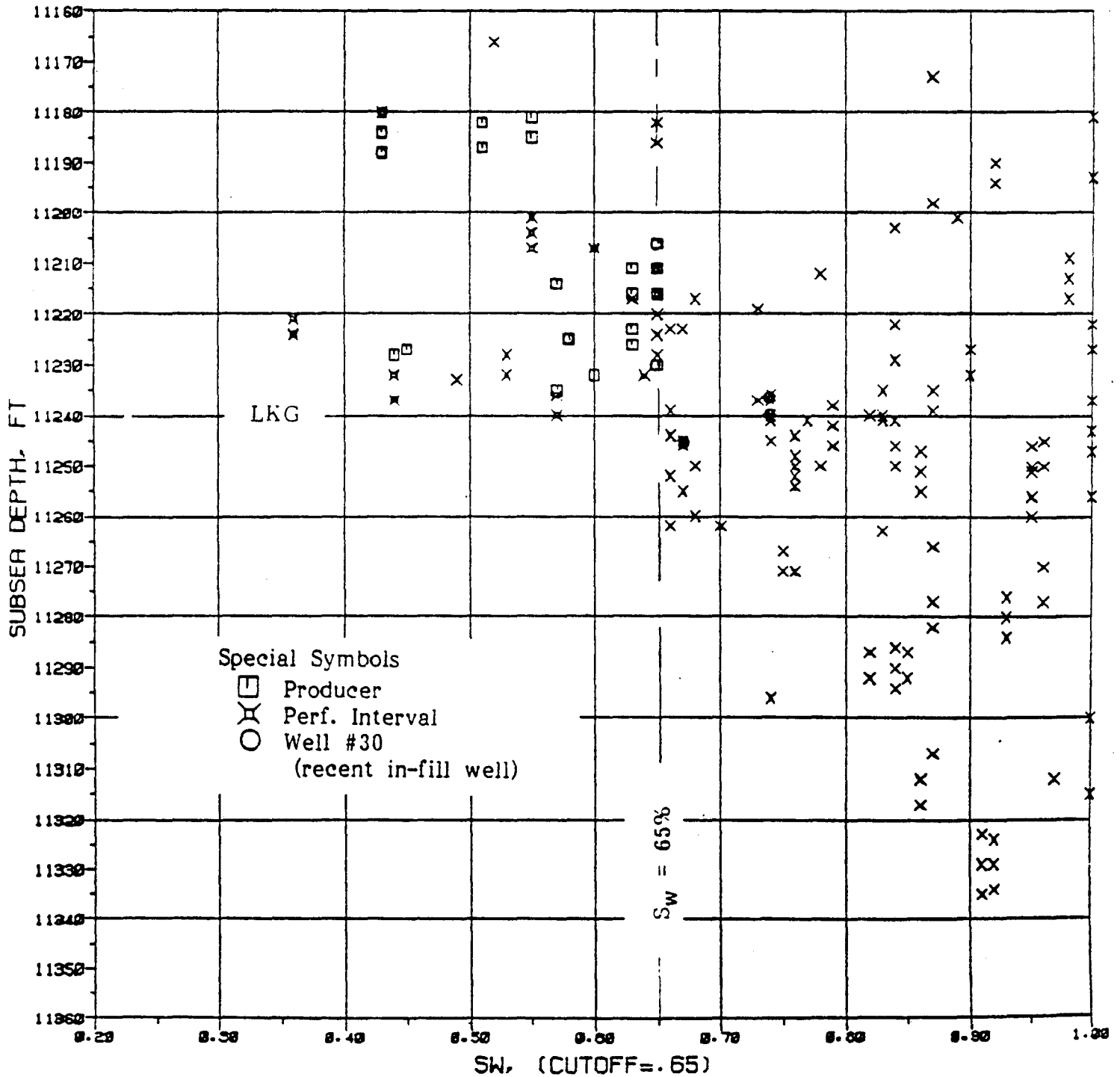
SW VS. SUBSEA DEPTH

E SAND (FRIO)   145 DATA,   X̄=   0.833 Ȳ=11320.683
L. HACKBERRY SD.   TYPE   LINER   EXPNT   POWER   LOGAR
PORT ARTHUR FIELD   EQ.   Y=A+BX   Y=A.E^BX Y=A.X^B Y=A+BLX
JEFFERSON CO., TEXAS   A =   11211.   11209.   11340.   11340.
APP. GWC = -11296 FT   B =   131.217 0.012   0.008   94.503
                       R =   0.341   0.066   0.062   0.299

EACH SYMBOL REPRESENTS APPROX. 5 FT. INTERVAL

SUBSEA DEPTH, FT

LKG

Special Symbols
⊡   Producer
✕   Perf. Interval
○   Well #30
    (recent in-fill well)

$S_W = 65\%$

SW, (CUTOFF=.65)

153
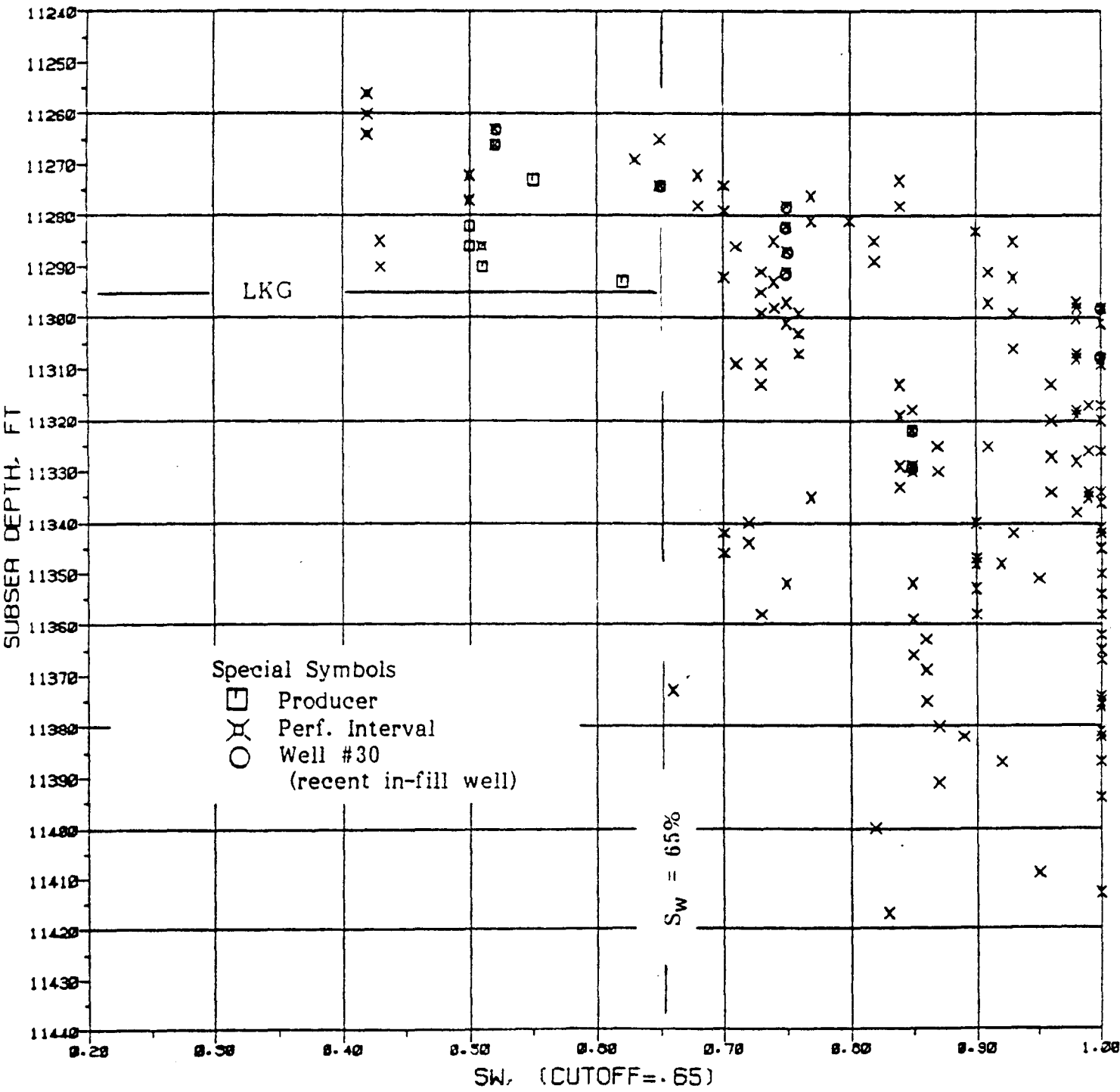
FIG. D-6   SW VS. SUBSEA DEPTH

LOWER E AND F SANDS   196 DATA,   X̄=   0.833   Ȳ=11472.832
L. HACKBERRY SD.   TYPE   LINER   EXPNT   POWER   LOGAR
PORT ARTHUR FIELD   EQ.   Y=A+BX   Y=A.E^BX   Y=A.X^B   Y=A+BLX
JEFFERSON CO., TEXAS   A =   11143.   11153.   11532.   11533.
APP. GWC = -11368 FT   B =   396.385   0.034   0.027   308.557
                               R =   0.125   0.308   0.316   0.125
           EACH SYMBOL REPRESENTS APPROX. 5 FT. INTERVAL   ⟩

154
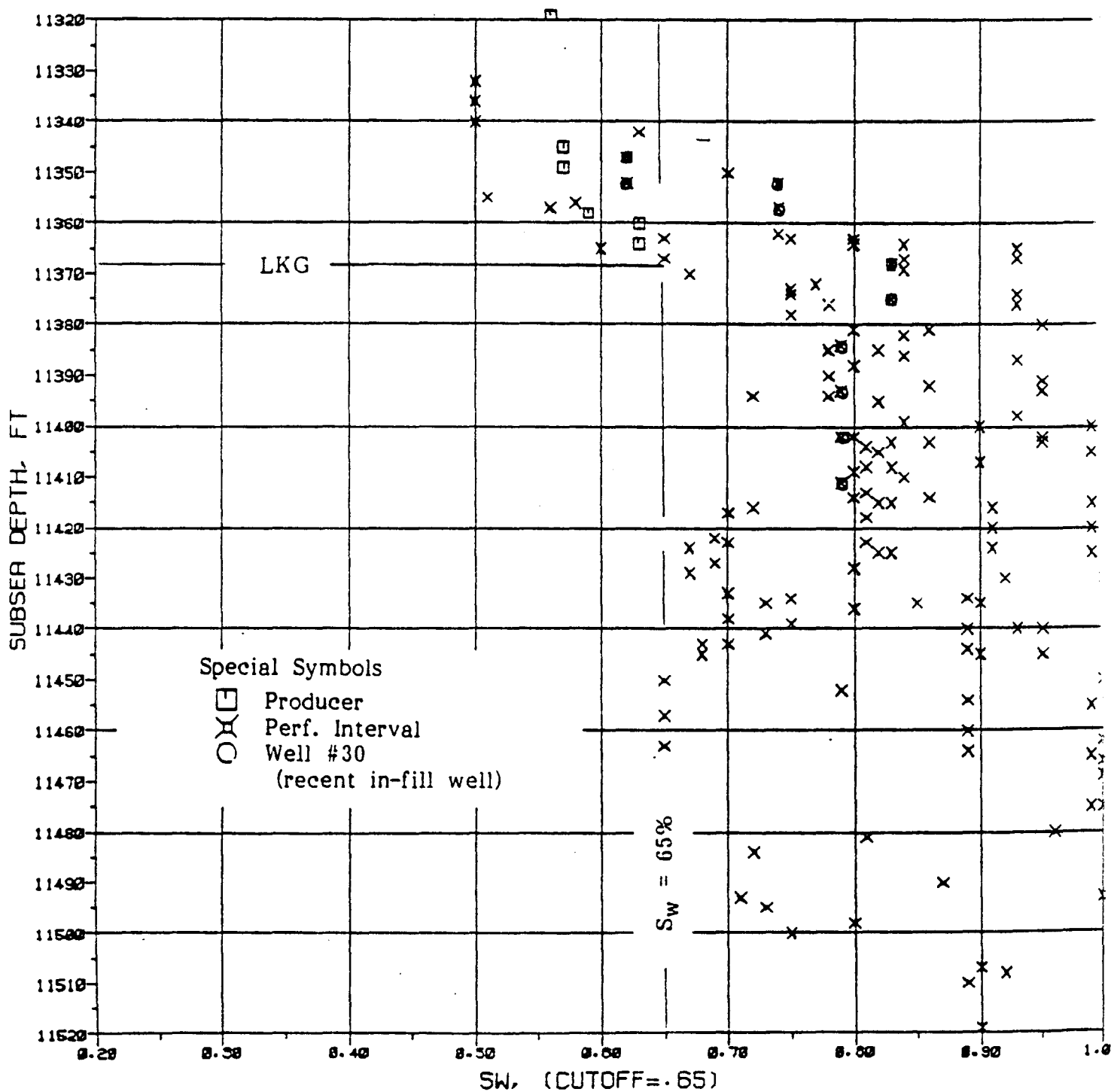
FIG. D-7   SW VS. SUBSEA DEPTH

G SAND (FRIO)
L. HACKBERRY SD.
PORT ARTHUR FIELD
JEFFERSON CO., TEXAS
APP. GWC = -11470 FT

	58 DATA,	$\bar{X}=$ 0.756	$\bar{Y}=$11483.000	
TYPE	LINER	EXPNT	POWER	LOGAR
EQ.	Y=A+BX	Y=A.E^{BX}	Y=A.X^{B}	Y=A+BLX
A =	11372.	11372.	11515.	11515.
B =	146.693	0.013	0.009	103.733
R =	0.328	0.327	0.315	0.309

EACH SYMBOL REPRESENTS APPROX. 5 FT. INTERVAL

Special Symbols
⊡ Producer
⋈ Perf. Interval
○ Well #30
(recent in-fill well)

LKG

$S_W = 65\%$

SUBSEA DEPTH FT

SW, (CUTOFF=.65)

155
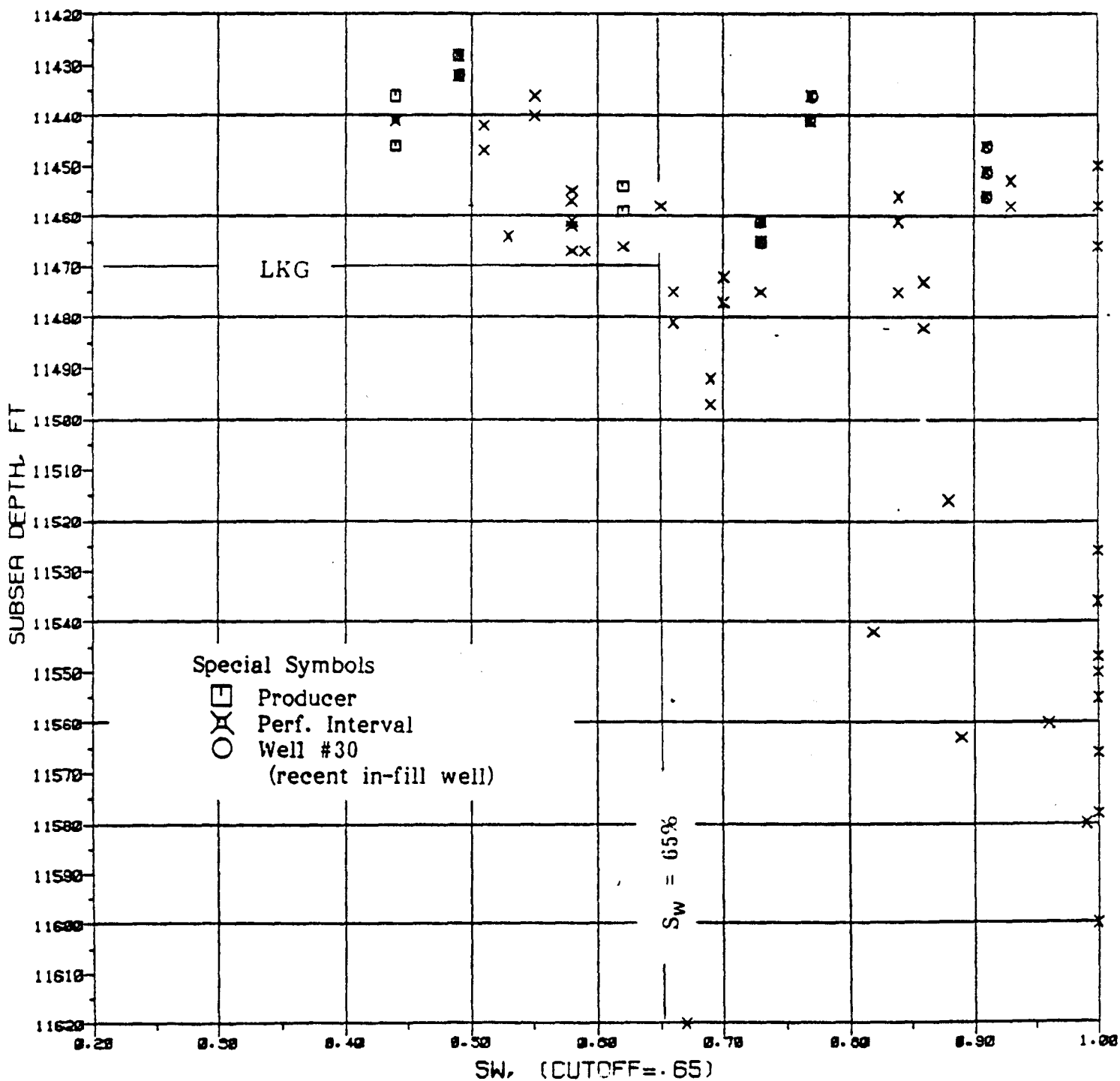
FIG. D-8   SW VS. SUBSEA DEPTH

B2 THRU G SANDS
L. HACKBERRY SD.
PORT ARTHUR FIELD
JEFFERSON CO., TEXAS

763 DATA, $\bar{X}=$ 0.756 $\bar{Y}=$11483.000

TYPE	LINER	EXPNT	POWER	LOGAR
EQ.	$Y=A+BX$	$Y=A \cdot E^{BX}$	$Y=A \cdot X^B$	$Y=A+BLX$
A =	11048.	11372.	11515.	11515.
B =	326.887	0.013	0.009	103.733
R =	0.120	0.327	0.315	0.309

EACH SYMBOL REPRESENTS APPROX. 5 FT. INTERVAL

156
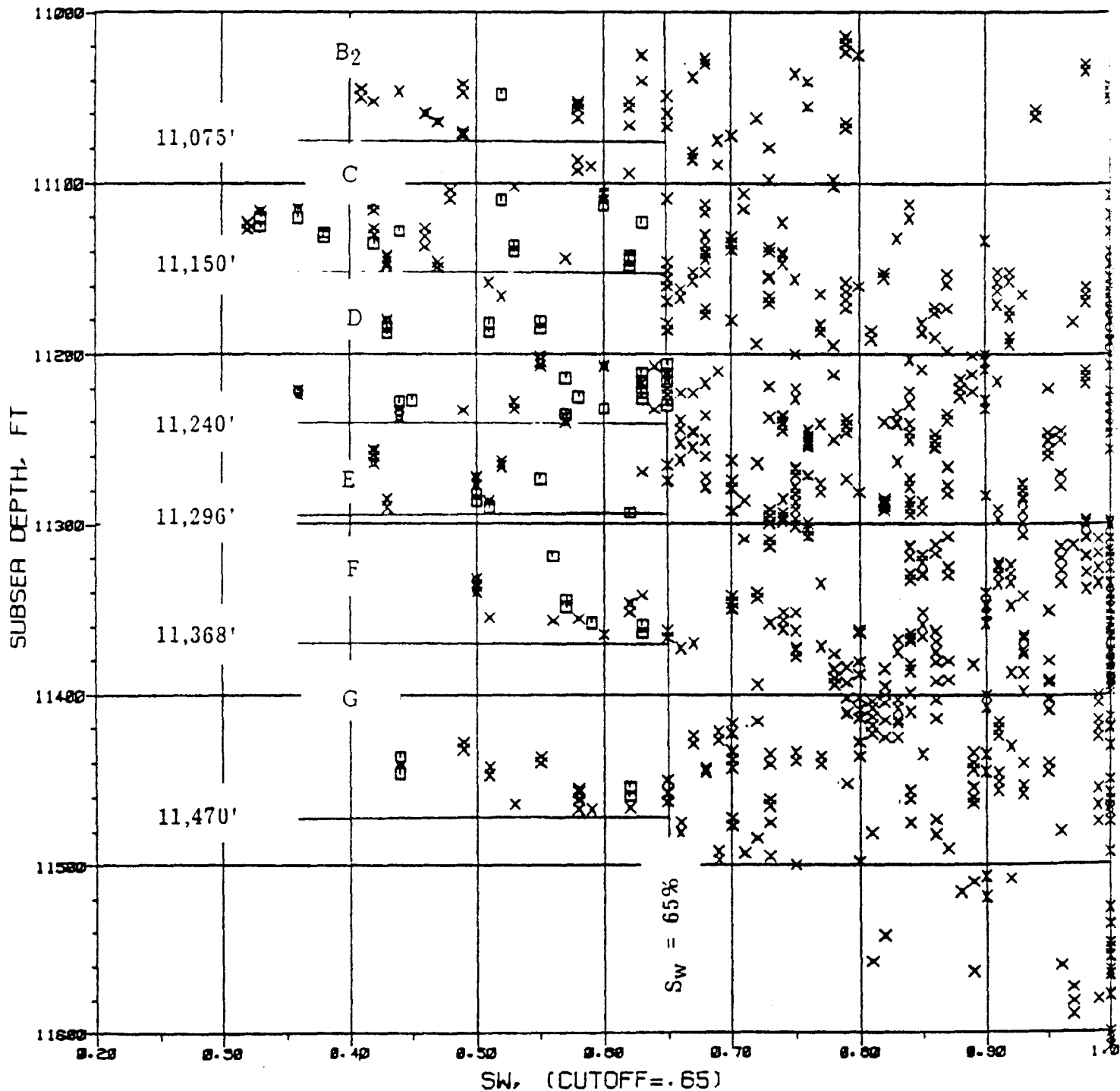
FIG. D-9   POROSITY VS. S DEPTH

WELL NO. 37
L. HACKBERRY SD.
PORT ARTHUR FIELD
JEFFERSON CO., TEXAS
DEVIATED WELL

83 DATA, $\bar{X}$= 0.260 $\bar{Y}$=11478.735

TYPE	LINER	EXPNT	POWER	LOGAR
EQ.	Y=A+BX	Y=A.E^{BX}	Y=A.X^{B}	Y=A+BLX
A =	11827.	11830.	11205.	11205.
B =		-0.117	-0.017	-195.672
R =	0.124	0.123	0.077	0.078

EACH SYMBOL REPRESENTS APPROX. 5 FT. INTERVAL

157
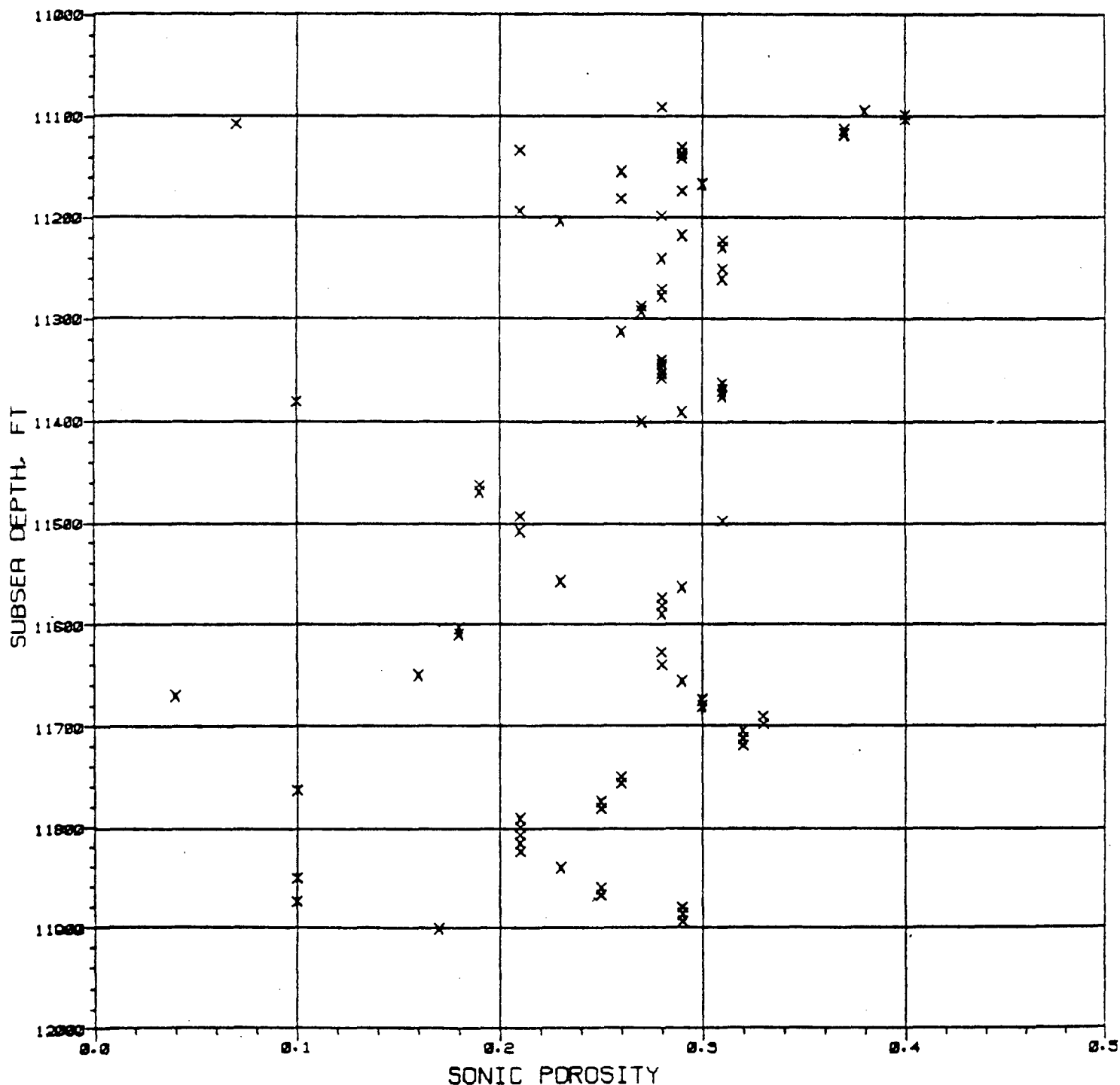
SW VS. SUBSEA DEPTH

WELL NO. 37
L. HACKBERRY SD.
PORT ARTHUR FIELD
JEFFERSON CO., TEXAS
DEVIATED WELL

83 DATA, $\bar{X}=$ 0.870 $\bar{Y}=11478.735$

TYPE	LINER	EXPNT	POWER	LOGAR
EQ.	$Y=A+BX$	$Y=A.E^{BX}$	$Y=A.X^B$	$Y=A+BLX$
A =	10658.	10681.	11592.	11594.
B =	943.429	0.082	0.068	773.367
R =	0.169	0.169	0.176	0.175

EACH SYMBOL REPRESENTS APPROX. 5 FT. INTERVAL

SUBSEA DEPTH FT

SW, (CUTOFF=.65)

158
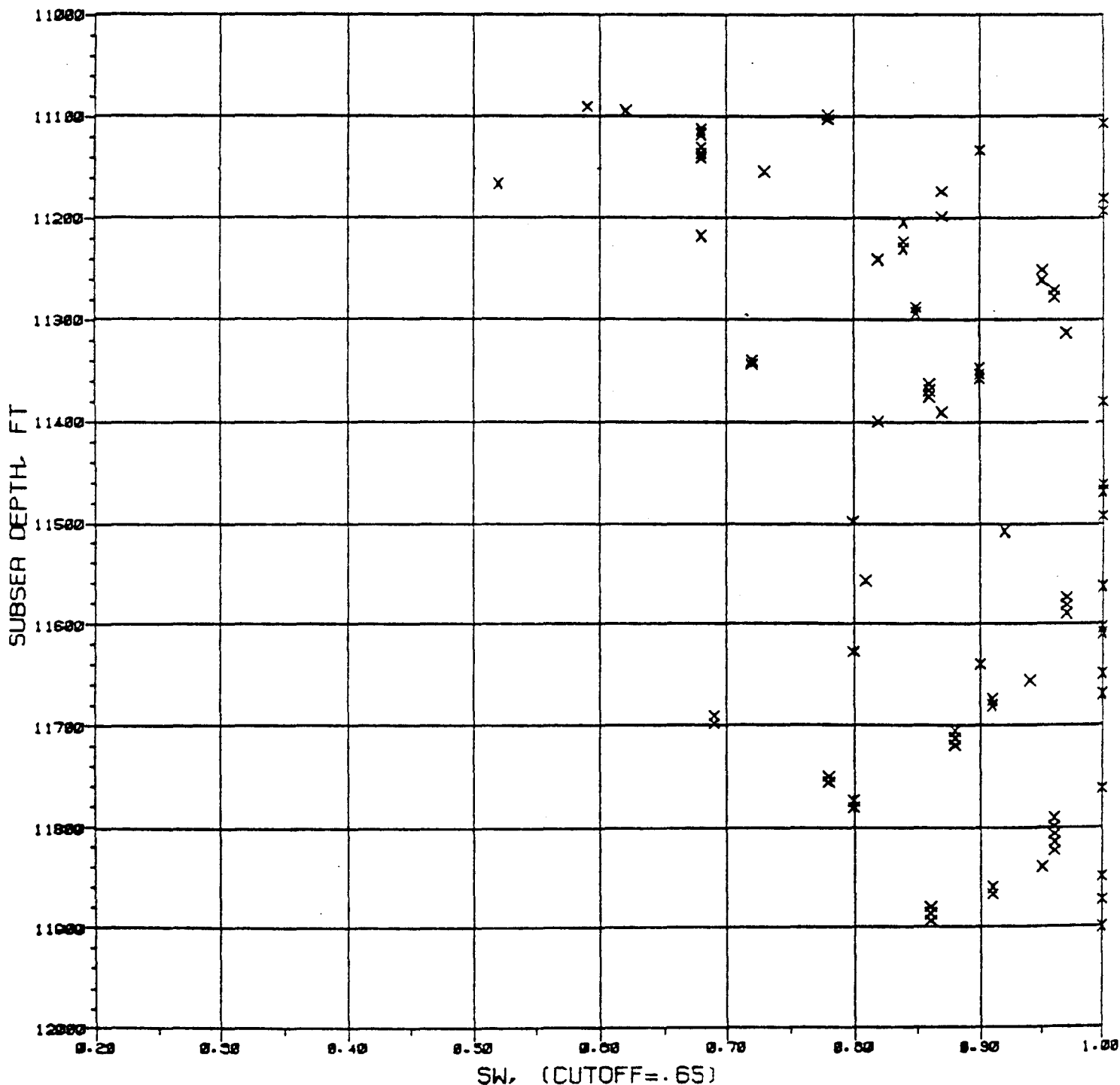
FIG. D-11   POROSITY VS. SW

WELL NO. 37   83 DATA, X̄ =   0.260 Ȳ =   0.870
L. HACKBERRY SD.   TYPE   LINER   EXPNT   POWER   LOGAR
PORT ARTHUR FIELD   EQ.   Y=A+BX   Y=A.E^{BX} Y=A.X^B Y=A+BLX
JEFFERSON CO., TEXAS   A =   1.129   1.169   0.661   0.643
DEVIATED WELL   B =   -0.995   -1.171   -0.190   -0.162
                         R =   0.360   0.324   0.249   0.282
        EACH SYMBOL REPRESENTS APPROX. 5 FT. INTERVAL

159
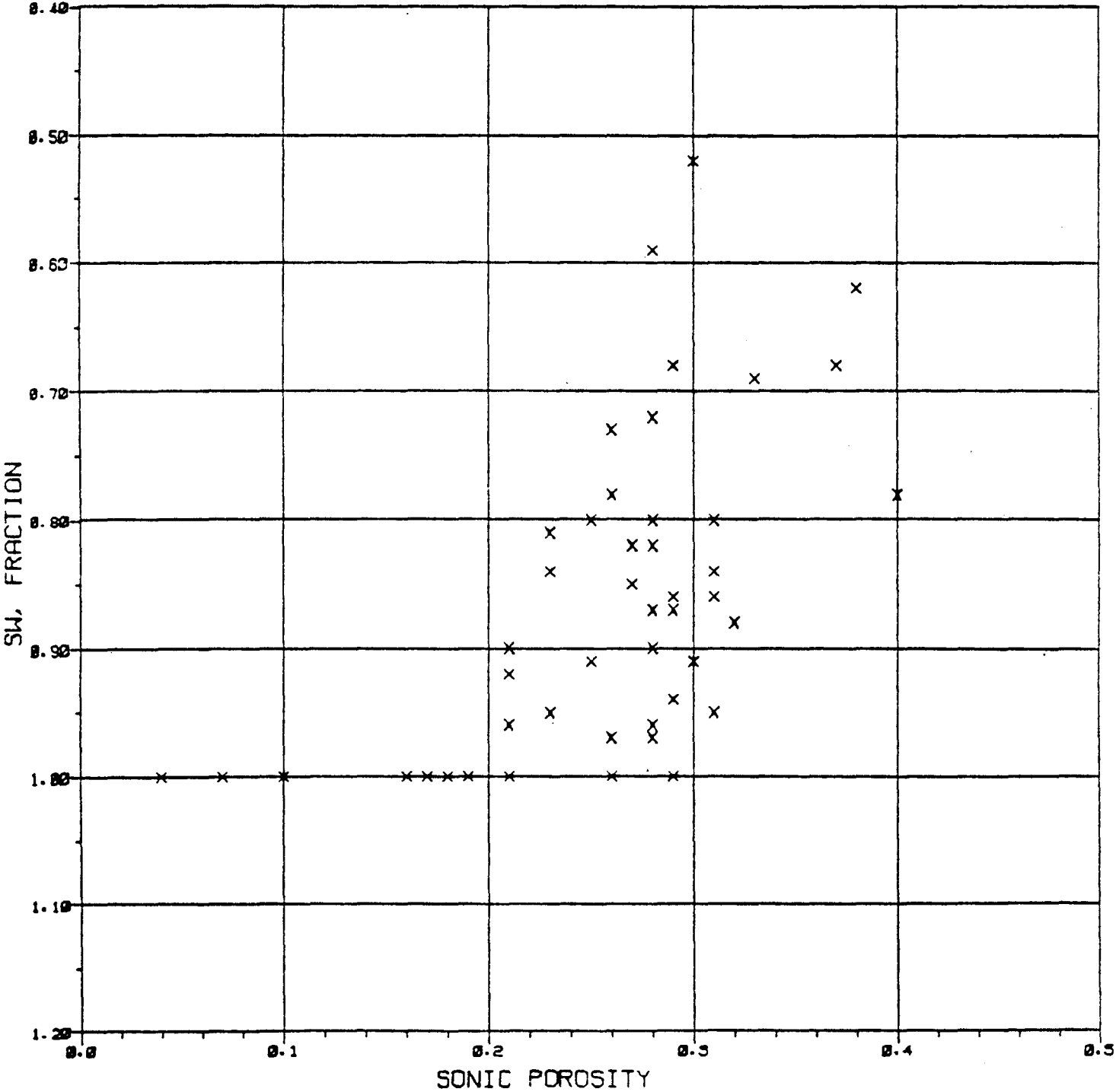
Part 3

DETAILED LOG EVALUATION BY WELL
FOR B_2 THROUGH H SANDS

LOG ANALYSIS

Well #1

Type	Interval	Net	Sp	RS	Rt	ϕ	S_w	hg	Vol.	Remarks
			SAND, FT.		**LOG READ**			**ANALYSIS**		
B_2	11,070-073	3	12	2.2	2.20	.26	.41	3	.46	R_t corrected
	TOTAL	3				.26	.41	3	.46	LKG = -11,053'
C	11,144-160	16	58	2.0	1.80	.26	.46	16	2.25	
	11,160-170	10	58	1.0	.77	.26	.74			
	11,170-179	9	58	.7	.52	.26	.92			
	11,181-190	9	58	.7	.44	.26	1.00			
	11,190-197	7	58	.8	.59	.26	.86			
	11,201-208	7	58	.9	.71	.26	.77			
	11,211-217	6	15	1.2	.80	.26	.72			
	11,225-230	5	20	1.7	1.00	.26	.64			Lower C
	TOTAL	69				.26	.46	16	2.25	LKG = -11,140'
D	11,245-256	11	45	0.9	.56	.26	.90			
	11,263-273	10	50	0.7	.50	.26	.90			
	TOTAL	21								
E	11,282-288	6	35	1.4	1.00	.26	.65			Not Counted
	11,290-300	10	40	0.9	.63	.26	.84			
	11,302-330	28	40	0.7	.53	.26	.93			
	11,331-358	27	45	0.8	.50	.26	.96			
	TOTAL	71						0	0	
F	11,380-426	40	40	0.7	.53	.26	.93			
	11,432-440	8	30	1.1	.83	.26	.72			
	11,440-450	10	20	1.1	.91	.26	.69			
	11,455-466	11	35	0.8	.53	.26	.93			
	11,466-480	14	6	1.2	1.00	.26	.65			
	11,480-487	7	35	1.7	1.00	.26	.65			
	TOTAL	90						0	0	
G	11,501-503	-	7							Poor sand
	11,503-510	-	6							Not Counted
	TOTAL	0						0	0	
H	None									

162

Log Analysis

Well #5

Type	SAND, FT. Interval	Net	LOG READ Sp	RS	Rt	ANALYSIS Ø	Sw	hq	Vol	Remarks
B₂	11,107-111	4	2	0.8	.77	.30	.69			
	Total	4						0	0	
C	11,140-161	3	−	0.9	.71	.30	.73			Shaly
	11,164-173	9	45	1.4	.87	.30	.65	9	.95	
	11,173-176	3	45	1.2	.71	.30	.73			
	11,179-181	2	42	.9	.60	.30	.80			
	11,183-187	4	50	.8	.45	.30	.93			
	11,194-226	26	50	.5	.40	.30	1.00			
	11,232-248	16	55	.6	.50	.30	.88			Lower 'C'
	Total	63				.30	.65	9	.95	GWC = -11,153'
D	11,255-266	11	40	0.8	.69	.30	.74			
	11,268-277	9	35	0.8	.67	.30	.76			
	11,280-284	4	40	1.1	.77	.30	.70			
	11,289-293	4	25	0.9	.67	.30	.76			
	11,294-306	12	42	0.6	.45	.30	.93			
	Total	40						0	0	
E	11,315-325	8	6	0.7	.71	.28	.75			
	11,327-335	8	38	1.1	.74	.28	.73			
	11,353-357	4	30	0.7	.67	.28	.77			
	11,357-375	18	55	0.4	.38	.28	1.00			
	11,380-406	20	50	0.4	.40	.28	1.00			
	Total	58						0	0	
F	11,406-430	22	45	0.3	.36	.29	1.00			
	11,433-448	15	40	0.5	.49	.29	.91			
	11,460-470	10	50	0.5	.45	.29	.95			
	11,470-473	3	30	0.7	.63	.29	.79			
	Total	50						0	0	
G	11,481-487	6	35	1.8	1.30	.29	.53	6	.82	
	Total	6				.29	.53	6	.82	LKG = -11,467'
H	11,554-560	6	40	0.9	.71	.30	.73			
	11,560-571	11	35	0.6	.53	.30	.86			
	11,574-580	6	40	0.7	.77	.30	.70			
	11,580-588	8	40	1.7	.83	.30	.67			
	Total	31						0	0	

LOG ANALYSIS

Well #6

Type	Interval	Net	Sp	RS	Rt	Ø	S_w	hg	Vol.	Remarks
B$_2$	11,058-061	3	5	.7	.7	.30	.76			
	TOTAL	3						0	0	
C	11,120-125	5	20	1.1	1.00	.30	.63	5	.56	
	11,127-133	6	52	2.0	1.40	.30	.52	6	.86	Perf: 11,130-135'
	11,133-142	9	52	2.9	2.70	.30	.36	9	1.73	
	11,147-154	7	50	2.5	2.40	.30	.38	7	1.30	
	11,170-181	11	54	1.7	.87	.30	.67			Lower C
	TOTAL	38				.30	.45	27	4.45	GWC = -11,135'
D	11,200-210	10	18	0.9	1.25	.30	.55	10	1.35	Upper D stringer
	11,218-228	10	40	1.3	1.25	.30	.55	10	1.35	Perf: 11,218-228'
	11,228-231	3	38	1.1	1.00	.30	.63	3	.33	
	11,231-236	5	42	1.4	1.18	.30	.57	5	.65	
	11,236-240	4	40	1.0	.77	.30	.73			
	11,240-244	4	44	1.1	1.00	.30	.63	4	.44	
	11,252-255	3	47	1.2	1.18	.30	.57	3	.39	
	11,255-266	11	48	0.8	.67	.30	.79			
	11,269-273	4	30	0.9	.91	.30	.66			
	TOTAL	54				.30	.57	35	4.51	LKG = -11,236'
E	11,290-294	4	25	1.4	1.25	.31	.55	4	.56	
	11,297-303	6	15	0.7	.63	.31	.80			Perf: 11,296-301'
	11,303-311	8	55	1.5	1.43	.31	.51	8	1.22	
	11,311-370	51	55	0.4	.43	.31	.98			
	11,370-374	4	30	0.9	.90	.31	.66			Lower E stringer
	TOTAL	73				.31	.52	12	1.78	LKG = -11,292'
F	11,380-383	3	45	0.6	.63	.30	.80			
	11,383-397	14	50	0.5	.48	.30	.93			
	11,397-413	14	40	0.6	.63	.30	.80			
	11,416-430	14	50	0.5	.50	.30	.90			
	11,430-436	6	35	0.8	.63	.30	.80			
	11,441-450	9	30	0.9	.87	.30	.56			
	TOTAL	60						0	0	

Log Analysis, Well #6 cont.

Type	SAND, FT. Interval	Net	LOG READ Sp	RS	Rt	ANALYSIS ∅	S_w	hg	Vol.	Remarks
G	11,458-468	10	40	1.6	1.45	.29	.51	10	1.42	
	11,470-480	10	50	0.6	.49	.29	.93			
	TOTAL	20				.29	.51	10	1.42	LKG = -11,449'
H	11,500-508	8	12	0.7	.77	.28	.73			
	11,508-512	4	42	0.6	.67	.28	.79			
	11,512-517	5	28	0.7	.83	.28	.70			
	11,517-525	5	22	0.7	.67	.28	.79			Shaly
	11,525-590	65	50	0.4	.45	.28	.98			
	TOTAL	87						0	0	

165

Log Analysis
Well #11

Type	SAND, FT. Interval	Net	LOG READ Sp	RS	Rt	∅	ANALYSIS Sw	hg	Vol.	Remarks
B$_2$	11,056-059	3	15	1.3	1.30	.26	.60	3	.31	R$_t$ corrected
	11,063-066	3	21	1.4	1.40	.26	.58	3	.33	R$_t$ corrected
	T o t a l	6				.26	.59	6	.64	LKG = -11,046
C	11,130-138	8	58	3.4	2.50	.26	.42	8	1.21	
	11,142-150	8	60	3.2	2.50	.26	.42	8	1.21	
	11,155-160	5	27	1.3	.91	.26	.73			
	11,164-170	6	61	7.0	2.00	.26	.47	6	.83	
	11,170-181	11	64	1.0	.67	.26	.87			
	11,183-187	4	30	1.2	.83	.26	.77			
	T o t a l	42				.26	.43	22	3.25	GWC = -11,150'
D	11,200-208	8	50	1.4	1.11	.24	.65	8	.67	Upper 'D'
	11,208-215	7	50	0.8	.59	.24	.92			
	11,218-224	6	50	1.0	.63	.24	.89			
	11,227-240	13	50	0.8	.53	.24	.98			
	11,240-250	10	50	0.7	.50	.24	1.00			
	11,255-260	5	45	0.9	.50	.24	1.00			
	11,262-273	11	50	1.7	.63	.24	.76			
	T o t a l	60				.24	.65	8	.67	LKG = -11,168'
E	11,293-300	7	25	1.0	.83	.25	.77			
	11,300-306	6	45	1.0	.63	.25	.90			
	11,309-314	5	35	1.7	.91	.25	.73			
	11,327-330	3	20	1.8	.95	.25	.71			
	11,334-346	12	60	0.8	.71	.25	.84			
	11,346-366	16	50	0.7	.53	.25	.99			
	11,376-392	16	50	0.6	.42	.25	1.00			
	11,397-402	5	45	0.9	.67	.25	.87			Lower 'E' stringer
	T o t a l	70						0	0	
F	11,406-420	14	55	0.7	.50	.25	1.00			
	11,426-433	7	50	1.0	.74	.25	.84			
	11,435-448	13	55	0.7	.48	.25	1.00			
	11,448-452	4	30	0.9	.63	.25	.92			
	11,452-465	13	25	1.1	.95	.25	.73			
	T o t a l	51						0	0	
G	11,475-481	6	40	3.0	1.11	.25	.65	6	.53	LKG = -11,461'
	T o t a l	6							.53	

196

Well #11 cont'd.

Type	SAND, FT. Interval	Net	LOG READ Sp	RS	Rt	ø	ANALYSIS Sw	hg	Vol.	Remarks
H	11,521-527	6	20	1.4	1.25	.25	.63			N/C, stratic. trap
	Total	6						0	0	

Log Analysis

Well #12

Type	SAND, FT. Interval	Net	LOG READ Sp	RS	Rt	ϕ	ANALYSIS Sw	hq	Vol	Remarks
B_2	11,118									Top of B_2
C	11,180-189	9	65	7.0	1.11	.27	.66			
	11,189-194	5	65	1.0	.62	.27	.91			
	11,197-202	5	65	3.0	1.00	.27	.70			Shaly
	11,205-210	5	65	2.0	.71	.27	.85			
	11,215-230	15	65	.6	.45	.27	1.00			Lower "C"
	11,232-239	7	60	1.1	.63	.27	.91			
	Total	46						0	0	
D	11,253-261	8	40	0.8	0.67	.27	.87			
	11,261-270	9	60	1.2	0.50	.27	1.00			Upper 'D'
	11,273-280	7	60	0.8	0.50	.27	1.00			stringer
	11,284-290	6	45	1.3	0.67	.27	.87			
	11,304-317	13	50	1.0	0.71	.27	.84			
	11,317-324	7	60	0.9	0.53	.27	1.00			
	11,324-330	6	38	0.9	0.67	.27	.87			
	11,330-340	10	60	1.0	0.53	.27	1.00			
	11,340-360	18	50	1.0	0.63	.27	.91			
	Total	84						0	0	
E	11,370-374	4	10	2.0	.91	.26	.75			
	11,376-400	24	60	0.5	.42	.26	1.00			
	11,400-404	4	60	0.8	.67	.26	.89			
	11,404-418	14	50	0.5	.42	.26	1.00			
	Total	46						0	0	
F	11,422-450	28	50	0.7	.53	.26	.99			
	11,450-470	20	45	0.9	.63	.26	.90			
	11,470-498	28	50	0.8	.53	.26	.99			
	11,500-508	8	45	4.0	.95	.26	.72			
	11,510-520	10	50	1.4	.91	.26	.73			
	11,523-546	23	45	1.0	.63	.26	.90			
	Total	117						0	0	
G	11,560-564	4	55	0.9	.77	.25	.82			
	11,564-576	12	55	0.6	.42	.25	1.00			
	11,580-604	24	60	0.6	.45	.25	1.00			
	Total	40						0	0	
H	None									

Type	SAND, FT. Interval	Net	LOG READ Sp	RS	Rt	ANALYSIS ϕ	Sw	hg	Vol	Remarks
B_2	11,063-068	5	26	2.6	1.82	.31	.44	5	.87	
	11,070-078	8	21	1.4	1.00	.31	.62	8	.94	
	Total	13				.31	.55	13	1.81	LKG = -11,058'
C	11,117-119	2	6	1.0	.74	.31	.73			
	11,124-127	3	11	1.3	.77	.31	.71			
	11,134-148	14	42	3.5	3.13	.31	.33	14	2.91	Perf; 11,136-144'
	11,152-158	6	40	2.4	2.00	.31	.42	6	1.08	
	11,161-167	6	30	1.6	1.00	.31	.62	6	.71	
	11,170-173	3	30	1.2	.83	.31	.68			
	11,176-180	4	30	2.2	1.43	.31	.51	(4)		Not counted
	Total	38				.31	.42	26	4.70	LKG = -11,147'
D	11,200-210	10	42	1.8	1.33	.30	.51	10	1.47	Upper 'D' stringer
	11,225-229	4	20	1.3	1.00	.30	.60	4	.48	Perforated
	11,229-239	10	22	1.4	0.85	.30	.66			11,225-11,243'
	11,239-245	6	40	5.0	2.50	.30	.36	6	1.15	
	11,245-250	5	40	2.0	1.67	.30	.45	5	.83	
	11,250-255	5	40	1.2	1.00	.30	.60	5	.60	
	11,255-260	5	40	1.1	0.71	.30	.73			
	Total	45				.30	.50	30	4.53	GWC = -11,235'
E	11,274-286	12	38	2.5	2.00	.29	.42	12	2.02	Perf; 11,276-286'
	11,289-300	11	20	1.1	.83	.29	.68			
	11,300-308	8	40	3.5	1.43	.29	.50	8	1.16	
	11,308-320	12	40	0.7	.49	.29	.91			
	11,324-334	10	42	0.6	.42	.29	.99			Clean wet
	11,336-342	6	38	2.0	1.18	.29	.56	6	.77	Lower 'E' stringer
	Total	59				.29	.48	26	3.95	GWC = -11,288/-11,322'
F	11,350-363	13	40	1.7	1.50	.27	.50	13	1.76	Perf; 11,350-359'
	11,363-370	7	36	1.4	1.20	.27	.57	7	.81	Rt corr.
	11,370-375	4	25	1.0	0.74	.27	.74			Shale imbeded
	11,375-381	6	40	1.2	1.10	.27	.59	6	.66	Rt corr.
	11,382-392	10	38	0.9	.59	.27	.84			
	11,392-400	8	20	1.0	.71	.27	.75			
	11,400-408	8	38	0.8	.59	.27	.84			
	11,408-416	8	30	0.9	.67	.27	.78			
	11,416-422	6	40	0.8	.59	.27	.84			
	11,422-430	8	20	0.9	.63	.27	.81			
	11,430-445	15	38	1.0	.63	.27	.81			
	Total	93				.27	.55	26	3.23	LKG = -11,361'
G	11,454-466	9	40	1.8	1.25	.26	.55	9	1.05	
	11,466-490	24	43	0.6	.40	.26	1.00			

	Type	SAND, FT. Interval	Net	LOG READ			ANALYSIS				Remarks
				Sp	RS	Rt	O	Sw	hq	Vol	
(Cont'd)	G	11,490-497	7	20	0.8	.56	.26	.86			
		T o t a l	40				.26	.55	9	1.05	GWC = -11,446'
	H	11,530-541	11	40	0.8	.59	.24	.83			Non-productive
		11,544-564	20	40	0.7	.54	.24	.87			Massive sand
		11,564-600	36	40	0.6	.45	.24	.95			
		T o t a l	67						0	0	

170

LOG ANALYSIS

Well #23

Type	Interval	Net	Sp	RS	Rt	Ø	S_w	hg	Vol.	Remarks
	SAND, FT.			**LOG READ**			**ANALYSIS**			
B_2	11,060-070	10	36	2.0	1.54	.29	.49	10	1.48	
	11,070-085	15	38	1.7	1.11	.29	.58	15	1.83	
	11,085-090	5	40	1.6	.91	.29	.65	5	.51	
	11,090-094	4	36	1.6	.80	.29	.70			
	11,100-107	7	38	1.6	.87	.29	.67			
	TOTAL	**41**				.29	.56	30	3.82	GWC = -11,070'
C	11,128-135	7	38	1.9	1.05	.28	.60	7	.78	Perf: 11,128-131
	11,145-151	6	39	21	1.82	.28	.44	6	.94	
	11,154-161	7	10	1.8	1.33	.28	.53	7	.92	
	11,161-170	9	40	1.5	1.00	.28	.62	9	.96	
	11,170-177	7	40	1.0	.62	.28	.82			
	11,186-191	5	40	1.8	.91	.28	.65	(5)		N/C
	11,191-200	9	22	1.2	.83	.28	.68			
	TOTAL	**50**					.56	29	3.60	GWC = -11,150'
D	11,234-250	10	10	1.2	.81	.26	.63	10	.96	
	11,252-259	7	40	2.0	1.11	.26	.57	7	.78	Perf: 11,251-256
	11,262-268	6	42	1.4	.83	.26	.67			
	11,268-272	4	43	1.1	.63	.26	.78			
	TOTAL	**27**				.26	.61	17	1.74	LKG = -11,239
E	11,290-299	9	40	2.0	1.43	.24	.50	9	1.08	Perf: 11,290-299
	11,299-302	3	10	1.0	.67	.24	.77			
	11,302-310	8	30	1.1	.77	.24	.71			
	11,310-316	6	40	1.3	1.00	.24	.62	6	.55	
	11,316-330	14	40	0.6	.43	.24	.98			
	11,332-350	18	45	0.5	.38	.24	1.00			
	11,356-370	14	40	0.7	.50	.24	.90			Lower E stringer
	TOTAL	**72**				.24	.55	15	1.63	LKG = -11,296

Log Analysis, Well #23 cont.

Type	Interval	Net	Sp	RS	Rt	$\varnothing$	S_w	hg	Vol.	Remarks
	S A N D , F T .			**L O G R E A D**			**A N A L Y S I S**			
F	11,374-380	6	38	1.2	1.20	.24	.56	6	.63	Rt corr.
	11,382-388	6	35	1.0	1.00	.24	.60	6	.58	Rt corr.
	11,390-395	5	30	0.9	.67	.24	.77			
	11,395-430	33	40	0.6	.45	.24	.95			
	11,430-450	20	35	0.8	.59	.24	.83			
	11,450-460	10	40	0.8	.56	.24	.85			
	11,460-470	10	38	1.0	.83	.24	.68			
	T O T A L	90				.24	.58	12	1.21	LKG = -11,368
G	11,480-490	10	25	1.8	1.11	.24	.58	10	1.01	
	11,490-500	10	10	0.9	.80	.24	.70			
	T O T A L	20				.24	.58	10	1.01	LKG = -11,470
H	11,520-525	5	10	1.0	.83	.24	.68			
	11,525-530	5	20	1.2	.87	.24	.66			
	11,530-570	40	42	0.5	.42	.24	1.00			
	11,570-600	30	42	0.6	.45	.24	.95			
	11,600-620	20	44	1.0	.48	.24	.93			
	11,620-670	50	41	0.6	.50	.24	.90			
	T O T A L	150						0	0	

Log Analysis

Well #24

Type	SAND, FT. Interval	Net	Sp	RS	Rt	ϕ	Sw	hq	Vol	Remarks
B₂	11,070-077	3	18	3.0	2.00	.27	.42	3	.47	Thin bed corr.
	11,085-087	2	12	1.5	1.00	.27	.62	2	.21	Thin bed corr.
	Total	5				.27	.50	5	.68	LKG = -11,067'
C	11,120-124	4	36	1.3	1.30	.25	.53	4	.47	Thin bed corr.
	11,160-169	8	51	2.2	1.90	.25	.43	8	1.14	
	11,169-186	17	55	.9	.50	.25	.91			
	11,189-205	16	55	.8	.42	.25	1.00			Lower 'D'
	Total	45					.82	12	1.61	GWC = -11,149'
D	11,241-246	4	20	1.0	.83	.25	.67			
	11,246-259	13	55	2.0	1.82	.25	.44	13	1.82	Perf; 11,250-257
	11,259-273	14	55	0.8	.56	.25	.84			
	11,273-280	5	55	3.0	.83	.25	.67			
	Total	36				.25	.44	13	1.82	GWC = -11,240'
E	11,309-315	6	40	1.0	.77	.25	.70			
	11,317-329	12	42	1.2	.67	.25	.76			
	11,332-360	28	45	0.5	.42	.25	.99			
	11,360-372	12	25	0.9	.77	.25	.70			
	11,378-385	7	42	1.4	.95	.25	.63	7	.65	
	11,385-391	6	0	0.5	.56	.25	.84			Perf; 11,387-391
	Total	71				.25	.63	7	.65	GWC = -11,366'
F	11,402-449	47	42	0.7	.59	.25	.82			
	11,450-466	16	30	0.8	.77	.25	.70			
	Total	63						0	0	
G	11,474-484	10	50	0.8	.56	.25	.84			
	11,484-490	6	50	4.0	1.04	.25	.59			N/C, hard streak
	11,490-500	6	45	0.7	.56	.25	.84			
	Total	22				.25	.59	0	. 0	
H	None									

LOG ANLYSIS

Well #27

Type	SAND, FT. Interval	Net	LOG READ Sp	RS	Rt	ANALYSIS $\emptyset$	S_w	hg	Vol.	Remarks
B$_2$	11,160-163	3	28	3.5	1.11	.24	.63	(3)		Not Counted
	11,173-180	7	40	1.9	1.00	.24	.67			
	T O T A L	10						0	0	
C	None									Fault-out
D	None									Fault-out
E	None									Fault-out
F	None									Fault-out
G	None									Fault-out
F	None									Fault-out
H	None									Fault-out

174

Log Analysis

Well #28

	SAND, FT.		LOG READ			ANALYSIS				
Type	Interval	Net	Sp	RS	Rt	Ø	Sw	hq	Vol	Remarks
B$_2$	11,130-135	5	47	2.8	.70	.25	.84			
	11,137-142	5	44	1.3	.70	.25	.84			
	Total	10						0	0	
C	11,200-210	10	58	1.9	.67	.25	.85			
	11,210-213	3	58	.9	.47	.25	1.00			
	11,217-230	13	56	1.3	.60	.25	.90			
	11,230-233	3	50	1.0	.62	.25	.89			
	11,237-248	11	25	1.5	.83	.25	.75			Lower 'D'
	Total	40						0	0	
D	11,259-264	5	40	1.7	.71	.24	.83			
	11,264-280	15	50	1.0	.56	.24	.95			
	11,280-286	6	30	1.8	.71	.24	.83			
	Total	26						0	0	
E	11,300-303	2	5	1.2	.77	.24	.80			
	11,305-315	8	35	1.4	.74	.24	.82			
	11,317-321	4	30	2.1	.91	.24	.73			
	11,336-341	5	35	1.3	.69	.24	.85			
	11,343-350	4	20	0.9	.61	.24	.91			
	11,350-367	17	56	0.7	.37	.24	1.00			
	11,369-374	4	42	1.7	.56	.24	.95			Lower 'E' stringer
	Total	44						0	0	
F	11,378-390	12	45	1.3	.77	.24	.80			
	11,392-408	16	50	0.8	.45	.24	1.00			
	11,408-430	20	42	0.9	.56	.24	.95			
	11,431-447	16	42	0.8	.51	.24	1.00			
	11,449-489	40	40	1.0	.63	.24	.89			
	11,490-499	9	43	0.9	.50	.24	1.00			
	11,500-503	3	25	1.4	.74	.24	.81			
	11,510-517	7	20	1.6	.95	.24	.71			
	Total	123						0	0	
G	11,532-540	8	25	1.1	.65	.24	.88			
	11,541-552	11	60	0.7	.40	.24	1.00			
	11,553-560	7	55	0.8	.45	.24	1.00			
	11,563-580	17	57	0.7	.42	.24	1.00			
	11,580-586	6	58	1.7	.63	.24	.89			
	Total	49						0	0	
H	11,641-650	9	8	1.3	.91	.24	.73			
	Total	9						0	0	

Log Analysis

Well #29

Type	SAND, FT. Interval	Net	Sp	RS	Rt	ϕ	Sw	hg	Vol	Remarks
B$_2$	11,072-076	4	22	1.1	.71	.32	.76			
	11,076-079	3	45	1.6	.95	.32	.65	3	.33	Rt corr.
	11,079-083	4	45	1.4	.77	.32	.72			
	11,093-095	2	15	2.0	.83	.32	.69			
	T o t a l	13				.32	.65	3	.33	LKG = -11,060'
C	11,132-135	3	12	1.9	.80	.28	.71			
	11,140-143	3	8	1.3	.74	.28	.74			
	11,157-160	3	8	1.3	.74	.28	.74			
	11,173-177	4	55	1.5	.71	.28	.75			
	11,177-191	14	56	.9	.45	.28	.98			
	11,191-199	8	57	1.1	.50	.28	.92			
	11,203-212	9	57	1.2	.62	.28	.81			Lower 'C'
	T o t a l	44						0	0	
D	11,240-247	7	20	1.4	.91	.28	.65	7	.69	
	11,253-259	6	50	1.9	1.54	.28	.49	6	.86	
	11,261-267	6	50	1.3	.67	.28	.77			
	11,270-276	6	40	1.5	.83	.28	.68			
	11,280-285	5	35	1.6	.83	.28	.68			
	T o t a l	30				.28	.57	13	1.55	LKG = -11,240'
E	11,301-306	5	40	1.0	.63	.26	.82			
	11,308-316	8	30	1.3	.77	.26	.73			
	11,316-344	25	50	0.9	.42	.26	1.00			
	11,346-354	8	25	1.1	.61	.26	.84			
	11,356-366	10	35	0.9	.50	.26	.83			
	11,368-390	22	30	1.0	.59	.26	.85			
	11,390-405	15	50	0.8	.40	.26	1.00			
	T o t a l	93						0	0	
F	11,410-416	6	30	1.7	.77	.26	.72			
	11,418-432	14	40	1.0	.63	.26	.80			
	11,432-448	16	42	1.0	.50	.26	.91			
	11,450-460	10	40	1.4	.71	.26	.75			
	11,460-464	4	15	1.2	.83	.26	.68			
	T o t a l	50						0	0	
G	11,474-482	8	40	2.0	1.11	.26	.58	8	.87	
	11,491-503	12	40	1.8	.90	.26	.66			
	T o t a l	20				.26	.58	8	.87	LKG = -11,463'

Well #29 cont'd.

Type	SAND, FT. Interval	Net	LOG READ Sp	RS	Rt	ANALYSIS Ø	Sw	hq	Vol	Remarks
II	11,521-528	7	35	1.8	1.05	.26	.60	(7)		
	11,528-534	6	7	1.2	.87	.26	.67	0	0	
	T o t a l	13						0	0	

Type	SAND, FT. Interval	Net	Sp	LOG READ RS	Rt	Ø	ANALYSIS Sw	hg	Vol	Remarks
B$_2$	11,050									Top of B$_2$
	11,065-068	3	20	1.0	.83	.26	.63	3	.29	
	11,069-078	9	53	2.1	1.82	.26	.41	9	1.38	
	T o t a l	12				.26	.46	12	1.67	LKG = -11,052'
C	11,111-115	4	12	1.4	.95	.25	.58	4	.42	
	11,117-120	3	8	1.0	.95	.25	.58	3	.32	
	11,128-137	9	75	2.0	1.33	.25	.48	9	1.17	
	11,142-161	19	80	1.0	.36	.25	1.00			
	11,168-172	4	40	1.3	1.00	.25	.57	4	.43	Lower 'C'
	11,178-190	12	80	.6	.29	.25	1.00			
	T o t a l	51				.25	.53	20	2.34	LKG = -11,111/-11,146'
D	11,204-215	11	45	2.0	1.67	.24	.43	11	1.50	Perf; 11,204-208'
	11,230-245	14	45	1.2	.80	.24	.65	14	1.18	
	11,248-254	6	40	1.6	1.00	.24	.58	6	.60	
	11,254-260	6	30	1.1	.80	.24	.65	6	.50	
	11,260-269	9	40	1.1	.63	.24	.74			
	11,269-273	4	25	1.2	.77	.24	.67			
	T o t a l	50				.24	.49	37	3.78	LKG = -11,234'
E	11,287-294	6	50	2.0	1.20	.24	.52	6	.69	
	11,298-302	4	55	1.2	.80	.24	.65	4	.34	
	11,302-320	18	55	1.2	.63	.24	.75			
	11,320-340	20	55	0.8	.36	.24	1.00			
	11,345-360	15	45	1.0	.50	.24	.85			Lower 'E' stringer
	T o t a l	63				.24	.57	10	1.03	LKG = -11,276'
F	11,370-380	10	50	1.6	.85	.26	.62	10	.99	
	11,380-389	9	50	1.6	.63	.26	.74			
	11,391-405	14	50	1.0	.50	.26	.83			
	11,405-442	35	40	1.2	.56	.26	.79			
	T o t a l	68				.26	.62	10	.99	LKG = -11,354'
G	11,452-460	8	45	1.4	1.25	.28	.49	8	1.14	
	11,460-470	10	50	1.1	.56	.28	.77			
	11,470-485	15	50	0.7	.42	.28	.91			
	11,485-494	9	20	0.9	.63	.28	.73			
	T o t a l	42				.28	.49	8	1.14	LKG = -11,434'
H	11,540-612	72	53	0.9	.38	.26	.97			
	T o t a l	72						0	0	

178

Type	SAND, FT. Interval	Net	LOG READ Sp	RS	Rt	ANALYSIS Ø	Sw	hq	Vol	Remarks
B$_2$	11,067-070	3	40	2.5	1.40	.28	.52	3	.40	
	11,077-081	4	45	1.8	1.80	.28	.46	4	.60	Thin bed corr.
	11,082-087	5	50	1.7	1.70	.28	.47	5	.74	Perf; 11,077-101'
	11,088-095	7	49	1.6	1.60	.28	.49	7	1.00	
	11,097-100	3	43	1.1	.77	.28	.73			
	Total	22				.28	.48	19	2.74	GWC = -11,075'
C	11,120-125	8	45	1.7	1.11	.25	.60	8	.80	
	11,141-149	8	45	4.5	3.33	.25	.32	8	1.36	
	11,149-161	12	35	1.3	.83	.25	.70			
	11,161-170	9	50	2.2	2.00	.25	.43	9	1.28	
	11,172-183	11	50	0.5	.42	.25	1.00			
	11,183-193	10	27	1.0	.77	.25	.73			
	Total	58				.25	.45	25	3.44	GWC = -11,150'
D	11,230-235	3	5	0.6	0.67	.25	.78			
	11,235-240	4	10	1.2	1.00	.25	.63	4	0.37	
	11,240-246	6	15	1.1	0.91	.25	.66			
	11,246-255	8	50	1.8	1.33	.25	.53	8	0.94	
	11,257-268	9	55	1.3	0.91	.25	.66			
	Total	30				.25	.56	12	1.31	LKG = -11,235'
E	11,287-292	5	25	1.2	1.00	.24	.63	5	0.44	
	11,292-303	9	30	1.0	0.83	.24	.70			
	11,303-312	9	50	1.8	2.00	.24	.43	9	1.23	
	11,312-348	33	45	0.5	0.45	.24	.98			
	11,352-370	18	50	0.5	0.42	.24	1.00			
	11,373-379	6	40	1.5	1.18	.24	.58	6	0.60	Lower 'E' stringer
	Total	80				.24	.53	20	2.27	LKG = -11,292/-11,359'
F	11,381-388	7	35	1.0	.87	.26	.65	7	.64	
	11,388-392	4	55	0.9	.83	.26	.67			
	11,392-419	26	45	0.8	.63	.26	.78			
	11,421-432	11	45	0.7	.56	.26	.83			
	11,434-446	12	40	1.2	.77	.26	.70			
	Total	60				.26	.65	7	.64	GWC = -11,368'
G	11,454-470	15	58	3.5	1.82	.26	.44	15	2.18	Perf; 11,458-463'
	11,472-486	10	20	1.1	1.00	.26	.62			Low perm not counted
	Total	25				.26	.44	15	2.18	

179

Well #31 cont'd.

Type	SAND, FT. Interval	Net	LOG READ Sp	RS	Rt	ϕ	ANALYSIS Sw	hg	Vol	Remarks
H	11,520-600	80	58	0.4	.42	.25	1.00			Massive clean
	11,600-653	53	61	0.5	.50	.25	0.92			Wet sand
	T o t a l	133						0	0	

Log Analysis

Well #32

Type	SAND, FT. Interval	Net	LOG READ Sp	RS	Rt	φ	ANALYSIS Sw	hq	Vol	Remarks
B₂	11,060-065	5	51	1.2	.63	.31	.80			
	11,065-072	7	51	.7	.45	.31	.98			
	11,085-187	2	25	1.3	.91	.31	.65	2	.22	
	11,090-093	3	27	1.5	1.11	.31	.58	3	.39	
	T o t a l	17				.31	.61	5	.61	LKG = -11,056'
C	11,138-140	2	15	1.0	.67	.27	.78			
	11,144-147	3	19	1.5	.91	.27	.65	3	.28	
	11,165-168	3	22	1.3	.83	.27	.68			
	11,173-188	15	59	.8	.42	.27	1.00			
	11,191-199	7	59	1.8	.91	.27	.65	(7)		N/C
	11,200-209	9	57	.6	.42	.27	1.00			
	11,211-222	11	60	.7	.38	.27	1.00			
	11,230-234	4	62	1.1	.67	.27	.78			
	T o t a l	54				.27	.65	3	.28	LKG = -11,110'
D	11,263-270	7	50	1.0	.91	.28	.65	7	.69	
	11,270-280	10	50	0.8	.59	.28	.83			
	11,282-295	13	35	1.2	.56	.28	.86			
	T o t a l	30				.28	.65	7	.69	LKG = -11,233'
E	11,320-323	3	40	1.3	.71	.29	.74			
	11,328-338	10	45	1.8	.71	.29	.74			
	11,340-364	24	50	0.5	.40	.29	1.00			
	11,364-370	6	50	0.8	.56	.29	.85			
	11,377-382	5	15	1.0	.95	.29	.63	5	.54	Lower 'E' stringer
	T o t a l	48				.29	.63	5	.54	LKG = -11,345'
F	11,390-394	4	40	1.6	1.40	.28	.51	4	.55	Thin bed corr.
	11,395-415	19	35	1.0	.71	.28	.75			
	11,416-456	40	35	0.7	.56	.28	.86			
	11,463-480	17	40	0.8	.63	.28	.80			
	T o t a l	80				.28	.51	4	.55	LKG = -11,357'
G	11,490-497	7	15	1.2	1.11	.28	.58	3	.35	hq was reduced
	11,501-507	6	15	1.2	1.00	.28	.62	3	.32	
	11,510-520	10	10	0.8	.74	.28	.73			
	T o t a l	23				.28	.60	6	.67	LKG = -11,470'
H	None									

181

Log Analysis

Well #34

Type	SAND, FT. Interval	Net	LOG READ Sp	RS	Rt	ϕ	ANALYSIS Sw	hg	Vol	Remarks
B$_2$	11,208-215	3	3	1.0	.83	.29	.86			
	Total	3						0	0	
C	11,272-282	10	40	4.3	1.90	.25	.54	(10)		N/C, hard streak
	11,290-297	7	45	1.7	.90	.25	.82			
	11,304-316	12	58	1.1	.67	.25	.97			
	11,316-323	7	50	1.5	.77	.25	.90			
	11,336-350	14	60	1.8	.77	.25	.90			Lower 'C'
	Total	50						0	0	
D	11,360-368	8	50	0.7	1.33	.25	.66			Upper 'D'
	11,368-380	10	30	1.2	.83	.25	.85			Upper 'D'
	11,390-400	10	40	2.0	1.03	.25	.76			
	11,400-408	8	45	1.3	.77	.25	.89			
	11,408-423	12	30	1.7	1.05	.25	.75			
	11,428-435	7	15	1.5	1.11	.25	.73			
	Total	55						0	0	
E	11,450-454	3	5	1.4	.87	.25	.83			
	11,454-465	11	40	0.6	.50	.25	1.00			
	11,465-470	5	45	1.7	.63	.25	1.00			
	11,472-480	8	35	1.0	.83	.25	.85			
	Total	27						0	0	
F	11,486-492	6	30	1.4	.45	.24	1.00			
	11,492-500	8	45	1.0	.63	.24	1.00			
	11,500-510	10	50	2.1	1.25	.24	.69			
	11,510-520	10	42	1.1	.63	.24	1.00			
	11,520-528	8	50	1.8	.56	.24	1.00			
	11,530-535	5	50	0.9	.59	.24	1.00			
	11,535-545	10	45	1.0	.77	.24	.91			
	11,545-568	23	43	1.0	.63	.24	1.00			
	11,572-584	12	30	1.3	.91	.24	.83			
	11,584-590	6	35	5.0	1.25	.24	.69			
	11,590-600	10	50	1.1	.63	.24	1.00			
	11,610-620	10	38	1.8	1.11	.24	.74			
	Total	118						0	0	
G	11,640-650	10	50	3.0	1.25	.24	.91			
	11,652-668	16	52	1.6	.77	.24	.69			
	Total	26						0	0	

H   None

Log Analysis

Well #35

Type	SAND, FT. Interval	Net	LOG READ Sp	RS	Rt	ϕ	ANALYSIS Sw	hg	Vol	Remarks
B_2	11,130-143	13	38	1.1	.77	.31	.79			
	11,143-150	7	38	3.0	1.00	.31	.68			
	11,150-155	5	38	1.5	.83	.31	.75			
	11,157-170	13	42	.7	.45	.31	1.00			
	11,173-180	7	42	.8	.56	.31	.94			
	11,180-187	7	42	2.1	.77	.31	.79			
	T o t a l	52						0	0	
C	11,216-220	4	15	1.2	.83	.31	.75			
	11,225-229	4	15	1.2	.67	.31	.85			
	11,238-240	2	5	.9	.62	.31	.89			
	11,252-255	3	10	1.2	1.00	.31	.68			
	11,280-284	4	35	1.9	.90	.31	.72			
	11,289-292	3	35	1.2	.77	.31	.79			
	T o t a l	20						0	0	
D	11,312-316	4	20	1.7	.87	.24	.74			
	11,328-337	9	40	1.0	.67	.24	.86			
	11,340-355	12	40	0.9	.59	.24	.92			
	T o t a l	25						0	0	
E	11,373-382	6	5	1.2	.91	.24	.73			Shaly
	11,425-430	5	45	0.9	.56	.24	.95			
	11,430-433	2	45	0.7	.48	.24	1.00			
	11,433-438	4	45	1.2	.71	.24	.83			
	T o t a l	17						0	0	
F	11,445-454	9	45	0.6	.42	.24	1.00			
	11,454-458	4	45	1.1	.56	.24	.95			
	11,458-490	32	45	0.5	.38	.24	1.00			
	T o t a l	45						0	0	
G	11,497-500	3	5	0.8	.67	.24	.86			
	11,505-517	9	20	1.4	1.00	.24	.69			Hard streak?
	T o t a l	12						0	0	
H	None									

Log Analysis

Well #36

Type	SAND, FT. Interval	Net	Sp	RS	Rt	ϕ	Sw	hg	Vol	Remarks
B_2	11,335-343	5	10	0.8	.70	.27	.83			TVD = 11,150'
	11,343-350	7	15	1.6	1.00	.27	.68			
	11,360-382	20	15	1.2	.77	.27	.79			
	11,382-390	8	50	0.7	.53	.27	.97			
	Total	40						0	0	
C	11,400-410	10	55	0.7	.50	.29	1.00			TVD = 11,215'
	11,410-422	10	15	1.2	1.00	.29	–			Very shaly
	11,422-432	10	55	0.6	.56	.29	.95			
	11,435-447	11	55	0.6	.45	.29	1.00			
	Total	41						0	0	
D	11,464-470	6	40	1.8	1.05	.28	.66			TVD = 11,279'
	11,470-480	9	50	1.8	.83	.28	.75			
	11,480-490	10	50	0.4	.63	.28	.87			
	11,490-500	8	40	1.0	.70	.28	.82			
	Total	33						0	0	
E	11,530-540	10	45	0.8	.63	.27	.87			TVD = 11,325'
	11,553-560	7	42	0.8	.56	.27	.92			
	11,563-590	27	53	0.3	.30	.27	1.00			
	11,590-598	8	53	0.6	.56	.27	.92			
	Total	52						0	0	
F	11,603-630	27	42	0.5	.50	.28	.99			TVD = 11,418'
	11,630-678	45	42	0.6	.60	.28	.89			
	11,678-690	10	45	0.5	.53	.28	.96			
	11,690-700	10	60	1.0	.63	.28	.87			
	11,700-710	10	60	4.0	.83	.28	.75			
	11,710-730	18	60	0.8	.60	.28	.89			
	Total	120						0	0	
G	11,752-768	15	40	0.8	.53	.28	.96			TVD = 11,567'
	11,778-790	12	45	0.5	.50	.28	.99			
	11,792-820	26	45	0.5	.40	.28	1.00			
	11,820-830	10	45	4.0	1.00	.28	.67			Hard streak
	Total	63						0	0	

H   None

LOG ANALYSIS

Well #37

Type	Interval	Net	Sp	RS	Rt	$\emptyset$	S_w	hg	Vol.	Remarks
B$_2$	None									
C	11,285-289	4	40	1.8	.95	.28	.59	4	.46	TVD = 11,088' Subsea
	11,289-293	4	65	1.5	.50	.38	.62	4	.58	Porosity Questionable
	11,293-302	9	70	1.1	.30	.40	.78			
	11,302-307	5	70	18.0	1.00	.07	1.00			Hard Streak
	11,307-317	10	60	1.2	.45	.37	.68			
	11,325-328	3	50	2.2	.70	.29	.68			
	11,328-331	3	60	3.0	.75	.21	.90			
	11,331-340	9	40	1.3	.70	.29	.68			
	11,348-354	6	20	2.0	.75	.26	.73			
	TOTAL	53				.33	.61	8	1.04	
D	11,360-367	7	55	2.2	1.00	.30	.52	7	1.01	TVD = 11,163' Subsea
	11,367-374	7	61	1.2	.42	.29	.87			
	11,374-383	9	65	1.6	.38	.26	1.00			
	11,388-392	4	58	2.5	.55	.21	1.00			
	11,392-398	6	60	1.0	.45	.28	.87			
	11,398-402	4	56	1.8	.68	.23	.84			
	11,412-415	3	42	1.5	.65	.29	.68			
	11,416-432	14	56	1.2	.40	.31	.84			
	11,435-440	5	60	1.7	.50	.28	.82			
	11,444-464	20	70	1.3	.32	.31	.95			
	11,464-478	14	70	1.6	.38	.28	.96			
	11,482-494	10	60	1.3	.50	.27	.85			
	11,506-514	8	60	1.6	.42	.26	.97			
	TOTAL	111				.30	.52	7	1.01	
E	11,535-543	8	42	1.3	.60	.28	.72			TVD = 11,338' Subsea
	11,543-557	14	57	1.4	.40	.28	.90			
	11,557-575	18	62	1.2	.36	.31	.86			
	11,575-581	6	65	7.0	.60	.10	1.00			Hard Streak
	11,586-592	6	58	1.4	.40	.29	.87			
	11,595-605	10	50	1.6	.51	.27	.82			
	TOTAL	62						0	0	

185

Log Analysis, Well #37

Type	SAND, FT. Interval	Net	LOG READ Sp	RS	Rt	ANALYSIS Ø	S$_w$	hg	Vol.	Remarks
F	11,620									TVD = 11,423' Subsea
	11,656-675	15	45	1.8	.65	.19	1.00			
	11,688-693	5	70	2.2	.51	.21	1.00			
	11,693-703	10	68	1.2	.41	.31	.80			
	11,703-708	5	68	2.3	.65	.21	.92			
	11,752-758	6	55	1.7	.70	.23	.81			
	11,758-766	8	65	.6	.25	.29	1.00			
	11,966-790	24	65	.9	.35	.28	.97			
	11,798-810	12	58	2.0	.70	.18	1.00			
	11,820-829	9	50	1.5	.50	.28	.80			
	11,834-844	10	60	1.1	.40	.28	.90			
	11,844-850	6	57	2.0	.57	.16	1.00			
	11,850-858	8	60	.9	.35	.29	.94			
	11,864-869	5	54	3.1	1.20	.04	1.00			Hard Streak
	11,869-882	13	60	1.0	.35	.30	.91			
	11,822-899	17	50	.9	.48	.33	.69			
	11,899-920	21	60	.9	.33	.32	.88			
	11,944-956	12	52	1.3	.60	.26	.78			
	11,956-964	8	52	3.2	.90	1.0	1.00			
	11,968-984	14	58	1.4	.61	.25	.80			
	11,984-12,026	42	58	1.8	.60	.21	.96			
	12,032-041	9	60	1.5	.52	.23	.95			
	12,041-054	13	58	4.0	.70	.10	1.00			
	12,054-068	14	62	1.5	.48	.25	.91			
	12,068-073	5	60	1.7	.65	.10	1.00			
	12,073-095	22	61	1.2	.41	.29	.86			
	12,095-102	7	40	2.1	.80	.17	1.00			
	TOTAL	320						0	0	

G   None

H   None

Part 4

IN-PLACE GAS VOLUME MAPS BY SAND
FOR B_2 THROUGH G SANDS

PORT ARTHUR FIELD
JEFFERSON COUNTY, TEXAS

B$_2$ SANDSTONE
HYDROCARBON PORE VOLUME
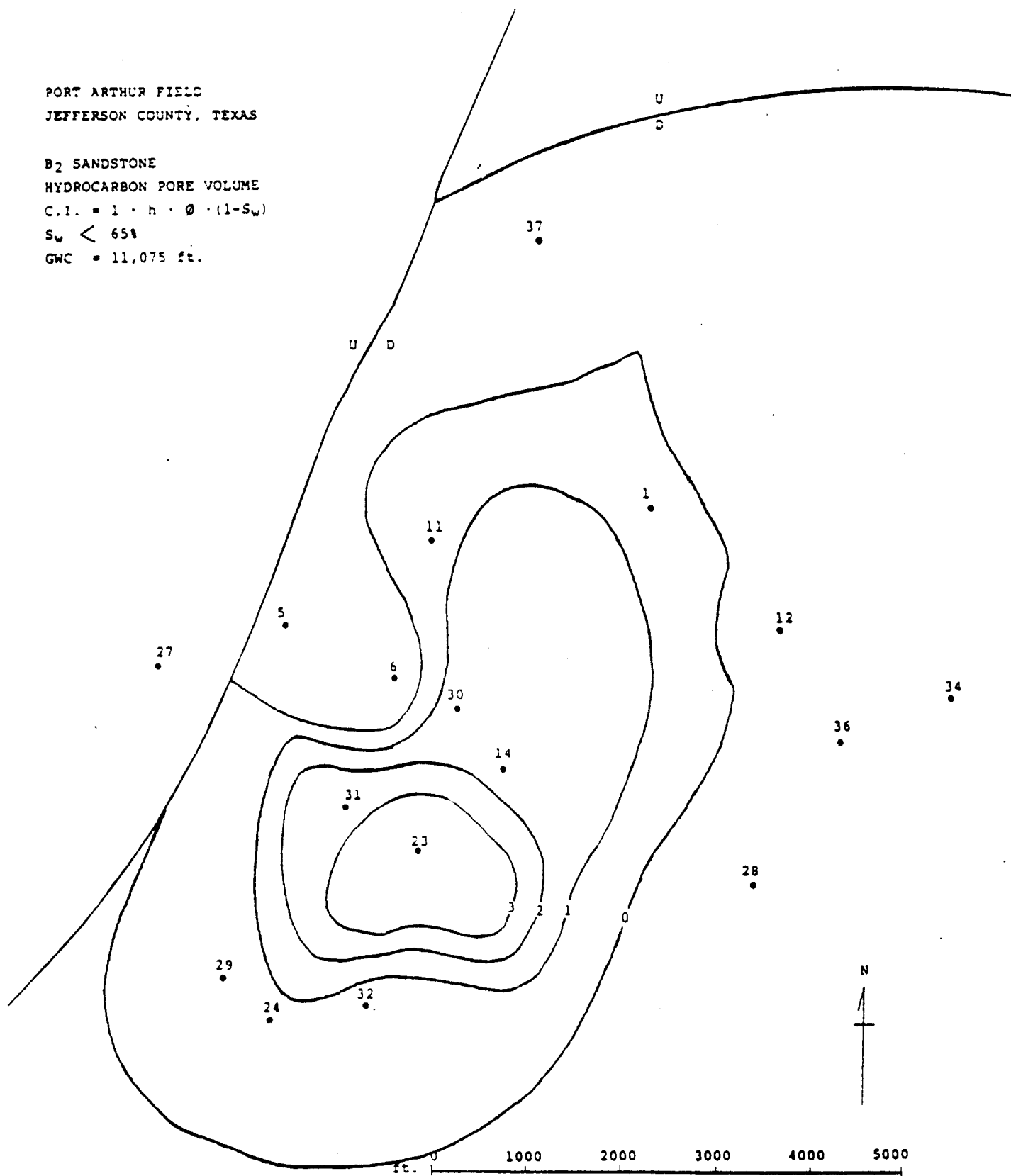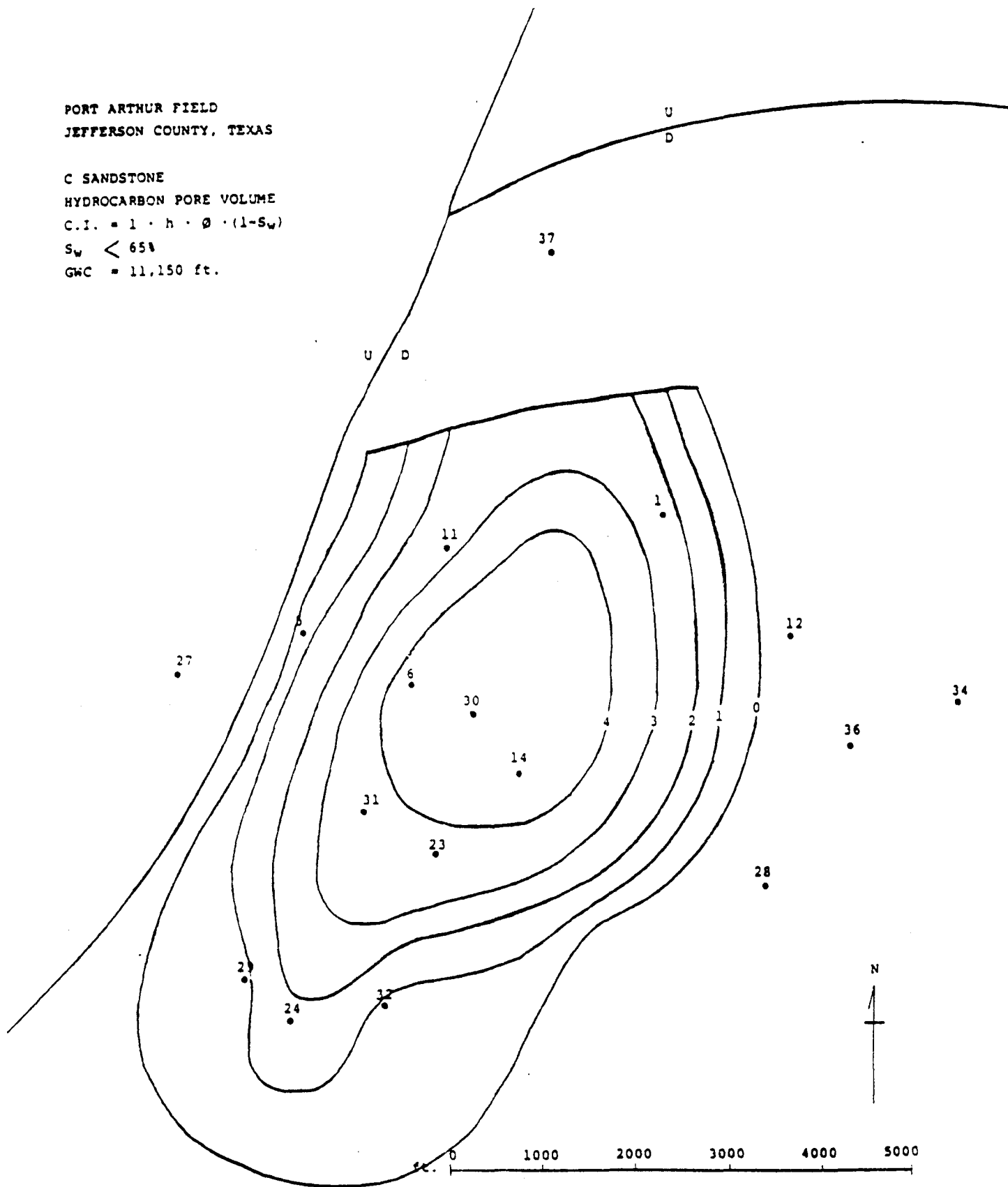C.I. = 1 · h · Ø · (1-S$_w$)
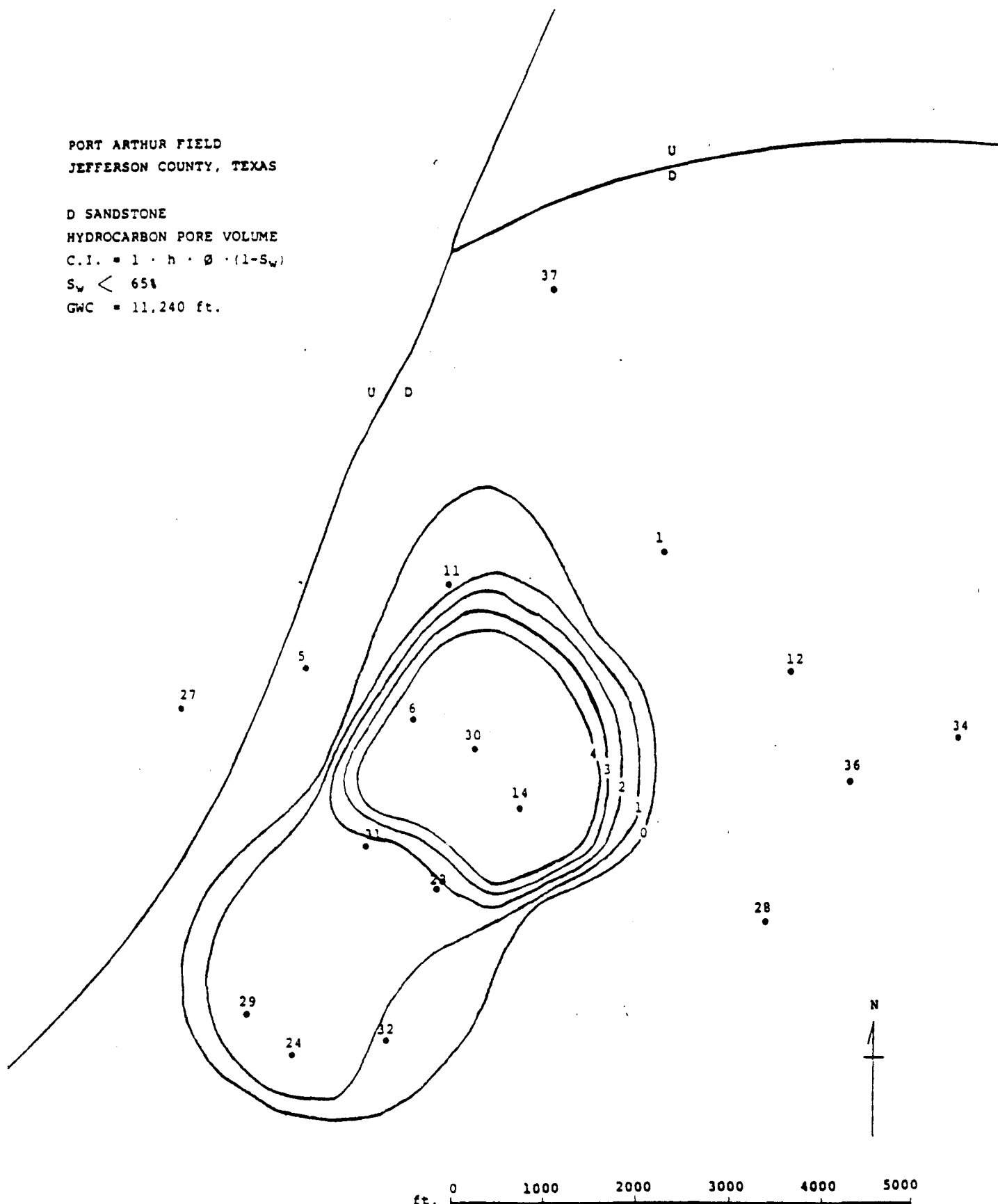S$_w$ < 65%
GWC = 11,075 ft.

Figure D-12. In-place gas volume map; contours show thickness (ft) of B$_2$ sandstone where S$_g$ > 35 percent, Port Arthur field.

188

PORT ARTHUR FIELD
JEFFERSON COUNTY, TEXAS

C SANDSTONE
HYDROCARBON PORE VOLUME
C.I. $= 1 \cdot h \cdot \emptyset \cdot (1-S_w)$
$S_w < 65\%$
GWC $= 11,150$ ft.

Figure D-13. In-place gas volume map; contours show thickness (ft) of C sandstone where $S_g > 35$ percent, Port Arthur field.

189

PORT ARTHUR FIELD
JEFFERSON COUNTY, TEXAS

D SANDSTONE
HYDROCARBON PORE VOLUME
C.I. = 1 · h · $\emptyset$ · $(1-S_w)$
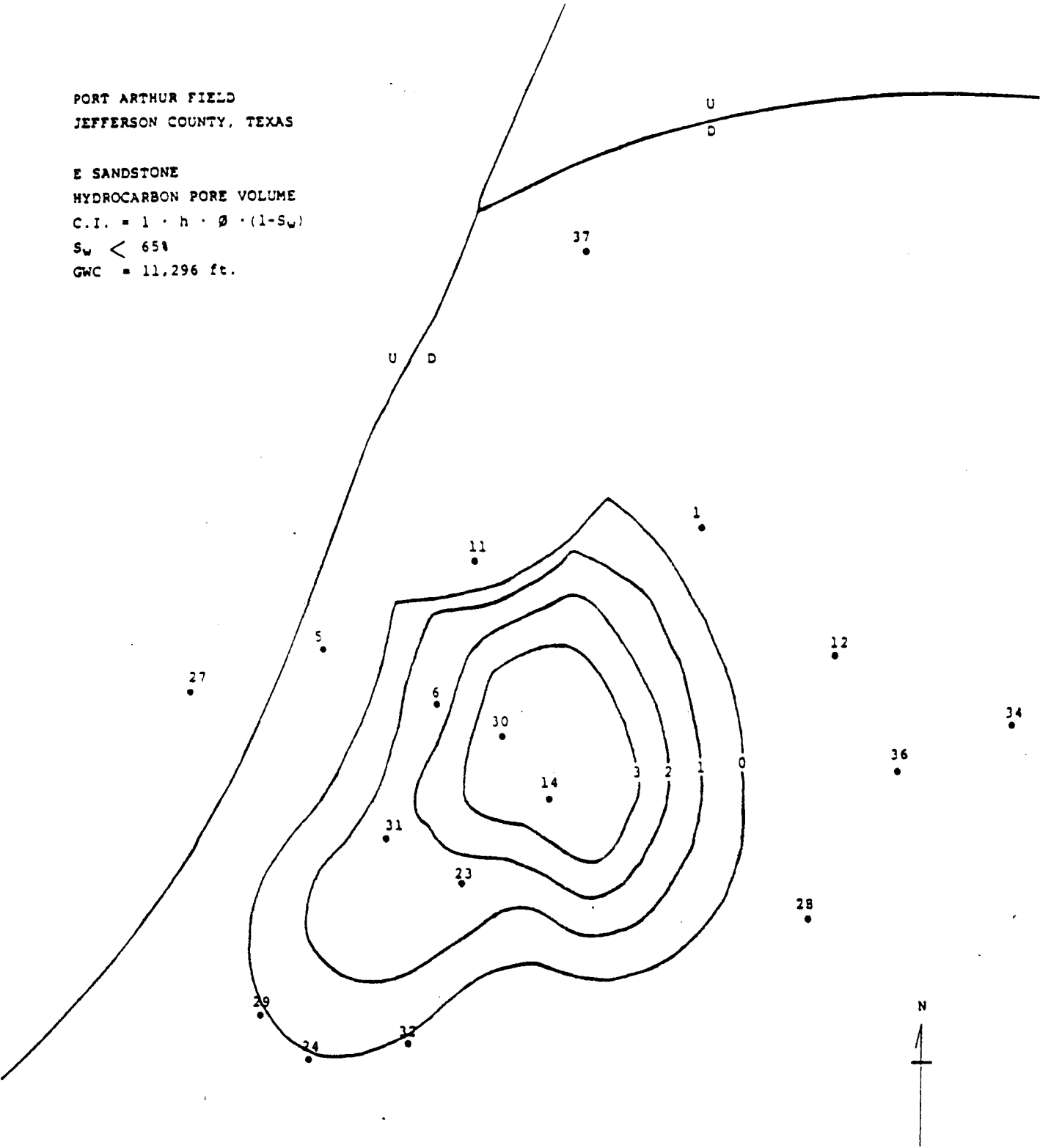$S_w < 65\%$
GWC = 11,240 ft.

Figure D-14. In-place gas volume map; contours show thickness (ft) of D sandstone where $S_g > 35$ percent, Port Arthur field.

190

PORT ARTHUR FIELD
JEFFERSON COUNTY, TEXAS

E SANDSTONE
HYDROCARBON PORE VOLUME
$C.I. = 1 \cdot h \cdot \emptyset \cdot (1-S_w)$
$S_w < 65\%$
$GWC = 11,296$ ft.

Figure D-15. In-place gas volume map; contours show thickness (ft) of E sandstone where $S_g > 35$ percent, Port Arthur field.

PORT ARTHUR FIELD
JEFFERSON COUNTY, TEXAS

F SANDSTONE
HYDROCARBON PORE VOLUME
$C.I. = 1 \cdot h \cdot \emptyset \cdot (1-S_w)$
$S_w < 65\%$
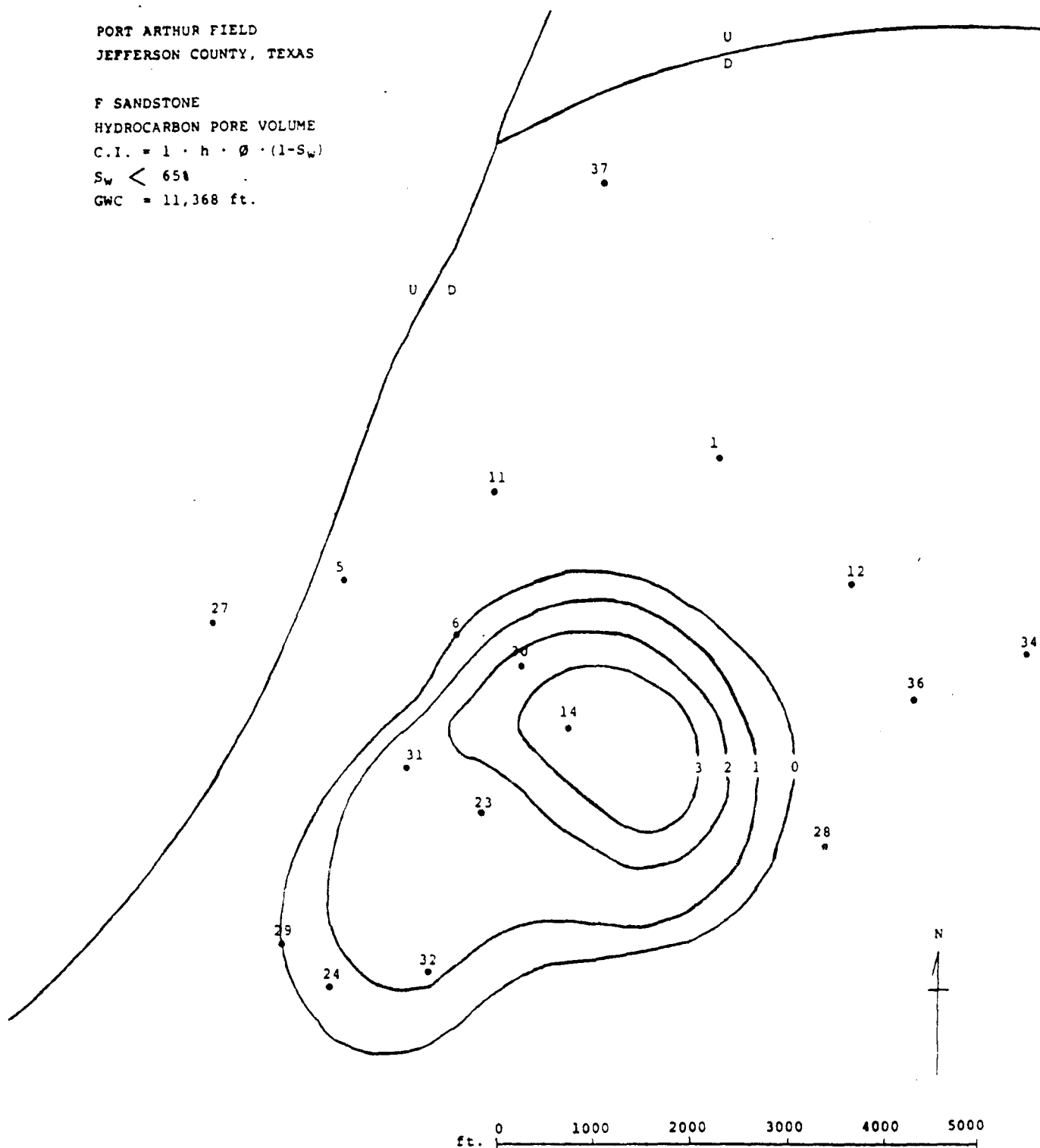$GWC = 11,368 \text{ ft.}$

Figure D-16. In-place gas volume map; contours show thickness (ft) of F sandstone where $S_g > 35$ percent, Port Arthur field.

192

PORT ARTHUR FIELD
JEFFERSON COUNTY, TEXAS

G SANDSTONE
HYDROCARBON PORE VOLUME
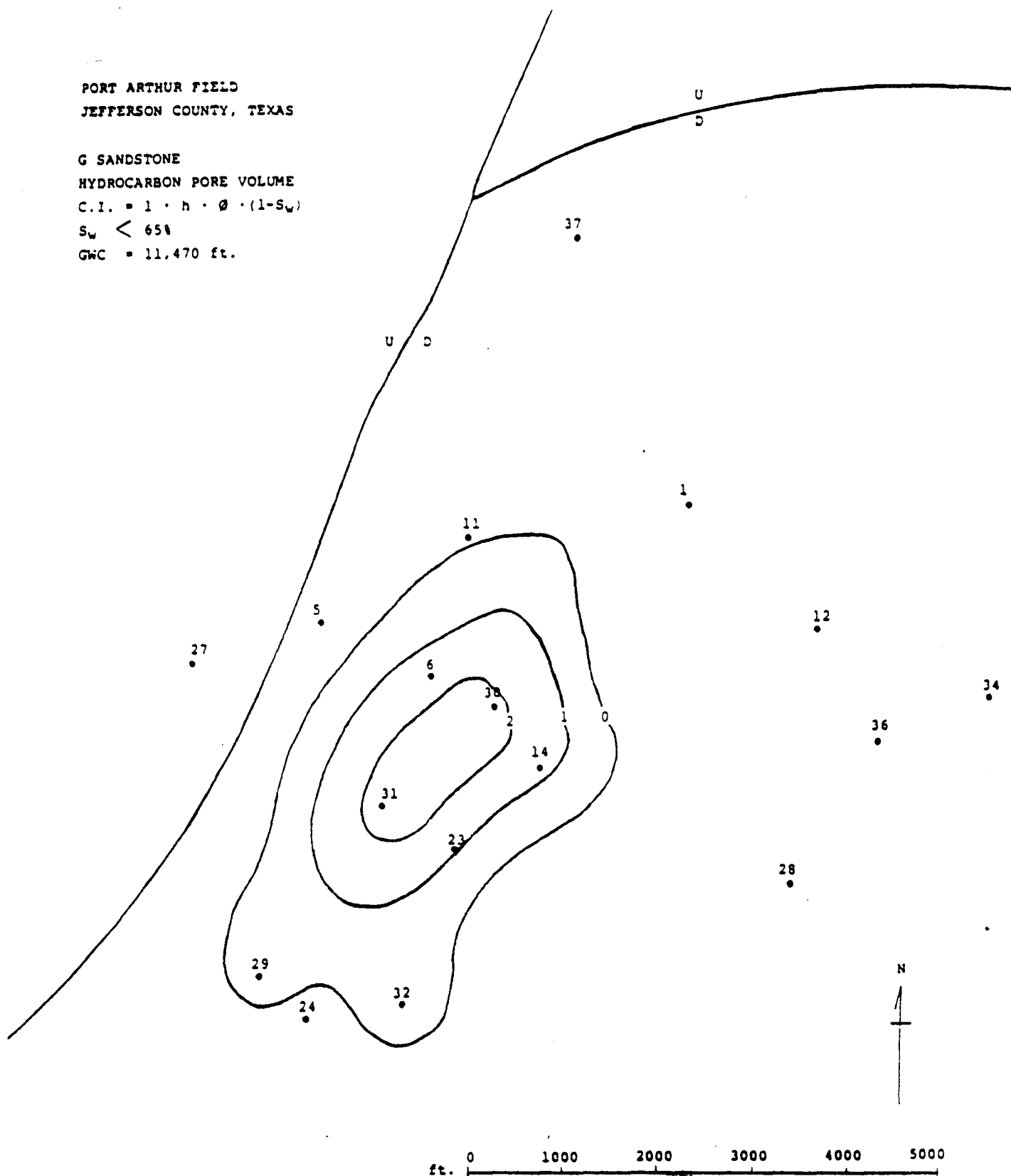C.I. = 1 · h · Ø ·(1-S$_w$)
S$_w$ < 65%
GWC = 11,470 ft.

Figure D-17. In-place gas volume map; contours show thickness (ft) of G sandstone where S$_g$ > 35 percent, Port Arthur field.

193

APPENDIX E: METRIC CONVERSION FACTORS

Customary Unit		Conversion Factor		Preferred Metric Unit
acre	x	0.4046856	=	ha (hectares)*
acre-ft	x	1,233.482	=	m^3
acre-ft	x	0.1233482	=	ha-m
bbl (42 gals)	x	0.158983	=	m^3
bbl/acre-ft	x	0.0001288931	=	m^3/m^3
bbl/d	x	0.1589873	=	m^3/d
°C	+	273.1500	=	°K
°F		(°F - 32)/1.8	=	°C
ft	x	0.3048	=	m
gal	x	0.003785412	=	m^3
lb/gal	x	119.8264	=	kg/m^3
md	x	0.0009869233	=	μm^2
mi	x	1.609344	=	km
mi^2	x	2.589988	=	km^2
psi	x	6.894757	=	kPa
psi/ft	x	22.62059	=	kPa/m
scf (std ft^3)	x	0.02831685	=	m^3
scf/bbl	x	0.1801175	=	std m^3/m^3

*1 ha (hectare) = 10,000 m^2 (2.47 acres)

APPENDIX F: NOMENCLATURE

A.F.I.T. = after federal income tax

bbl = barrel, 42-gallon capacity

B.F.I.T. = before federal income tax

BHP = bottom-hole pressure, psi

BHSIP = bottom-hole shut-in pressure, psi

BHT = bottom-hole temperature, °F

Bscf = billion standard cubic feet

B_w = water formation volume factor, dimensionless

°C = degrees Celsius (centigrade)

CH_4 = methane

C_p = compaction correction factor

D = depth, feet

d = day

DST = drill-stem test

F = formation factor

°F = degrees Fahrenheit

FPG = formation pressure gradient, psi/ft

GOR = gas-to-oil ratio

GP = geopressure

GWC = gas/water contact

m = cementation factor

md = millidarcy

mi = mile or miles

MMscf = million standard cubic feet

Mscf = thousand standard cubic feet

Appendix F: (continued)

R_{sh} = shale resistivity, ohm-meters

R_{mf} = mud filtrate resistivity, ohm-meters

S_g = gas saturation percent or fraction of pore volume

S_w = water saturation, percent or fraction of pore volume

T_L = temperature measured in borehole and recorded on well log header, °F

ΔT_f = transit time of fluid contained in pore spaces of rock, μsec/ft

ΔT_{log} = transit time from acoustic log, μsec/ft

ΔT_m = transit time of solid matrix material of rock, μsec/ft

WHSIP = wellhead shut-in pressure, psi

Z = gas compressibility factor, dimensionless